

PHASE 2 INITIAL BOREHOLE DRILLING AND TESTING, IGNACE AREA

*Thin Section Petrography and Lithogeochemical
Analysis of Core Samples from IG_BH01 through
IG_BH04*

APM-REP-01332-0464

January 2024

Nuclear Waste Management Organization (NWMO)

nwmo

NUCLEAR WASTE
MANAGEMENT
ORGANIZATION

SOCIÉTÉ DE GESTION
DES DÉCHETS
NUCLÉAIRES



Nuclear Waste Management Organization
22 St. Clair Avenue East, 4th Floor
Toronto, Ontario
M4T 2S3
Canada

Tel: 416-934-9814
Web: www.nwmo.ca

Phase 2 Initial Borehole Drilling and Testing, Ignace Area.

Thin Section Petrography and Lithogeochemical Analysis of Core Samples from IG_BH01 through IG_BH04

APM-REP-01332-0464

January 2024

Nuclear Waste Management Organization

Document History

Title:	Phase 2 Initial Borehole Drilling and Testing, Ignace Area. Thin Section Petrography and Lithogeochemical Analysis of Core Samples from IG_BH01 through IG_BH04		
Report Number:	APM-REP-01332-0464		
Revision:	R000	Date:	January 2024
Author Company(s)	Nuclear Waste Management Organization		
Authored by:	Nuclear Waste Management Organization (NWMO)		
Accepted by:	Andrew Parmenter (Geoscience Director)		

Revision Summary		
Revision Number	Date	Description of Changes/Improvements
R000	2024-01	Initial issue

1. INTRODUCTION

Lithogeochemistry and optical petrography provide important information about the composition, petrogenesis, alteration, and deformation of the host and accessory rock types of the Revell batholith. Whole rock (major element) and trace element analyses are performed on each sample, in addition to a detailed qualitative optical petrographic description. The goal of this work is to further understand and classify the host and accessory rock types of the batholith, to identify outlier or unusual rock types, and to better understand the types and locations of alteration throughout the rock mass.

In general, whole rock geochemistry provides a breakdown of the major cations present in the sample (Si, Ti, Al, Fe, Mn, Mg, Ca, Na, K, and P) which aid in rock classification and understanding the conditions of melting and/or the subsequent crystallization history of the batholith. Trace element geochemistry provides a breakdown of elements in the sample in concentrations less than 0.1 wt. %. Most commonly, these trace elements substitute for major elements (listed above) in the rock-forming minerals. Trace elements can help identify geological processes and combined with major elements, can identify the original tectonic setting of igneous rocks.

Qualitative optical petrography provides a detailed description of the minerals present in each sample, their form, interrelationship, and any deformation they may have undergone. Point-counting provides a relative amount of major minerals, allowing for classification of igneous rocks on a QAPF diagram. Additionally, the presence of accessory minerals and their relationship to the rock-forming minerals provide valuable information on post-cooling processes and fluid movement. The petrographic report and associated high-quality thin section photographs are an essential part of understanding the host and subordinate rock types present in the Revell batholith.

This report documents the results of Thin Section Petrography and Lithogeochemical Analysis of Core Samples from IG_BH01 through IG_BH04. This work was complete as part of Phase 2 Initial Borehole Drilling and Testing, Ignace Area. The analyses and reporting were completed by ACTLABS.

Results documented within this report are divided into two parts:

- A) Thin Section Petrographic Analysis
- B) Lithogeochemical Analysis

2. SCOPE OF LABORATORY WORK

The work associated with Phase 2 Geoscientific Preliminary Assessment, Lithochemical analysis of samples from IG_BH01 through IG_BH04 in Ignace was undertaken by Activations Laboratories, which is a mineral laboratory with ISO 17025:2017 accreditation.

All samples are prepared on arrival at Activation Laboratories in Thunder Bay using the following methodology: samples are crushed to 80% passing 2 mm, riffle split (250 g) and pulverized using a mild steel mill to 95% passing 105 µm. All samples are then analyzed for major and trace elements using the techniques described below. Note that any analyses listed below with a 4 in their code are added to the 4Lithores suite to account for specific elements.

4Lithores

Crushed samples are fused with lithium metaborate/tetraborate and the resulting molten bead is digested in a weak nitric acid solution. The liquid is analyzed for major and trace elements using Inductively-Coupled Plasma Mass Spectroscopy (ICP-MS) and Inductively-Coupled Plasma Optical Emission Spectroscopy (ICP-OES).

4B1

4B1 is used to obtain accurate levels of base metals (Cu, Pb, Zn, Ni, and Ag). A 4-acid (near-total) digestion is used, which is a combination of hydrofluoric, nitric, perchloric, and hydrochloric acids. The solution is analyzed with ICP-OES.

4B – INAA

4B-INAA is used principally to analyze concentrations of As, Sb, W, and moderate levels of Cr. Instrumental Neutron Activation Analysis (INAA) is an analytical technique dependent on measuring induced gamma radiation in the sample by irradiation with neutrons. The source of neutrons is a nuclear reactor. Each element emits a unique signature of gamma radiation which can be measured and analyzed on a high-purity Ge detector.

QOP

A qualitative optical petrography report is completed for each sample. Thin sections are prepared by ACTLABS and a petrographic analysis using transmitted and reflective light microscopy (including modal mineralogy, thin section description, and photomicrographs) is completed by a qualified person.

4F – C, S

This analysis measures total carbon and sulphur. An accelerator material is added to the sample, and the inductive elements of the sample and accelerator couple with the high frequency field of the induction furnace, causing the sample to combust in the pure oxygen environment. During combustion, sulphur- and carbon-bearing elements are reduced, releasing sulphur and carbon, which bond with oxygen to form SO_2 , CO , and CO_2 (majority CO_2). Sulphur and carbon dioxide are measured by infrared spectroscopy.

A) Thin Section Petrographic Analysis



Petrographic Report
on Polished Thin Section
A23-01966

Reviewed By:
Dr. Mahdi Ghobadi

Date:
7/20/2023

Table of Contents

Conditions and Disclaimer.....	4
1. Introduction.....	5
Terminology.....	6
2. Summary of Results.....	7
3. Petrographic Descriptions.....	23
Sample 1: A23-01966-1-IG_BH04_MG051.....	23
Sample 2: A23-01966-2-IG_BH04_MG052.....	28
Sample 3: A23-01966-3-IG_BH04_MG053.....	31
Sample 4: A23-01966-4-IG_BH04_MG054.....	34
Sample 5: A23-01966-5-IG_BH04_MG055.....	36
Sample 6: A23-01966-6-IG_BH04_MG056.....	38
Sample 7: A23-01966-7-IG_BH04_MG057.....	41
Sample 8: A23-01966-8-IG_BH04_MG058.....	44
Sample 9: A23-01966-9-IG_BH04_MG059.....	48
Sample 10: A23-01966-10-IG_BH04_MG060.....	51
Sample 11: A23-01966-11-IG_BH04_MG061.....	54
Sample 12: A23-01966-12-IG_BH04_MG062.....	58
Sample 13: A23-01966-13-IG_BH04_MG063.....	62
Sample 14: A23-01966-14-IG_BH04_MG064.....	66
Sample 15: A23-01966-15-IG_BH04_MG065.....	69
Sample 16: A23-01966-16-IG_BH04_MG066.....	73
Sample 17: A23-01966-17-IG_BH04_MG067.....	76
Sample 18: A23-01966-18-IG_BH04_MG068.....	80
Sample 19: A23-01966-19-IG_BH04_MG069.....	84
Sample 20: A23-01966-20-IG_BH04_MG070.....	87
Sample 21: A23-01966-21-IG_BH04_MG071.....	90
Sample 22: A23-01966-22-IG_BH04_MG072.....	94
Sample 23: A23-01966-23-IG_BH04_MG073.....	97
Sample 24: A23-01966-24-IG_BH04_MG074.....	100
Sample 25: A23-01966-25-IG_BH04_MG075.....	103
Sample 26: A23-01966-26-IG_BH04_MG076.....	106
Sample 27: A23-01966-27-IG_BH04_MG077.....	110
Sample 28: A23-01966-28-IG_BH04_MG078.....	113
Sample 29: A23-01966-29-IG_BH04_MG079.....	115
Sample 30: A23-01966-30-IG_BH04_MG080.....	118
Sample 31: A23-01966-31-IG_BH04_MG081.....	121
Sample 32: A23-01966-32-IG_BH04_MG082.....	124
Sample 33: A23-01966-33-IG_BH04_MG083.....	127
Sample 34: A23-01966-34-IG_BH04_MG084.....	129
Sample 35: A23-01966-35-IG_BH04_MG085.....	132
Sample 36: A23-01966-36-IG_BH01_LG046.....	136
Sample 37: A23-01966-37-IG_BH02_LG027.....	138
Sample 38: A23-01966-38-IG_BH02_LG028.....	141
Sample 39: A23-01966-39-IG_BH02_LG029.....	144
Sample 40: A23-01966-40-IG_BH02_LG030.....	147
Sample 41: A23-01966-41-IG_BH03_LG023.....	150
Sample 42: A23-01966-42-IG_BH04_MG086.....	153
Sample 43: A23-01966-43-IG_BH04_MG087.....	156
Sample 44: A23-01966-44-IG_BH04_MG088.....	159

Sample 45: A23-01966-45-IG_BH04_MG089.....	162
Sample 46: A23-01966-46-IG_BH02_LG031.....	165
Sample 47: A23-01966-47-IG_BH02_LG032.....	169
Sample 48: A23-01966-48-IG_BH02_LG033.....	172
Sample 49: A23-01966-49-IG_BH02_LG034.....	175
Sample 50: A23-01966-50-IG_BH01_LG047.....	179
Sample 51: A23-01966-51-IG_BH01_LG048.....	183
Appendix 1. Glossary of Microstructural and Petrologic Terms Used in the Text.....	186
Appendix 2. Bibliography.....	188

1. Introduction

The present “Petrographic Description” provides the following information:

- (i) the petrographic rock classification;
- (ii) microstructural description;
- (iii) a table with the modal percentage and average grain size for each mineral; and
- (iv) description of the minerals in decreasing order of abundance.

Terminology

Grain Size

Following the aforementioned classification systems, the grain size classifications used in this report are:

very coarse grained:	greater than 16 mm
coarse grained:	from 2 mm to 16 mm
medium grained:	from 0.25 mm to 2 mm
fine grained:	from 0.032 mm to 0.25 mm
very fine grained:	from 0.004 mm to 0.032 mm
cryptocrystalline:	less than 0.004 mm (4 μ m).

Alteration

If the rock is altered, the alteration intensity is described by indices, and the molar percentage of these indices is shown below (see Gifkins et al. 2005). If the alteration is replacing a specific mineral, it is specified in the description, and these percentages are referred to the specific mineral, and need to be recalculated considering the modal percentage of the mineral in the rock.

Alteration Index	Mass Change %
subtle	<1
weak	<10
moderate	5-30
strong	15-60
intense	15-100

2. Summary

Sample 1: A23-01966-1-IG_BH04_MG051—White mica-altered tonalite & Felsitic rock & Quartz vein & K-feldspar veinlets—Anhedral and subhedral plagioclase, anhedral quartz, poikilitic K-feldspar, and randomly oriented biotite define a granular texture occurring in the upper and lower part of the section (Domains A). The granular domain is associated and probably transitioning to a fine-grained inequigranular and felsitic Domain B consisting of quartz and plagioclase. An up to 5.5 mm thick quartz vein crosscut the fine-grained felsitic domain and K-feldspar-rich veinlets reactivated the vein walls and crosscut the granular and fine-grained felsitic host domains.

Alteration: white mica: moderate after plagioclase in Domain A; epidote: weak around the quartz vein; chlorite-white mica: weak after biotite; pyrite: subtle in Domain B

Sample 2: A23-01966-2-IG_BH04_MG052—White mica-epidote-altered tonalite & Biotite schist & Calcite veinlets—This section comprises two compositionally and texturally different domains. In Domain A, subhedral and inequigranular plagioclase crystals prevail over anhedral crystals of quartz, randomly oriented and anhedral biotite and sparse epidote alteromorphs after biotite defines a granular texture. In Domain B, fine-grained biotite is iso-oriented and defines a continuous schistosity. Subordinate quartz and epidote define a granolepidoblastic texture.

Alteration: white mica-epidote: weak after plagioclase in Domain B; epidote: weak to strong after biotite in Domain B; pyrite: subtle; iron oxides: subtle after pyrite

Sample 3: A23-01966-3-IG_BH04_MG053—Biotite schist—Irregularly shaped and lenticular microlithons of calcite, calcite and quartz, and quartz are wrapped by a continuous and disharmonically folded schistosity defined by biotite, and subordinate quartz, plagioclase, and epidote.

Alteration/metamorphism: epidote-chlorite: weak after biotite

Sample 4: A23-01966-4-IG_BH04_MG054—Quartz-biotite-albite granofels—Fine- to medium-grained poikiloblastic albite, randomly oriented biotite, and subordinate quartz and calcite define a xenoblastic granular texture.

Sample 5: A23-01966-5-IG_BH04_MG055—Calcite crystal & Chlorite-schist—This section comprises a single crystal of calcite (~15mm by 29 mm) and a small portion of biotite schist.

Sample 6: A23-01966-6-IG_BH04_MG056—Tonalite—Subhedral and inequigranular plagioclase crystals prevail over anhedral crystals of quartz, randomly oriented and anhedral biotite and sparse crystals of anhedral K-feldspar, all of which define a granular texture.

Alteration: white mica-epidote: weak after plagioclase; iron oxides: subtle

Sample 7: A23-01966-7-IG_BH04_MG057—Tonalite & Orthogneiss—This section comprises two

domains. Domain A is a granular aggregate of plagioclase, quartz, and biotite. In Domain B, the plagioclase forms anhedral porphyroclasts immersed within a fine-grained matrix of quartz, plagioclase and biotite. The clustering and iso-oriented lamellae of biotite define a discontinuous schistosity wrapping the plagioclase porphyroclasts.

Alteration/Metamorphism: white mica-epidote(?): subtle after plagioclase in Domain A; epidote: weak in Domain B

Sample 8: A23-01966-8-IG_BH04_MG058—Tonalite & K-feldspar-biotite-quartz schist & Orthogneiss—This section comprises three different compositional and textural domains. In Domain A, subhedral plagioclase, anhedral quartz and subordinate biotite define a coarse-grained granular texture. Domain B comprises fine-grained quartz, heterogeneously distributed K-feldspar and fine-grained iso-oriented lamellae of biotite. In Domain C, plagioclase porphyroclasts are rotated within a fine-grained matrix of quartz and plagioclase and are wrapped by discontinuous and sub-parallel cleavage domains of biotite.

Alteration/Metamorphism: epidote-white mica: subtle to weak after plagioclase; epidote-white mica: weak in Domain C; carbonate: subtle in Domain C

Sample 9: A23-01966-9-IG_BH04_MG059—Tonalite—Subhedral and inequigranular plagioclase crystals prevail over anhedral crystals of quartz, randomly oriented and anhedral biotite and sparse crystals of anhedral K-feldspar, all of which define a granular texture.

Alteration: white mica-epidote: weak after plagioclase; epidote: subtle

Sample 10: A23-01966-10-IG_BH04_MG060—Tonalite—Subhedral and inequigranular plagioclase crystals prevail over anhedral crystals of quartz, randomly oriented and anhedral biotite and sparse crystals of anhedral K-feldspar, all of which define a granular texture.

Alteration: white mica-epidote: weak after plagioclase; epidote: subtle

Sample 11: A23-01966-11-IG_BH04_MG061—Tonalite & Microtonalite(?) & Epidote-biotite-quartz-white mica sheared domain—This section comprises three domains. Domain A is a granular aggregate of euhedral and subhedral plagioclase, anhedral quartz, biotite, and subordinate poikilitic K-feldspar. Domain B shows a similar composition to Domain A, and the plagioclase is inequigranular. The two domains are divided by an up to 1.5 mm thick schistose Domain C consisting of white mica, quartz, biotite, and epidote.

Alteration/Metamorphism: white mica-epidote(?): subtle after plagioclase; moderate to strong in the 1.5 mm thick shear domain

Sample 12: A23-01966-12-IG_BH04_MG062—Microquartz-diorite & Epidote-Fe-chlorite-altered microgranodiorite/microquartz-monzodiorite—This section shows a compositional heterogeneity, which generated two irregular sub-domains. In the upper and lower parts of the section (Domains A), subhedral plagioclase prevails over anhedral quartz and randomly oriented flakes of biotite. Domain B comprises plagioclase, quartz, which is more abundant than in Domain A, K-feldspar, and sparse Fe-chlorite and epidote replacing biotite.

Alteration: Fe-chlorite: moderate to strong after biotite in Domain B; epidote: weak after biotite in Domain B; sericite-epidote: moderate after plagioclase in Domain B; epidote:

subtle after plagioclase in Domain A; chalcopyrite: subtle in Domain B

Sample 13: A23-01966-13-IG_BH04_MG063—Chlorite-altered microquartz-diorite & Epidote-chlorite-sericite-altered microgranodiorite/microquartz-monzodiorite—This section is compositionally similar to Sample 12 and shows a compositional heterogeneity. In the upper and lower parts of the section (Domains A), subhedral plagioclase prevails over anhedral quartz and randomly oriented flakes of biotite. Domain B comprises plagioclase, quartz, and sparse Fe-chlorite and epidote replacing biotite.

Alteration: Fe-chlorite: moderate to strong after biotite in Domain B; epidote: weak after biotite in Domain B; sericite-epidote-K-feldspar: moderate after plagioclase in Domain B; epidote: subtle after plagioclase in Domain A; chalcopyrite: subtle in Domain B

Sample 14: A23-01966-14-IG_BH04_MG064—Microquartz-diorite & Microgranodiorite/microquartz-monzodiorite & Tonalite—This section is compositionally similar to Sample 12 and 13 (quartz-diorite and microgranodiorite); however, its heterogeneity is more complex and includes Domain C (tonalite). The medium-grained magmatic rock is subdivided into a relatively fresh Domain A comprising plagioclase, quartz, and biotite, and a Domain B comprising plagioclase, quartz, K-feldspar, and biotite. Both domains are crosscut by a coarser-grained and more leucocratic Domain C comprising plagioclase, quartz, K-feldspar, and biotite.

Alteration: epidote: weak after biotite; sericite-epidote: subtle after plagioclase; epidote: subtle

Sample 15: A23-01966-15-IG_BH04_MG065—Albite-epidote-actinolite-chlorite granofels & Chlorite schist & Quartz vein—Most of this section consists of xenoblastic and randomly oriented crystals of amphibole, albite, chlorite and epidote. These minerals define a xenoblastic and isotropic texture in the mid- and upper part of the section. In the lower part, Chlorite is concentrated within irregular cleavage domains associated with K-feldspar microlithons defining a spaced schistosity. A quartz vein is ~2 mm thick, is oriented parallel to the schistosity defined by the chlorite domains and K-feldspar microlithons in the lower part of the section.

Sample 16: A23-01966-16-IG_BH04_MG066—Pyrite-calcite-chlorite-retrometamorphosed actinolite schist—Amphibole, chlorite, and relic biotite define a rough schistosity, which is disharmonically folded and wraps lenticular and irregularly shaped microlithons comprising plagioclase, chlorite, calcite, and quartz.

Alteration/Metamorphism: chlorite: moderate to strong after biotite; calcite: moderate; pyrite: subtle

Sample 17: A23-01966-17-IG_BH04_MG067—Chlorite-retrometamorphosed biotite schist—Tightly folded cleavage domains of chlorite and biotite define a crenulated schistosity associated with fine-grained granoblastic domains of calcite and quartz. The chlorite partially overprinted the biotite, which likely defined the schistosity during the folding event.

Alteration/Metamorphism: chlorite: moderate to strong after biotite; calcite: moderate; chalcopyrite: subtle

- Sample 18: A23-01966-18-IG_BH04_MG068—Microtonalite & Epidote-Fe-chlorite-sericite microgranodiorite/microquartz-monzodiorite & K-feldspar veinlet—This section comprises a relatively fresh Domain A comprising plagioclase, quartz, biotite, and K-feldspar and a Domain B comprising plagioclase, quartz, K-feldspar, and biotite. The boundary between the two domains is gradual and point to a magmatic mingling process.
- Alteration: sericite-epidote: subtle after plagioclase in Domain A; moderate after plagioclase in Domain B; Fe-chlorite-epidote-titanite: strong after biotite in Domain B.
- Sample 19: A23-01966-19-IG_BH04_MG069—Chlorite-Sericite-altered microtonalite & Quartz vein—A ~10 mm thick quartz vein crosscut a medium-grained granular texture defined by anhedral plagioclase, quartz, and biotite.
- Alteration: white mica: weak to moderate after plagioclase; chlorite>titanite: moderate to strong after biotite
- Sample 20: A23-01966-20-IG_BH04_MG070—White mica-chlorite-altered microdiorite(?) & Chlorite-K-feldspar-altered schist—This section comprises a schistose domain, which is defined by preferentially iso-oriented clusters of chlorite, fine-grained xenoblastic K-feldspar, and calcite, and in the left part of the section (right part of the offcut) the schist wraps angular and irregularly shaped fragments of a dioritic(?) rock comprising plagioclase, quartz, chlorite, and subordinate microcline. Calcite crosscuts the schist and the diorite.
- Alteration/Metamorphism: chlorite: strong after biotite; K-feldspar: weak in the schist calcite: weak to moderate; white mica: moderate after plagioclase, weak in the schist
- Sample 21: A23-01966-21-IG_BH04_MG071—Chlorite-altered microtonalite & Chlorite-retrometamorphosed biotite schist—A granular domain (A) comprising anhedral plagioclase, quartz, and chlorite after biotite define an irregular contact with a fine-grained schistose domain comprising chlorite, quartz and calcite.
- Alteration/Metamorphism: white mica: moderate after plagioclase; chlorite>titanite: moderate to strong after biotite; calcite-epidote: subtle to weak in Domain A and after the plagioclase
- Sample 22: A23-01966-22-IG_BH04_MG072—Calcite-Fe-chlorite-albite-altered foliated microdiorite—Fine-grained xenoblastic aggregates of plagioclase (albite) and fine-grained lamellae and clusters of lamellae of chlorite are associated with subordinate calcite and define a weak foliation within the pseudomorphic texture.
- Alteration: chlorite>titanite: strong after biotite; albite: strong after plagioclase; calcite: weak to moderate; pyrite-chalcopyrite: subtle
- Sample 23: A23-01966-23-IG_BH04_MG073—Microgranodiorite/microquartz-monzodiorite—Subhedral and weakly altered plagioclase is intergrown with anhedral quartz, interstitial K-feldspar, and randomly oriented and Fe-chlorite-epidote-altered biotite.
- Alteration: Fe-chlorite-epidote: moderate to strong after biotite; sericite-epidote: weak after plagioclase

- Sample 24: A23-01966-24-IG_BH04_MG074—Chlorite-altered tonalite & Chlorite-retrogressed orthoschist—This heterogeneous section comprises a medium-grained central part, in which subhedral plagioclase crystals and anhedral quartz define a granular texture, and fine-grained upper and lower part, in which granoblastic plagioclase, quartz, and xenoblastic chlorite define a roughly foliated domains.
- Alteration: chlorite-titanite: strong after biotite; white mica: weak to moderate after the plagioclase; calcite: weak; pyrite: subtle
- Sample 25: A23-01966-25-IG_BH04_MG075—Microquartz-diorite & Epidote-chlorite-sericite-altered microgranodiorite/microquartz-monzodiorite—This section comprises two different domains: Domain A, the less altered domain, comprises subhedral and weakly altered plagioclase associated with anhedral quartz and randomly oriented biotite. Domain B is probably generated by the alteration surrounding an irregular epidote veinlet and comprises moderately altered plagioclase, chlorite-altered biotite, and quartz.
- Alteration: Chlorite>titanite: strong after biotite in Domain B; subtle to weak in Domain A; K-feldspar: weak to moderate in Domain B; sericite-epidote: weak after plagioclase in Domain A; moderate to strong in Domain B
- Sample 26: A23-01966-26-IG_BH04_MG076—Epidote-albite-biotite granofels & Biotite schist—Two domains occur in this section. A fine-grained xenoblastic and relatively homogeneous and isotropic aggregate of albite, epidote and biotite (Domain A), and a roughly schistose Domain B comprising clusters of biotite, fine-grained and xenoblastic albite and epidote, and vein-like domains of calcite and subordinate quartz and biotite.
- Sample 27: A23-01966-27-IG_BH04_MG077—Calcite-epidote-biotite schist—Iso-oriented and medium-grained lamellae of biotite, subordinate xenoblasts of calcite, epidote, and fine-grained plagioclase and quartz define a continuous schistosity in this relatively homogeneous section.
- Sample 28: A23-01966-28-IG_BH04_MG078—Meta-tonalite(?)—Inequigranular plagioclase crystals are intergrown with fine-grained and subordinate crystals of quartz, epidote, chlorite, biotite, and titanite. The epidote and chlorite define irregular clusters imparting a subtle anisotropy to the granular texture.
- Alteration/Metamorphism: epidote: moderate; Fe-chlorite: weak to moderate after biotite; white mica: subtle after plagioclase; titanite: subtle
- Sample 29: A23-01966-29-IG_BH04_MG079—Chlorite-sericite-altered microtonalite—Subhedral and anhedral plagioclase prevails over interstitial quartz and K-feldspar, and together with chlorite-rich pseudomorphs after biotite define a relatively homogeneous granular texture.
- Alteration: sericite-epidote: moderate after plagioclase; Fe-chlorite-epidote-titanite: subtle to strong after biotite
- Sample 30: A23-01966-30-IG_BH04_MG080—Fe-chlorite-sericite-altered microgranodiorite—In this section, subhedral plagioclase crystals are intergrown with quartz, interstitial K-feldspar and randomly oriented biotite. The biotite is heterogeneously altered in different parts of the section.

Alteration: sericite-epidote: subtle to moderate after plagioclase; Fe-chlorite-titanite: subtle to strong after biotite

Sample 31: A23-01966-31-IG_BH04_MG081—Tonalite—Subhedral and inequigranular plagioclase crystals, anhedral crystals of quartz, randomly oriented and anhedral biotite and poikilitic K-feldspar define a granular texture.

Alteration: white mica-epidote: weak after plagioclase; epidote: subtle

Sample 32: A23-01966-32-IG_BH04_MG082—Tonalite—Subhedral and inequigranular plagioclase crystals, anhedral crystals of quartz, randomly oriented and anhedral biotite and poikilitic K-feldspar define a granular texture.

Alteration: white mica-epidote: weak after plagioclase; epidote: subtle

Sample 33: A23-01966-33-IG_BH04_MG083—Sericite-altered tonalite—Subhedral and anhedral crystals of plagioclase, anhedral quartz, and subhedral biotite define a granular texture, in which very fine-grained sericite weakly to moderately altered the plagioclase.

Alteration: white mica: weak to moderate after plagioclase; pyrite: subtle; iron oxides: strong after pyrite

Sample 34: A23-01966-34-IG_BH04_MG084—Tonalite—Subhedral and inequigranular plagioclase crystals, anhedral crystals of quartz, randomly oriented and anhedral biotite define a granular texture.

Alteration: white mica-epidote: weak to strong after plagioclase; chlorite: weak after the biotite; epidote>>iron oxides: subtle

Sample 35: A23-01966-35-IG_BH04_MG085—Fe-chlorite-K-feldspar-altered tonalite & Epidote-K-feldspar veinlet—Euhedral and subhedral crystals of plagioclase and quartz define a granular texture associated with randomly oriented pseudomorphs of chlorite after biotite. The concentration of K-feldspar alteration around an irregular epidote-K-feldspar veinlet defines a second compositional sub-domain in the lower part of this granular rock.

Alteration: Fe-chlorite: strong after biotite; K-feldspar: weak to moderate after plagioclase in the lower part; saussurite (epidote+sericite): weak to moderate after the plagioclase in the upper part

Sample 36: A23-01966-36-IG_BH01_LG046—Sericite-altered tonalite—Subhedral plagioclase crystals are immersed within a medium-grained anhedral aggregate of quartz and, together with randomly oriented lamellae of biotite, define a granular texture.

Alteration: white mica>>epidote: weak to moderate after plagioclase

Sample 37: A23-01966-37-IG_BH02_LG027—Chlorite-white mica-altered felsitic rock—Inequigranular and anhedral crystals of quartz, plagioclase, and randomly oriented lamellae of white mica define a granular texture. A quartz-vein crosscut the fragmental texture and is fractured and filled in by chlorite and white mica.

Alteration: chlorite: strong after biotite; white mica: weak; limonite: weak; rutile-pyrite: subtle

- Sample 38: A23-01966-38-IG_BH02_LG028—Chlorite-altered plagioclase-phyric quartz-diorite & K-feldspar-quartz veinlet—Subhedral phenocrysts of plagioclase are randomly oriented within a fine-grained granophyric aggregate of plagioclase and quartz hosting anhedral biotite. A K-feldspar-quartz veinlet crosscut the porphyritic section.
- Alteration: K-feldspar: weak; sericite-earthy and unresolved: weak to moderate after plagioclase; chlorite: moderate to strong after biotite
- Sample 39: A23-01966-39-IG_BH02_LG029—Sericite-epidote-altered plagioclase-phyric microtonalite—Subhedral and anhedral plagioclase phenocrysts are randomly oriented within a fine-grained groundmass of quartz, biotite, and plagioclase. Anhedral crystals of epidote and white mica overprinted the porphyritic texture.
- Alteration: white mica: weak to moderate after plagioclase; subtle to weak after the groundmass; epidote: weak in the groundmass
- Sample 40: A23-01966-40-IG_BH02_LG030—Fe-chlorite-plagioclase-calcite granofels—Inequigranular and xenoblastic crystals of calcite, plagioclase, and irregularly shaped patches of fine-grained Fe-chlorite define a granular, xenoblastic, and relatively homogeneous texture.
- Alteration/Metamorphism: Calcite-plagioclase: strong; chlorite: weak; white mica: weak after plagioclase
- Sample 41: A23-01966-41-IG_BH03_LG023—Epidote-Fe-chlorite-retrogressed schist—This section shows a heterogeneous composition and texture. In the upper part, fine-grained K-feldspar crystals are mixed with fine-grained flakes of chlorite and xenoblastic epidote. In most of the mid to lower part of the section, abundant Fe-chlorite define a rough continuous schistosity, which wraps angular fragments of fine-grained chlorite, epidote, and quartz.
- Alteration/Metamorphism: Fe-chlorite: strong; epidote-K-feldspar: moderate; quartz-calcite-earthy and unresolved: weak
- Sample 42: A23-01966-42-IG_BH04_MG086—White mica-chlorite-retrogressed biotite schist—Lenticular and irregular microlithons of plagioclase, quartz, and biotite are wrapped by cleavage domains of chlorite and subordinate white mica. The chlorite and white mica replaced iso-oriented biotite and all the phyllosilicates define a spaced and rough schistosity.
- Alteration/Metamorphism: chlorite: strong after biotite; white mica: weak; earthy and unresolved: moderate to strong after plagioclase; rutile: subtle
- Sample 43: A23-01966-43-IG_BH04_MG087—Chlorite-calcite-white mica-altered albitite—Anhedral and subhedral plagioclase, subordinate patches of fine-grained Fe-chlorite and interstitial calcite define a granular xenomorphic texture.
- Alteration: white mica: weak after plagioclase; Fe-chlorite-calcite: weak
- Sample 44: A23-01966-44-IG_BH04_MG088—Chlorite-sericite-altered tonalite & Sheared iron oxides-white mica-calcite veins—Subhedral plagioclase crystals are immersed within a medium-grained anhedral aggregate of quartz and, together with randomly oriented

lamellae of biotite, define a granular texture, which is crosscut by 1 mm thick micro-shear zone filled in by iso-oriented flakes of white mica and calcite.

Alteration: white mica>>epidote: weak to moderate after plagioclase; chlorite: moderate to strong after biotite; iron oxides: subtle

Sample 45: A23-01966-45-IG_BH04_MG089—Chlorite-epidote-white mica-altered tonalite—This section comprises inequigranular and anhedral crystals of plagioclase, quartz, biotite, and subordinate K-feldspar. The composition is similar to other tonalitic samples (e.g., Samples 6, 9, 10, 31, 32, and 34). Texturally, this sample show a finer-grained nature, probably due to the post- or late-magmatic re-crystallization of the quartzofeldspathic minerals.

Alteration: white mica-titanite-chlorite-epidote: weak to moderate after plagioclase; chlorite: weak after the biotite; epidote>iron oxides: subtle

Sample 46: A23-01966-46-IG_BH02_LG031—Orthogneiss—This section is compositionally similar to Sample 45. In some domains of this section, the plagioclase and subordinate K-feldspar define porphyroclastic domains immersed within a fine-grained matrix of quartz and the epidote and the white mica, which partially to completely replaced randomly oriented lamellae of biotite, define discontinuous sub-parallel cleavage domains imparting a gneissose texture.

Alteration: white mica-epidote: weak after plagioclase, and weak to strong after biotite

Sample 47: A23-01966-47-IG_BH02_LG032—Chlorite-sericite-altered tonalite & Sheared calcite-K-feldspar-quartz vein(?)—This section comprises 2 domains. Subhedral plagioclase, and anhedral quartz, K-feldspar, and biotite define the granular texture in Domain A. A fine-grained tabular and sheared Domain B is made up of fine-grained quartz, K-feldspar, calcite and white mica crosscut the granular Domain A.

Alteration: sericite-epidote: weak to moderate after the plagioclase; Fe-chlorite>epidote: strong after biotite; pyrite: subtle; iron oxides: strong after pyrite

Sample 48: A23-01966-48-IG_BH02_LG033—Fe-chlorite-calcite-altered tonalite & Plagioclase-phyric andesite(?)—This section comprises two Domains. In the upper part of the section (Domain A), anhedral and subhedral plagioclase and quartz, patches of calcite and pseudomorphs of Fe-chlorite after biotite define a granular texture. In the lower part (Domain B), anhedral and subhedral phenocrysts of plagioclase are immersed within a very fine-grained groundmass of plagioclase and subordinate quartz.

Alteration: white mica-epidote: weak after plagioclase; Fe-chlorite: strong after biotite; calcite: weak in Domain A

Sample 49: A23-01966-49-IG_BH02_LG034—Brecciated chlorite-sericite-altered tonalite—Subhedral plagioclase, and anhedral quartz, K-feldspar, and biotite define the granular texture, which is crosscut by intersecting fractures filled in by white mica, chlorite and limonitic material.

Alteration: sericite: moderate after the plagioclase; Fe-chlorite: strong after biotite; pyrite: subtle; iron oxides: weak after pyrite

Sample 50: A23-01966-50-IG_BH01_LG047—Chlorite-white mica-altered tonalite & White mica-orthoschist—Most of this section comprises anhedral crystals of plagioclase, anhedral quartz, and randomly oriented biotite (Domain A). These minerals define a relatively homogeneous and isotropic granular texture. In the upper part of the section (Domain B), porphyroclasts of plagioclase and K-feldspar are immersed within a schistose matrix of fine-grained plagioclase and white mica.

Alteration: white mica: weak after plagioclase in Domain A; weak to moderate after biotite in Domain A; chlorite: weak to strong after biotite in Domain A; iron oxides: strong after unknown mineral

Sample 51: A23-01966-51-IG_BH01_LG048—White mica-altered tonalite & White mica-quartz schist—Anhedral and white mica-altered plagioclase crystals are associated with anhedral quartz and randomly oriented biotite and define a relatively homogeneous and isotropic granular texture. In the lower left part of the section, a sheared domain comprises cleavage domains of white mica, lenticular microlithons of quartz, and subordinate fine-grained plagioclase.

Alteration: white mica: moderate after plagioclase; weak after biotite; titanite: subtle after biotite

Table 1: List of samples with their magnetic susceptibility and petrographic classification following the recommendations of Gillespie et al. (2011), Gillespie and Styles (1999), and Robertson (1999).

Sample No.	Sample ID	Magnetic Susceptibility	Rock Type	Alteration/Metamorphism
01	A23-01966-1- IG_BH04_MG051	0.07	White mica-altered tonalite & Felsitic rock & Quartz vein & K-feldspar veinlets	white mica: moderate after plagioclase in Domain A; epidote: weak around the quartz vein; chlorite-white mica: weak after biotite; pyrite: subtle in Domain B
02	A23-01966-2- IG_BH04_MG052	0.079	White mica-epidote-altered tonalite & Biotite schist & Calcite veinlets	white mica-epidote: weak after plagioclase in Domain B; epidote: weak to strong after biotite in Domain B; pyrite: subtle; iron oxides: subtle after pyrite
03	A23-01966-3- IG_BH04_MG053	0.121	Biotite schist	epidote-chlorite: weak after biotite
04	A23-01966-4- IG_BH04_MG054	0.125	Quartz-biotite-albite granofels	
05	A23-01966-5- IG_BH04_MG055	0.004	Calcite crystal & Chlorite-schist	
06	A23-01966-6- IG_BH04_MG056	0.111	Tonalite	white mica-epidote: weak after plagioclase; iron oxides: subtle
07	A23-01966-7- IG_BH04_MG057	0.066	Tonalite & Orthogneiss	white mica-epidote(?): subtle after plagioclase in Domain A; epidote: weak in Domain B
08	A23-01966-8- IG_BH04_MG058	0.056	Tonalite & K-feldspar-biotite-quartz schist & Orthogneiss	epidote-white mica: subtle to weak after plagioclase; epidote-white mica: weak in Domain C; carbonate: subtle in Domain C
09	A23-01966-9- IG_BH04_MG059	0.091	Tonalite	white mica-epidote: weak after plagioclase; epidote: subtle
10	A23-01966-10- IG_BH04_MG060	0.081	Tonalite	white mica-epidote: weak after plagioclase; epidote: subtle
11	A23-01966-11- IG_BH04_MG061	0.106	Tonalite & Microtonalite(?) & Epidote-biotite-quartz-white mica sheared domain	white mica-epidote(?): subtle after plagioclase; moderate to strong in the 1.5 mm thick shear domain

Sample No.	Sample ID	Magnetic Susceptibility	Rock Type	Alteration/Metamorphism
12	A23-01966-12- IG_BH04_MG062	0.061	Microquartz-diorite & Epidote-Fe-chlorite-altered microgranodiorite/microquartz-monzodiorite	Fe-chlorite: moderate to strong after biotite in Domain B; epidote: weak after biotite in Domain B; sericite-epidote: moderate after plagioclase in Domain B; epidote: subtle after plagioclase in Domain A; chalcopyrite: subtle in Domain B
13	A23-01966-13- IG_BH04_MG063	0.052	Chlorite-altered microquartz-diorite & Epidote-chlorite-sericite-altered microgranodiorite/microquartz-monzodiorite	Fe-chlorite: moderate to strong after biotite in Domain B; epidote: weak after biotite in Domain B; sericite-epidote-K-feldspar: moderate after plagioclase in Domain B; epidote: subtle after plagioclase in Domain A; chalcopyrite: subtle in Domain B
14	A23-01966-14- IG_BH04_MG064	0.128	Microquartz-diorite & Microgranodiorite/microquartz-monzodiorite & Tonalite	epidote: weak after biotite; sericite-epidote: subtle after plagioclase; epidote: subtle
15	A23-01966-15- IG_BH04_MG065	0.161	Albite-epidote-actinolite-chlorite granofels & Chlorite schist & Quartz vein	
16	A23-01966-16- IG_BH04_MG066	0.086	Pyrite-calcite-chlorite-retrometamorphosed actinolite schist	chlorite: moderate to strong after biotite; calcite: moderate; pyrite: subtle
17	A23-01966-17- IG_BH04_MG067	0.133	Chlorite-retrometamorphosed biotite schist	chlorite: moderate to strong after biotite; calcite: moderate; chalcopyrite: subtle
18	A23-01966-18- IG_BH04_MG068	0.134	Microtonalite & Epidote-Fe-chlorite-sericite microgranodiorite/microquartz-monzodiorite & K-feldspar veinlet	sericite-epidote: subtle after plagioclase in Domain A; moderate after plagioclase in Domain B; Fe-chlorite-epidote-titanite: strong after biotite in Domain B.
19	A23-01966-19- IG_BH04_MG069	0.026	Chlorite-Sericite-altered microtonalite & Quartz vein	white mica: weak to moderate after plagioclase; chlorite>titanite: moderate to strong after biotite

Sample No.	Sample ID	Magnetic Susceptibility	Rock Type	Alteration/Metamorphism
20	A23-01966-20- IG_BH04_MG070	0.186	White mica-chlorite-altered microdiorite(?) & Chlorite-K-feldspar-altered schist	chlorite: strong after biotite; K-feldspar: weak in the schist calcite: weak to moderate; white mica: moderate after plagioclase, weak in the schist
21	A23-01966-21- IG_BH04_MG071	0.14	Chlorite-altered microtonalite & Chlorite-retrometamorphosed biotite schist	white mica: moderate after plagioclase; chlorite>titanite: moderate to strong after biotite; calcite-epidote: subtle to weak in Domain A and after the plagioclase
22	A23-01966-22- IG_BH04_MG072	0.164	Calcite-Fe-chlorite-albite-altered foliated microdiorite	chlorite>titanite: strong after biotite; albite: strong after plagioclase; calcite: weak to moderate; pyrite-chalcopyrite: subtle
23	A23-01966-23- IG_BH04_MG073	0.028	Microgranodiorite/microquartz-monzodiorite	Fe-chlorite-epidote: moderate to strong after biotite; sericite-epidote: weak after plagioclase
24	A23-01966-24- IG_BH04_MG074	0.067	Chlorite-altered tonalite & Chlorite-retrogressed orthoschist	chlorite-titanite: strong after biotite; white mica: weak to moderate after the plagioclase; calcite: weak; pyrite: subtle
25	A23-01966-25- IG_BH04_MG075	0.058	Microquartz-diorite & Epidote-chlorite-sericite-altered microgranodiorite/microquartz-monzodiorite	chlorite>titanite: strong after biotite in Domain B; subtle to weak in Domain A; K-feldspar: weak to moderate in Domain B; sericite-epidote: weak after plagioclase in Domain A; moderate to strong in Domain B
26	A23-01966-26- IG_BH04_MG076	0.099	Epidote-albite-biotite granofels & Biotite schist	
27	A23-01966-27- IG_BH04_MG077	0.158	Calcite-epidote-biotite schist	
28	A23-01966-28- IG_BH04_MG078	0.025	Meta-tonalite(?)	epidote: moderate; Fe-chlorite: weak to moderate after biotite; white mica: subtle after plagioclase; titanite: subtle

Sample No.	Sample ID	Magnetic Susceptibility	Rock Type	Alteration/Metamorphism
29	A23-01966-29- IG_BH04_MG079	0.048	Chlorite-sericite-altered microtonalite	sericite-epidote: moderate after plagioclase; Fe-chlorite-epidote-titanite: subtle to strong after biotite
30	A23-01966-30- IG_BH04_MG080	0.035	Fe-chlorite-sericite-altered microgranodiorite	sericite-epidote: subtle to moderate after plagioclase; Fe-chlorite-titanite: subtle to strong after biotite
31	A23-01966-31- IG_BH04_MG081	0.039	Tonalite	white mica-epidote: weak after plagioclase; epidote: subtle
32	A23-01966-32- IG_BH04_MG082	0.07	Tonalite	white mica-epidote: weak after plagioclase; epidote: subtle
33	A23-01966-33- IG_BH04_MG083	0.025	Sericite-altered tonalite	white mica: weak to moderate after plagioclase; pyrite: subtle; iron oxides: strong after pyrite
34	A23-01966-34- IG_BH04_MG084	0.296	Tonalite	white mica-epidote: weak to strong after plagioclase; chlorite: weak after the biotite; epidote>>iron oxides: subtle
35	A23-01966-35- IG_BH04_MG085	0.056	Fe-chlorite-K-feldspar-altered tonalite & Epidote-K-feldspar veinlet	Fe-chlorite: strong after biotite; K-feldspar: weak to moderate after plagioclase in the lower part; saussurite (epidote+sericite): weak to moderate after the plagioclase in the upper part
36	A23-01966-36- IG_BH01_LG046	0.04	Sericite-altered tonalite	white mica>>epidote: weak to moderate after plagioclase
37	A23-01966-37- IG_BH02_LG027	0.015	Chlorite-white mica-altered felsitic rock	chlorite: strong after biotite; white mica: weak; limonite: weak; rutile-pyrite: subtle
38	A23-01966-38- IG_BH02_LG028	0.059	Chlorite-altered plagioclase-phyrlic quartz-diorite & K-feldspar-quartz veinlet	K-feldspar: weak; sericite-earthy and unresolved: weak to moderate after plagioclase; chlorite: moderate to strong after biotite

Sample No.	Sample ID	Magnetic Susceptibility	Rock Type	Alteration/Metamorphism
39	A23-01966-39- IG_BH02_LG029	0.057	Sericite-epidote-altered plagioclase-phyric microtonalite	white mica: weak to moderate after plagioclase; subtle to weak after the groundmass; epidote: weak in the groundmass
40	A23-01966-40- IG_BH02_LG030	0.041	Fe-chlorite-plagioclase-calcite granofels	calcite-plagioclase: strong; chlorite: weak; white mica: weak after plagioclase
41	A23-01966-41- IG_BH03_LG023	0.09	Epidote-Fe-chlorite-retrogressed schist	Fe-chlorite: strong; epidote-K-feldspar: moderate; quartz-calcite-earthy and unresolved: weak
42	A23-01966-42- IG_BH04_MG086	0.033	White mica-chlorite-retrogressed biotite schist	chlorite: strong after biotite; white mica: weak; earthy and unresolved: moderate to strong after plagioclase; rutile: subtle
43	A23-01966-43- IG_BH04_MG087	0.028	Chlorite-calcite-white mica-altered albitite	white mica: weak after plagioclase; Fe-chlorite-calcite: weak
44	A23-01966-44- IG_BH04_MG088	0.025	Chlorite-sericite-altered tonalite & Sheared iron oxides-white mica-calcite veins	white mica>>epidote: weak to moderate after plagioclase; chlorite: moderate to strong after biotite; iron oxides: subtle
45	A23-01966-45- IG_BH04_MG089	0.05	Chlorite-epidote-white mica-altered tonalite	white mica-titanite-chlorite-epidote: weak to moderate after plagioclase; chlorite: weak after the biotite; epidote>iron oxides: subtle
46	A23-01966-46- IG_BH02_LG031	0.032	Orthogneiss	white mica-epidote: weak after plagioclase, and weak to strong after biotite
47	A23-01966-47- IG_BH02_LG032	0.043	Chlorite-sericite-altered tonalite & Sheared calcite-K-feldspar-quartz vein(?)	sericite-epidote: weak to moderate after the plagioclase; Fe-chlorite>epidote: strong after biotite; pyrite: subtle; iron oxides: strong after pyrite

Sample No.	Sample ID	Magnetic Susceptibility	Rock Type	Alteration/Metamorphism
48	A23-01966-48- IG_BH02_LG033	0.025	Fe-chlorite-calcite-altered tonalite & Plagioclase-phyric andesite(?)	white mica-epidote: weak after plagioclase; Fe-chlorite: strong after biotite; calcite: weak in Domain A
49	A23-01966-49- IG_BH02_LG034	0.023	Brecciated chlorite-sericite-altered tonalite	sericite: moderate after the plagioclase; Fe-chlorite: strong after biotite; pyrite: subtle; iron oxides: weak after pyrite
50	A23-01966-50- IG_BH01_LG047	0.061	Chlorite-white mica-altered tonalite & White mica-orthoschist	white mica: weak after plagioclase in Domain A; weak to moderate after biotite in Domain A; chlorite: weak to strong after biotite in Domain A; iron oxides: strong after unknown mineral
51	A23-01966-51- IG_BH01_LG048	0.028	White mica-altered tonalite & White mica-quartz schist	white mica: moderate after plagioclase; weak after biotite; titanite: subtle after biotite

3. Petrographic Descriptions

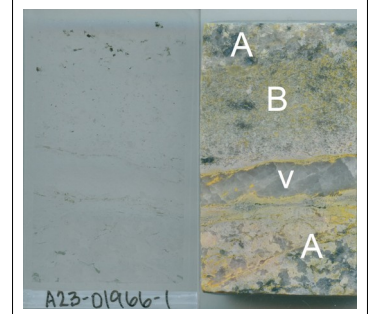
Sample 1: A23-01966-1-IG_BH04_MG051

White mica-altered tonalite

Felsitic rock

Quartz vein

K-feldspar veinlets



Anhedral and subhedral plagioclase, anhedral quartz, poikilitic K-feldspar, and randomly oriented biotite define a granular texture occurring in the upper and lower part of the section (Domains A). The granular domain is associated and probably transitioning to a fine-grained inequigranular and felsitic Domain B consisting of quartz and plagioclase. An up to 5.5 mm thick quartz vein crosscut the fine-grained felsitic domain and K-feldspar-rich veinlets reactivated the vein walls and crosscut the granular and fine-grained felsitic host domains.

Alteration: **white mica:** moderate after plagioclase in Domain A; **epidote:** weak around the quartz vein; **chlorite-white mica:** weak after biotite; **pyrite:** subtle in Domain B

Mineral	Alteration/Weathering Mineral	Modal %	Size Range (mm)
Domain A: tonalite (38% of PTS)			
plagioclase	white mica	34- 35	up to 2.5 long
quartz		18- 19	up to 2 long
K-feldspar			up to 6 long
biotite	chlorite±white mica	5- 6	up to 1.2 long
zircon		tr	up to 0.05
Domain B: fine-grained felsitic (~45% of PTS)			
quartz		22- 23	up to 0.5
plagioclase		20- 21	up to 0.7
	white mica	1- 2	up to 0.2
	epidote	tr	up to 0.1
	pyrite	tr	up to 0.03

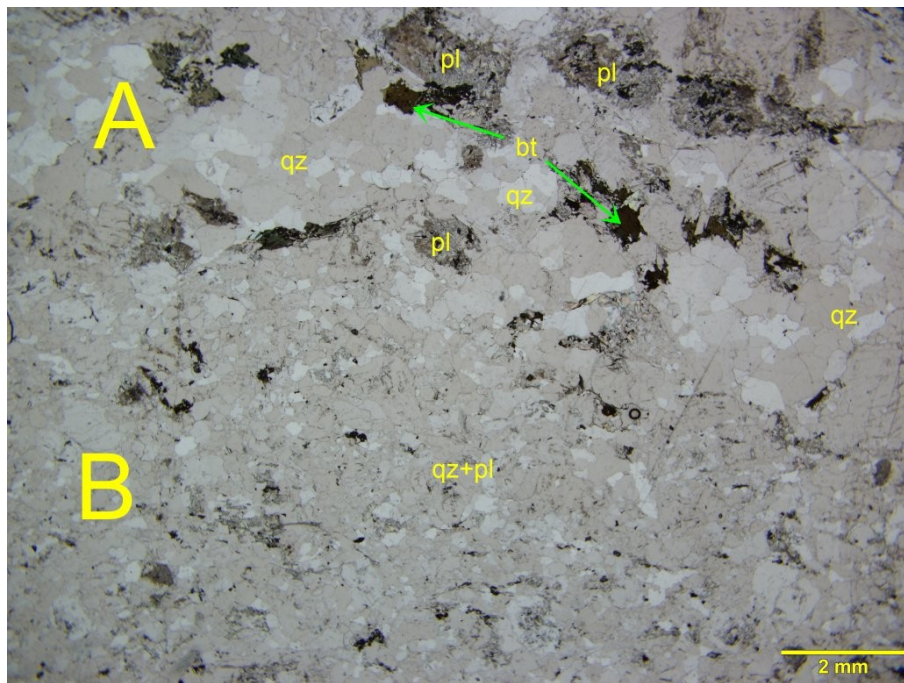
Mineral	Alteration/Weathering Mineral	Modal %	Size Range (mm)
quartz vein (~15% of PTS)			
quartz		15	up to 7.5 long
calcite		tr	up to 0.2 long
K-feldspar veinlets (~2% of PTS)			
K-feldspar		2	up to 0.2

Plagioclase forms anhedral and subhedral crystals (up to 2.5 mm long) immersed within the medium-grained anhedral quartz in the medium-grained tonalite. Fine-grained flakes of white mica weakly to moderately altered the plagioclase in Domain A. In Domain B, the plagioclase and quartz dominate the composition and define a fine-grained interlobate texture that I tentatively interpret as a leucocratic differentiate from the tonalitic rock. This domain shows sharp and transitional boundaries with Domain A (Photomicrograph 1a) and is crosscut by the 5.5 mm thick quartz vein. Around the vein, irregular selvages(?) of very fine-grained quartz, plagioclase, and sparse patches of epidote (see Photomicrographs 1d and 1e) are reactivated by irregular veinlets of K-feldspar.

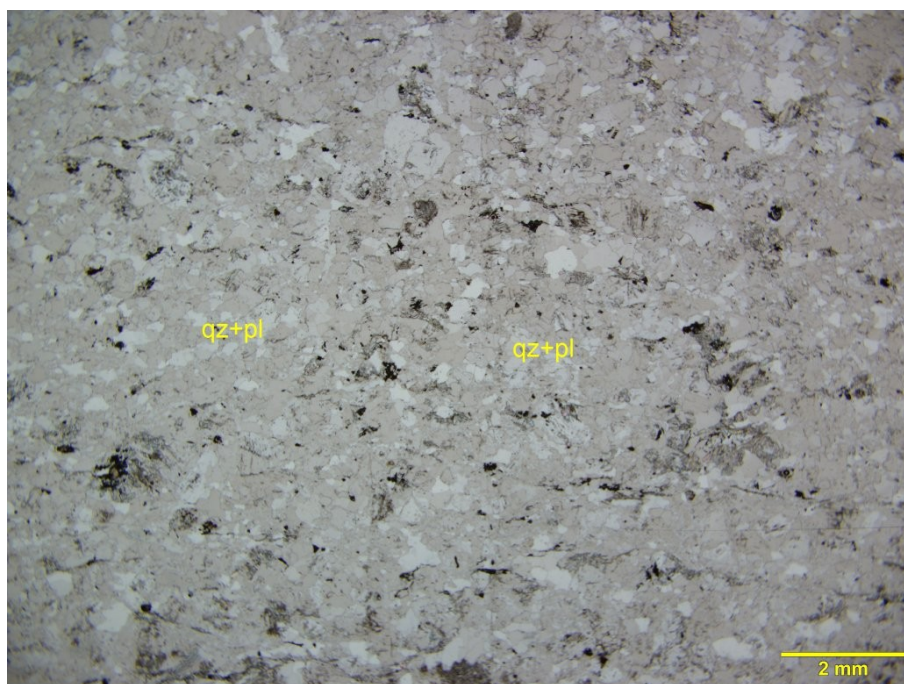
Quartz forms fine- to medium-grained monomineralic aggregates in Domain A. In Domain B, the quartz is fine-grained anhedral, and it is finely intergrown with the plagioclase. In the vein, the quartz crystals are up to 7.5 mm long, show interlobate crystal boundaries, and display a strong undulose extinction. Calcite veinlets crosscut the quartz vein; however, they do not continue in the selvages or host rock (Photomicrograph 1e).

K-feldspar occurs within the coarse-grained granular texture as poikilitic crystals (up to 6 mm long) enclosing subhedral plagioclase crystals. This texture is a recurrent feature of the tonalite described in this report. K-feldspar filled in irregular veinlets reactivating the quartz vein-walls and crosscutting Domain A and B at low angle with respect to the sub-parallel boundaries (see image of the stained offcut above). The K-feldspar veinlets are distinguished by their yellow staining colour.

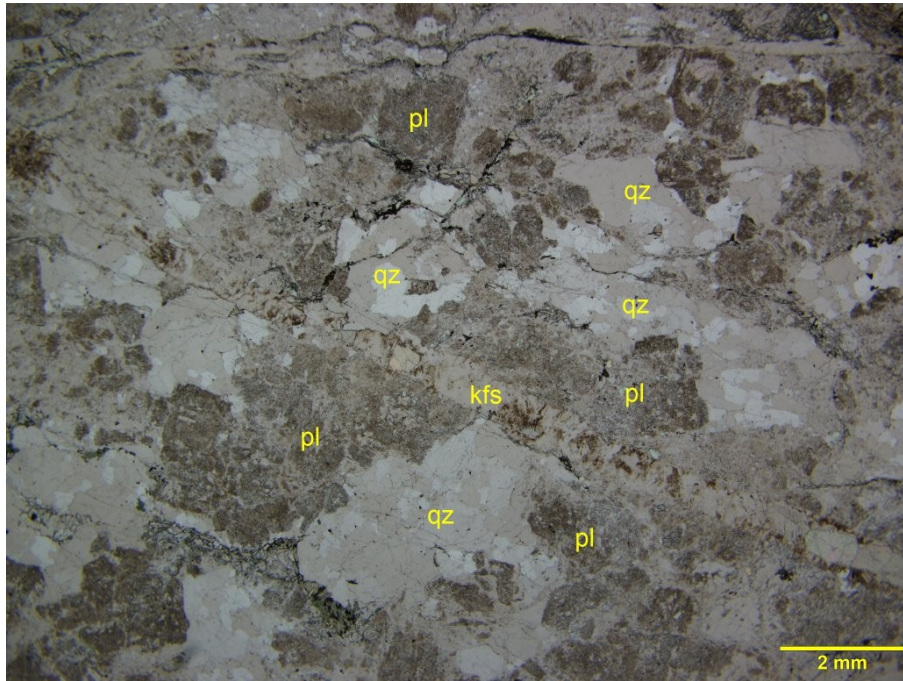
Biotite is fine- to medium-grained and occurs as randomly oriented lamellae in Domain A. The biotite is distinguished by its strong brown pleochroism. Chlorite and white mica weakly altered some biotite crystals.



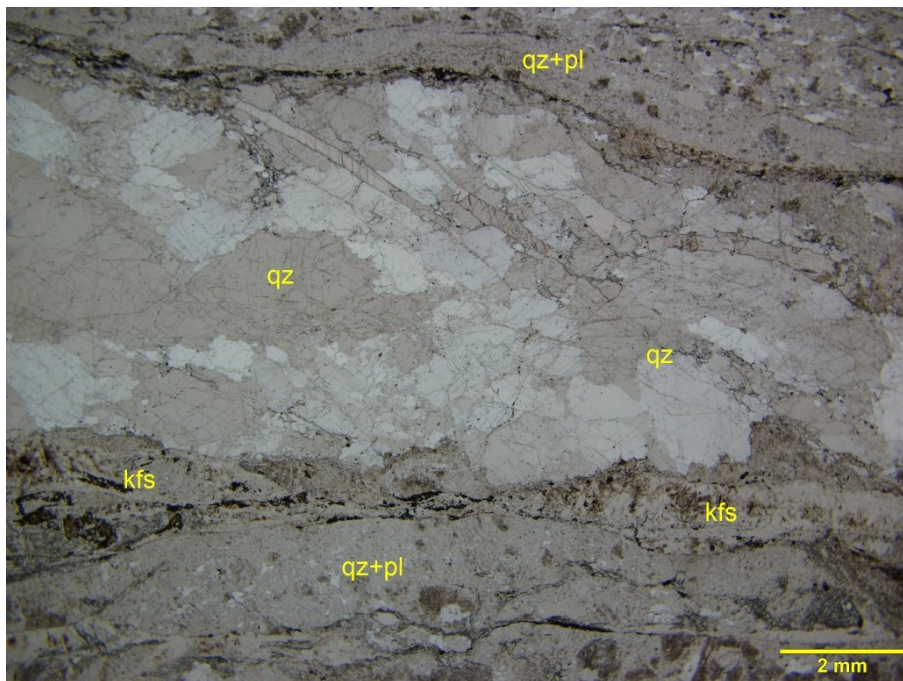
Photomicrograph 1a: The boundary between the granular domain A (A) and Domain B (B) is apparently transitional and suggests a genetic relation between the two. Plane-polarized transmitted light.



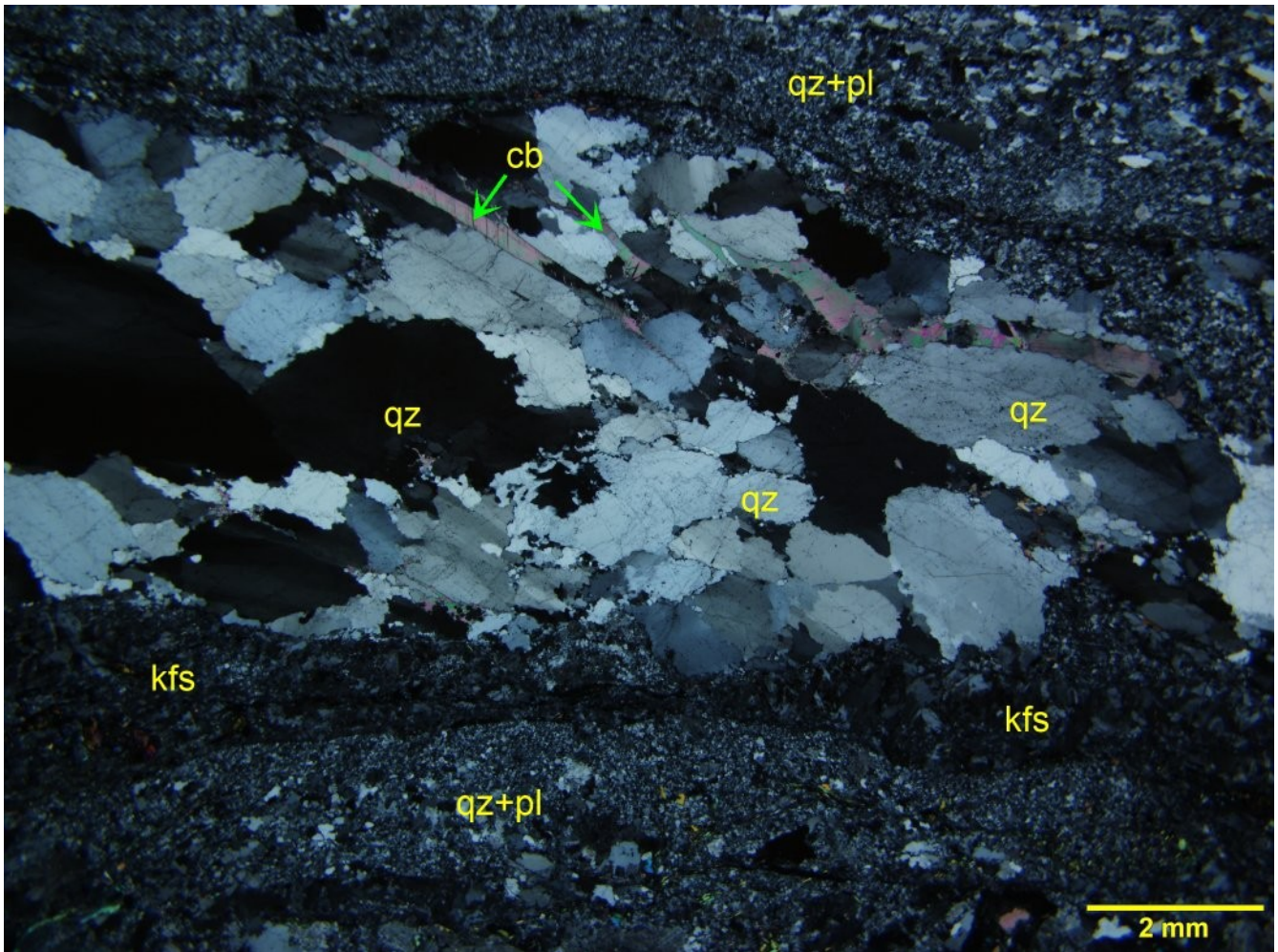
Photomicrograph 1b: Domain B is dominated by fine-grained quartz and plagioclase (qz+pl). Plane-polarized transmitted light.



Photomicrograph 1c: Domain A—Moderately altered plagioclase (pl) and quartz (qz) define a granular texture, which is crosscut by a K-feldspar veinlet (kfs). Plane-polarized transmitted light.



Photomicrograph 1d: The quartz vein (qz) is surrounded by thin domains (selvages?) of quartz and plagioclase (qz+pl), which are reactivated by K-feldspar veinlets (kfs). Plane-polarized transmitted light.



Photomicrograph 1e: Same area as shown in Photomicrograph 1d. Under Crossed polarizers transmitted light, the very fine-nature of the quartz and plagioclase selvages, the fine-grained nature of the K-feldspar veinlets (kfs), and the coarse-grained and deformed quartz in the vein are shown.

Sample 2: A23-01966-2-IG_BH04_MG052

White mica-epidote-altered tonalite

Biotite schist

Calcite veinlets



This section comprises two compositionally and texturally different domains. In Domain A, subhedral and inequigranular plagioclase crystals prevail over anhedral crystals of quartz, randomly oriented and anhedral biotite and sparse epidote alteromorphs after biotite defines a granular texture. In Domain B, fine-grained biotite is iso-oriented and defines a continuous schistosity. Subordinate quartz and epidote define a granolepidoblastic texture.

Alteration: white mica-epidote: weak after plagioclase in Domain B; **epidote:** weak to strong after biotite in Domain B; **pyrite:** subtle; **iron oxides:** subtle after pyrite

Mineral	Alteration/Weathering Mineral	Modal %	Size Range (mm)
Domain A: biotite schist (~40% of PTS)			
biotite		24- 25	up to 0.5 long
quartz		10- 11	up to 0.2
epidote		5- 7	up to 0.05
calcite-rich veinlets			
calcite	calcite	1	up to 1 long
pyrite→iron oxides	pyrite→iron oxides	tr	up to 1 long
Domain B: tonalite (60% of PTS)			
plagioclase	white mica-titanite-epidote	34- 35	up to 2.5 long
quartz		18- 19	up to 2, rare up to 4 long
biotite	epidote	5- 6	up to 2 long
[?]	epidote	2.5- 3	up to 0.4
zircon		tr	up to 0.05
	pyrite→iron oxides	tr	0.01

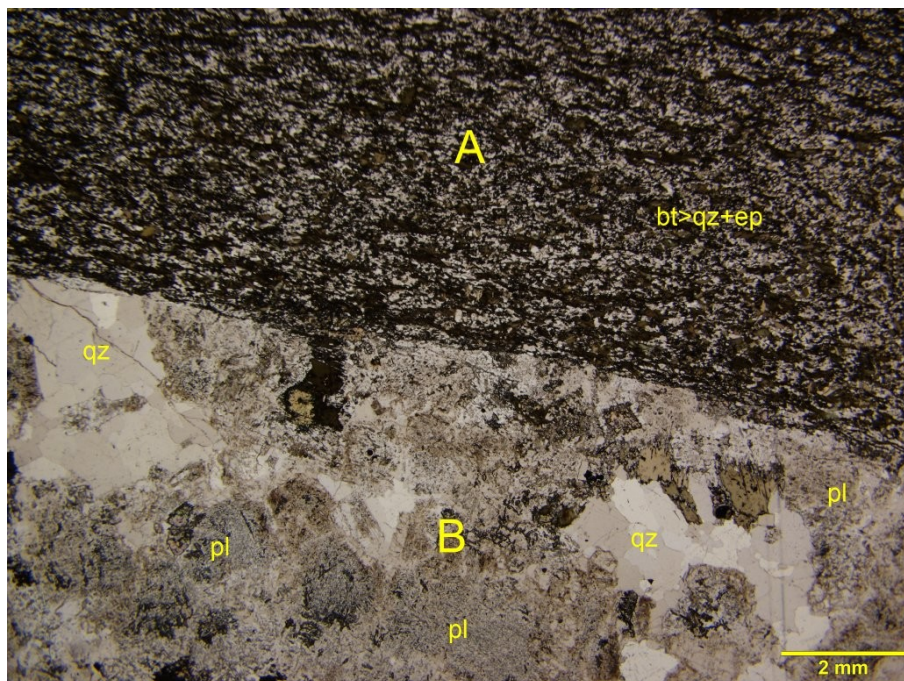
Plagioclase forms subhedral crystals ranging from 0.3 mm to 2.5 mm across and imparting a granular texture to Domain B (Photomicrograph 2a and 2b). Fine-grained flakes of **white mica** and subordinate

epidote moderately altered the plagioclase crystals, which under plane-polarized transmitted light are easily distinguished from the inclusion-free quartz (Photomicrographs 2a and 2b).

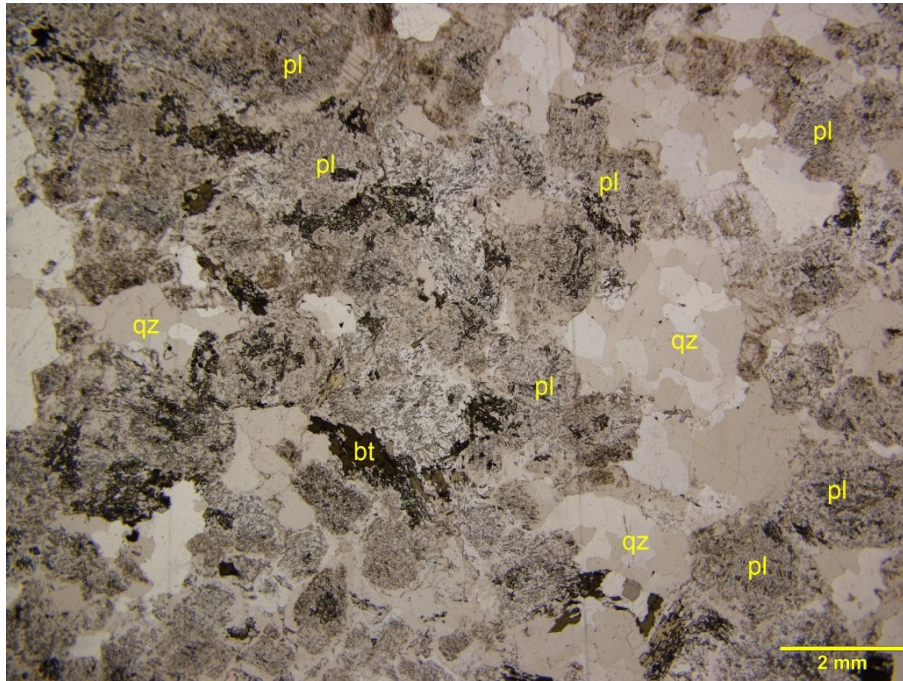
Quartz forms monomineralic and irregularly shaped aggregates in Domain B (Photomicrographs 2a and 2b) and is fine-grained and subordinate to the biotite in the schistose Domain A (Photomicrographs 2a and 2c). In Domain A, the blocky and anhedral quartz crystals range from 0.2 mm to 4 mm long and, in some cases, may be derived from the re-crystallization of quartz phenocrysts.

Biotite is dispersed as randomly oriented anhedral lamellae in the Domain B. In this magmatic domain, Biotite or another ferromagnesian mineral are partially to completely replaced by fine-grained **epidote** and hosts abundant very fine-grained zircon crystals. Within Domain A, the biotite is fine-grained (up to 0.5 mm long) and its iso-orientation defines a continuous schistosity (Photomicrograph 2a and 2c). In this domain, the biotite is associated with fine-grained blocky crystals of quartz and homogeneously dispersed and fine-grained epidote crystals. Irregular carbonate-rich veinlets crosscut the schistosity at low angles (Photomicrograph 2c).

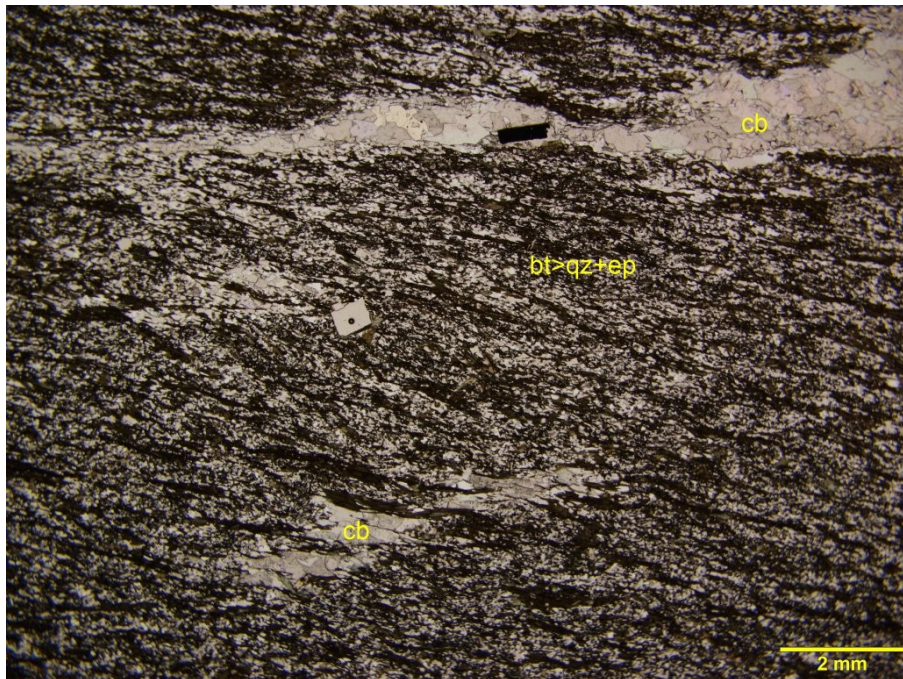
Pyrite is very rare and is dispersed as subhedral crystals within the quartz in Domain B and within the carbonate-rich veinlets in Domain A. Iron oxides subtly altered the pyrite.



Photomicrograph 2a: Domain A (A) and Domain B (B) display a sharp boundary sub-parallel to the schistosity defined by the biotite in Domain A. Plane-polarized transmitted light.



Photomicrograph 2b: Domain B—Weakly to moderately altered plagioclase (pl) quartz (qz) and randomly oriented biotite define a granular texture. Plane-polarized transmitted light.



Photomicrograph 2c: Domain A—Biotite prevails over fine-grained quartz and epidote (bt>qz+ep) and defines a continuous schistosity crosscut by calcite-rich veinlets (cb). Plane-polarized transmitted light.

Sample 3: A23-01966-3-IG_BH04_MG053



Biotite schist

Irregularly shaped and lenticular microlithons of calcite, calcite and quartz, and quartz are wrapped by a continuous and disharmonically folded schistosity defined by biotite, and subordinate quartz, plagioclase, and epidote.

Alteration/metamorphism: epidote-chlorite: weak after biotite

Mineral	Alteration/Metamorphic Mineral	Modal %	Size Range (mm)
biotite	chlorite	60- 62	up to 0.5 long
calcite		15- 20	up to 1 in the microlithons
quartz		15- 20	up to 0.2, up to 1.2 long in the microlithons
epidote	epidote	4- 5	up to 0.15
plagioclase(?)		2- 4	up to 0.2
	magnetite	tr	up to 0.1

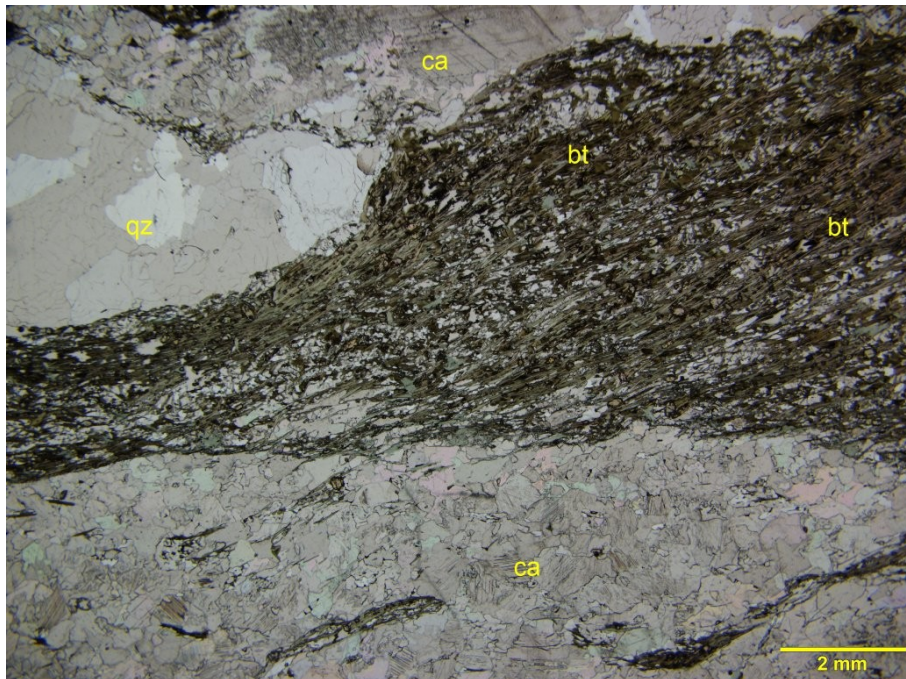
Biotite prevails over the fine-grained xenoblastic crystals of quartz, plagioclase, and epidote in the schistose portion of this section. The schistosity is continuous and it is disharmonically folded within the biotite-rich layers (Photomicrograph 3a). The biotite is partially overprinted by fine-grained epidote and epitaxial chlorite. Very fine-grained crystals of zircon are disseminated within the biotite lamellae.

Calcite forms fine- to medium-grained (up to 1 mm long) interlobate crystals concentrated within irregular and lenticular microlithons (Photomicrographs 3b and 3c), which are wrapped by the schistosity. The calcite is distinguished by its high relief, extreme birefringence, and by its brisk reaction to cold dilute (10%) HCl.

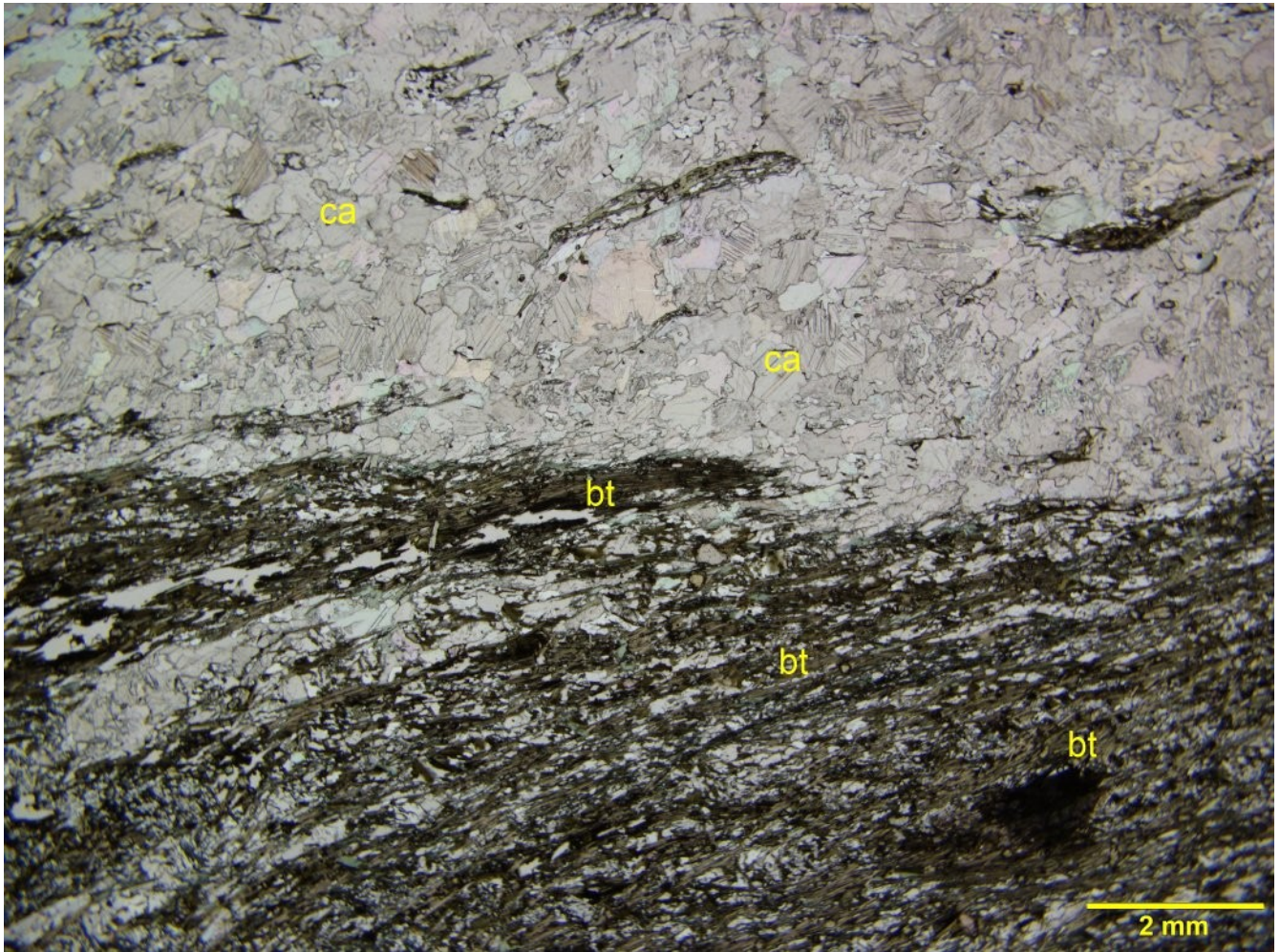
Quartz is fine-grained and it is relatively homogeneously dispersed within the biotite-rich domains. In these domains, the quartz is associated with fine-grained crystals of epidote, and plagioclase; however, the plagioclase was not positively distinguished and its occurrence is tentatively interpreted because of the occurrence of crystals with low relief and lower birefringence than the quartz.



Photomicrograph 3a: The biotite define a continuous and disharmonically folded schistosity and is associated with fine-grained quartz, epidote, and plagioclase. Plane-polarized transmitted light.



Photomicrograph 3b: The biotite-rich schistose domains (bt) wrap calcite (ca) and quartz (qz) microlithons. Plane-polarized transmitted light.



Photomicrograph 3c: Within the calcite-rich microlithons, some rafts of biotite-rich cleavage domains are immersed. Plane-polarized transmitted light.

Sample 4: A23-01966-4-IG_BH04_MG054



Quartz-biotite-albite granofels

Fine- to medium-grained poikiloblastic albite, randomly oriented biotite, and subordinate quartz and calcite define a xenoblastic granular texture.

Mineral	Alteration/Metamorphic Mineral	Modal %	Size Range (mm)
	plagioclase (albite)	45- 47	up to 0.4
	biotite	40- 42	0.02 to 0.6 long
	epidote	8- 10	up to 0.1
	quartz	2- 4	up to 0.2
	calcite	2- 3	up to 0.6
	titanite	tr	up to 0.2
	pyrite→iron oxides	tr	up to 0.1

Plagioclase (albite) forms xenoblastic and poikiloblastic crystals (up to 0.4 mm across) hosting fine grained crystals of epidote and biotite. In very rare instances, the plagioclase show albite twinnings. The plagioclase’s refractive indexes are lower than those of the quartz, thus indicating that the plagioclase is **albite**.

Biotite occurs as inequigranular (0.02 to 0.6 mm long) and xenoblastic flakes and lamellae, which are randomly oriented and intergrown with the more abundant plagioclase and the subordinate quartz. Most biotite is homogeneously dispersed. In some cases (see Photomicrograph 4a), irregular clusters of medium-grained crystals occur.

Quartz forms sparse and xenoblastic crystals up to 0.2 mm across. Most crystals are inclusion-free. In some crystals small inclusions of epidote may occur.

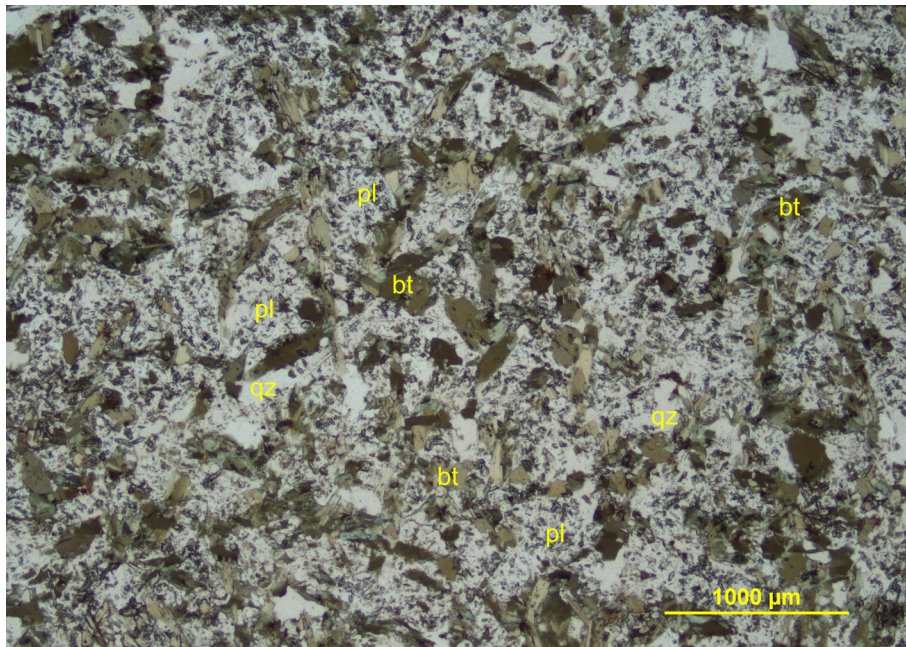
Calcite forms xenoblastic crystals up to 0.6 mm across. The calcite shows high relief and extreme birefringence under the microscope and briskly reacts to cold dilute (10%) HCl.

Titanite is rare and forms fine-grained xenoblastic crystals disseminated within the granofels.

Very rare crystals of **pyrite** (up to 0.1 mm across) are partially replaced by a thin rim of **iron oxides**.



Photomicrograph 4a: Clusters of medium-grained and randomly oriented biotite are dispersed within the granular texture. Plane-polarized transmitted light.



Photomicrograph 4b: Poikiloblastic albite (pl), randomly oriented biotite (bt) and subordinate quartz (qz) define a granofelsic texture. Plane-polarized transmitted light.

Sample 5: A23-01966-5-IG_BH04_MG055

Calcite crystal

Chlorite-schist



This section comprises a single crystal of calcite (~15mm by 29 mm) and a small portion of biotite schist.

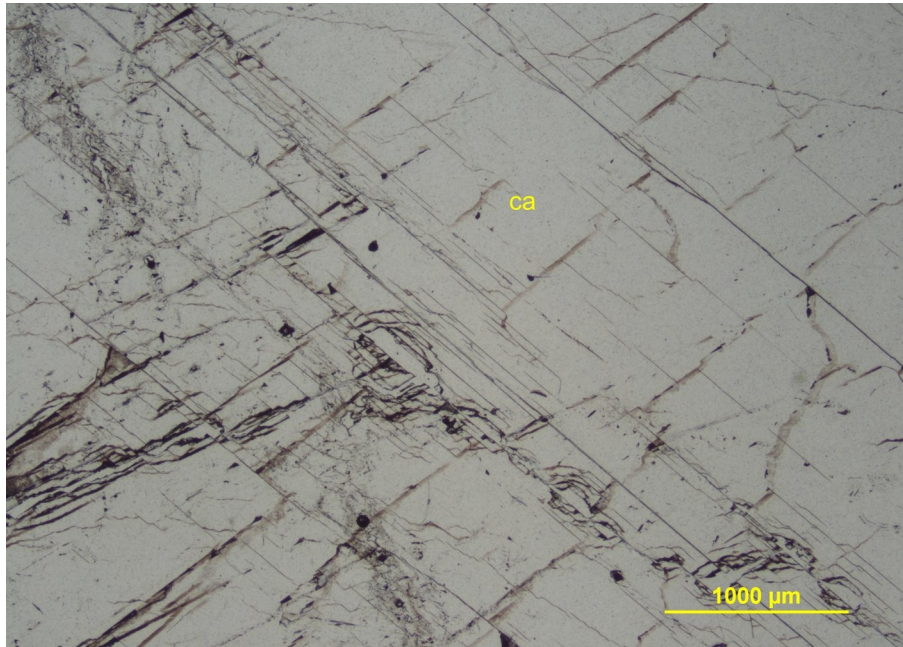
Mineral	Alteration/Metamorphic Mineral	Modal %	Size Range (mm)
calcite		97- 98	~15mm by 29 mm
	chlorite	2- 3	up to 0.2 long
	quartz	tr	0.05
	pyrite	tr	up to 0.5

Calcite occurs as a single crystal (~15mm by 29 mm). The nature of calcite is determined by its high relief, extreme birefringence and two cleavages oriented at ~120°. The calcite crystal is fresh (Photomicrograph 5a) and near the contact with the schist encloses clusters of biotite and quartz (Photomicrograph 5b).

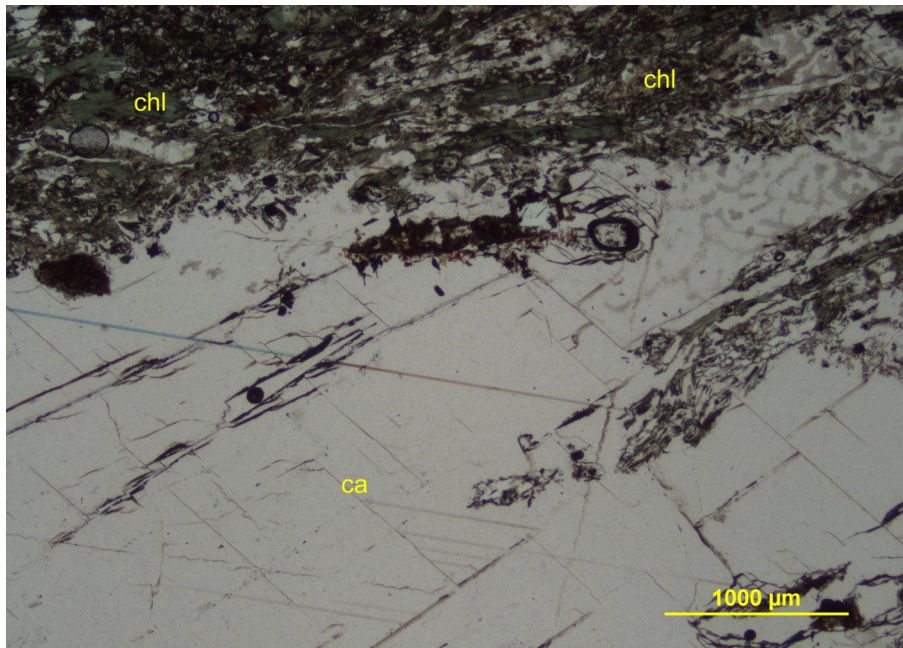
Chlorite is concentrated along the edge of the calcite crystal (Photomicrograph 5b). The rock fragment is 2 mm by 10 mm. From this small fragment, I interpret the rock as a chlorite-schist.

Quartz is subordinate to the chlorite within the rock fragment and the included fragments of schist within the calcite (Photomicrograph 5b).

Pyrite occurs as xenoblastic inclusions within the calcite (up to 0.5 mm across), and occurs as very fine-grained dispersions within the fragments of schist within the calcite.



Photomicrograph 5a: The calcite crystal (ca) is fresh and shows the typical cleavage systems. Plane-polarized transmitted light.



Photomicrograph 5b: The calcite is in contact with a chlorite-rich domain (chl) and encloses fragments of chlorite and quartz-bearing rock. Plane-polarized transmitted light.

Sample 6: A23-01966-6-IG_BH04_MG056

Tonalite

Subhedral and inequigranular plagioclase crystals prevail over anhedral crystals of quartz, randomly oriented and anhedral biotite and sparse crystals of anhedral K-feldspar, all of which define a granular texture.



Alteration: white mica-epidote: weak after plagioclase; **iron oxides:** subtle

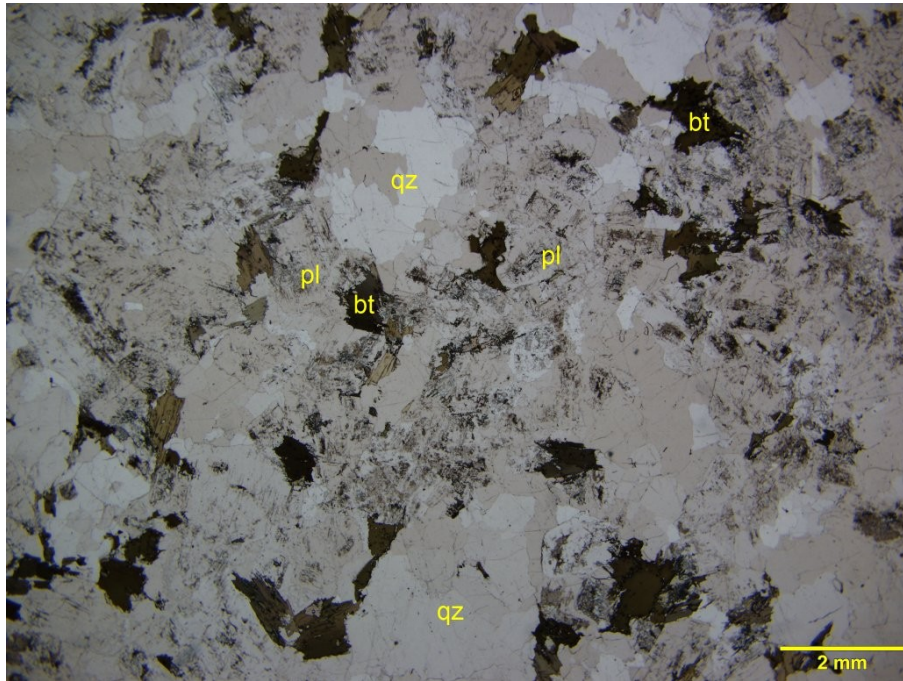
Mineral	Alteration/Weathering Mineral	Modal %	Size Range (mm)
plagioclase	white mica-epidote	55- 57	up to 2.5 long
quartz		28- 30	up to 2
biotite		8- 9	up to 2 long
K-feldspar (microcline)		5- 6	up to 5
zircon		tr	up to 0.05
	iron oxides	tr	0.01

Plagioclase is the prevailing mineral and forms subhedral crystals up to 2.5 mm long. The plagioclase shows Albite twinnings and its refractive indexes are lower than those of the quartz, thus indicating its composition is albitic. Fine-grained white mica flakes and anhedral epidote weakly altered the plagioclase. Some plagioclase crystals show a subhedral growth zoning.

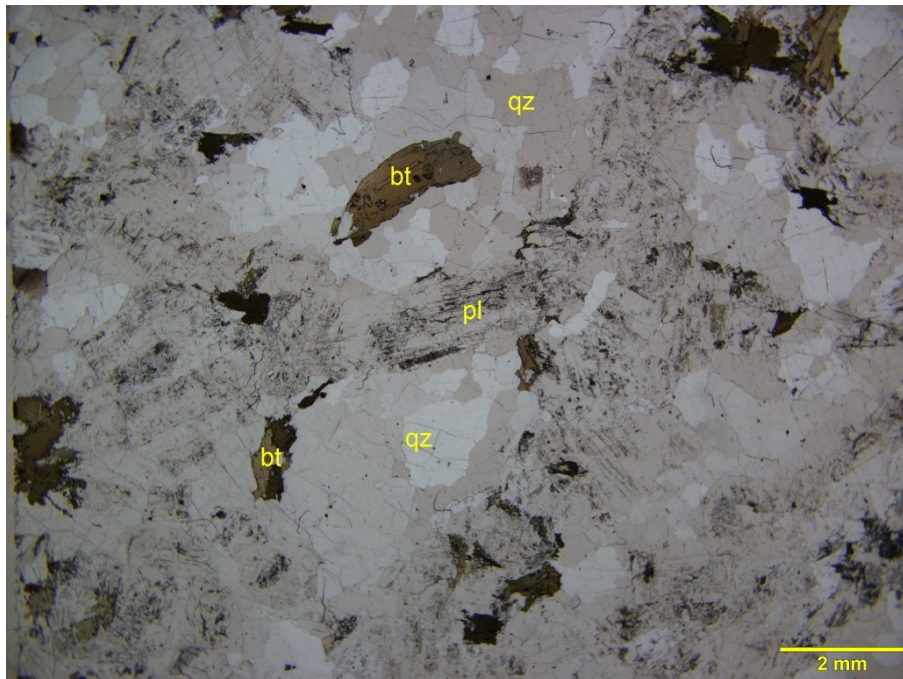
Quartz forms medium-grained anhedral crystals, which in some cases form monomineralic domains, likely the result of recrystallized quartz phenocrysts. Most crystals show a moderate undulose extinction.

Biotite is randomly oriented and occurs as fine to medium-grained (up to 2 mm long) subhedral and anhedral lamellae. The biotite hosts very fine-grained zircon, which generates the typical pleochroic halo within the biotite host. Rare epidote crystals overprinted the biotite.

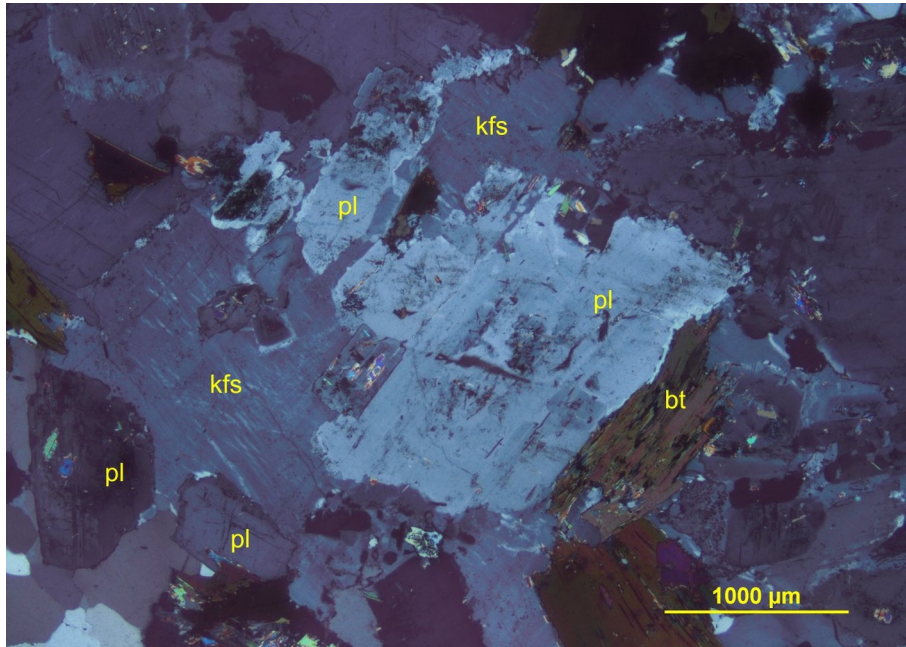
K-feldspar occurs as sparse patches (see yellow staining spots in the offcut’s image above), which under the microscope are poikilitic crystals (up to 5 mm across) including subhedral plagioclase and biotite (Photomicrographs 6c and 6d). Because of the Albite-Pericline (tartan) twinnings, the K-feldspar is **microcline**.



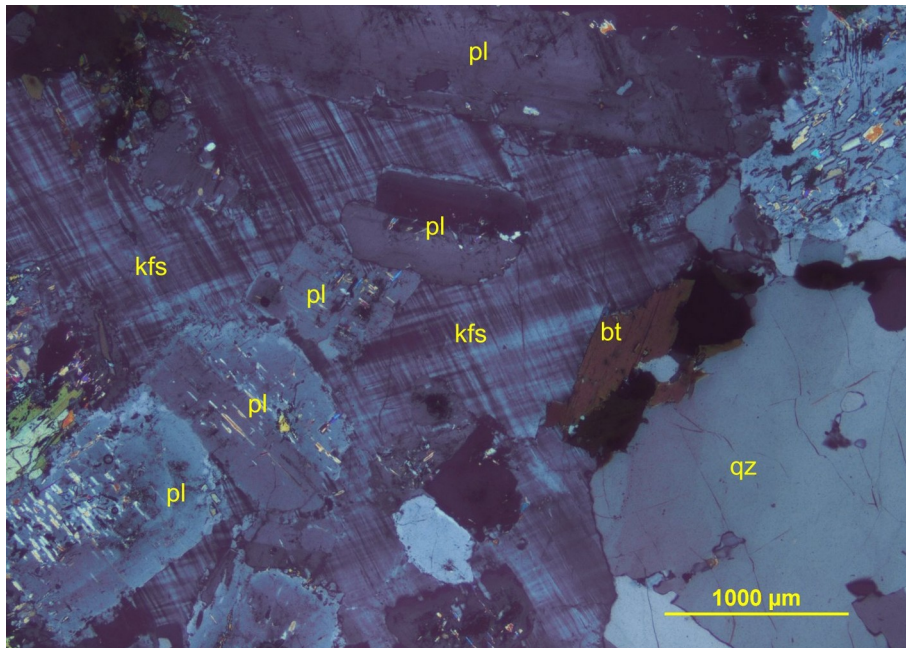
Photomicrograph 6a: Subhedral and weakly altered plagioclase (pl) anhedral quartz (qz) and randomly oriented biotite define a granular texture. Plane-polarized transmitted light.



Photomicrograph 6b: The quartz (qz) forms monomineralic domains, likely the result of recrystallized phenocrysts. Plane-polarized transmitted light.



Photomicrograph 6c: Poikilitic K-feldspar (kfs) encloses subhedral plagioclase (pl) and biotite (bt). Crossed polarizers transmitted light.

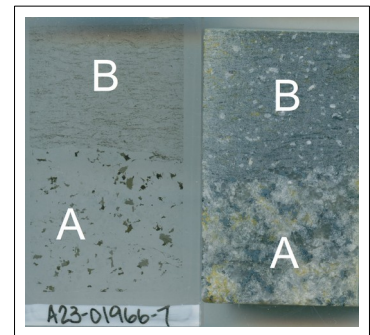


Photomicrograph 6d: The poikilitic K-feldspar (kfs) hosts subhedral plagioclase (pl), biotite (bt) and displays Albite-Pericline twinnings. Crossed polarizers transmitted light.

Sample 7: A23-01966-7-IG_BH04_MG057

Tonalite

Orthogneiss



This section comprises two domains. Domain A is a granular aggregate of plagioclase, quartz, and biotite. In Domain B, the plagioclase forms anhedral porphyroclasts immersed within a fine-grained matrix of quartz, plagioclase and biotite. The clustering and iso-oriented lamellae of biotite define a discontinuous schistosity wrapping the plagioclase porphyroclasts.

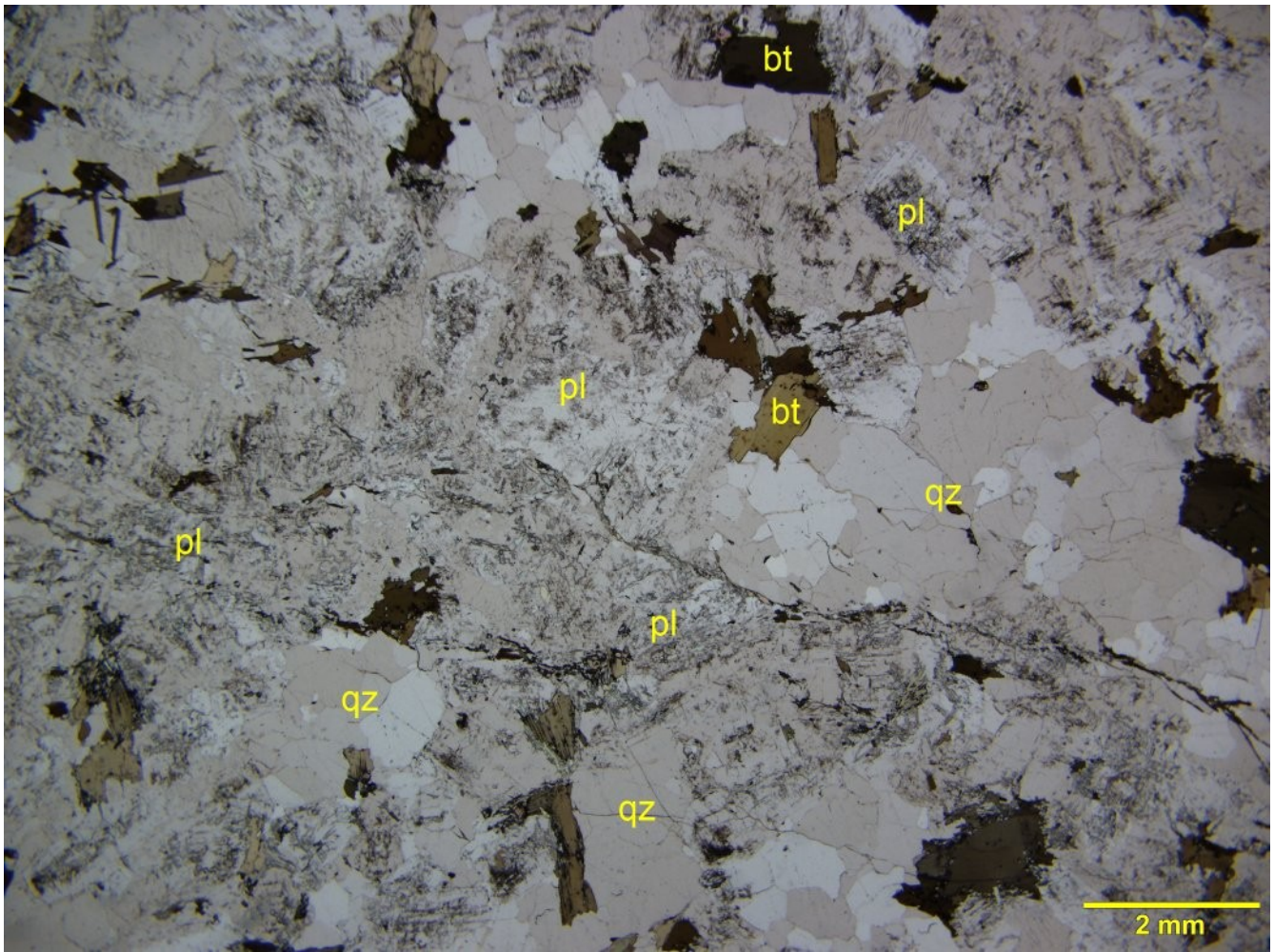
Alteration/Metamorphism: white mica-epidote(?): subtle after plagioclase in Domain A: epidote: weak in Domain B

Mineral	Alteration/Metamorphic Mineral	Modal %	Size Range (mm)
Domain A (~45% of PTS) tonalite			
plagioclase	white mica	22- 24	up to 2
quartz		16- 18	up to 2 long
biotite		4- 5	up to 1
K-feldspar		1- 2	up to 1.5
	titanite	tr	up to 0.5 long
zircon		tr	up to 0.02
Domain B (~55% of PTS) orthogneiss			
<i>porphyroclasts</i>			
plagioclase		5- 7	up to 1
<i>matrix</i>			
quartz		32- 34	up to 0.1
biotite		10- 12	up to 0.2 long
plagioclase		5- 10	
	epidote	1- 1.2	up to 0.2 long
	white mica	0.2- 0.4	up to 0.2 long
K-feldspar		tr	up to 0.1

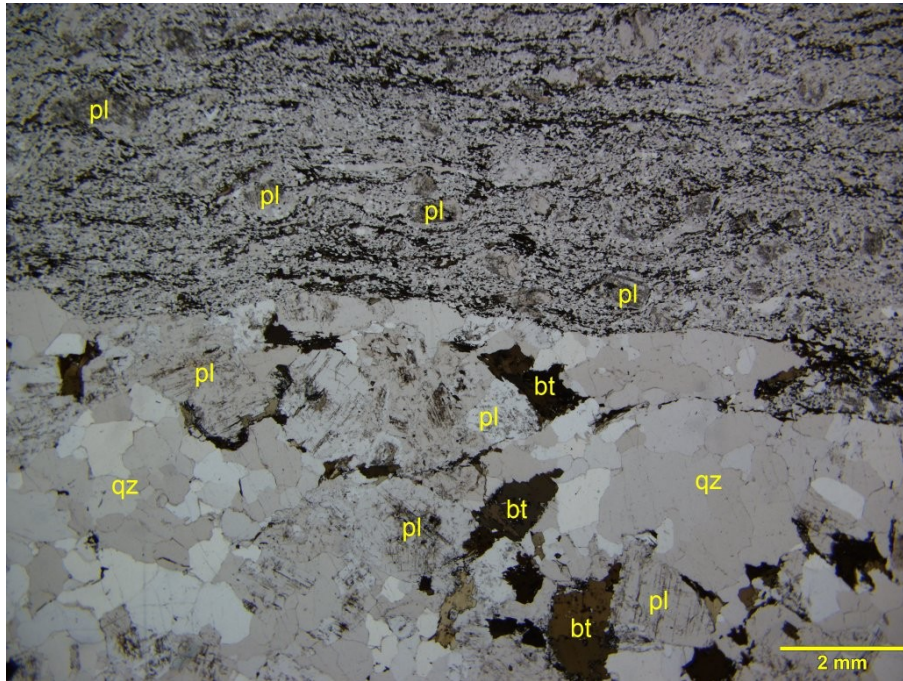
Plagioclase forms subhedral and anhedral crystals, which prevail over the quartz and the biotite and define a granular texture in Domain A (Photomicrograph 7a). A very fine-grained earthy and unresolved material (very fine-grained epidote?) weakly altered the plagioclase's core. In Domain B, the plagioclase forms anhedral and subhedral porphyroclasts (up to 1 mm across) rotated and wrapped by the schistosity defined by fine-grained iso-oriented lamellae of biotite and discontinuous biotite-rich cleavage domains.

Quartz forms inequigranular and anhedral crystals in the two domains. In Domain A, the quartz is up to 2 mm long. In Domain B is very fine-grained and forms blocky and anhedral crystals up to 0.1 mm across, and in this domain, the quartz is inter-grown with biotite and subordinate plagioclase and K-feldspar.

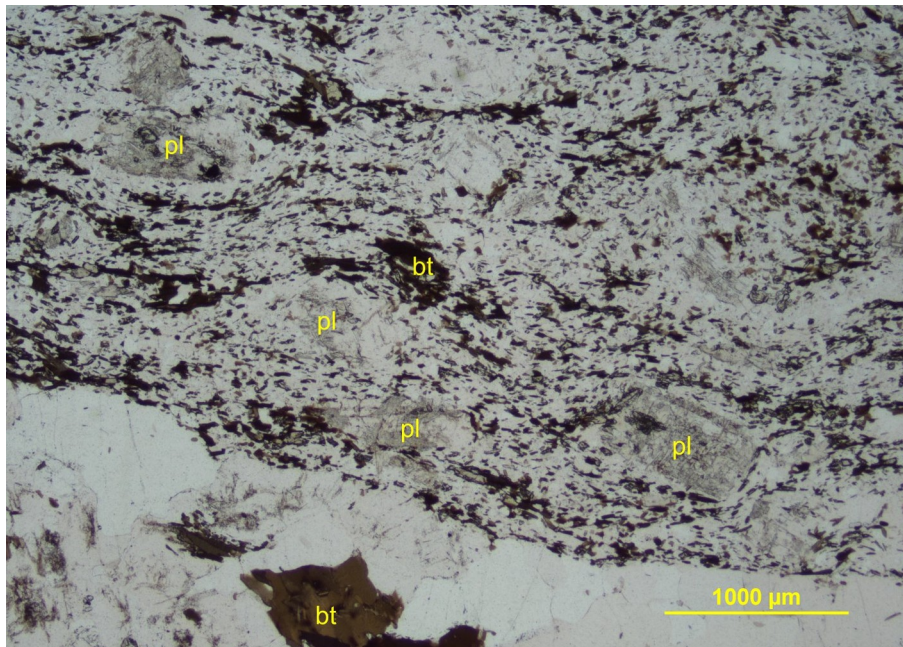
Biotite is fine- to medium-grained. In Domain A, the biotite is medium-grained (up to 2 mm long) and it is randomly oriented. In Domain B, the biotite is fine-grained, preferentially iso-oriented and define sub-parallel clusters imparting a continuous foliation to the fine-grained matrix of quartz (Photomicrographs 7b and 7c).



Photomicrograph 7a: Domain A—Under plane-polarized transmitted light, the plagioclase (pl) is distinguished by the earthy alteration products from the transparent quartz (qz). The plagioclase, quartz, and biotite define a relatively homogeneous granular texture.



Photomicrograph 7b: The sharp and irregular contact between the granular Domain A (below) and the foliated Domain B (above) is shown under plane-polarized transmitted light.



Photomicrograph 7c: Domain B—The plagioclase porphyroclasts (pl) are wrapped by the schistosity defined by the clustered and preferentially iso-oriented biotite (bt). Plane-polarized transmitted light.

Sample 8: A23-01966-8-IG_BH04_MG058



Tonalite

K-feldspar-biotite-quartz schist

Orthogneiss

This section comprises three different compositional and textural domains. In Domain A, subhedral plagioclase, anhedral quartz and subordinate biotite define a coarse-grained granular texture. Domain B comprises fine-grained quartz, heterogeneously distributed K-feldspar and fine-grained iso-oriented lamellae of biotite. In Domain C, plagioclase porphyroclasts are rotated within a fine-grained matrix of quartz and plagioclase and are wrapped by discontinuous and sub-parallel cleavage domains of biotite.

Alteration/Metamorphism: epidote-white mica: subtle to weak after plagioclase; epidote-white mica: weak in Domain C; carbonate: subtle in Domain C

Mineral	Alteration/Metamorphic Mineral	Modal %	Size Range (mm)
Domain A (~50% of PTS) tonalite			
plagioclase		24- 25	up to 2 long
quartz		20- 21	up to 2.5
biotite		4- 5	up to 1, rare up to 2 long
K-feldspar		tr	up to 0.6
Domain B (18% of PTS) K-feldspar-biotite-quartz schist			
quartz		9- 11	0.1 to 1
K-feldspar		6- 8	up to 0.4
plagioclase		1- 2	up to 0.4
biotite		1- 2	up to 0.4 long
Domain C (~32% of PTS) orthogneiss			
<i>porphyroclasts</i>			
plagioclase		5- 7	up to 1
<i>matrix</i>			
quartz		20- 21	up to 0.2
biotite		4- 5	up to 0.3 long
	epidote	1- 2	up to 0.2
	white mica	tr	up to 0.4 long
K-feldspar		tr	up to 0.1
	carbonate	tr	up to 0.2

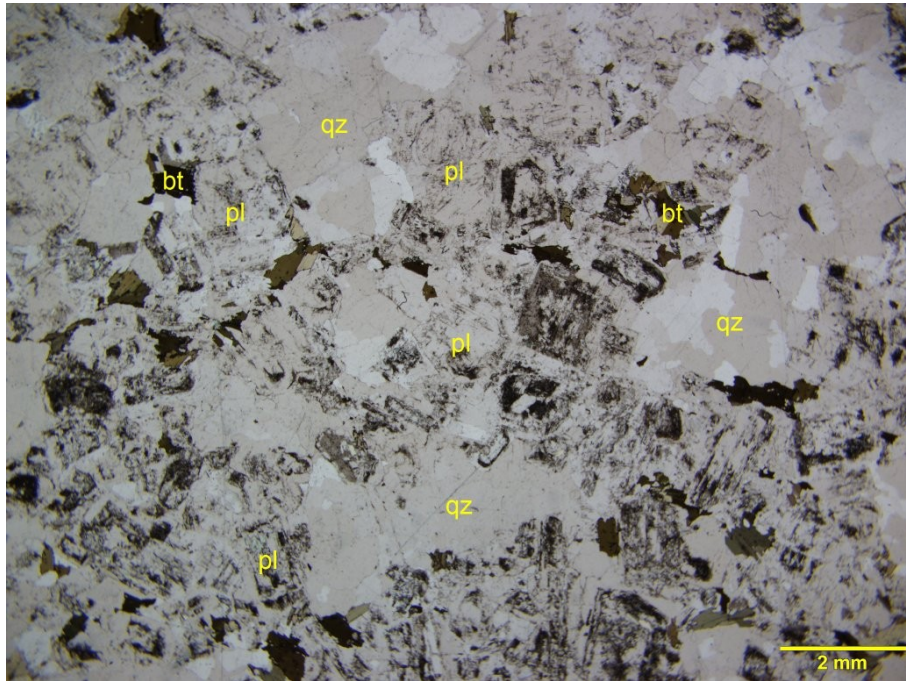
Plagioclase forms subhedral crystals, which prevail over the quartz and the biotite and define a granular texture in Domain A (Photomicrograph 8a). A very fine-grained earthy and unresolved material (very fine-grained epidote?) weakly altered the plagioclase's core. Subordinate flakes of white mica subtly to weakly altered some plagioclase crystals. In Domain C, the plagioclase forms anhedral porphyroclasts (up to 1 mm across) rotated and wrapped by the schistosity defined by fine-grained iso-oriented lamellae of biotite and discontinuous biotite-rich cleavage domains.

Quartz forms inequigranular and anhedral crystals in the three domains. In Domain A, the quartz is up to 2.5 mm long. In Domain B ranges from 0.1 mm to 1 mm across, and in Domain C, the quartz forms a fine-grained matrix associated with fine-grained plagioclase and biotite.

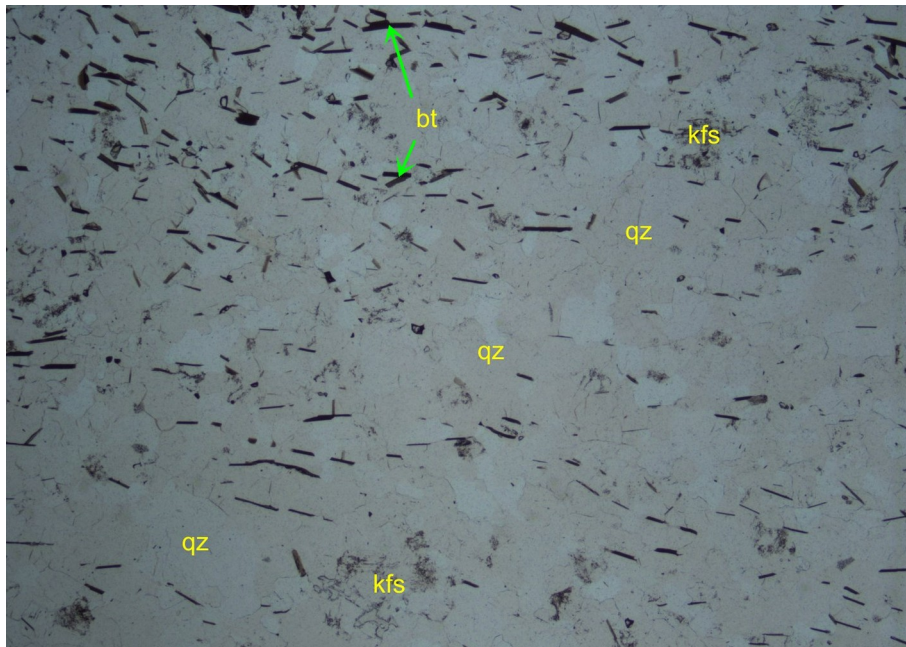
Biotite is fine- to medium-grained. In Domain A, the biotite is medium-grained (up to 2 mm long) and it is randomly oriented. In Domains B and C, the fine-grained lamellae of biotite define a continuous foliation within the fine-grained matrix of quartz associated with K-feldspar and subordinate plagioclase in Domain B) and with plagioclase in Domain C.

K-feldspar is concentrated within Domain B. In this domain, the fine-grained and anhedral crystals are heterogeneously dispersed within the fine-grained quartz. The abundance and distribution of the K-feldspar is shown in the stained offcut's image above.

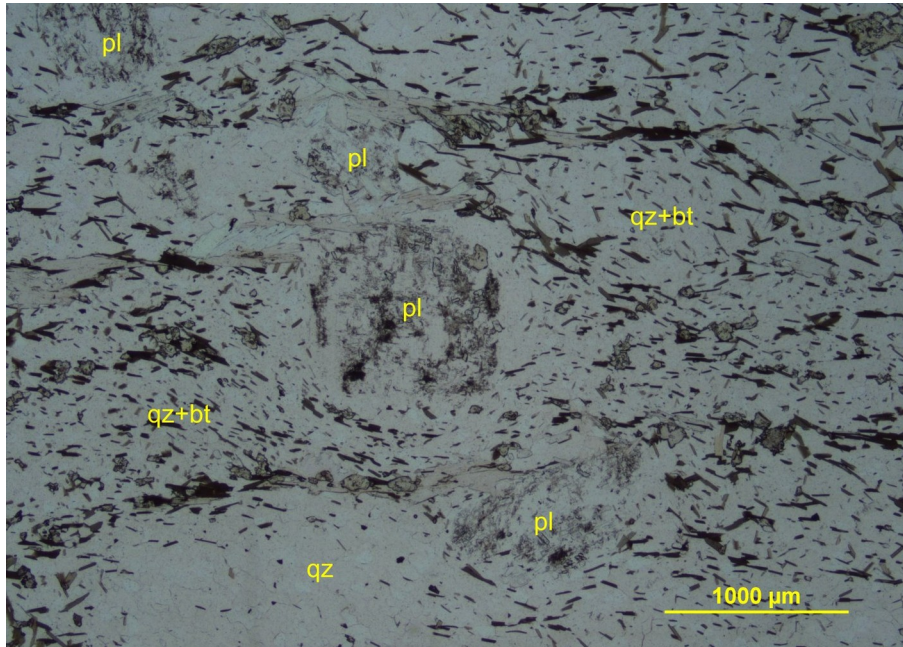
Epidote is fine-grained xenoblastic and is spatially associated with the biotite in Domain C. I interpret most of the very fine-grained and unresolved alteration products of plagioclase as very fine-grained epidote. Like the epidote, White mica is more abundant in Domain B, and forms fine- to medium-grained lamellae (up to 0.4 mm long) post-dating the biotite and showing a weak preferred dimensional orientation parallel to the schistosity.



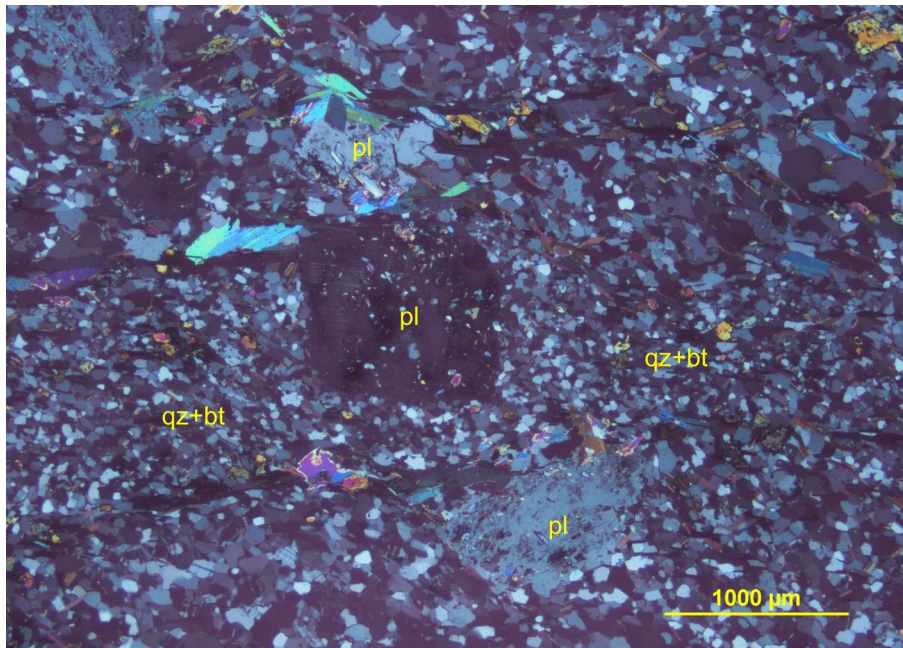
Photomicrograph 8a: Domain A—Subhedral plagioclase (pl) anhedral quartz (qz) and randomly oriented biotite (bt) define a granular texture. Plane-polarized transmitted light.



Photomicrograph 8b: Domain B—Abundant quartz (qz) and preferentially iso-oriented lamellae of biotite are associated with sparse K-feldspar crystals (kfs). Plane-polarized transmitted light.



Photomicrograph 8c: Domain C—Anhedral plagioclase porphyroclasts (pl) are immersed within a foliated matrix of quartz and biotite (qz+bt). Plane-polarized transmitted light.



Photomicrograph 8d: Domain C—Same area as shown in Photomicrograph 8c. Under crossed polarizers transmitted light, the plagioclase porphyroclasts are immersed within a fine-grained matrix of quartz and biotite (qz+bt).

Sample 9: A23-01966-9-IG_BH04_MG059

Tonalite

Subhedral and inequigranular plagioclase crystals prevail over anhedral crystals of quartz, randomly oriented and anhedral biotite and sparse crystals of anhedral K-feldspar, all of which define a granular texture.



Alteration: white mica-epidote: weak after plagioclase; **epidote:** subtle

Mineral	Alteration/Weathering Mineral	Modal %	Size Range (mm)
plagioclase (albite)	white mica-epidote	50- 52	up to 2.5 long
quartz		35- 37	up to 2
biotite		7- 9	up to 1.5 long, rare up to 2.5 across
K-feldspar (microcline)		3- 4	up to 5
	epidote	0.3- 0.5	up to 0.6 long
zircon		tr	up to 0.05

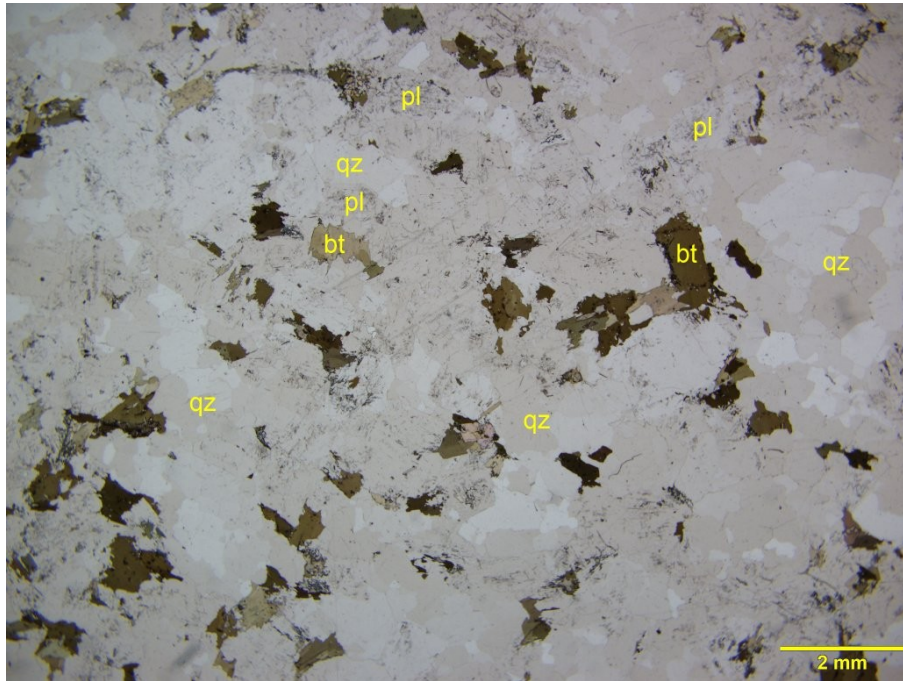
Plagioclase is forms subhedral crystals up to 2.5 mm long. The plagioclase shows Albite twinings and its refractive indexes are lower than those of the quartz, thus indicating its composition is albitic. Fine-grained white mica flakes and anhedral epidote weakly altered the plagioclase. Some plagioclase crystals show a subhedral growth zoning (Photomicrograph 9c).

Quartz forms medium-grained anhedral crystals. Like in Sample 6, the quartz forms monomineralic domains, which I interpret as the result of recrystallized quartz phenocrysts (Photomicrograph 9b). Most crystals show a moderate undulose extinction.

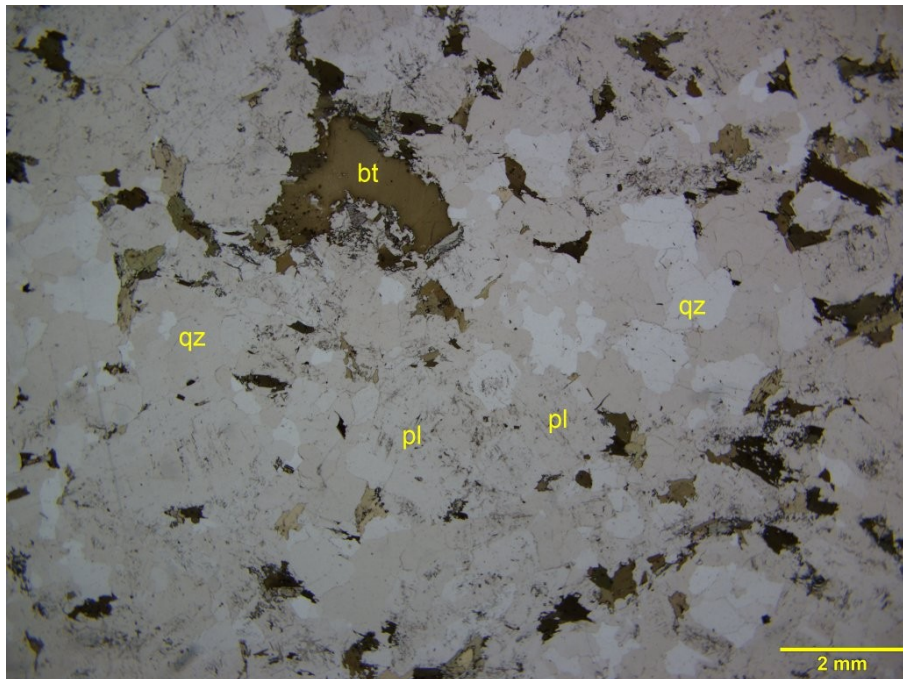
Biotite is randomly oriented and occurs as fine to medium-grained (up to 2.5 mm across) subhedral and anhedral lamellae. The biotite hosts very fine-grained zircon, which generates the typical pleochroic halo within the biotite host. Rare epidote crystals overprinted the biotite.

K-feldspar occurs as sparse patches (see yellow staining spots in the offcut’s image above), which are less abundant than in Sample 6.

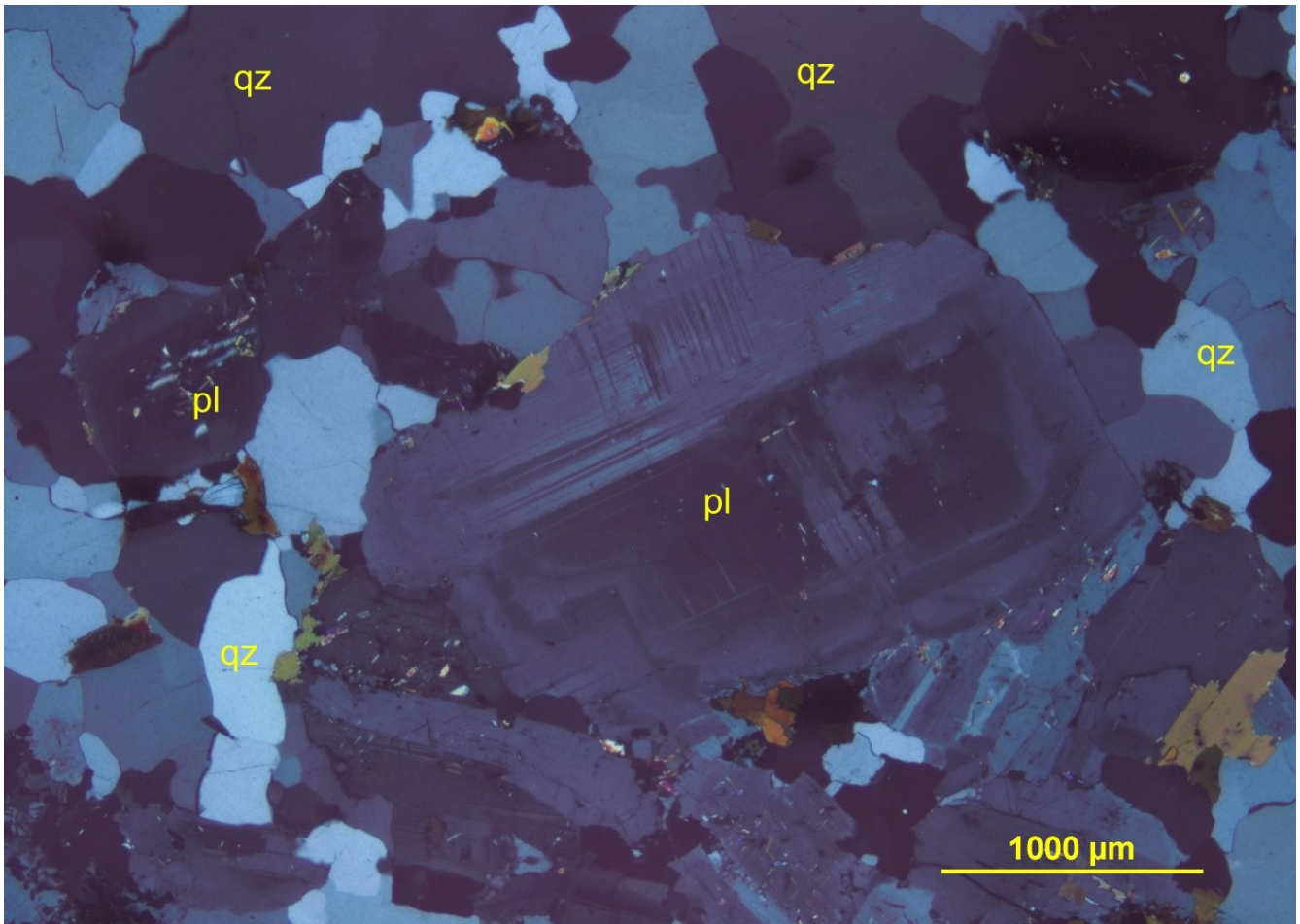
Epidote forms fine- to medium-grained (up to 0.6 mm long) anhedral crystals, which are spatially associated with the biotite and overprinted the plagioclase.



Photomicrograph 9a: Subhedral and weakly altered plagioclase (pl) anhedral quartz (qz) and randomly oriented biotite define a granular texture. Plane-polarized transmitted light.



Photomicrograph 9b: Like in Sample 6, the quartz (qz) forms monomineralic domains, likely the result of recrystallized phenocrysts. Plane-polarized transmitted light.

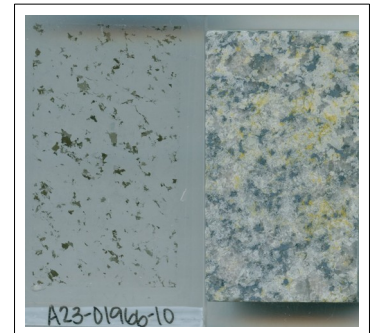


Photomicrograph 9c: Subhedral plagioclase (pl) displays a subhedral growth zoning and Albite twinnings. Crossed polarizers transmitted light.

Sample 10: A23-01966-10-IG_BH04_MG060

Tonalite

Subhedral and inequigranular plagioclase crystals prevail over anhedral crystals of quartz, randomly oriented and anhedral biotite and sparse crystals of anhedral K-feldspar, all of which define a granular texture.



Alteration: white mica-epidote: weak after plagioclase; **epidote:** subtle

Mineral	Alteration/Weathering Mineral	Modal %	Size Range (mm)
plagioclase (albite)	white mica-epidote	50- 52	up to 2.5 long
quartz		35- 37	up to 2
biotite		7- 9	up to 1.5 long, rare up to 2.5 across
K-feldspar (microcline)		3- 4	up to 5
	epidote	0.3- 0.5	up to 0.6 long
zircon		tr	up to 0.05

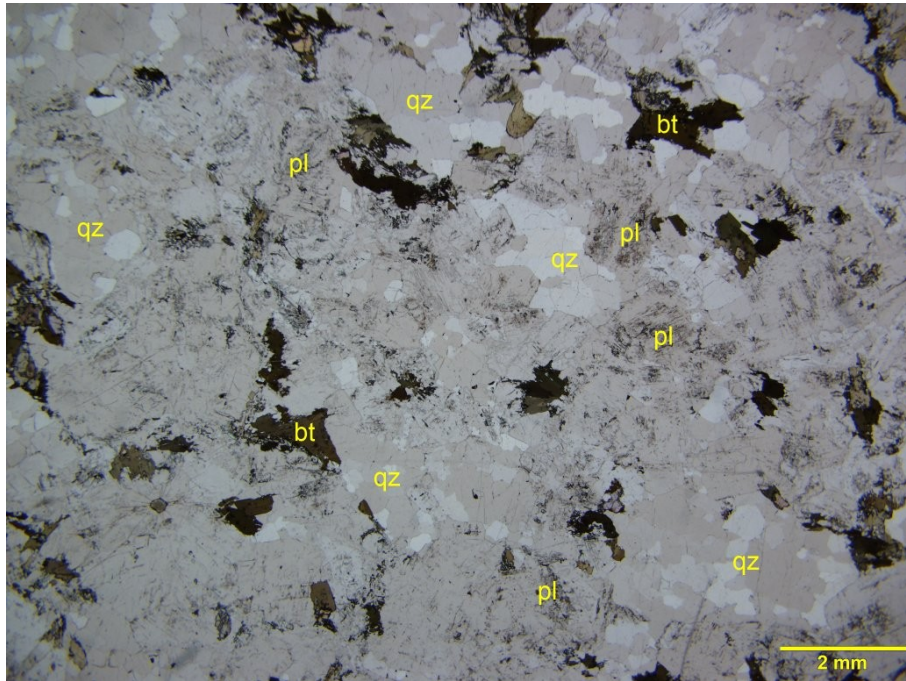
Plagioclase (albite) is the prevailing mineral and forms subhedral crystals up to 2.5 mm long. The plagioclase shows Albite twinnings and its refractive indexes are lower than those of the quartz, thus indicating its composition is **albitic**. Fine-grained white mica flakes and anhedral epidote altered the plagioclase. Under plane-polarized transmitted light, the alteration minerals overprinting the plagioclase are slightly more abundant than in Sample 6 and 9; however, the alteration intensity is still weak. Some plagioclase crystals show a subhedral growth zoning.

Quartz forms medium-grained anhedral crystals, which in some cases form monomineralic domains, likely the result of recrystallized quartz phenocrysts. Most crystals show a moderate undulose extinction.

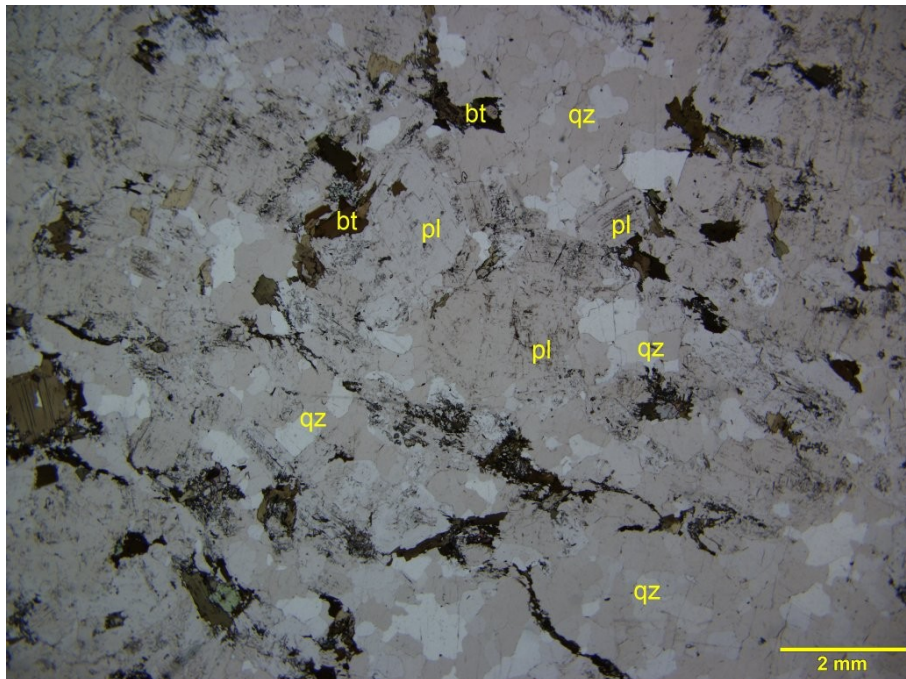
Biotite is randomly oriented and occurs as fine to medium-grained (up to 2.5 mm across) subhedral and anhedral lamellae. The biotite hosts very fine-grained zircon.

Rare **epidote** crystals (up to 0.6 mm long) overprinted the biotite and are dispersed within the plagioclase in association with fine-grained white mica flakes.

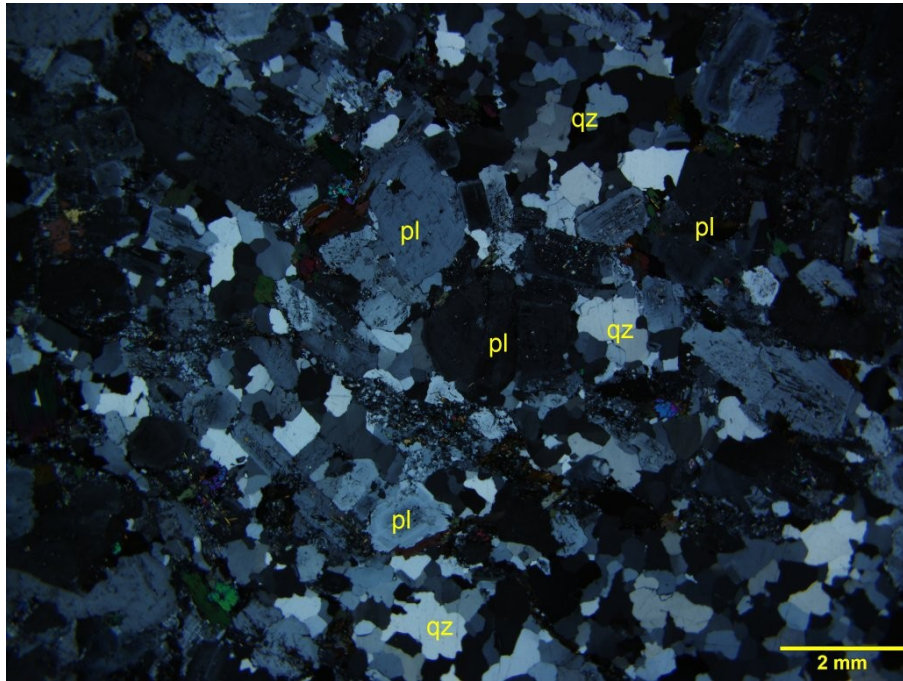
K-feldspar occurs as sparse patches (see yellow staining spots in the offcut's image above) showing Albite-Pericline (tartan) twinnings, thus indicating that the K-feldspar is **microcline**.



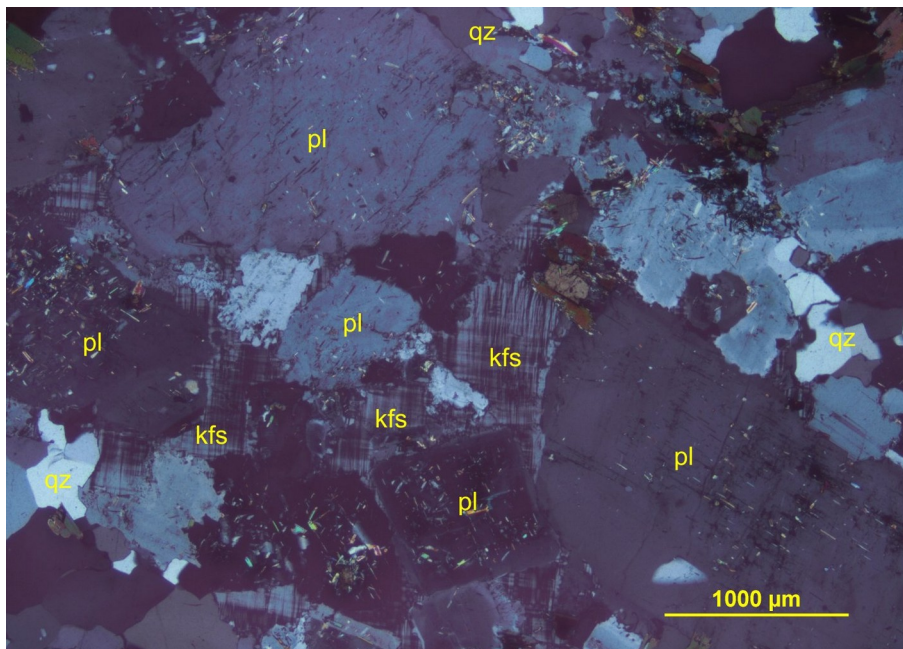
Photomicrograph 10a: Weakly altered plagioclase (pl), anhedral quartz (qz) and randomly oriented biotite define a granular texture. Plane-polarized transmitted light.



Photomicrograph 10b: The quartz (qz) forms monomineralic domains, likely the result of recrystallized phenocrysts. Plane-polarized transmitted light.



Photomicrograph 10c: Same area as shown in Photomicrograph 10c. Under crossed polarizers transmitted light, the plagioclase (pl) and quartz (qz) define a medium-grained granular texture.



Photomicrograph 10d: K-feldspar (kfs) occupies the interstices between the subhedral plagioclase crystals (pl) and biotite (bt). Crossed polarizers transmitted light.

Sample 11: A23-01966-11-IG_BH04_MG061

Tonalite

Microtonalite(?)

Epidote-biotite-quartz-white mica sheared domain



This section comprises three domains. Domain A is a granular aggregate of euhedral and subhedral plagioclase, anhedral quartz, biotite, and subordinate poikilitic K-feldspar. Domain B shows a similar composition to Domain A, and the plagioclase is inequigranular. The two domains are divided by an up to 1.5 mm thick schistose Domain C consisting of white mica, quartz, biotite, and epidote.

Alteration/Metamorphism: white mica-epidote(?): subtle after plagioclase; moderate to strong in the 1.5 mm thick shear domain

Mineral	Alteration/Metamorphic Mineral	Modal %	Size Range (mm)
Domain A (~55% of PTS) tonalite			
plagioclase	white mica	24- 25	up to 4
quartz		23- 24	up to 3
K-feldspar		4- 5	up to 5
biotite		2- 3	up to 1.2
magnetite(?)		tr	0.5
zircon		tr	0.01
Domain B (~39% of PTS) microtonalite(?)			
plagioclase		19- 20	0.5 to 4.5
quartz		15- 16	up to 0.5, rare up to 1.5
biotite		2- 3	up to 0.6
K-feldspar		1- 2	up to 1
Domain C: (~6% of PTS) shear zone			
white mica		2	up to 0.1
quartz		1.5	up to 0.1
biotite		1.5	up to 0.1
epidote		1	up to 0.1

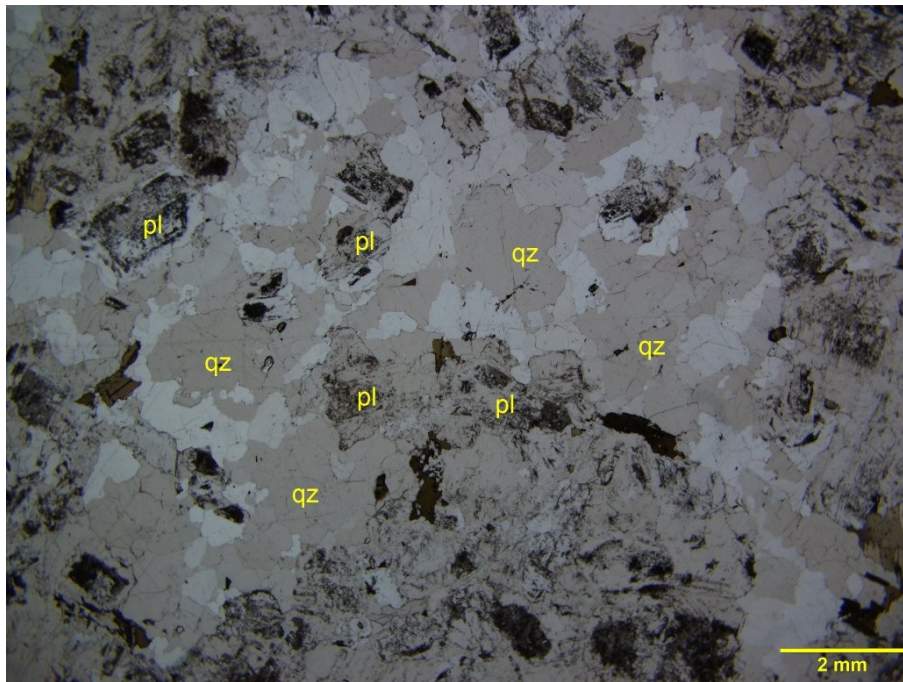
Plagioclase forms subhedral crystals immersed within the monomineralic aggregate of quartz and defines a granular texture in Domain A (Photomicrograph 11a). A very fine-grained earthy and

unresolved material (very fine-grained epidote?) weakly to moderately altered the plagioclase and helps to distinguish it from the quartz under plane-polarized transmitted light. In some plagioclase crystals, very fine-grained flakes of sericite are dispersed within the plagioclase, and in some others, a subhedral growth zoning occurs. In Domain B, the plagioclase forms anhedral and subhedral crystals ranging from 0.5 mm to 4.5 mm long, which are finely intergrown with the quartz (Photomicrograph 11c and 11d).

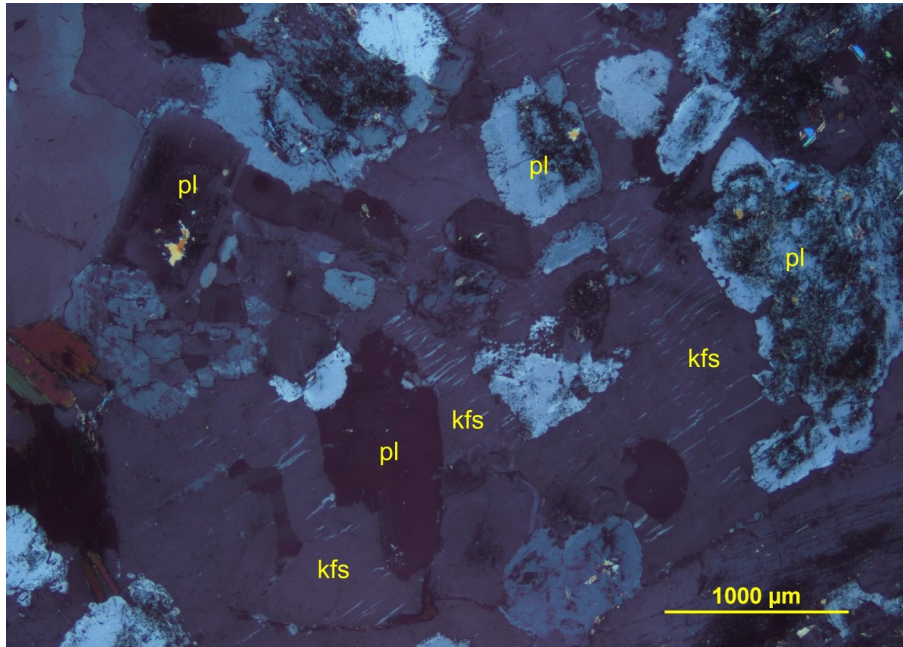
Quartz forms inequigranular and anhedral crystals in the two domains. In Domain A, the quartz is up to 3 mm across and mostly forms monomineralic aggregates. In Domain B, the quartz is fine-grained anhedral crystals are intergrown and interlobate with the plagioclase and the subordinate K-feldspar. Fine-grained white mica, quartz, biotite, and epidote form a 1.5 mm thick schistose domain dividing the isotropic domains A and B. The White mica is the mineral that defines an irregular schistosity in this domain (C in the image above), which I interpret as having generated during the shearing occurring between the two magmatic domains after their crystallization.

Biotite is fine- to medium-grained. In Domain A, the biotite is medium-grained (up to 1.2 mm long) and it is randomly oriented. In Domain B, the biotite is finer-grained than in Domain A and its crystals (up to 0.6 mm across) are mostly anhedral.

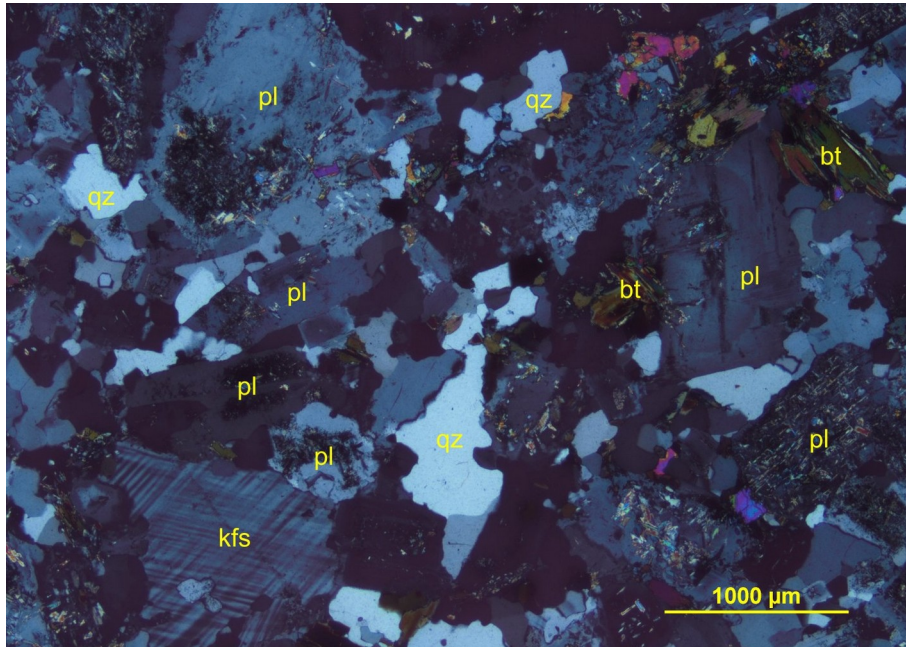
K-feldspar (microcline) forms sparse poikilitic crystals (up to 5 mm across) including subhedral plagioclase crystals in Domain A. This texture suggests a cogenetic nature of Domain A with some of the tonalite (e.g., Samples 6, 31, 32, 34, and 45). K-feldspar is fresh and shows Albite-Pericline twinnings indicating its triclinic nature. In Domain B, it is fine- to medium-grained and its anhedral crystals are dispersed within the anhedral plagioclase-quartz aggregate.



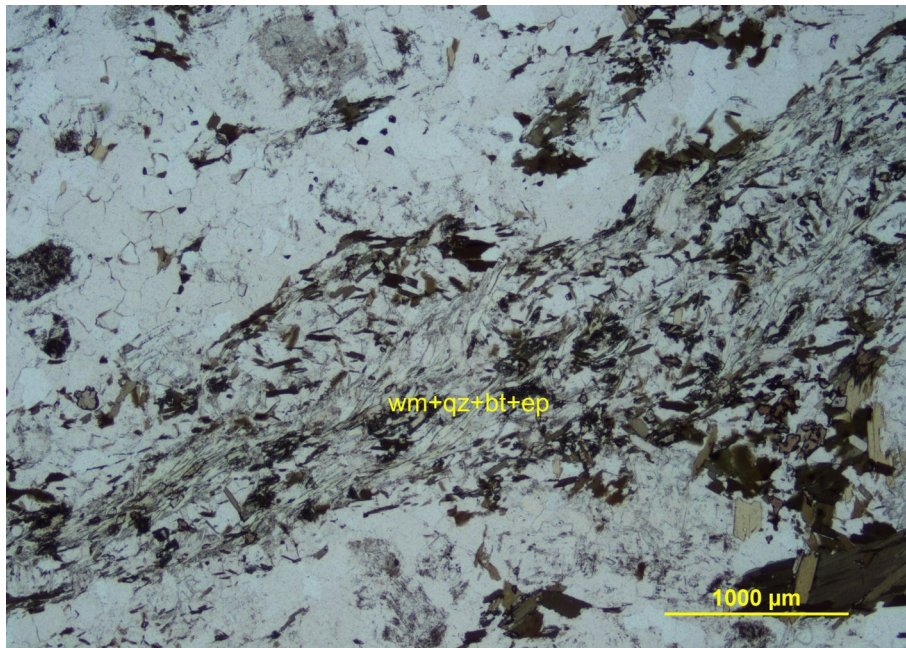
Photomicrograph 11a: Domain A—Subhedral plagioclase (pl) is immersed within monomineralic quartz (qz) and, together with biotite (bt) defines a granular texture. Plane-polarized transmitted light.



Photomicrograph 11b: Domain A—Poikilitic K-feldspar (kfs) host subhedral inclusions of plagioclase (pl). Crossed polarizers transmitted light.



Photomicrograph 11c: Domain B—Plagioclase (pl), quartz (qz) are inequigranular, anhedral, and on average, finer-grained than in Domain A. Crossed polarizers transmitted light.



Photomicrograph 11d: Domain C—an up to 1.5 mm thick schistose domain of white mica, quartz, biotite, and epidote (wm+qz+bt+ep) sharply divides Domain A and B. Plane-polarized transmitted light.

Sample 12: A23-01966-12-IG_BH04_MG062

Microquartz-diorite

Epidote-Fe-chlorite-altered microgranodiorite/microquartz-monzodiorite



This section shows a compositional heterogeneity, which generated two irregular sub-domains. In the upper and lower parts of the section (Domains A), subhedral plagioclase prevails over anhedral quartz and randomly oriented flakes of biotite. Domain B comprises plagioclase, quartz, which is more abundant than in Domain A, K-feldspar, and sparse Fe-chlorite and epidote replacing biotite.

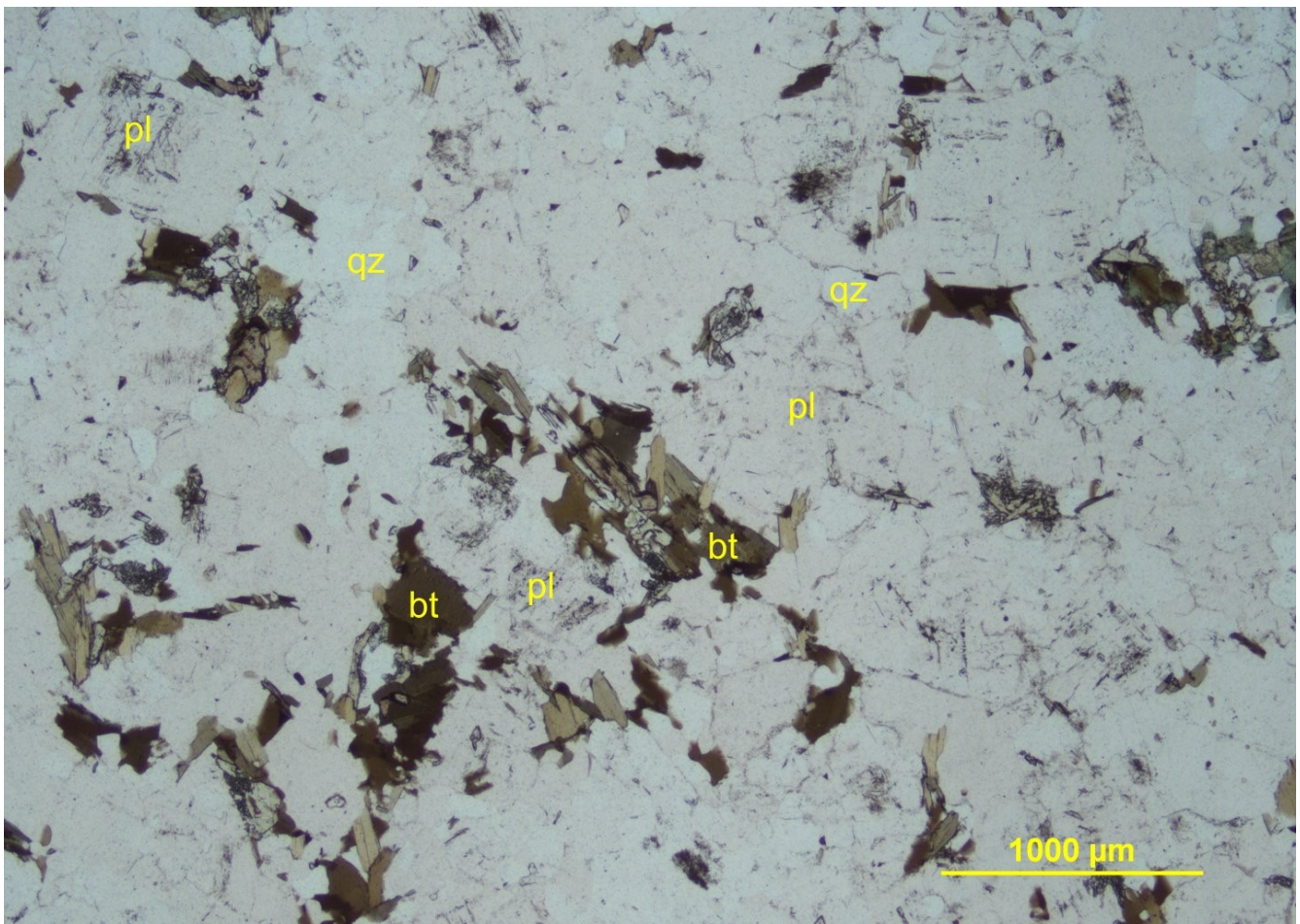
Alteration: Fe-chlorite: moderate to strong after biotite in Domain B; epidote: weak after biotite in Domain B; sericite-epidote: moderate after plagioclase in Domain B; epidote: subtle after plagioclase in Domain A; chalcopyrite: subtle in Domain B

Mineral	Alteration/Weathering Mineral	Modal %	Size Range (mm)
Domain A: microquartz-diorite (~78% of PTS)			
plagioclase		69- 70	up to 2.5
quartz		5- 6	up to 0.5
biotite		3- 4	up to 0.6
zircon		tr	0.01
Domain B altered microgranodiorite? (~22% of PTS)			
plagioclase	sericite-epidote	11- 12	up to 2.5
quartz		8- 9	up to 0.5
K-feldspar (microcline)		1- 2	up to 0.2
biotite	Fe-chlorite-epidote-titanite	1- 2	[up to 0.6]
zircon		tr	0.01

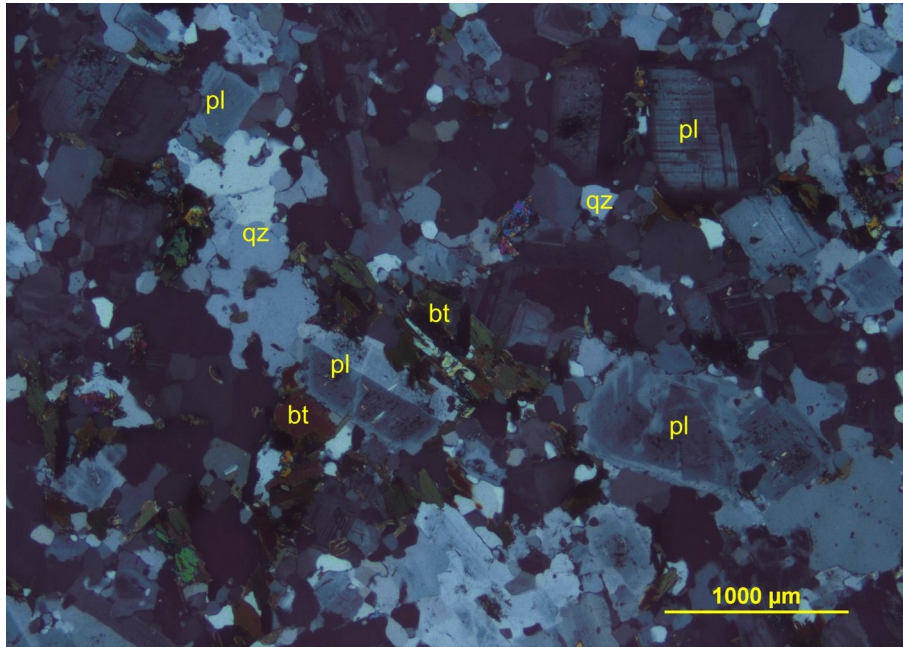
Plagioclase prevails in Domain A. The crystals are inequigranular (up to 2.5 mm long), and are relatively fresh. The randomly oriented plagioclase shows subhedral growth zoning and Albite twinings. The refractive indexes of plagioclase are lower than those of the quartz; therefore, the plagioclase’s rims are albitic. In Domain B, the plagioclase is inequigranular (up to 2.5 mm long) and the crystals are weakly to moderately altered. The alteration products comprise very fine-grained sericite, very fine-grained dispersions of epidote and interstitial K-feldspar. The occurrence of **K-feldspar** is also indicated by the yellow staining patches shown in the offcut’s image above.

Quartz is subordinate to the plagioclase and occurs as interstitial fine- to medium-grained crystals in Domain A (Photomicrographs 12a and 12b). In Domain B, the quartz is more abundant than in Domain B. In this domain, the alteration induced the crystallization of Fe-chlorite replacing biotite, and sparse anhedral crystals of epidote (Photomicrographs 12c and 12d).

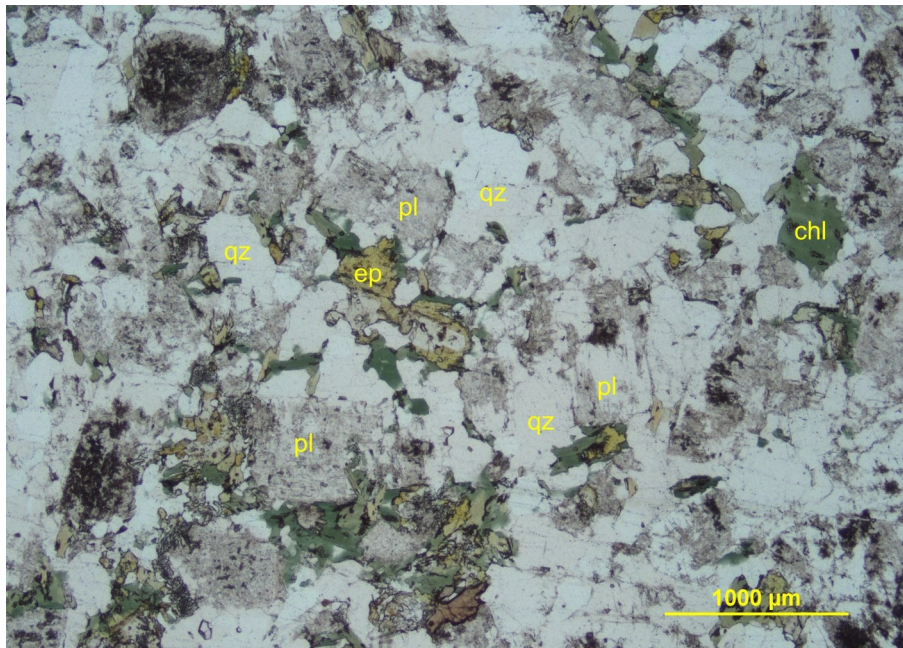
Biotite is fine- to medium-grained (up to 0.6 mm long) and the anhedral lamellae are randomly oriented within the plagioclase and quartz aggregate. The biotite hosts very fine-grained zircon inclusions and is relatively fresh in Domain A. In Domain B, the biotite is moderately to strongly altered to Fe-chlorite and epidote.



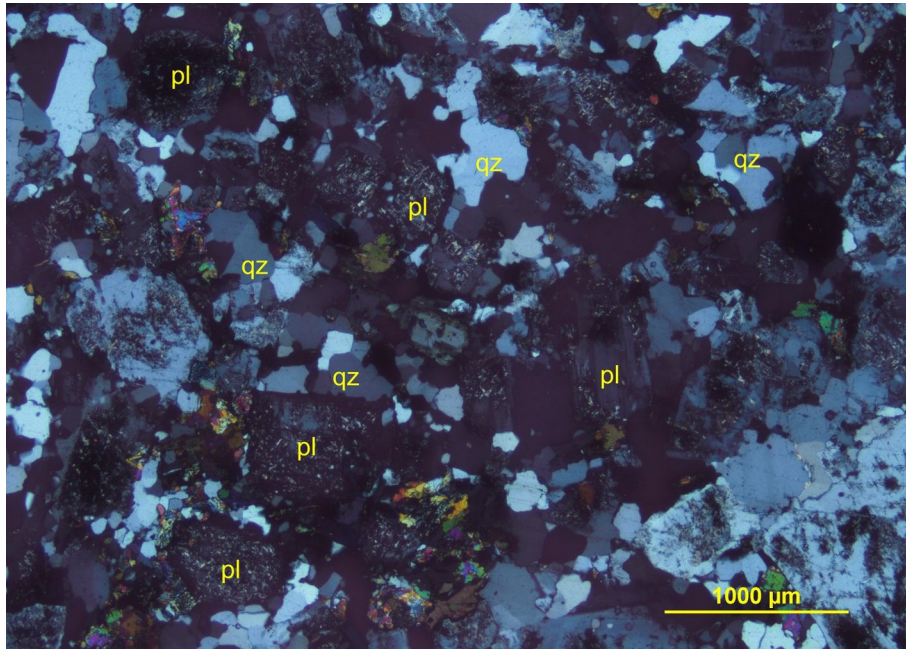
Photomicrograph 12a: Domain A—Relatively fresh plagioclase (pl) and quartz (qz) host randomly oriented biotite (bt). Plane-polarized transmitted light.



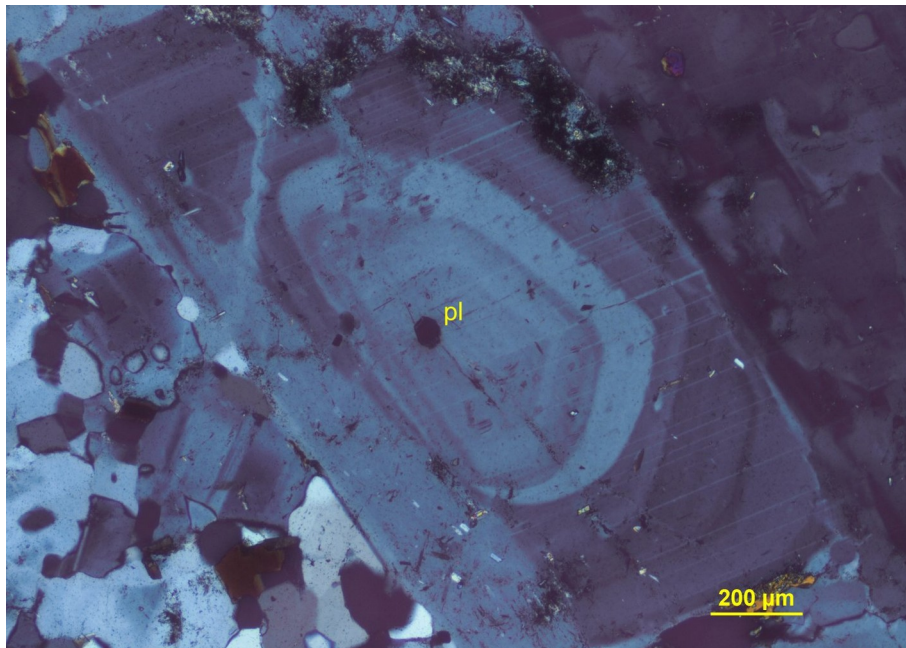
Photomicrograph 12b: Domain A—Same area as shown in Photomicrograph 12a. Under crossed polarizers transmitted light, the plagioclase displays a subhedral growth zoning within its fresh crystals.



Photomicrograph 12c: Domain B—The plagioclase (pl) crystals are moderately altered and the biotite is replaced by Fe-chlorite (chl) and epidote. Plane-polarized transmitted light.



Photomicrograph 12d: Domain B—Under crossed polarizers transmitted light the plagioclase is partially replaced by highly birefringent flakes of sericite and very fine-grained epidote.

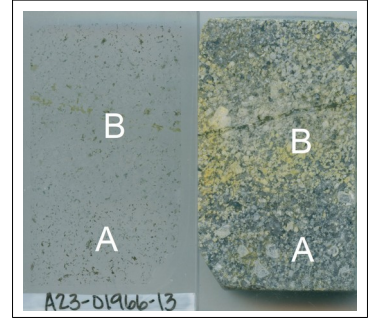


Photomicrograph 12e: Domain A—The plagioclase (pl) shows anhedronal and subhedronal growth zoning. Crossed polarizers transmitted light.

Sample 13: A23-01966-13-IG_BH04_MG063

Chlorite-altered microquartz-diorite

Epidote-chlorite-sericite-altered microgranodiorite/microquartz-monzodiorite



This section is compositionally similar to Sample 12 and shows a compositional heterogeneity. In the upper and lower parts of the section (Domains A), subhedral plagioclase prevails over anhedral quartz and randomly oriented flakes of biotite. Domain B comprises plagioclase, quartz, and sparse Fe-chlorite and epidote replacing biotite.

Alteration: Fe-chlorite: moderate to strong after biotite in Domain B; epidote: weak after biotite in Domain B; sericite-epidote-K-feldspar: moderate after plagioclase in Domain B; epidote: subtle after plagioclase in Domain A; chalcopyrite: subtle in Domain B

Mineral	Alteration/Weathering Mineral	Modal %	Size Range (mm)
Domain A: microquartz-diorite (~44% of PTS)			
plagioclase		26- 28	up to 2.5
quartz		15- 16	up to 0.5
biotite	Fe-chlorite-epidote-titanite	2- 3	up to 0.6
zircon		tr	0.01
Domain B altered microgranodiorite? (~55% of PTS)			
plagioclase		30- 32	up to 2.5
quartz		15- 16	up to 0.5
K-feldspar (microcline)		5- 10	up to 0.2
biotite	Fe-chlorite-epidote-titanite	3- 3.2	[up to 0.6]
zircon		tr	0.01
epidote-quartz vein (~1% of PTS)			
quartz		1	up to 1
epidote		tr	up to 1

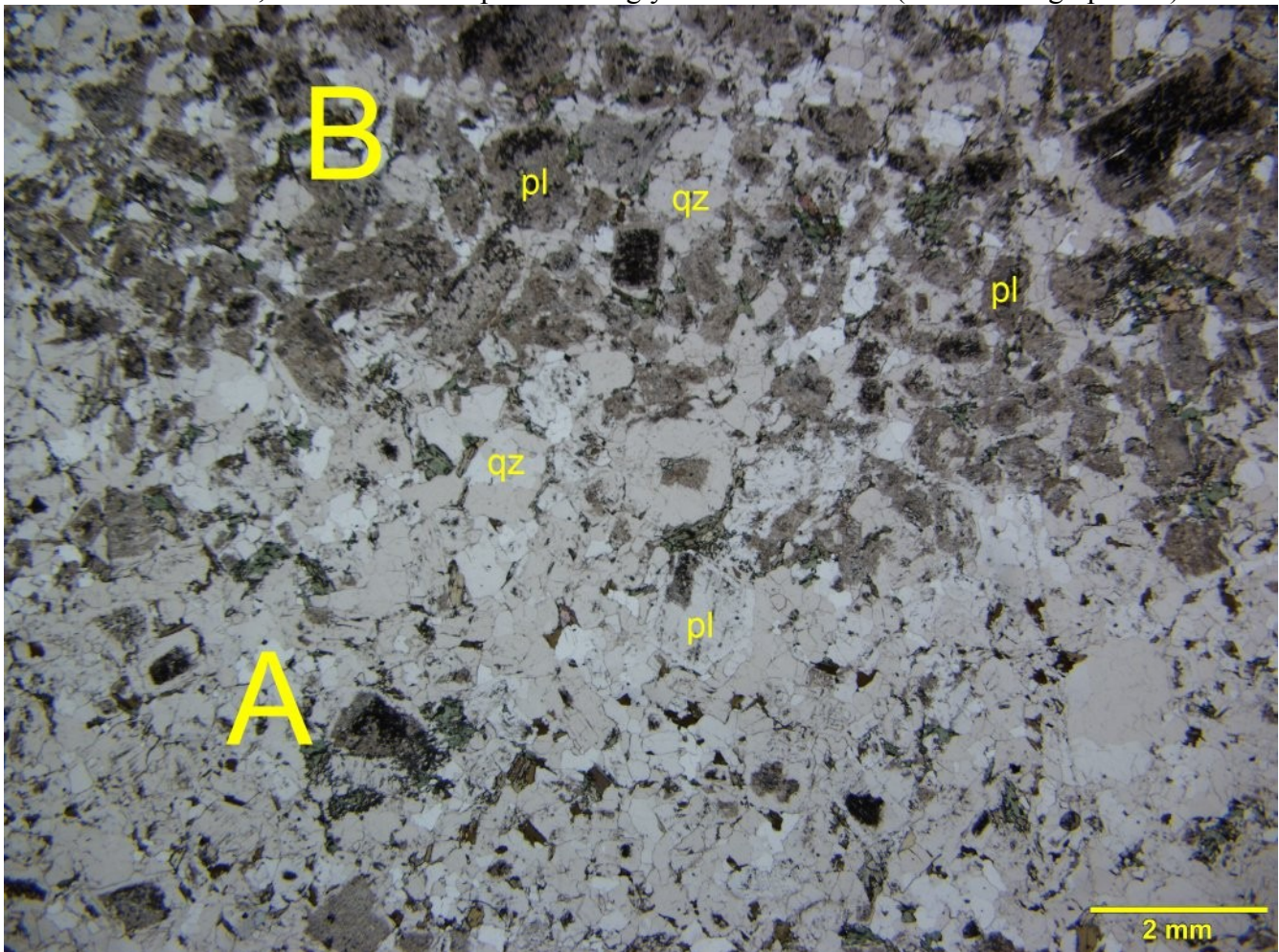
Plagioclase prevails in both domains. The crystals are inequigranular (up to 2.5 mm long), and are relatively fresh in Domains A. The randomly oriented plagioclase shows subhedral growth zoning and Albite twinnings. The refractive indexes of plagioclase are lower than those of the quartz; therefore, the plagioclase’s rims are albitic. In Domain B, the plagioclase is inequigranular (up to 2.5 mm long) and the crystals are weakly to moderately altered. The alteration products comprise very fine-grained

sericite, and very fine-grained dispersions of epidote.

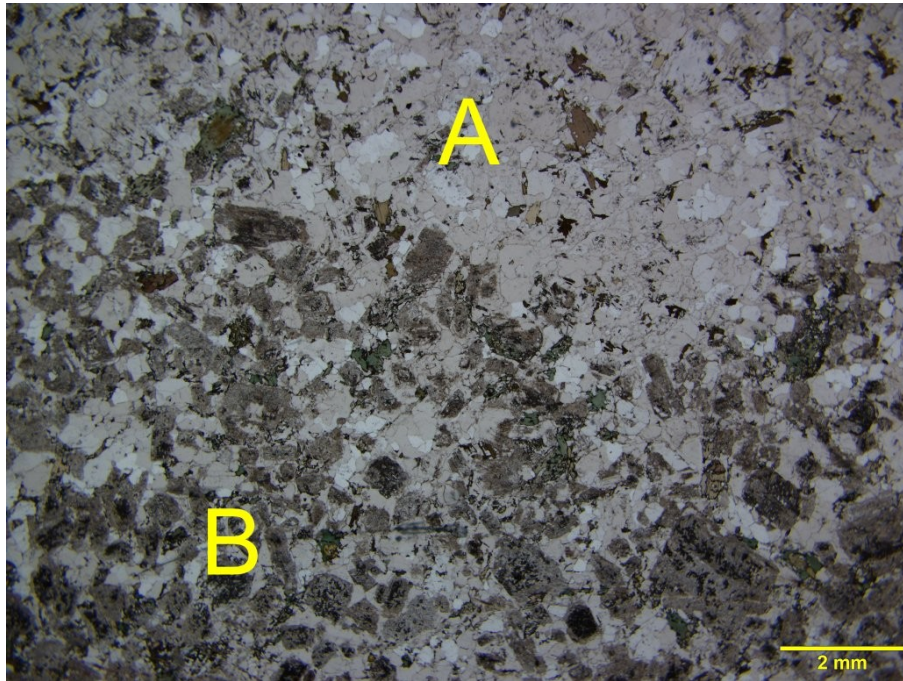
K-feldspar forms fine-grained interstitial crystals (Photomicrograph 13d) showing Albite-Pericline twinnings, thus indicating the K-feldspar is microcline.

Quartz is subordinate to the plagioclase and occurs as interstitial fine- to medium-grained crystals in Domain A (Photomicrographs 12a and 12b). In Domain B, the quartz is associated with interstitial K-feldspar, Fe-chlorite replacing biotite, and sparse anhedral crystals of epidote (Photomicrograph 13c).

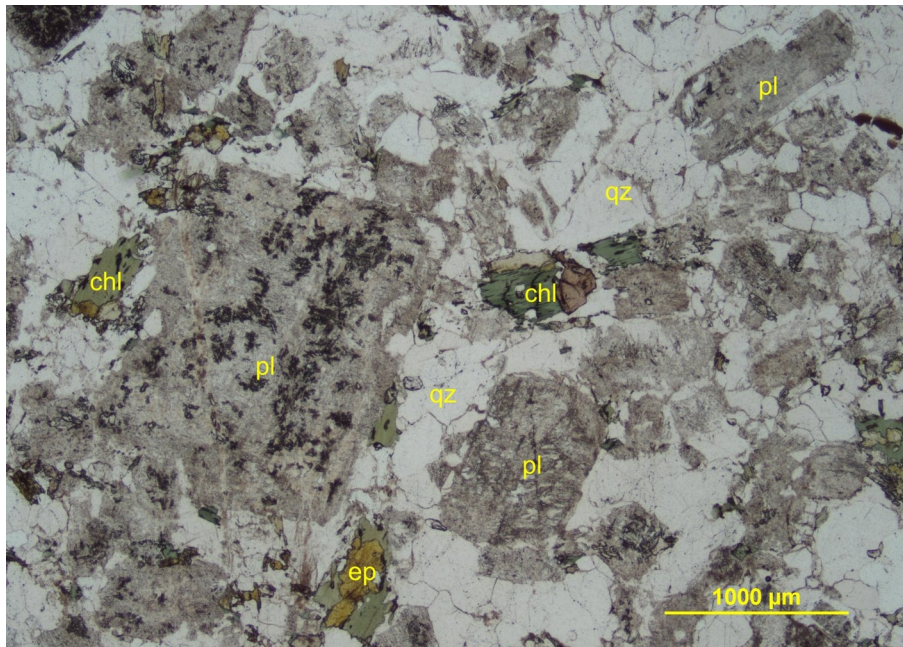
Biotite is fine- to medium-grained (up to 0.6 mm long) and the anhedral lamellae are randomly oriented within the plagioclase and quartz aggregate. The biotite hosts very fine-grained zircon inclusions and is relatively fresh in Domain A. In some cases, the Fe-chlorite moderately altered the biotite. In Domain B, Fe-chlorite and epidote strongly altered the biotite (Photomicrograph 13c).



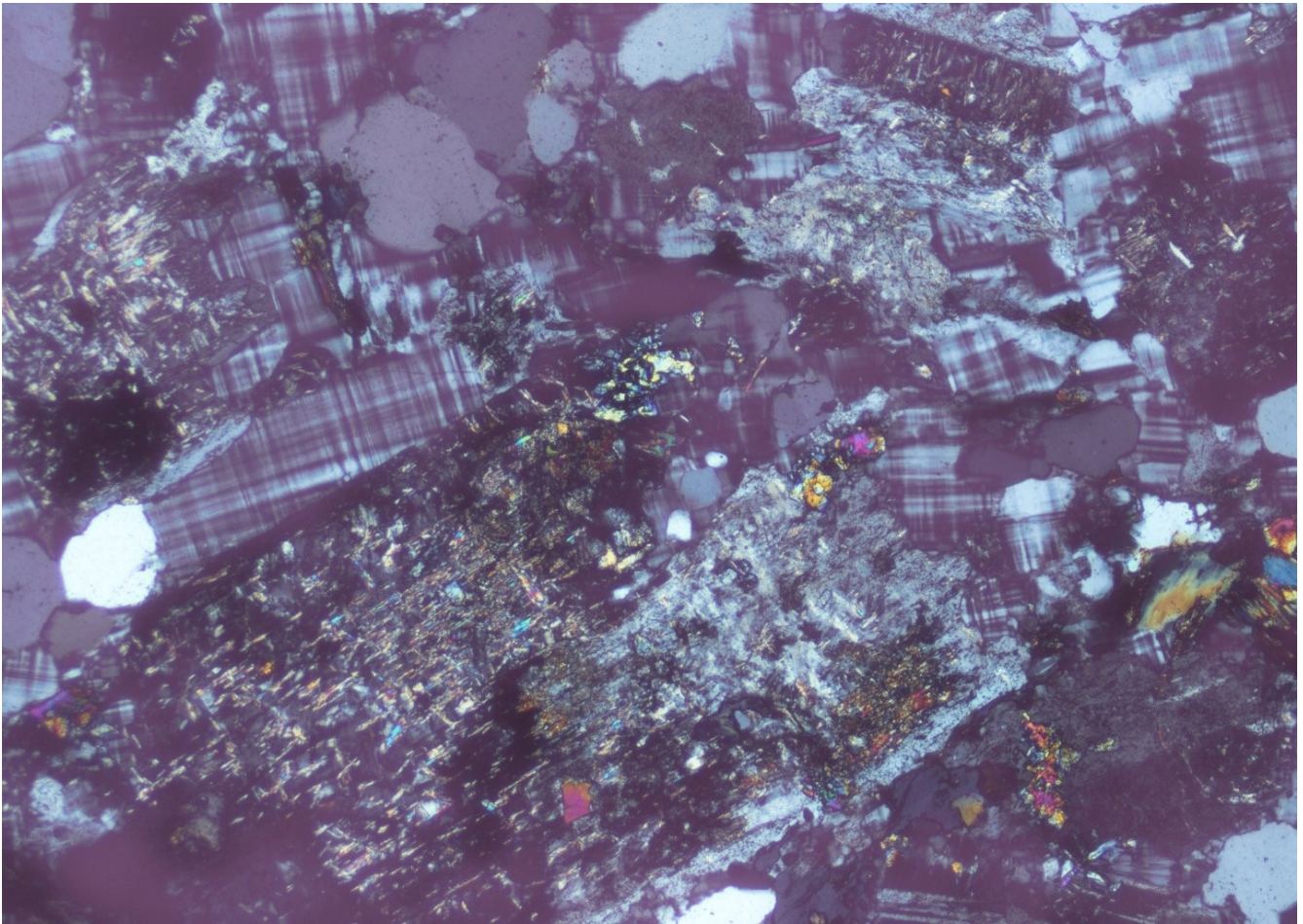
Photomicrograph 13a: The difference between Domains A and B (A and B respectively) is shown by the relatively fresh nature of plagioclase (pl) and biotite (bt) in Domain A, and the altered nature of the plagioclase in Domain B. Plane-polarized transmitted light.



Photomicrograph 13b: Another example of the different alteration intensity in Domain A (A) and Domain B (B). Plane-polarized transmitted light.



Photomicrograph 13c: Domain B—The plagioclase (pl) crystals are moderately altered to sericite and epidote, and the biotite is replaced by Fe-chlorite (chl) and epidote. Plane-polarized transmitted light.



Photomicrograph 13d: Domain B—Under crossed polarizers transmitted light the plagioclase is partially replaced by highly birefringent flakes of sericite and epidote, and interstitial K-feldspar (kfs) occurs.

Sample 14: A23-01966-14-IG_BH04_MG064

Microquartz-diorite

Microgranodiorite/microquartz-monzodiorite

Tonalite



This section is compositionally similar to Sample 12 and 13 (quartz-diorite and microgranodiorite); however, its heterogeneity is more complex and includes Domain C (tonalite). The medium-grained magmatic rock is subdivided into a relatively fresh Domain A comprising plagioclase, quartz, and biotite, and a Domain B comprising plagioclase, quartz, K-feldspar, and biotite. Both domains are crosscut by a coarser-grained and more leucocratic Domain C comprising plagioclase, quartz, K-feldspar, and biotite.

Alteration: epidote: weak after biotite; **sericite-epidote:** subtle after plagioclase; **epidote:** subtle

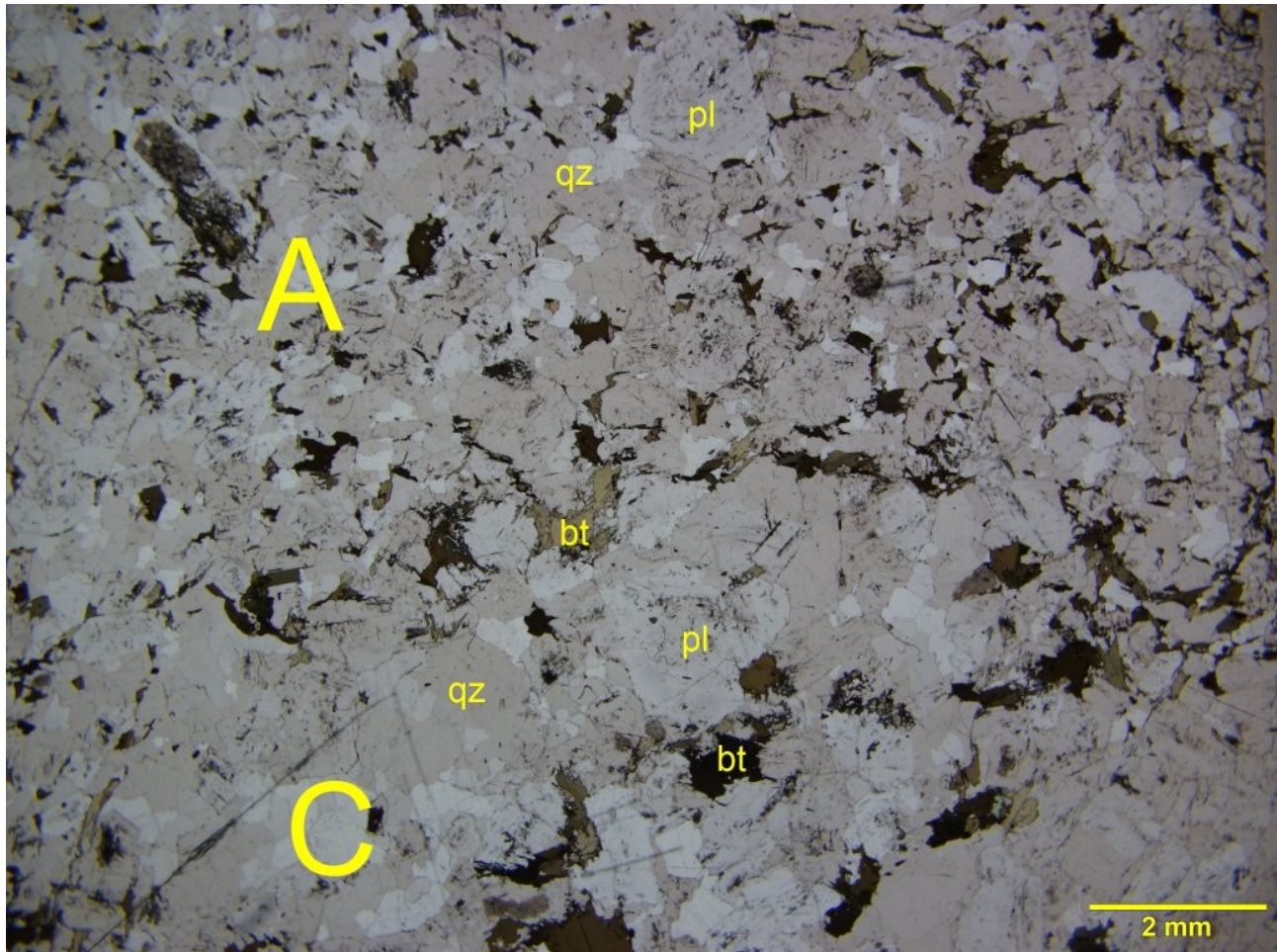
Mineral	Alteration/Weathering Mineral	Modal %	Size Range (mm)
Domain A: microquartz-diorite (~25% of PTS)			
plagioclase	sericite-epidote	14- 15	up to 2
quartz		5- 6	up to 0.5
biotite	epidote-titanite	4- 5	up to 0.4 long
zircon		tr	0.02
Domain B; microgranodiorite? (~25% of PTS)			
plagioclase	sericite-epidote	14- 15	up to 2
quartz		6- 7	up to 0.5
biotite	epidote-titanite	3- 4	0.02
K-feldspar		1- 2	up to 0.2
zircon		tr	up to 0.02
Domain C: tonalite (~50% of PTS)			
plagioclase	sericite-epidote	25- 26	up to 2
quartz		15- 16	up to 1
K-feldspar		5- 8	up to 7.5 long
biotite	epidote-titanite	3- 4	up to 1.5
zircon		tr	0.02

Plagioclase prevails in all domains. The crystals are inequigranular (up to 2 mm across), and are relatively fresh. Rare crystals are moderately altered to very fine-grained sericite and epidote. Most crystals show subhedral growth zoning and Albite twinnings. Like In Samples 12 and 13, the refractive indexes indicate the plagioclase is **albite**.

K-feldspar is heterogeneously dispersed in Domains B and C. In Domain B forms fine-grained interstitial crystals. In Domain C its poikilitic crystals are up to 7.5 mm long and host subhedral crystals of plagioclase (Photomicrograph 14c). This texture indicate the K-feldspar belongs to the magmatic crystallization stage.

Quartz forms fine- to medium-grained crystals subordinate to the plagioclase in Domain A and B, and medium-grained anhedral crystals (up to 0.6 mm across) in Domain C.

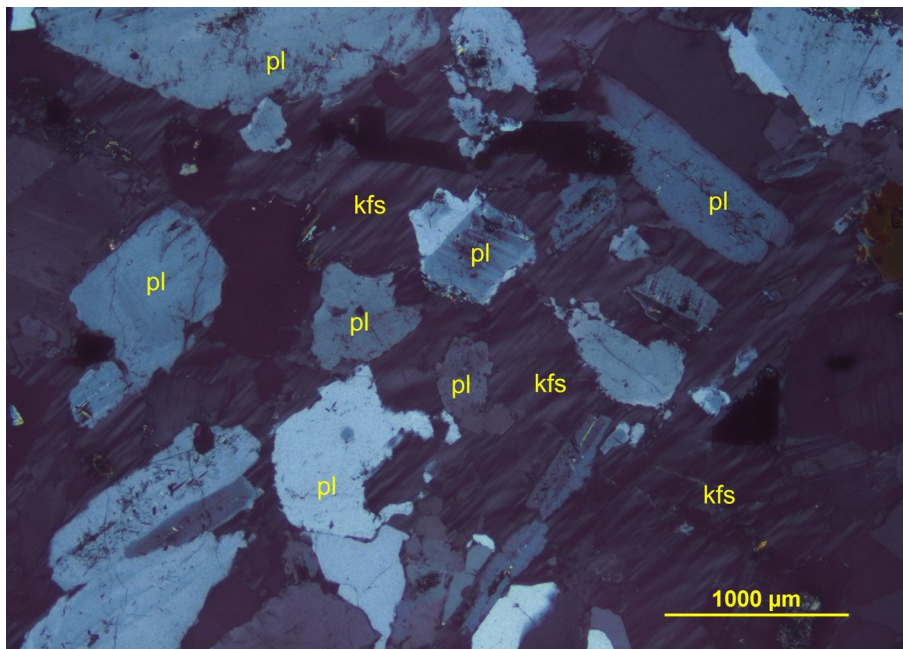
Biotite is fine- to medium-grained (up to 0.4 mm long) and randomly oriented within Domain A and B. It is coarser (up to 1.5 mm long) in Domain C. Despite its coarser size, the biotite is subordinate to the plagioclase and quartz and define a leucocratic domain easily distinguished in the offcut's image above. The biotite hosts very fine-grained zircon. Fine-grained anhedral crystals of **epidote** weakly altered the biotite.



Photomicrograph 14a: The main difference between Domain A and C is in the coarser grain-size of Domain B, and its lower content of biotite (bt) imparting a leucocratic nature. Plane-polarized transmitted light.



Photomicrograph 14b: Domain B—The biotite is randomly oriented and relatively homogeneously dispersed within the quartzofeldspathic aggregate. Plane-polarized transmitted light.



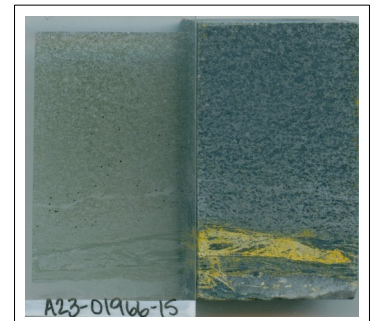
Photomicrograph 14c: Domain C. K-feldspar is poikilitic (kfs) and hosts subhedral crystals of plagioclase (pl). Crossed polarizers transmitted light.

Sample 15: A23-01966-15-IG_BH04_MG065

Albite-epidote-actinolite-chlorite granofels

Chlorite schist

Quartz vein



Most of this section consists of xenoblastic and randomly oriented crystals of amphibole, albite, chlorite and epidote. These minerals define a xenoblastic and isotropic texture in the mid- and upper part of the section. In the lower part, Chlorite is concentrated within irregular cleavage domains associated with K-feldspar microlithons defining a spaced schistosity. A quartz vein is ~2 mm thick, is oriented parallel to the schistosity defined by the chlorite domains and K-feldspar microlithons in the lower part of the section.

Mineral	Alteration/Metamorphic Mineral	Modal %	Size Range (mm)
granofels/schist (~95% of PTS)			
	Fe-chlorite	40- 42	up to 0.54 long
	actinolite	25- 27	up to 0.4 long
	epidote	15- 17	up to 0.3
	albite	5- 7	up to 0.2
	biotite	4- 5	up to 0.4 long
	K-feldspar	3- 4	0.02
	pyrite	0.1- 0.2	up to 0.3
quartz vein (~5% of PTS)			
	quartz	5	up to 0.6
	albite	tr	up to 1

Amphibole forms fine-grained xenoblastic crystals, which are randomly oriented and clustered in the mid and upper part of the section. The green colour and weak pleochroism with green tints suggests that the amphibole is **actinolite**. The amphibole is intergrown with Fe-chlorite.

Fe-chlorite is intergrown with the amphibole and in most cases is hardly distinguishable under plane-polarized transmitted light. Only the chlorite's low birefringence and straight extinction set it apart from the amphibole in the xenoblastic clusters (Photomicrograph 15b and 15c). Chlorite forms irregular and lenticular cleavage domains, which are associated with very fine-grained K-feldspar and quartz

microlithons (Photomicrograph 15a and 15d) in the lower part of the section. I interpret this schistose domain as generated by intense simple-shear, and the shear probably triggered the quartz-rich vein (Photomicrograph 15a). The chlorite epitaxially replaced biotite lamellae, which are distinguished by their stronger pleochroism and higher birefringence than the chlorite (Photomicrograph 15c).

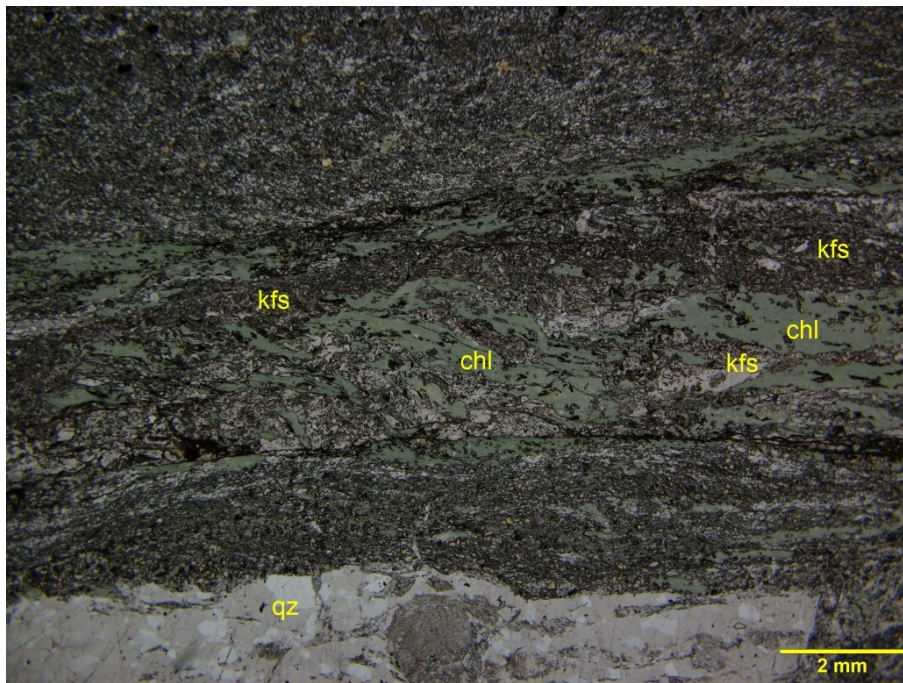
Epidote is disseminated as fine-grained xenoblastic crystals within the amphibole-chlorite clusters, and it forms very fine-grained inclusions hosted in the xenoblastic albite (Photomicrograph 15b and 15c).

Albite forms fine-grained xenoblastic and poikiloblastic crystals in the granofels (Photomicrograph 15b and 15c).

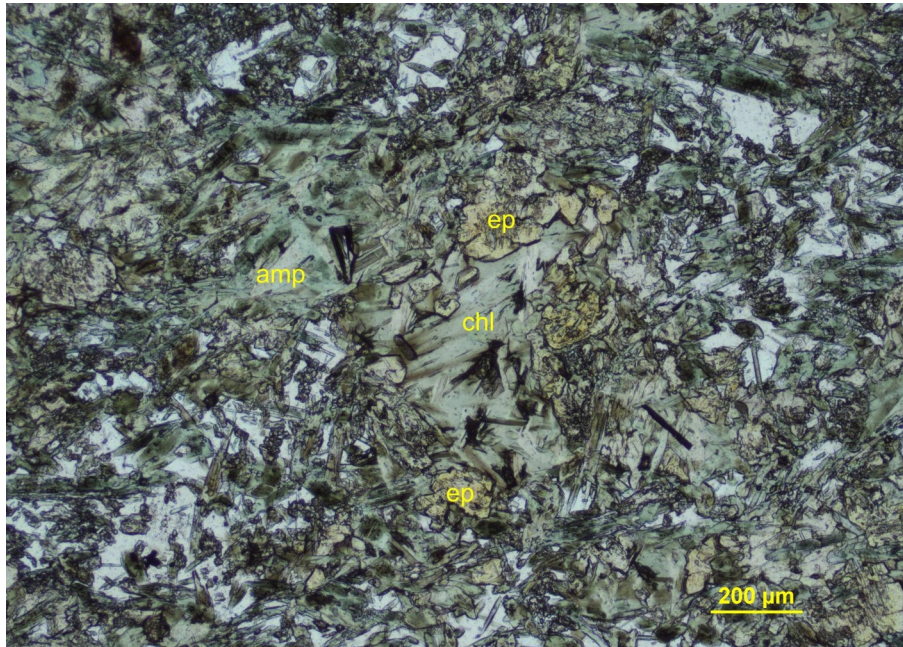
K-feldspar is concentrated within a 4 mm thick domain comprising irregular and lenticular cleavage domains of chlorite and very fine-grained microlithons of K-feldspar, quartz, and probable albite (Photomicrograph 15d).

Quartz is concentrated within a 2 mm thick vein in the lower part of the section (Photomicrograph 15a). The medium-grained (up to 0.6 mm across) blocky and interlobate crystals host sparse porphyroclasts (up to 1 mm across) of albite.

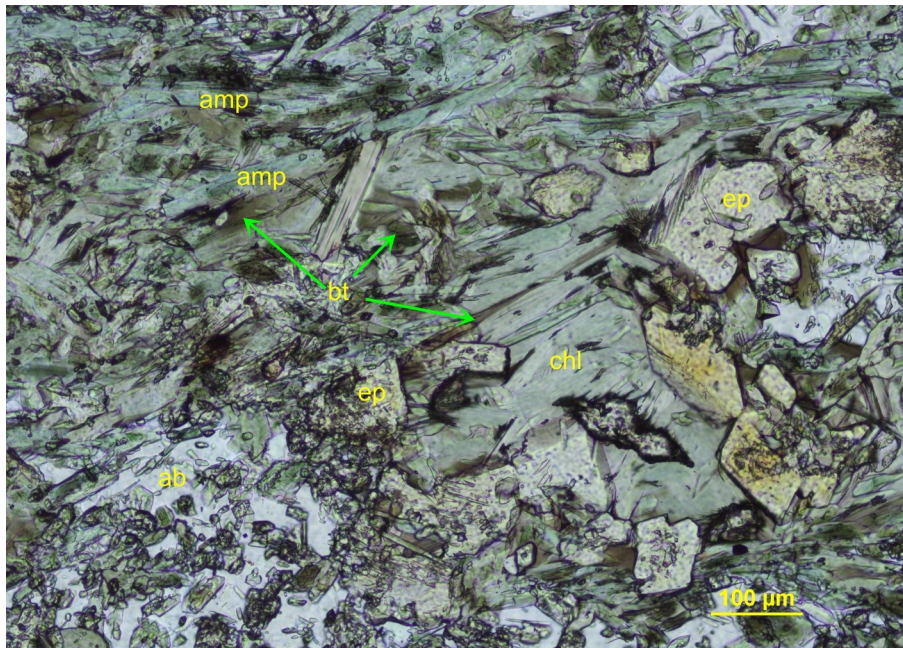
Pyrite is disseminated as fine-grained (up to 0.3 mm across) and subidioblastic crystals in the granofels.



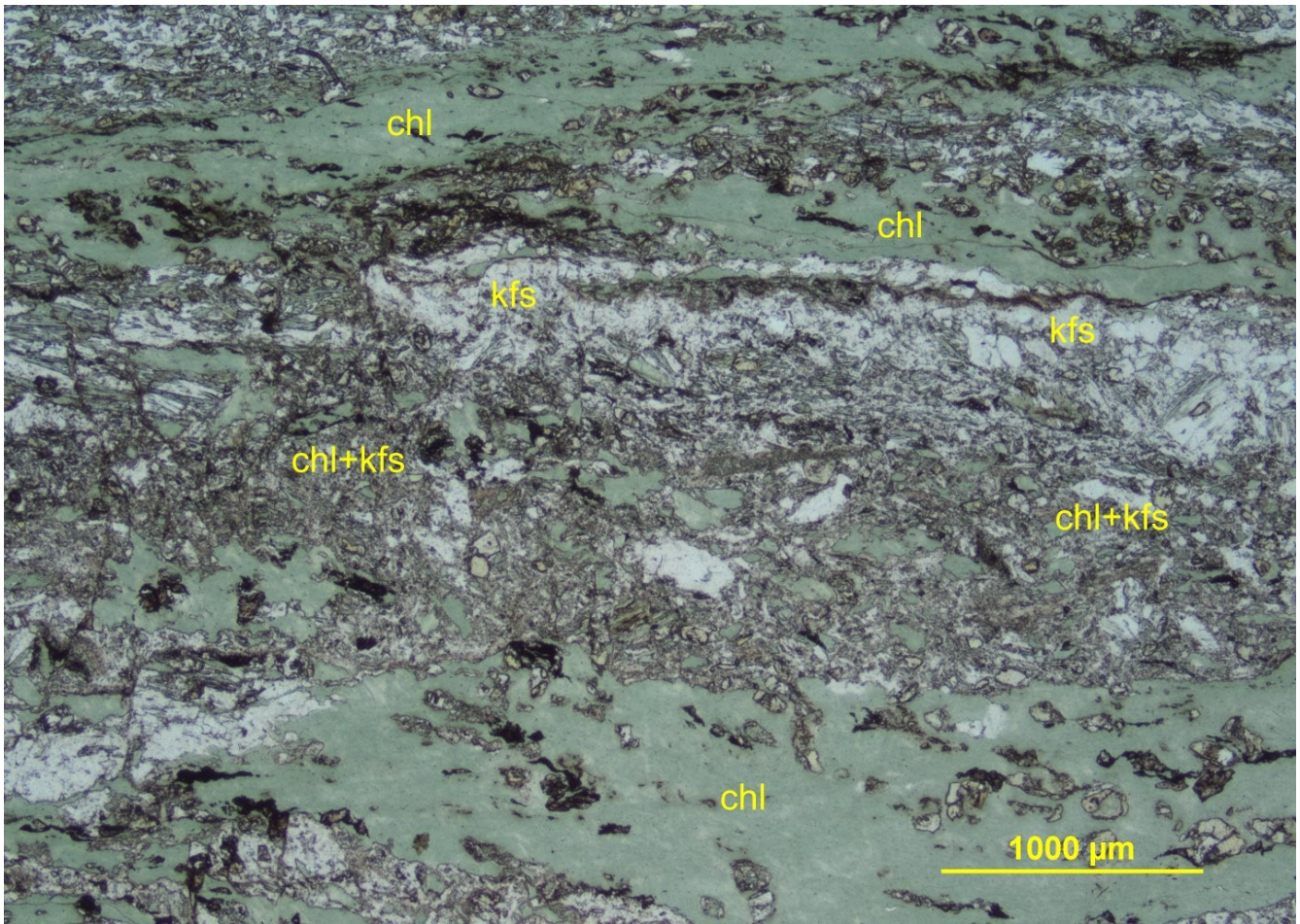
Photomicrograph 15a: The xenoblastic and isotropic texture of the granofels in the upper part of the photomicrograph is associated with a schistose texture defined by chlorite-rich cleavage domains (chl) and K-feldspar-rich microlithons (kfs). A quartz-vein (qz) is oriented parallel to the schistosity. Plane-polarized transmitted light.



Photomicrograph 15b: Amphibole (amp) and chlorite (chl) define irregular clusters overprinted by epidote (ep) in the granofels. Plane-polarized transmitted light.

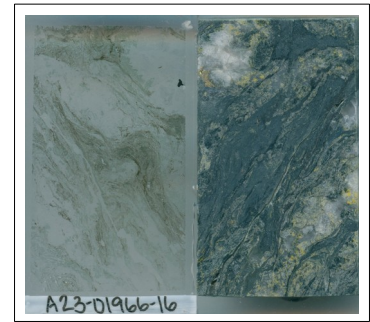


Photomicrograph 15c: Another example of the actinolite (amp) and chlorite (chl) clusters overprinted by xenoblastic epidote. The chlorite partially and epitaxially replaced biotite lamellae (bt). Albite (ab) is xenoblastic, poikiloblastic, and hosts very fine-grained epidote crystals. Plane-polarized transmitted light.



Photomicrograph 15d: In the sheared domain, the chlorite (chl) forms irregular cleavage domains alternated with very fine-grained microlithons of K-feldspar (kfs) and subordinate chlorite, quartz, and probable albite. Plane-polarized transmitted light.

Sample 16: A23-01966-16-IG_BH04_MG066



Pyrite-calcite-chlorite-retrometamorphosed actinolite schist

Amphibole, chlorite, and relic biotite define a rough schistosity, which is disharmonically folded and wraps lenticular and irregularly shaped microlithons comprising plagioclase, chlorite, calcite, and quartz.

Alteration/Metamorphism: **chlorite:** moderate to strong after biotite; **calcite:** moderate; **pyrite:** subtle

Mineral	Alteration/Metamorphic Mineral	Modal %	Size Range (mm)
plagioclase		33- 35	up to 6 long
[biotite?]	chlorite	30- 32	up to 0.4
actinolite		22- 24	up to 0.2 long
	calcite	10- 12	up to 1
quartz		2- 3	up to 0.4
biotite		1- 2	up to 0.5 long
	pyrite	tr	up to 1

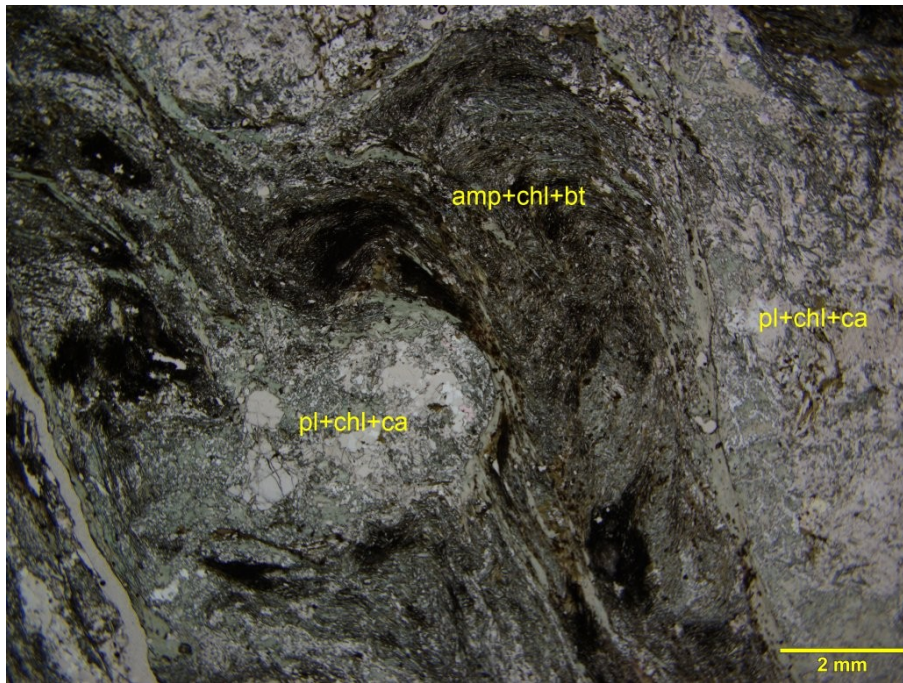
Amphibole forms elongated prisms and xenoblastic crystals, which are preferentially iso-oriented and concentrated within irregular cleavage domains. The amphibole shows a moderate relief, weak green pleochroism and oblique extinction of its elongate crystals, and I interpret these features as belonging to the **actinolite**-series.

Chlorite occurs as fine- to medium-grained xenoblastic crystals. It is intergrown with the actinolite in the cleavage domains, and it is intergrown with the plagioclase in the microlithons. Within the microlithons, the chlorite is heterogeneously dispersed as xenoblastic patches (up to 0.4 mm across). Chlorite partially and epitaxially replaced biotite relics (Photomicrograph 16d).

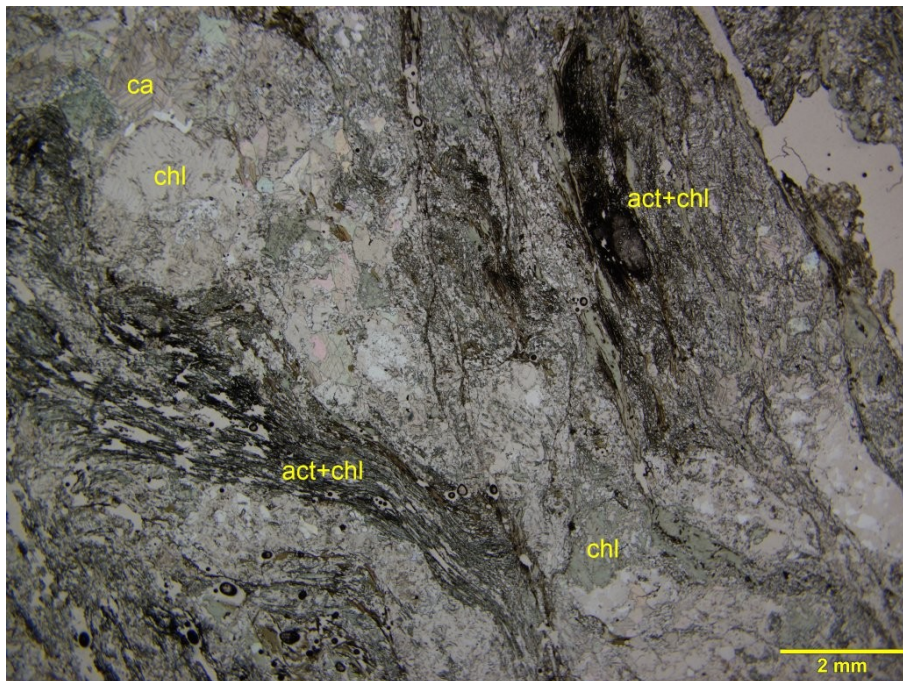
Plagioclase forms xenoblastic crystals concentrated within lenticular and irregularly shaped microlithons. In some microlithons, the plagioclase forms subidioblastic crystals up to 6 mm long. The coarse-grained plagioclase crystals show Albite twinnings, and are fractured and filled in by calcite (Photomicrograph 16c).

Quartz is subordinate to and it is spatially associated with the plagioclase in the granular microlithons.

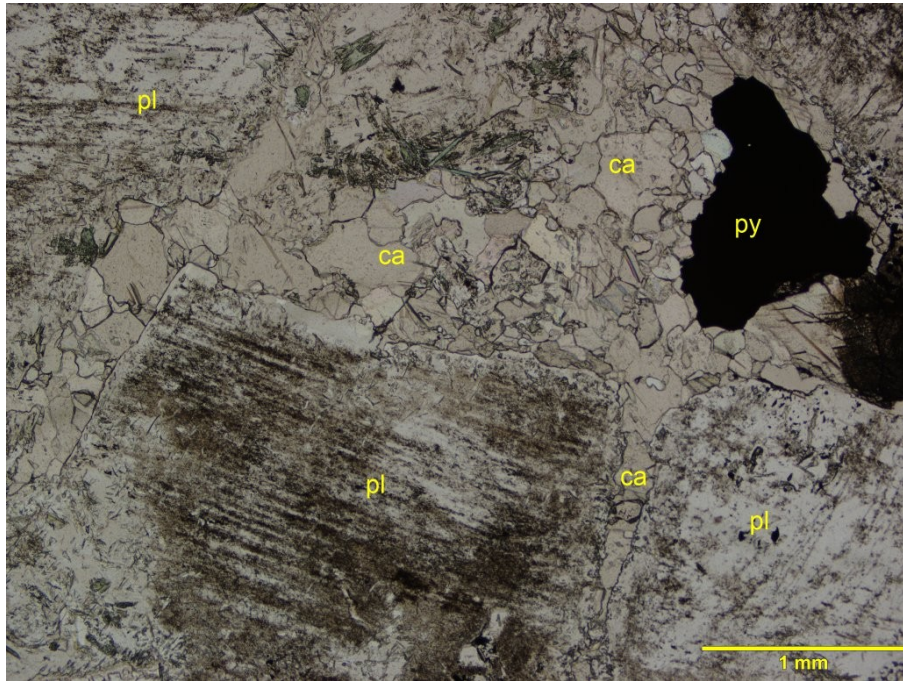
Very rare **pyrite** crystals (up to 1 mm across) are dispersed within the plagioclase and calcite microlithons.



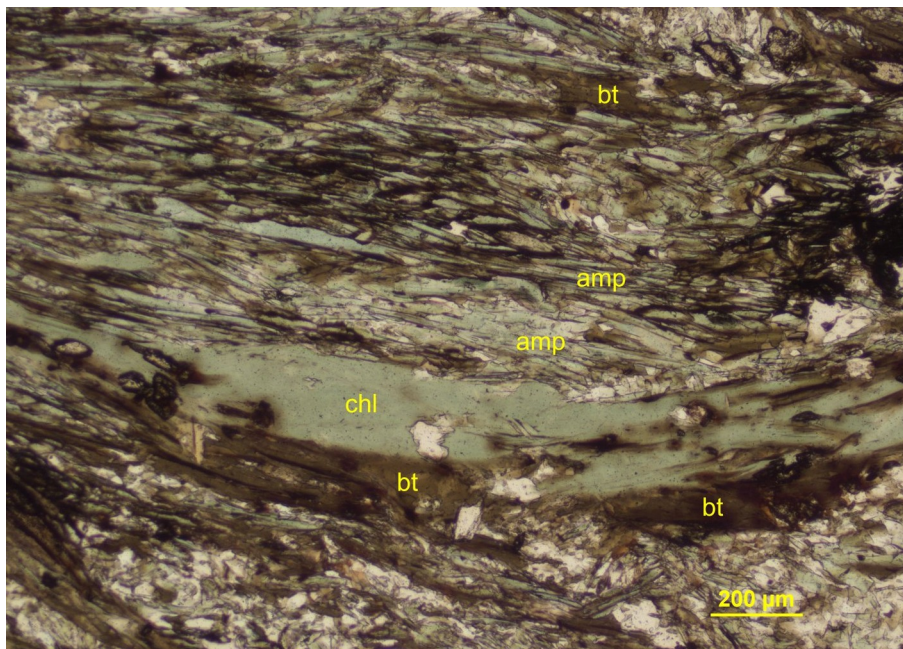
Photomicrograph 16a: The amphibole, chlorite, and biotite are concentrated within disharmonically folded cleavage domains, which wraps granular microlithons comprising plagioclase, chlorite, and calcite (pl+chl+ca). Plane-polarized transmitted light.



Photomicrograph 16b: Another example of the heterogeneous and disharmonically folded texture defined by the cleavage domains and the microlithons. Plane-polarized transmitted light.

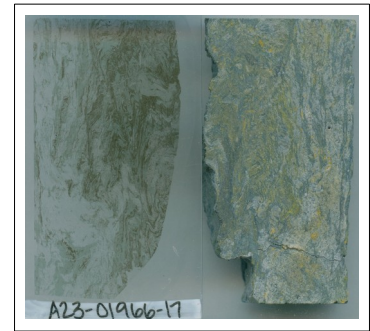


Photomicrograph 16c: In some microlithons, the plagioclase (pl) is fractured and filled in by calcite (ca). Very rare pyrite (py) is dispersed within the calcite-rich part of the microlithons. Plane-polarized transmitted light.



Photomicrograph 16d: Within the cleavage domains, it is the actinolite (amp) that mostly defines the schistosity. The chlorite (chl) partially replaced the biotite (bt), and crystallized during and after the deformation. Plane-polarized transmitted light.

Sample 17: A23-01966-17-IG_BH04_MG067



Chlorite-retrometamorphosed biotite schist

Tightly folded cleavage domains of chlorite and biotite define a crenulated schistosity associated with fine-grained granoblastic domains of calcite and quartz. The chlorite partially overprinted the biotite, which likely defined the schistosity during the folding event.

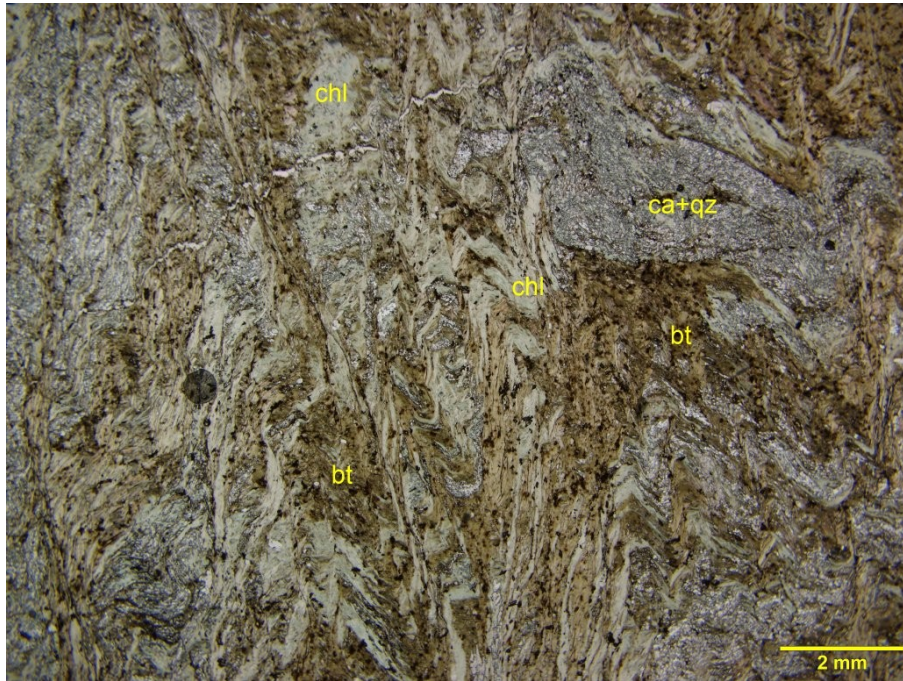
Alteration/Metamorphism: chlorite: moderate to strong after biotite; calcite: moderate; chalcopyrite: subtle

Mineral	Alteration/Metamorphic Mineral	Modal %	Size Range (mm)
biotite	chlorite	60- 62	up to 0.4
calcite		20- 22	up to 0.8
quartz		15- 17	up to 0.1
plagioclase(?)		1- 2	up to 0.1
	titanite	0.1- 0.2	up to 0.1
zircon		tr	up to 0.05
	chalcopyrite	tr	up to 0.05

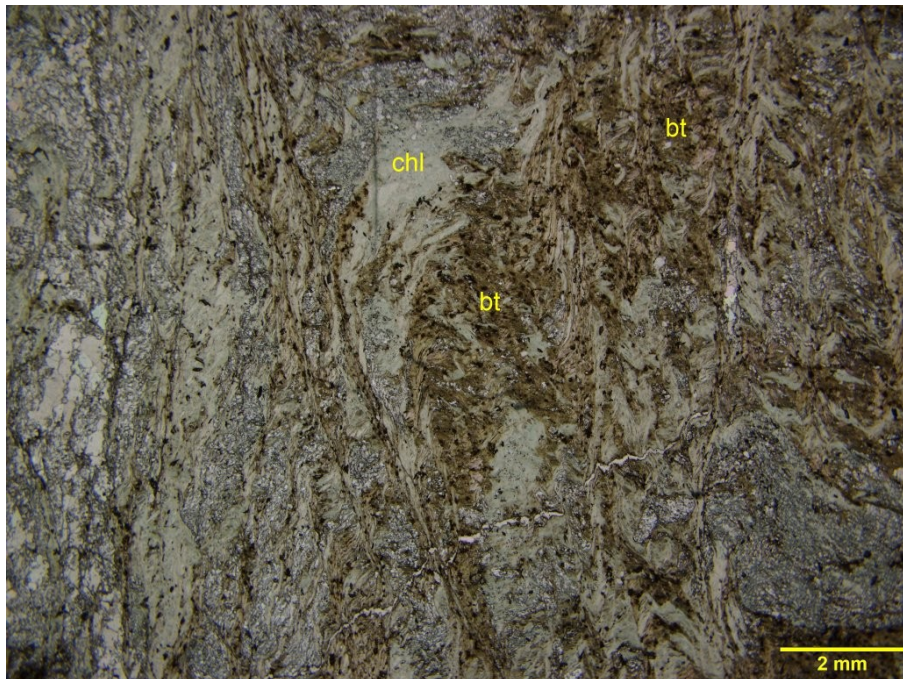
Chlorite moderately to strongly altered the biotite and define tightly folded cleavage domains (Photomicrographs 17a, 17b, 17d and 17e) and irregular patches filling the strain shadows between the calcite, quartz, and plagioclase microlithons. As already interpreted in the similar Sample 16, I interpret the biotite as the primary mineral defining the schistosity, and the the folded schistosity in this sample. The chlorite epitaxially replaced the **biotite** during the latest stages of the metamorphic event, and overprinted the schistosity as randomly oriented lamellae and flakes. The biotite hosts abundant and very fine-grained zircon, which is distinguished by its typical pleochroic halo generated in the hosting biotite.

Calcite forms fine-grained xenoblastic crystals, which together with the quartz and the plagioclase define the fine-grained granular microlithons.

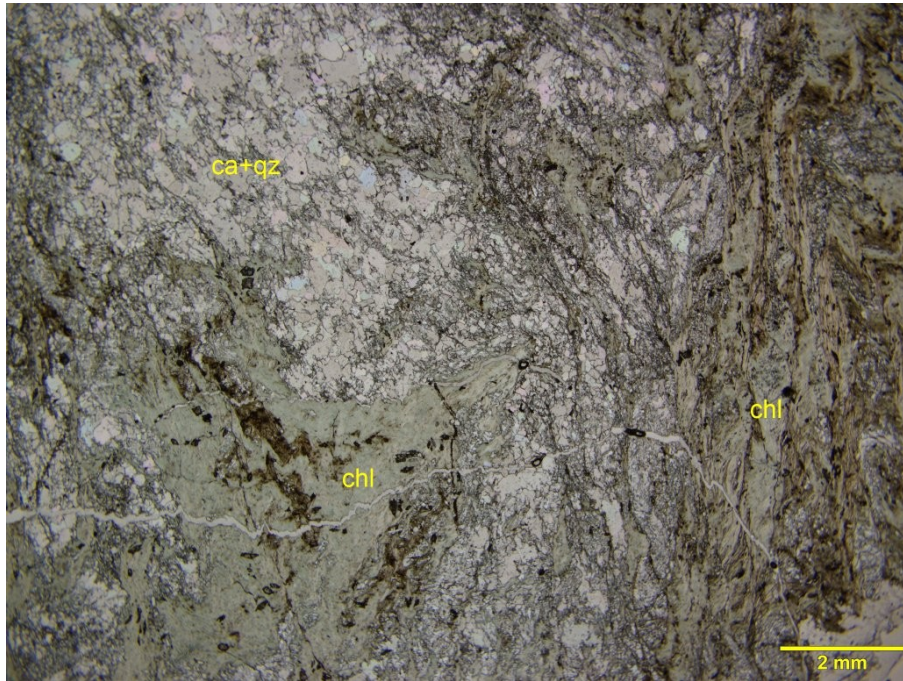
Quartz is fine-grained and it is subordinate to the calcite in the granoblastic microlithons. I suspect the occurrence of **plagioclase**; however, the plagioclase is not positively identified in this section.



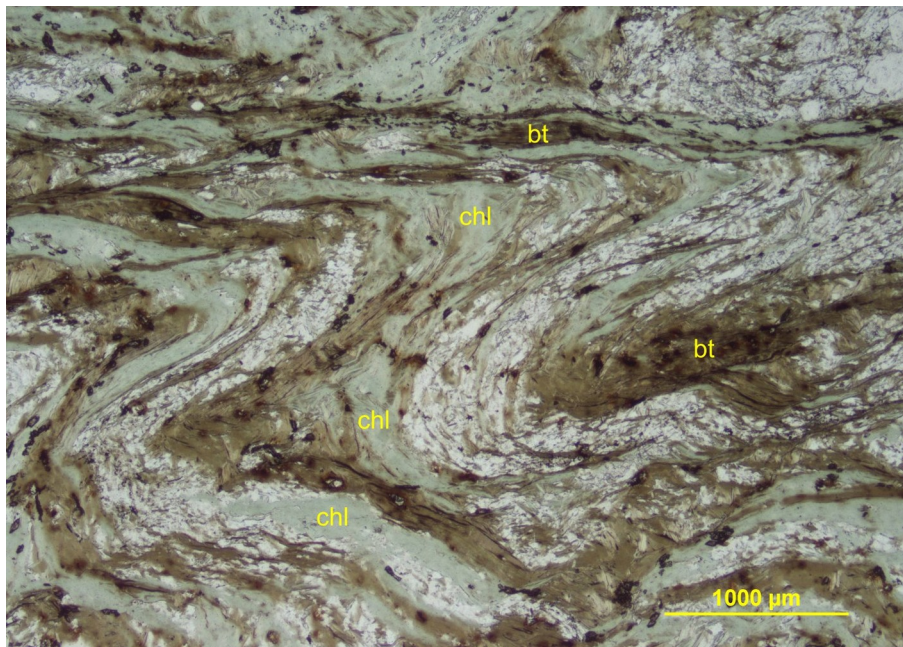
Photomicrograph 17a: Chlorite (chl) partially replaced the biotite (bt) and defines tightly folded cleavage domains. Plane-polarized transmitted light.



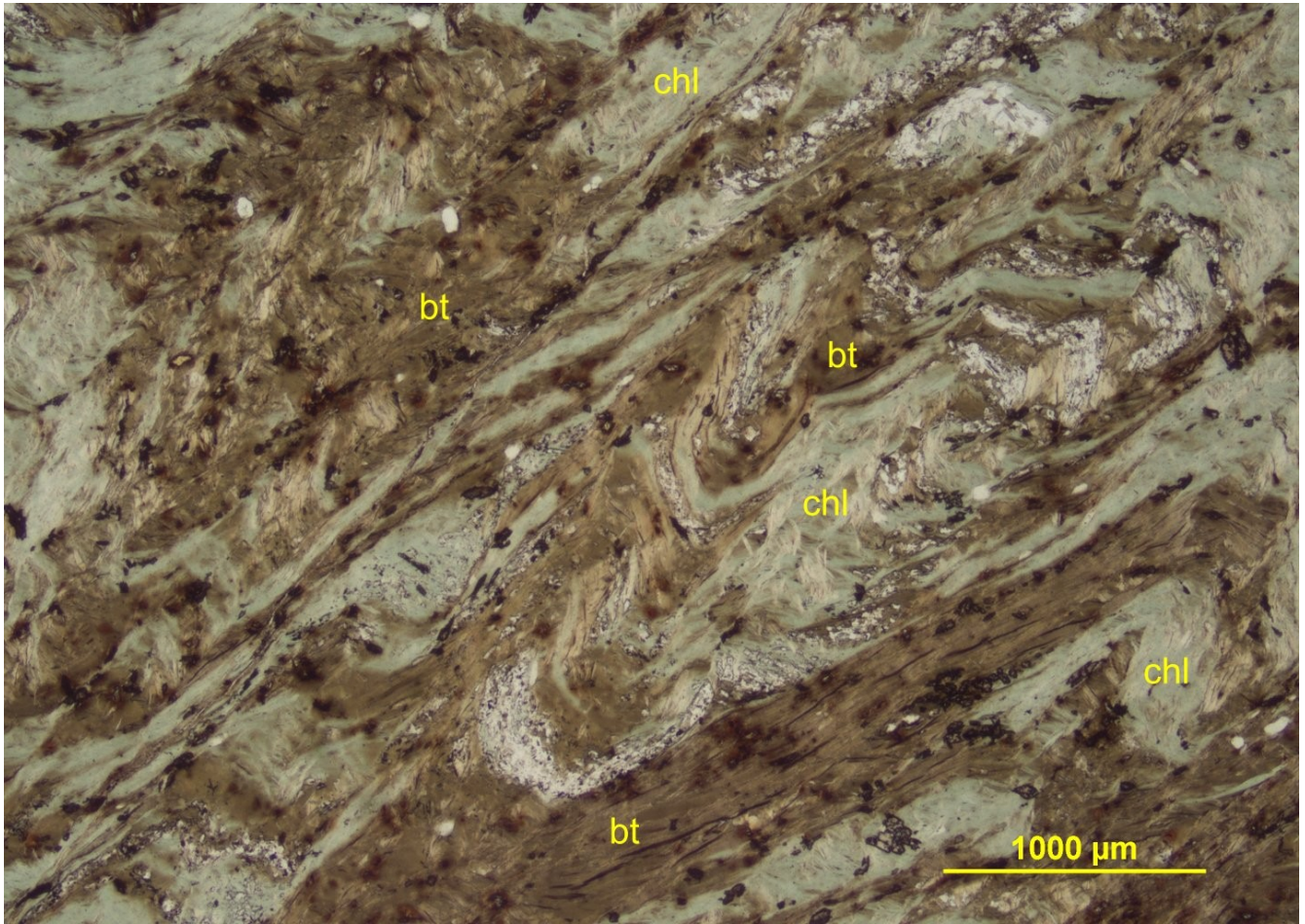
Photomicrograph 17b: Another example of the chlorite (chl) replacement of biotite in the tightly folded cleavage domains. Plane-polarized transmitted light.



Photomicrograph 17c: The chlorite-replaced domain (chl) in the lower left of this photomicrograph occupies the strain shadows between the calcite and quartz (ca+qz) microlithons. Plane-polarized transmitted light.



Photomicrograph 17d: The cleavage domains defined by the chlorite (chl) replacing the biotite (bt) are tightly and isoclinally folded and alternate with the granoblastic domains of quartz, chlorite and calcite. Plane-polarized transmitted light.



Photomicrograph 17e: Disharmonically folded biotite (bt) is partially replaced by chlorite (chl). Plane-polarized transmitted light.

Sample 18: A23-01966-18-IG_BH04_MG068



Microtonalite

Epidote-Fe-chlorite-sericite microgranodiorite/microquartz-monzodiorite

K-feldspar veinlet

This section comprises a relatively fresh Domain A comprising plagioclase, quartz, biotite, and K-feldspar and a Domain B comprising plagioclase, quartz, K-feldspar, and biotite. The boundary between the two domains is gradual and point to a magmatic mingling process.

Alteration: sericite-epidote: subtle after plagioclase in Domain A; moderate after plagioclase in Domain B; **Fe-chlorite-epidote-titanite:** strong after biotite in Domain B.

Mineral	Alteration/Weathering Mineral	Modal %	Size Range (mm)
Domain A: tonalite (~50% of PTS)			
plagioclase	sericite	23- 24	up to 2.5
quartz		22- 23	up to 0.5
K-feldspar		2- 3	up to 3
biotite	epidote-titanite	1.5- 2	
zircon		tr	
Domain B altered microgranodiorite? (~50% of PTS)			
plagioclase	sericite-epidote	11- 12	up to 2.5
quartz		8- 9	up to 0.5
K-feldspar (microcline)		1- 2	up to 0.2
biotite	Fe-chlorite-epidote-titanite	1- 2	[up to 0.6]
	calcite	tr	0.2
zircon		tr	0.01
K-feldspar veinlet (tr)			
K-feldspar		tr	up to 0.2

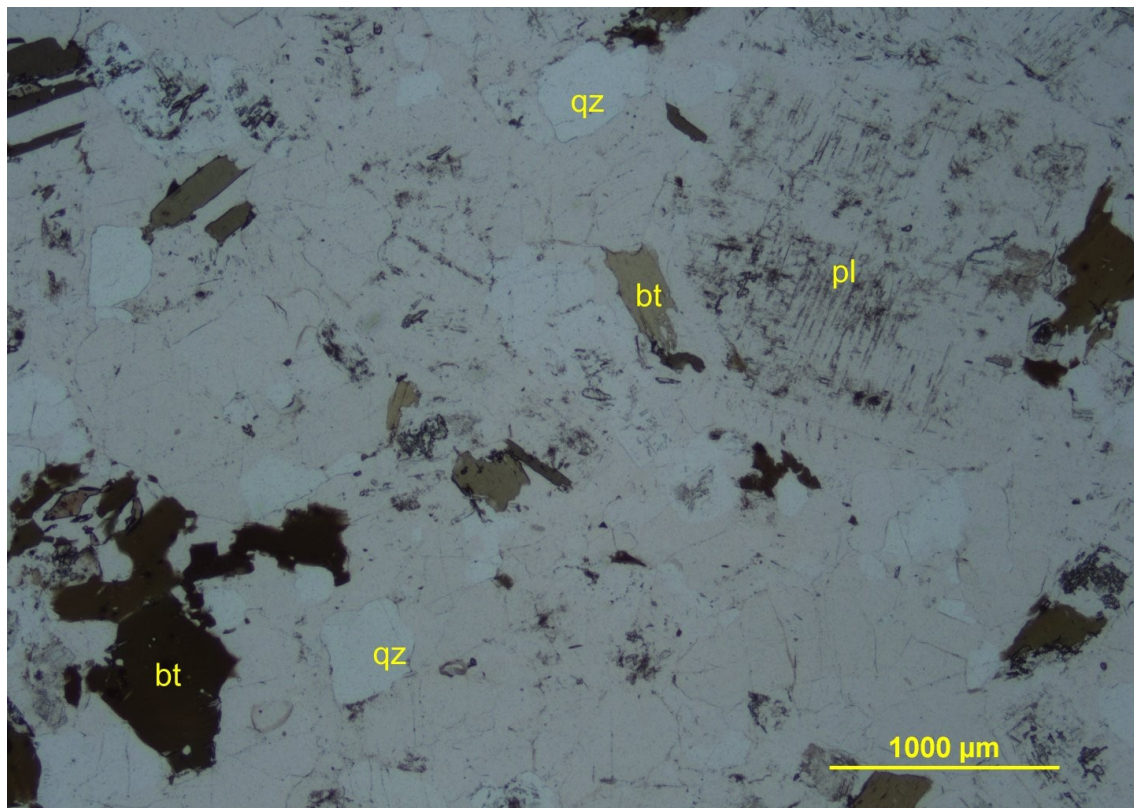
Plagioclase prevails in both domains. The crystals are inequigranular (up to 2 mm across), and are relatively fresh in Domain A. Rare crystals are moderately altered to very fine-grained **sericite** and epidote. In Domain B, the plagioclase (up to 2.5 mm long) crystals are weakly to moderately altered

(Photomicrograph 18d) to very fine-grained sericite and subordinate very fine-grained **epidote**.

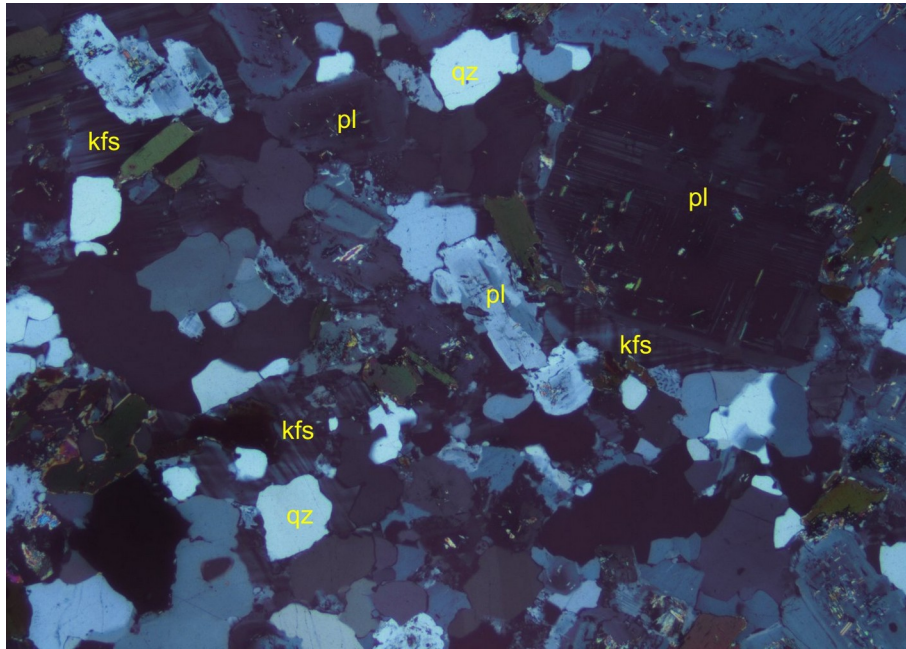
K-feldspar is heterogeneously dispersed in Domains A and B. In Domain A its poikilitic crystals are up to 3 mm across and hosts subhedral crystals of plagioclase and quartz (Photomicrograph 18c). This texture indicates the K-feldspar belongs to the magmatic crystallization stage. In Domain B, the K-feldspar is mostly fine-grained and interstitial and show Albite-Pericline twinnings in most of its occurrences. I would interpret also in this domain the K-feldspar as a primary magmatic mineral. A K-feldspar veinlet crosscut Domain B and show that the K-feldspar circulated in this domain after its magmatic crystallization.

Quartz forms fine- to medium-grained crystals subordinate to the plagioclase in both domains. In Domain A, the quartz is more abundant than in Domain B, and its amount is comparable to the plagioclase.

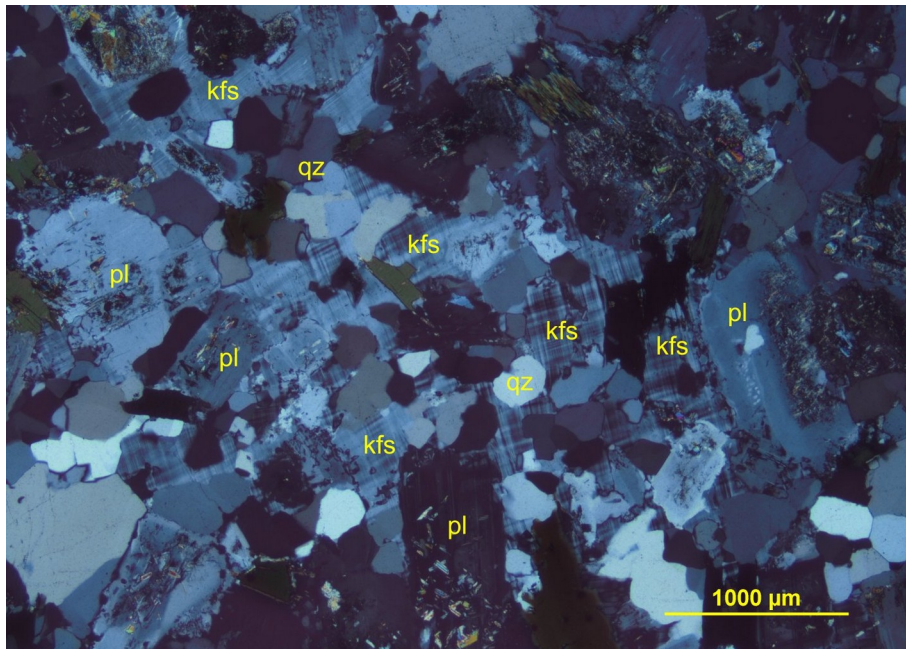
Biotite is fine- to medium-grained (up to 0.7 mm long), subhedral, and randomly oriented within Domain A (Photomicrograph 18a). In Domain B, the anhedral and up to 1 mm across biotite crystals are completely replaced by epitaxial **Fe-chlorite**, epidote, and **titanite** (Photomicrograph 18e).



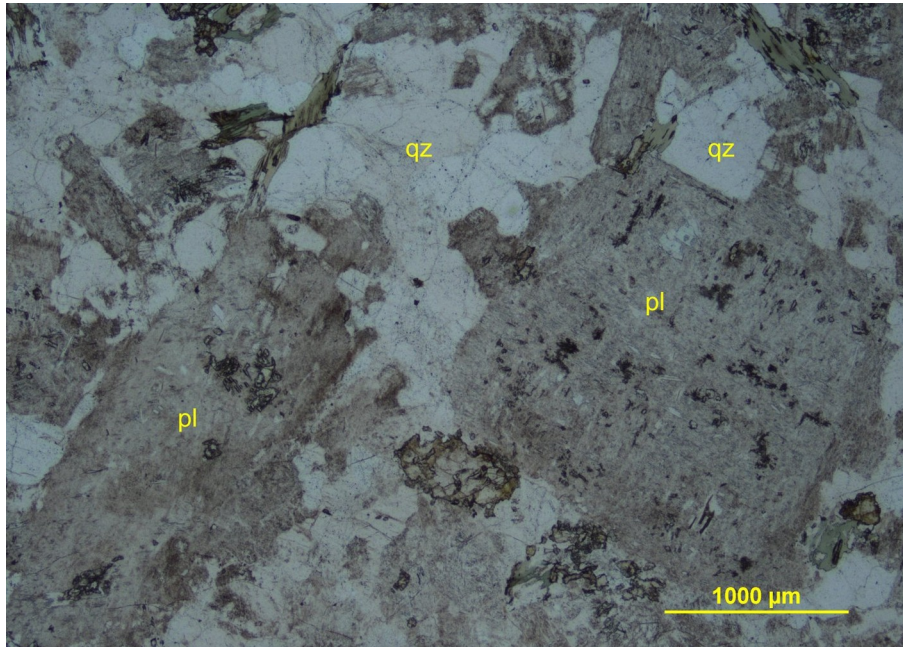
Photomicrograph 18a: Domain A—Plagioclase (pl) and quartz are associated with subordinate and randomly oriented biotite (bt) defining a granular and relatively unaltered texture. Plane-polarized transmitted light.



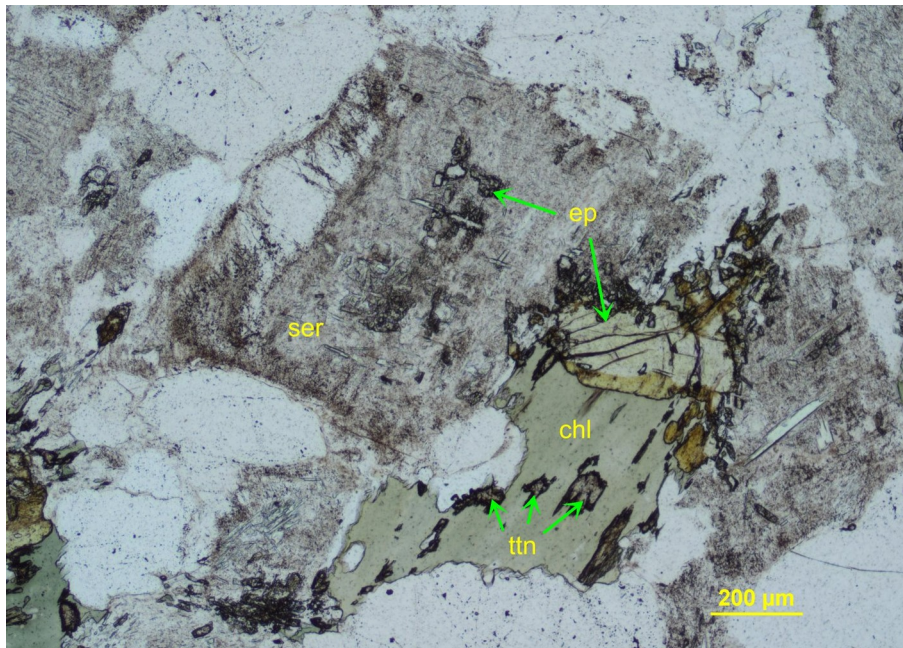
Photomicrograph 18b: Domain A—Same area as shown in Photomicrograph 18a, The plagioclase is relatively fresh and displays Albite twinings and in some cases growth zonation. The subhedral plagioclase (pl) is intergrown with interstitial K-feldspar (kfs) and quartz (qz). Crossed polarizers transmitted light.



Photomicrograph 18c: Domain A—Sparse poikilitic K-feldspar hosts plagioclase (pl) and quartz crystals (qz). Crossed polarizers transmitted light.

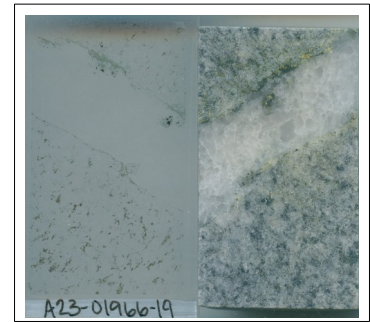


Photomicrograph 18d: Domain B—Subhedral plagioclase crystals are moderately altered and, together with the quartz, define a granular texture. Plane-polarized transmitted light.



Photomicrograph 18e: Domain B—Sericite (ser) and subordinate epidote (ep) moderately altered the plagioclase. Fe-chlorite (chl), epidote (ep) and titanite (ttn) completely replaced the biotite. Plane-polarized transmitted light.

Sample 19: A23-01966-19-IG_BH04_MG069



Chlorite-Sericite-altered microtonalite

Quartz vein

A ~10 mm thick quartz vein crosscut a medium-grained granular texture defined by anhedral plagioclase, quartz, and biotite.

Alteration: white mica: weak to moderate after plagioclase; **chlorite>titanite:** moderate to strong after biotite

Mineral	Alteration/Weathering Mineral	Modal %	Size Range (mm)
microtonalite (~75% of PTS)			
plagioclase (albite)	white mica	49- 50	up to 1
quartz		19- 20	up to 0.7
biotite	chlorite	4- 5	up to 0.3
zircon		tr	0.01
quartz vein (~25% of PTS)			
quartz		24- 25	up to 4 long
pyrite		0.1	up to 0.5
sphalerite		tr	up to 0.3 long
chalcopyrite		tr	up to 0.1

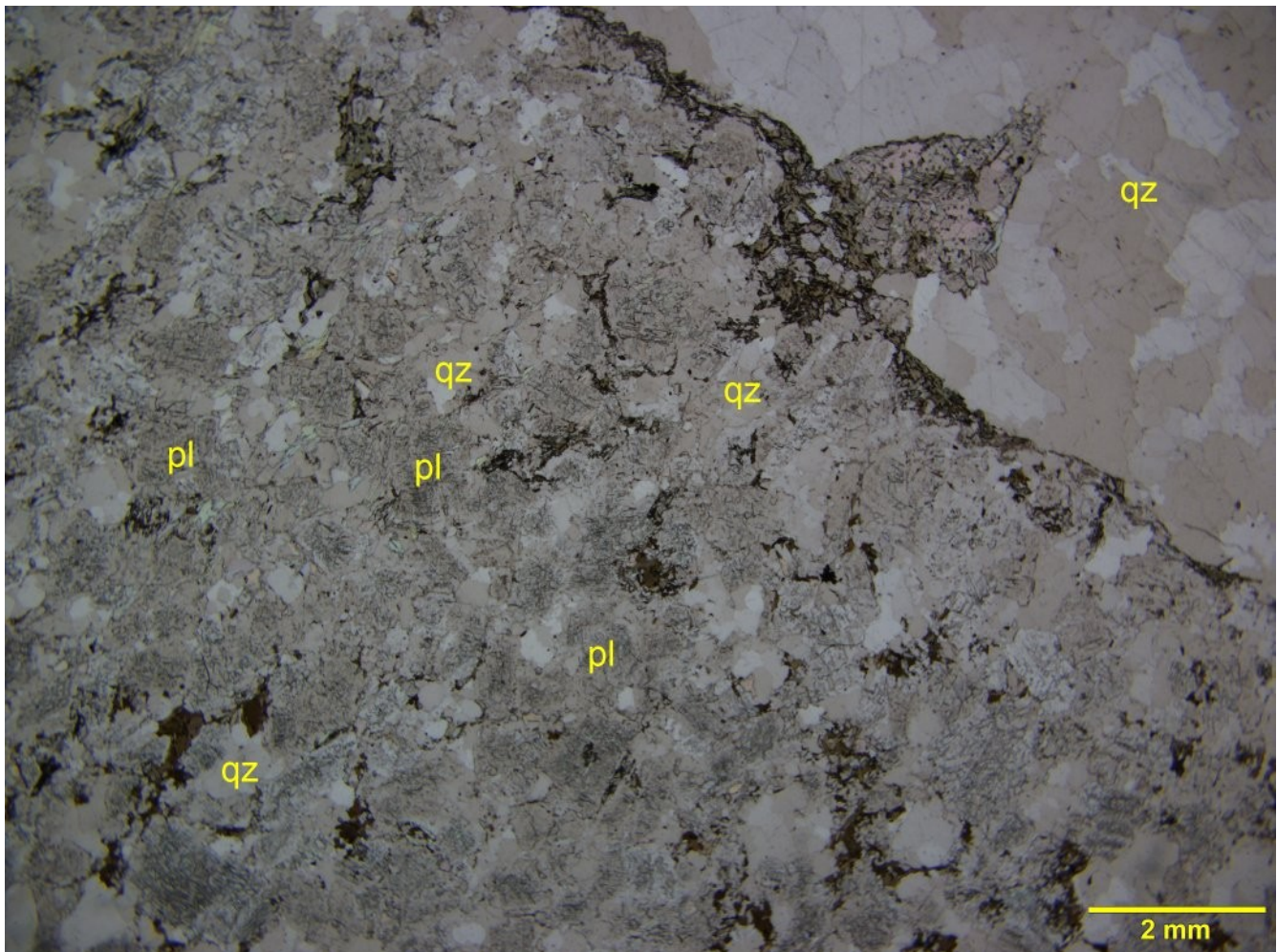
Plagioclase (albite) occurs as medium-grained (up to 1 mm across) anhedral crystals intergrown with the quartz and biotite. The plagioclase crystals show Albite twinings and refractive indexes lower than those of the quartz. Fine-grained flakes of white mica weakly to moderately altered the plagioclase crystals.

Quartz forms fine- to medium-grained crystals in the host rock and it is concentrated as coarse-grained (up to 4 mm long) crystals in the 10 mm thick quartz vein. Within the host rock, the quartz forms monomineralic crystal aggregates, and in some aggregates, the quartz forms polygonal crystal aggregates. Within the vein, the quartz shows interlobate crystal boundaries.

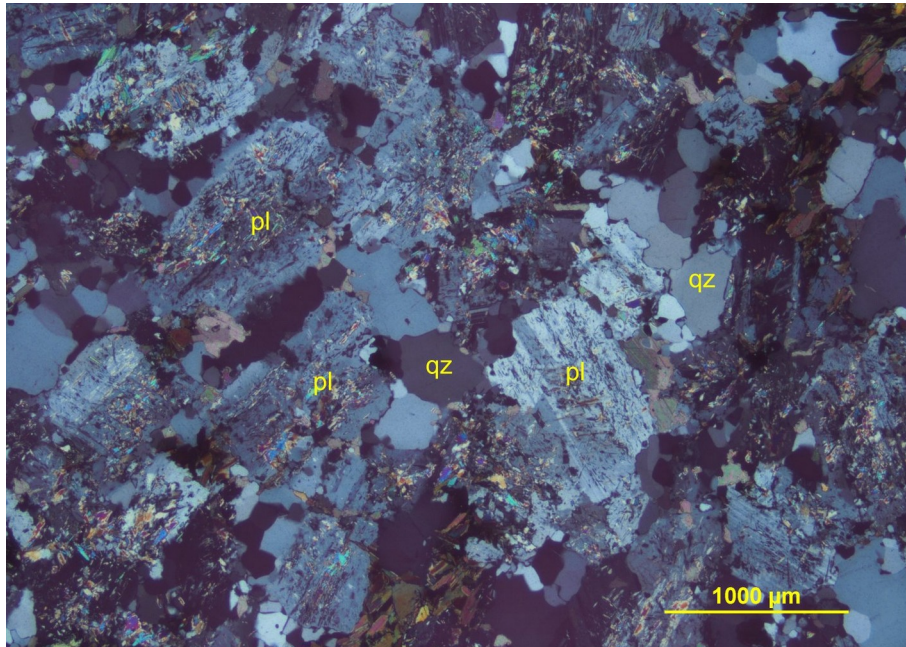
Biotite forms fine-grained crystals and crystal clusters within the interstitial positions between the plagioclase crystals and the quartz crystal aggregates. In some parts of the section, the chlorite moderately to strongly replaced the biotite. The epitaxial replacement is associated with very fine-

grained dispersions of titanite. The biotite hosts very fine-grained inclusions of **zircon**.

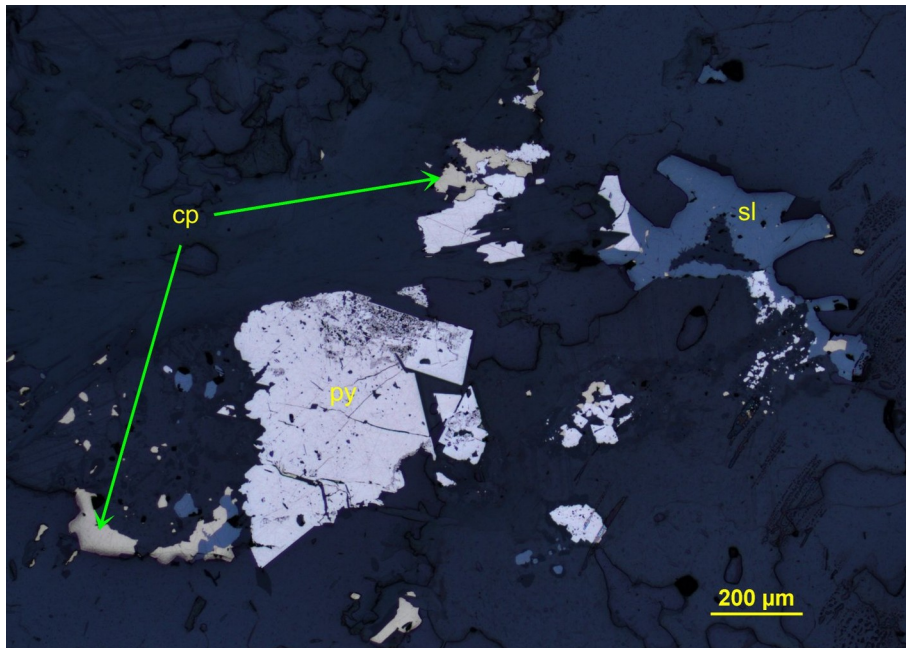
Pyrite is dispersed along the vein-walls as fine-grained anhedral and subhedral crystals. In one instance, the pyrite is associated with **sphalerite** and **chalcopyrite** (Photomicrograph 19c).



Photomicrograph 19a: Anhedra plagioclase (pl) and quartz (qz) and biotite define a granular texture, which is crosscut by a quartz vein (qz in the upper right part of the photomicrograph). Plane-polarized transmitted light.

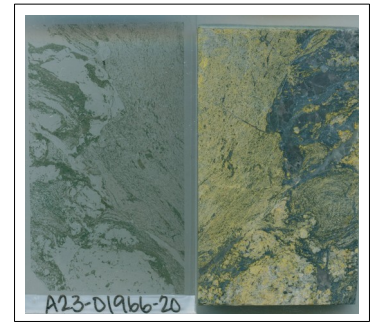


Photomicrograph 19b: Anhedral plagioclase (pl) and quartz define the granular texture in the host rock. Crossed polarizers transmitted light.



Photomicrograph 19c: Pyrite (py) occurs along the quartz vein-walls and is associated with subordinate sphalerite (sl) and chalcopyrite (cp). Plane-polarized reflected light.

Sample 20: A23-01966-20-IG_BH04_MG070



White mica-chlorite-altered microdiorite(?)

Chlorite-K-feldspar-altered schist

This section comprises a schistose domain, which is defined by preferentially iso-oriented clusters of chlorite, fine-grained xenoblastic K-feldspar, and calcite, and in the left part of the section (right part of the offcut) the schist wraps angular and irregularly shaped fragments of a dioritic(?) rock comprising plagioclase, quartz, chlorite, and subordinate microcline. Calcite crosscuts the schist and the diorite.

Alteration/Metamorphism: **chlorite:** strong after biotite; **K-feldspar:** weak in the schist **calcite:** weak to moderate; **white mica:** moderate after plagioclase, weak in the schist

Mineral	Alteration/Metamorphism Mineral	Modal %	Size Range (mm)
Domain A: schist (~55% of PTS)			
plagioclase		30- 32	up to 0.1
[biotite]	Fe-chlorite	15- 17	[up to 1.5 long]
	K-feldspar	5- 6	up to 0.1
	rutile	2- 4	up to 0.1
	calcite	1- 2	up to 0.1
Domain B: microdiorite (~30% of PTS)			
plagioclase		22- 23	up to 2.5
quartz		4- 5	up to 0.2
microcline		2- 4	up to 0.2
[biotite]	Fe-chlorite	1- 2	up to 0.2
	calcite	tr	up to 0.5
calcite veinlets and veins (~15% of PTS)			
calcite		15	up to 3.5 across
chalcopyrite		tr	up to 0.6 long

Plagioclase forms xenoblastic crystals (up to 2.5 mm long), which are intergrown with quartz in the fragments showing a granular texture. I interpret the plagioclase, quartz, chlorite, and microcline as fragments of a microdioritic rock. Fine-grained flakes of white mica moderately altered the plagioclase. Some plagioclase crystals are fresh and display Albite twinnings. Fine-grained lamellae of white mica overprinted the chlorite in the schistose domain. The plagioclase is fine-grained in the schist and prevails over fine-grained **K-feldspar**. Within the microdiorite, the K-feldspar is fresh and shows

Albite-Pericline twinnings indicating its triclinic nature.

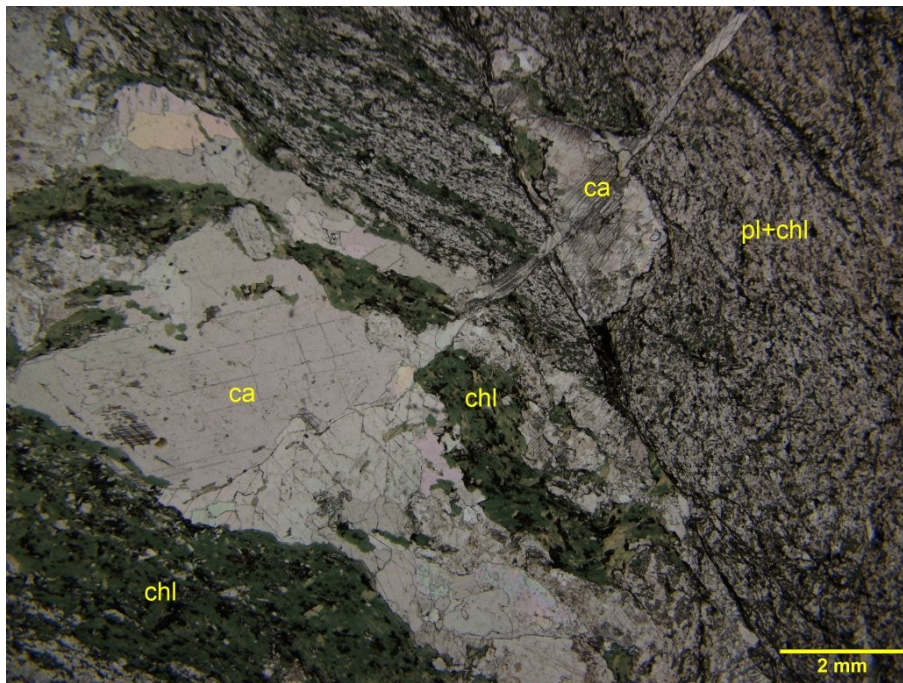
Fe-chlorite forms xenoblastic and preferentially iso-oriented flakes, lamellae, pseudomorphs (up to 1.5 mm long), and clusters defining the schistosity in the K-feldspar-bearing domain. The chlorite is randomly oriented in the plagioclase-rich granular domain. The chlorite shows a strong green colour under plane-polarized transmitted light, thus indicating its Fe-rich composition, and likely replaced biotite crystals in this section.

Fine-grained **rutile** crystals are disseminated within the schist and are iso-oriented and contribute to the schistosity defined by the chlorite.

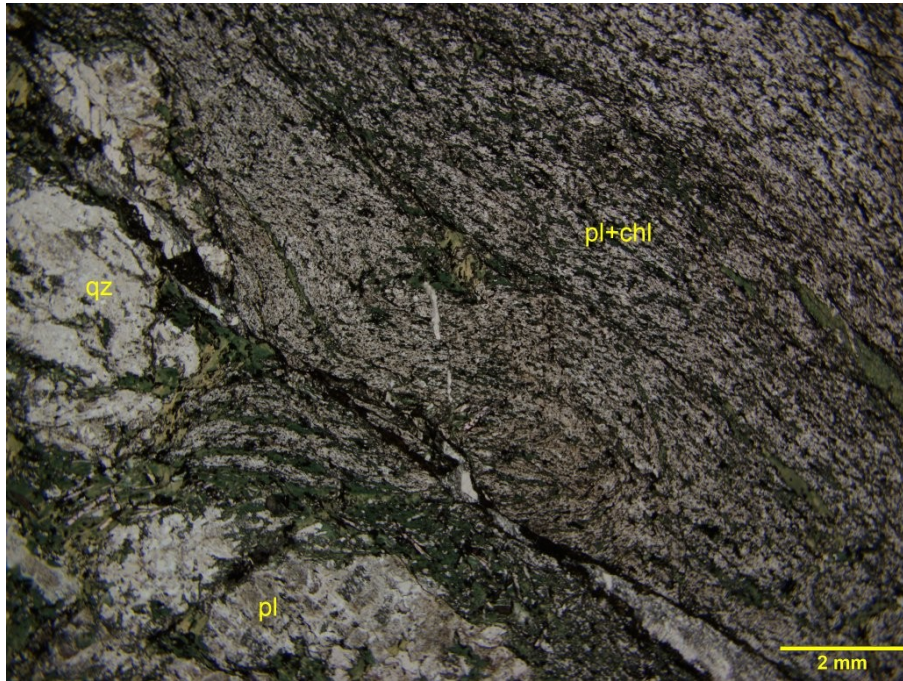
Quartz is subordinate to the plagioclase in the filling domains, and probably occurs as mixed with the fine-grained K-feldspar within the schist.

Calcite forms xenoblastic patches (up to 3.5 mm across) in the filling domains, and crosscut the schist as thin and discontinuous veinlets. The calcite briskly reacted to cold dilute (10%) HCl. In the upper left part of the section, the schist is brecciated and the K-feldspar-chlorite crushed aggregate is associated with xenoblastic patches of calcite.

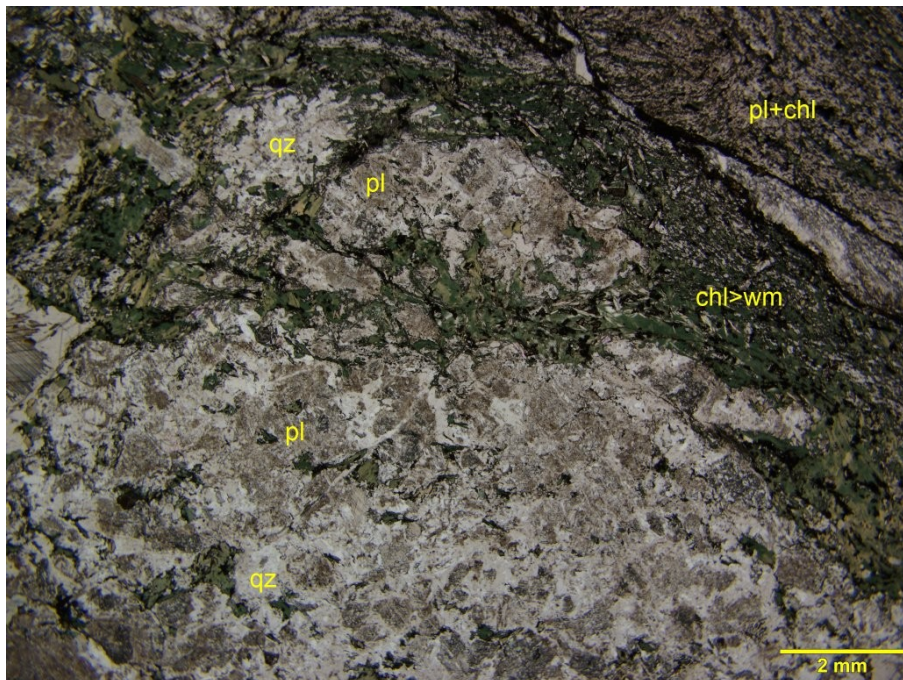
Rare **chalcopyrite** is spatially associated with the calcite within the veinlets and vein-like domains crosscutting the schist.



Photomicrograph 20a: The schist consists of fine-grained plagioclase and chlorite (pl+chl) and chlorite-rich domains (chl) filled in by calcite (ca). Plane-polarized transmitted light.

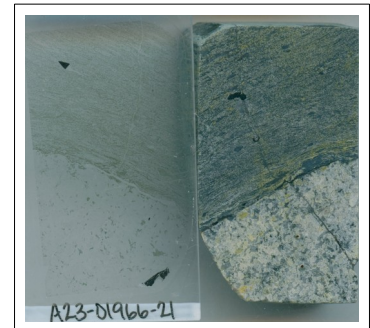


Photomicrograph 20b: The preferred dimensional orientation of the chlorite, likely replacing biotite in the K-feldspar-chlorite domain (pl+chl), defines the continuous schistosity. In the lower left part of the photomicrograph, fragments of granitoid rock (qz) and (pl) occur. Plane-polarized transmitted light.



Photomicrograph 20c: Plagioclase (pl) prevails over the quartz (qz) in the fragmented dioritic rock, which is wrapped by the schist. Plane-polarized transmitted light.

Sample 21: A23-01966-21-IG_BH04_MG071



Chlorite-altered microtonalite

Chlorite-retrometamorphosed biotite schist

A granular domain (A) comprising anhedral plagioclase, quartz, and chlorite after biotite define an irregular contact with a fine-grained schistose domain comprising chlorite, quartz and calcite.

Alteration/Metamorphism: white mica: moderate after plagioclase; **chlorite>titanite:** moderate to strong after biotite; **calcite-epidote:** subtle to weak in Domain A and after the plagioclase

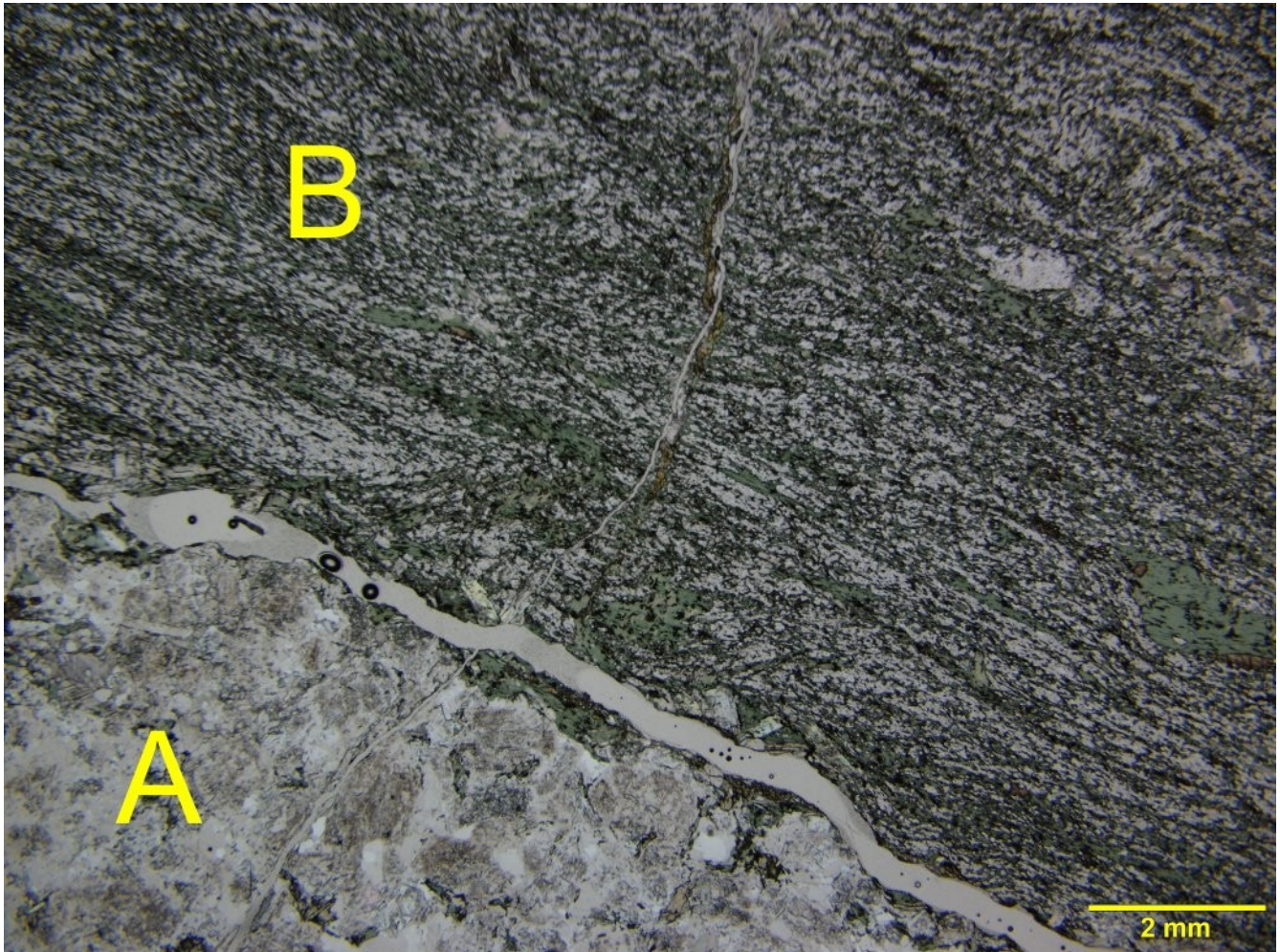
Mineral	Alteration/Weathering Mineral	Modal %	Size Range (mm)
Domain A: microtonalite (~40% of PTS)			
plagioclase (albite)	white mica-calcite-epidote	26- 28	up to 1
quartz		10- 12	up to 0.7
[biotite]	Fe-chlorite	2- 3	up to 0.6
	pyrite	0.5- 1	up to 4
	epidote	tr	up to 0.2
	calcite	tr	up to 0.1
zircon		tr	0.01
Domain : schist (~60% of PTS)			
[biotite	Fe-chlorite+titanite	35- 40	up to 0.4 long
	quartz (and plagioclase?)	18- 20	up to 0.2
	pyrite	tr	u1.5 long
	calcite	tr	up to 0.1
zircon		tr	0.01

Plagioclase (albite) occurs as medium-grained (up to 1 mm across) anhedral crystals in Domain A. The plagioclase crystals show Albite twinings and refractive indexes lower than those of the quartz. Fine-grained flakes of white mica moderately altered the plagioclase crystals.

Quartz forms fine- to medium-grained crystals in Domain A (Photomicrograph 21c and e) and it is subordinate to the chlorite in the schistose Domain B (Photomicrograph 21d). In this domain, the quartz filled in the strain shadow surrounding one idioblastic crystal of pyrite (Photomicrograph 21d), thus indicating the pyrite (and the quartz) crystallized during the deformation generating the schistosity. Like in Sample 19, I interpret the chlorite as having replaced the biotite after the deformation.

Fe-chlorite completely replaced medium-grained (up to 0.6 mm long) and randomly oriented biotite crystals in the granular texture of Domain A. IN Domain B, the chlorite completely and epitaxially replaced the iso-oriented biotite defining the continuous schistosity. Very fine-grained inclusions of **zircon** occur in the pseudomorphic chlorite and indicate that the parent mineral is biotite.

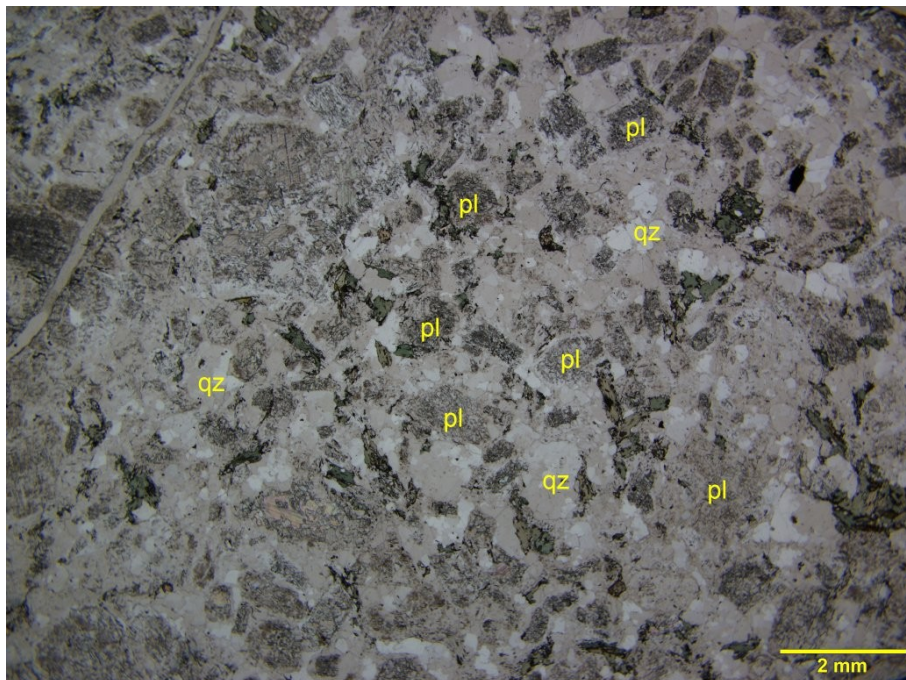
Pyrite occurs as one idioblastic crystal wrapped by the schistosity in Domain B (Photomicrograph 21d) and forms a xenoblastic crystal (up to 4 mm in the section) in the lower right part of the section in Domain A.



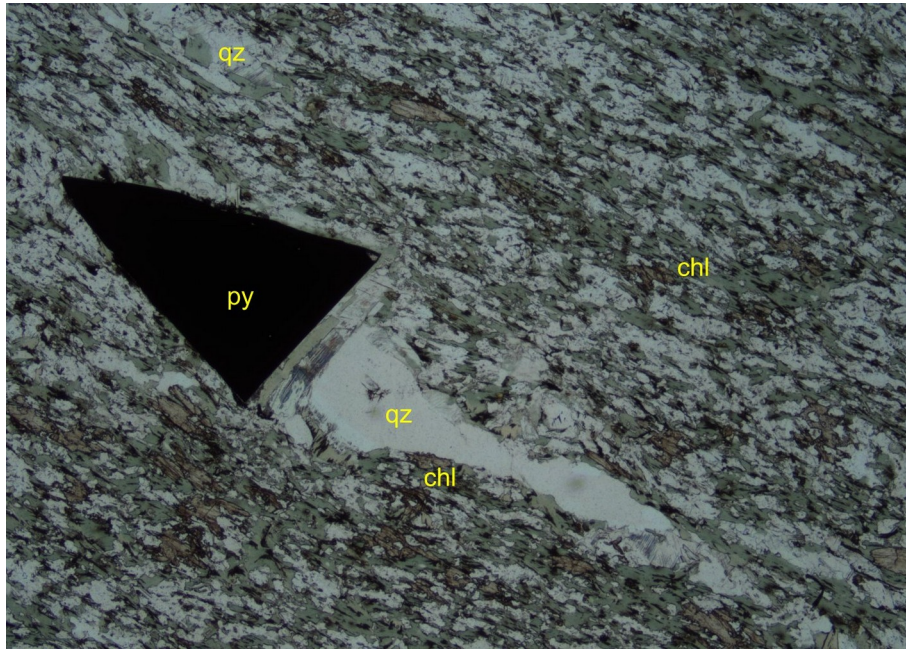
Photomicrograph 21a: The disjointed boundary between the granular Domain A (A) and the schistose Domain B (B) is shown here. Plane-polarized transmitted light.



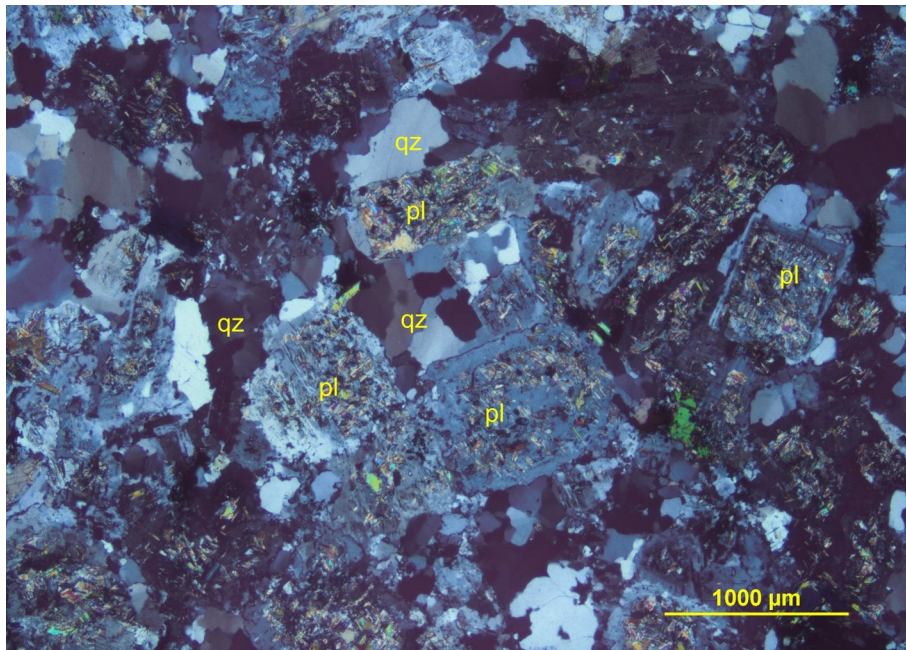
Photomicrograph 21b: Domain B—The schistosity is defined by iso-oriented and chlorite-replaced biotite. The texture is relatively homogeneous and is crosscut by irregular quartz-chlorite veinlets. Plane-polarized transmitted light.



Photomicrograph 21c: Domain A—The granular texture is defined by anhedral and moderately altered plagioclase (pl), quartz (qz) and chlorite-replaced biotite. Plane-polarized transmitted light.



Photomicrograph 21d: Domain B—Idioblastic pyrite (py) define a quartz (qz) and chlorite-calcite-filled strain shadow immersed within the schistosity. Plane-polarized transmitted light.



Photomicrograph 21e: Domain A—Anhedral and subhedral plagioclase (pl) and quartz (qz) define a granular texture. White mica selectively and moderately altered the plagioclase. Crossed polarizers transmitted light.

Sample 22: A23-01966-22-IG_BH04_MG072



Calcite-Fe-chlorite-albite-altered foliated microdiorite

Fine-grained xenoblastic aggregates of plagioclase (albite) and fine-grained lamellae and clusters of lamellae of chlorite are associated with subordinate calcite and define a weak foliation within the pseudomorphic texture.

Alteration: chlorite>titanite: strong after biotite; **albite:** strong after plagioclase; **calcite:** weak to moderate; **pyrite-chalcopyrite:** subtle

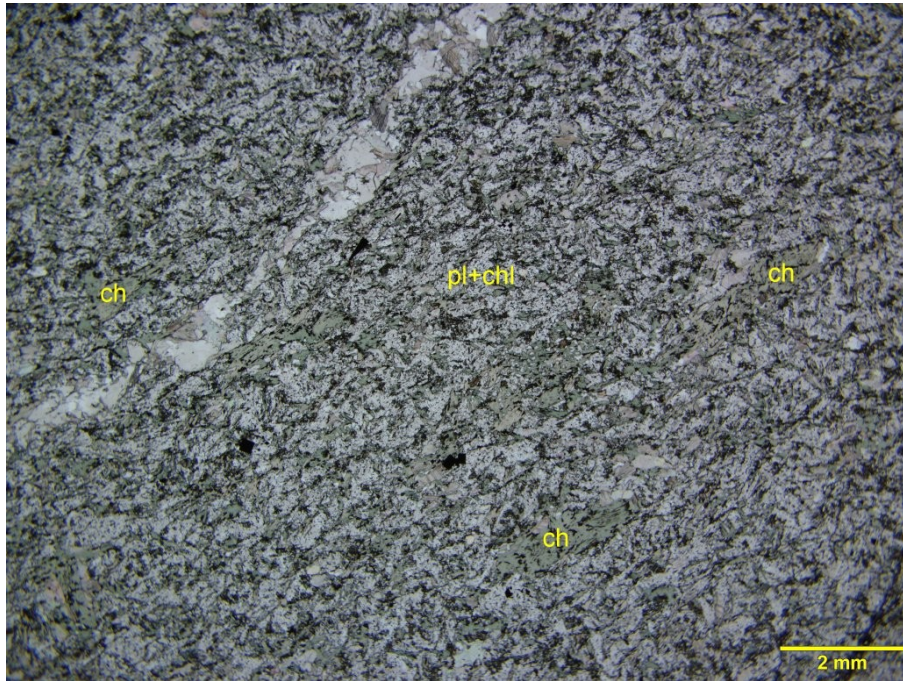
Mineral	Alteration/Weathering Mineral	Modal %	Size Range (mm)
plagioclase (albite)		70- 72	[up to 0.5]
[biotite]	Fe-chlorite-titanite	12- 15	up to 0.4, rare up to 1 long
calcite		5- 10	
	pyrite	tr	up to 0.2, rare up to 0.5
	chalcopyrite	tr	up to 0.02
zircon		tr	

Very fine- to fine-grained xenoblastic crystals of **plagioclase** (albite) are associated with fine-grained flakes and lamellae of chlorite and define a granular and weakly foliated texture (Photomicrographs 22a and 22b). The very fine-grained aggregates of albite re-crystallized plagioclase crystals (Photomicrographs 22c and 22d).

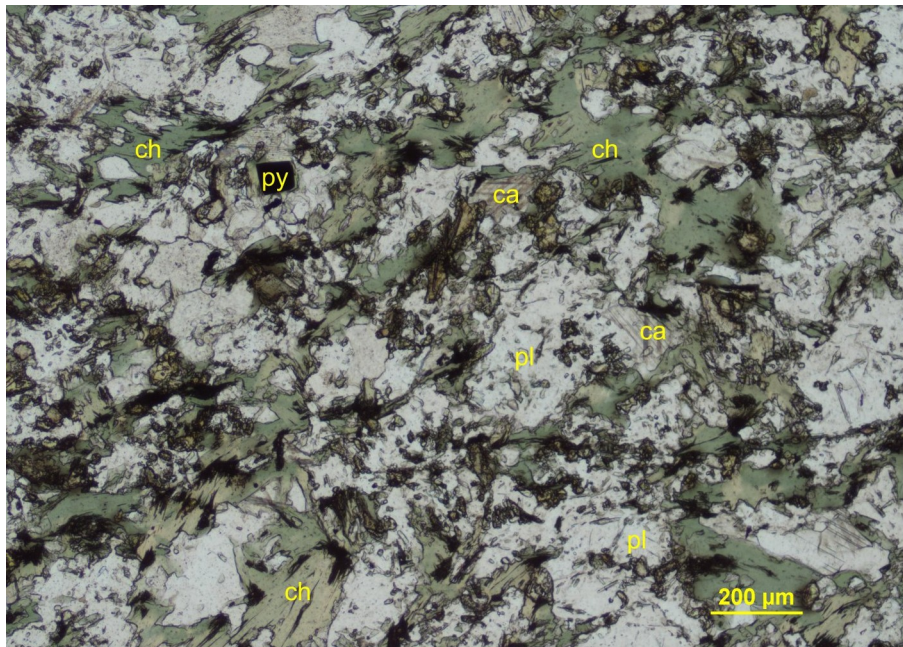
Fe-chlorite completely and epitaxially replaced biotite crystals. The pseudomorphs after biotite show a weak preferred dimensional orientation, which impart a weak foliation to the texture (Photomicrograph 22b). The chlorite replacing the biotite is associated with very fine-grained dispersions of titanite and very fine-grained zircon.

Calcite is subordinate to the albite and chlorite and it is relatively homogeneously dispersed within the pseudomorphic texture.

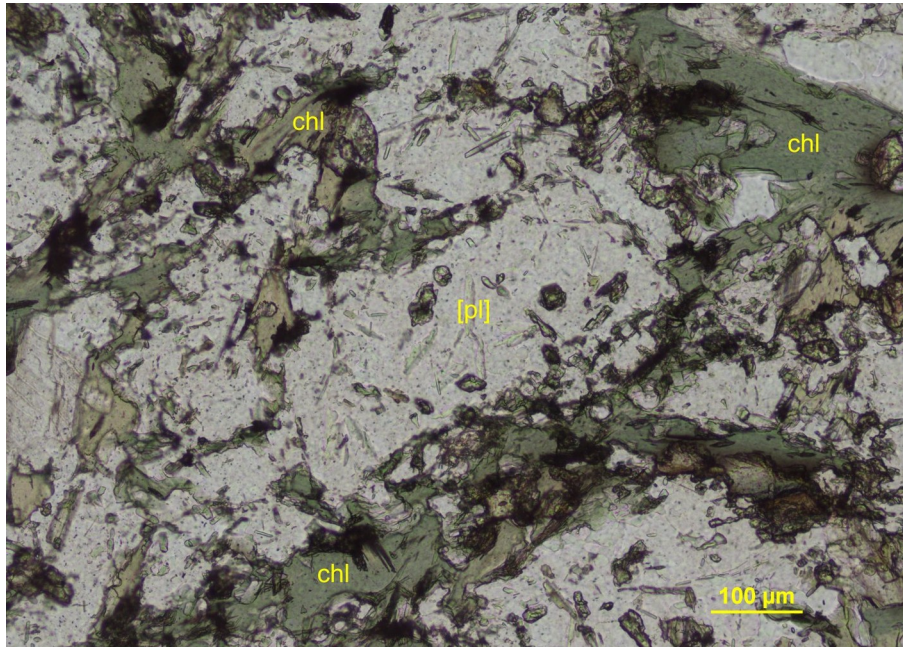
Very rare idiomorphic **pyrite** and very fine-grained xenoblastic **chalcopyrite** are disseminated within the section.



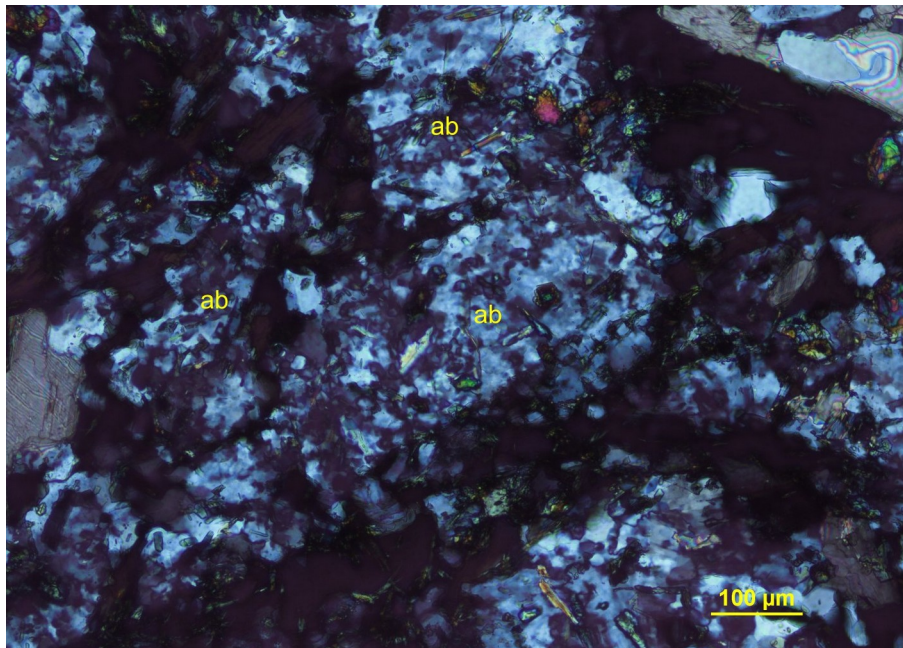
Photomicrograph 22a: The fine-grained chlorite and the clusters of chlorite (chl) define a weak foliation in the granular texture. Plane-polarized transmitted light.



Photomicrograph 22a: The fine-grained flakes of chlorite (chl) show a weak preferred dimensional orientation, likely inherited from the parent biotite crystals. Plane-polarized transmitted light.



Photomicrograph 22c: Apparent subidioblastic crystals of plagioclase [pl] are associated with xenoblastic chlorite (chl). Plane-polarized transmitted light.



Photomicrograph 22d: Same area as shown in Photomicrograph 22c. Under crossed polarizers transmitted light, the apparent plagioclase crystal consists of very fine-grained interlobate crystals of albite (ab).

Sample 23: A23-01966-23-IG_BH04_MG073

Microgranodiorite/microquartz-monzodiorite

Subhedral and weakly altered plagioclase is intergrown with anhedral quartz, interstitial K-feldspar, and randomly oriented and Fe-chlorite-epidote-altered biotite.



Alteration: Fe-chlorite-epidote: moderate to strong after biotite; **sericite-epidote:** weak after plagioclase

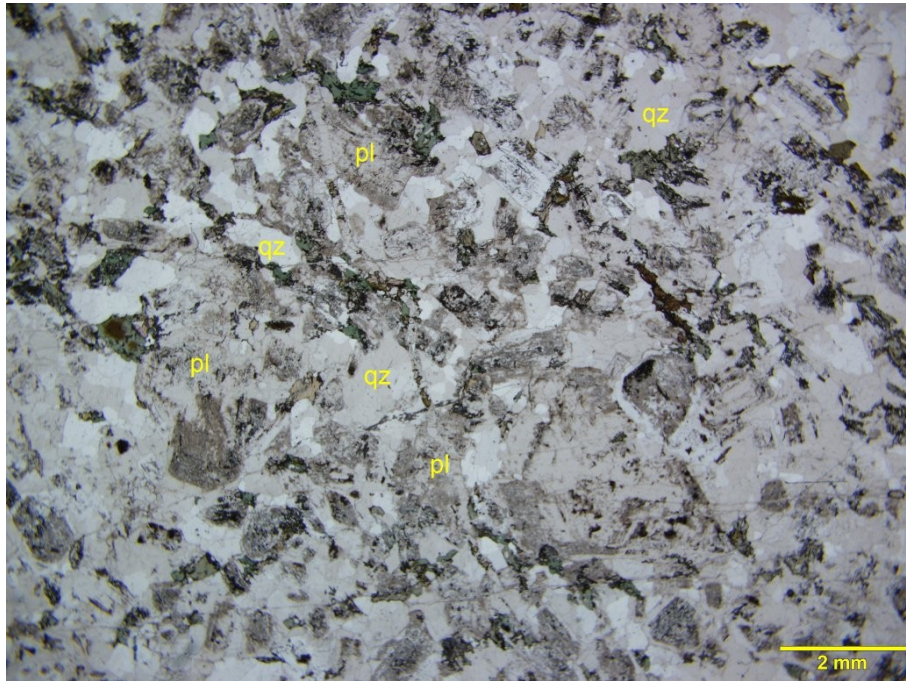
Mineral	Alteration/Weathering Mineral	Modal %	Size Range (mm)
plagioclase	sericite-epidote	60- 62	up to 2, rare up to 4
quartz		22- 23	up to 0.5
K-feldspar		10- 11	up to 0.2
biotite	Fe-chlorite-epidote	5- 6	up to 1.4 long
piemontite(?)		tr	up to 2 long
zircon		tr	up to 0.02

Plagioclase forms inequigranular (up to 2.5 mm long, and very rare up to 4 mm across) subhedral and randomly oriented crystals. Very fine- to fine-grained flakes of sericite subtly to weakly altered the plagioclase. The plagioclase, at least along its rims, is albitic, as indicated by its refractive indexes lower than those of quartz.

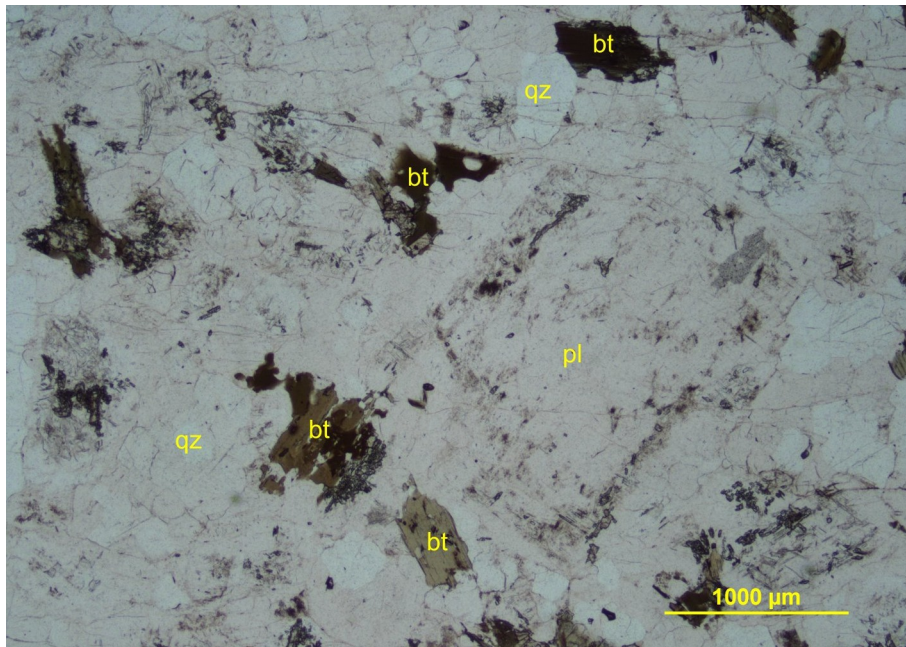
Quartz forms anhedral crystals ranging from 0.05 mm to 1 mm across. In some cases, the quartz forms monomineralic aggregates, which probably are recrystallized larger crystals of quartz.

Biotite occurs in Domain A as fine- to medium-grained (up to 1 mm long) and randomly oriented lamellae. Fe-chlorite and epidote moderately to strongly altered the biotite crystals.

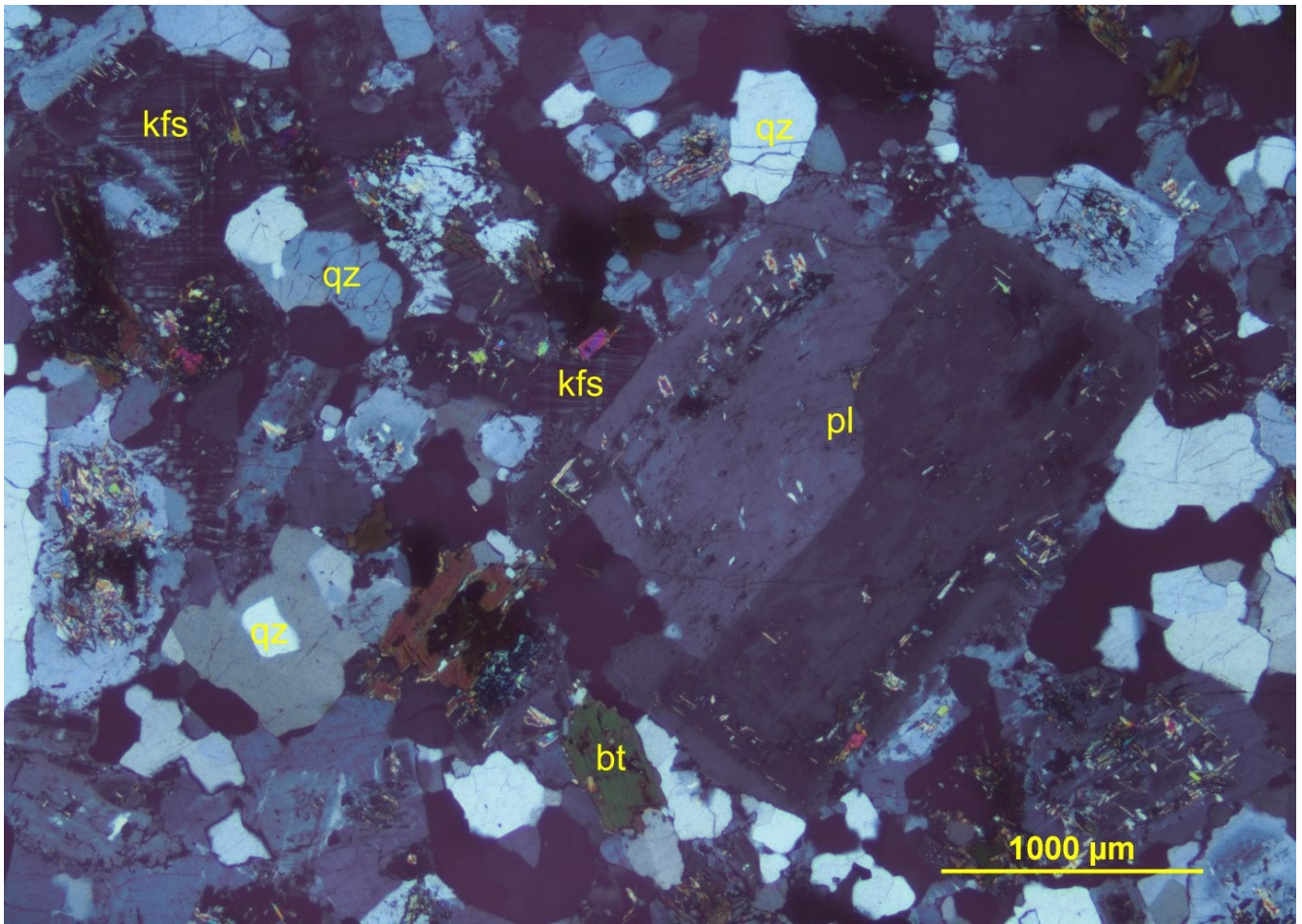
K-feldspar is disseminated as fine-grained interstitial crystals displaying their typical Albite-Pericline twinnings. Because of the shape, position in the texture, and transparent nature, I interpret the K-feldspar as a late magmatic mineral; therefore, I interpret this rock as a microgranodiorite.



Photomicrograph 23a: Weakly altered plagioclase, quartz, and strongly altered biotite define a granular texture. Plane-polarized transmitted light.



Photomicrograph 23b: Detail of the granular texture. In this photomicrograph, the plagioclase is only subtly altered and is intergrown with quartz (qz), K-feldspar, and relatively fresh biotite (bt). Plane-polarized transmitted light.



Photomicrograph 23c: Same area as shown in Photomicrograph 23b. Interstitial K-feldspar is fresh and displays Albite-Pericline twinnings. Crossed polarizers transmitted light.

Sample 24: A23-01966-24-IG_BH04_MG074



Chlorite-altered tonalite

Chlorite-retrogressed orthoschist

This heterogeneous section comprises a medium-grained central part, in which subhedral plagioclase crystals and anhedral quartz define a granular texture, and fine-grained upper and lower part, in which granoblastic plagioclase, quartz, and xenoblastic chlorite define a roughly foliated domains.

Alteration: chlorite-titanite: strong after biotite; **white mica:** weak to moderate after the plagioclase; **calcite:** weak; **pyrite:** subtle

Mineral	Alteration/Weathering Mineral	Modal %	Size Range (mm)
altered tonalite (~60% of PTS)			
plagioclase		32- 33	up to 2.5
quartz		20- 22	up to 0.8
[biotite?]	chlorite-titanite	2- 2.5	
	calcite	2- 2.2	up to 0.
	pyrite	tr	up to 0.2
zircon		tr	0.02
schist (~40% of PTS)			
plagioclase		20- 21	up to 0.1
[biotite?]	chlorite-titanite	10- 12	up to 0.4
quartz		6- 7	up to 0.1
	calcite	2- 3	up to 0.15
zircon		tr	0.02

Quartz forms anhedral crystals intergrown with the moderately altered plagioclase in the granular domain (see the lighter central part of the offcut). And occurs as fine-grained granoblastic aggregates associated with the chlorite (see the darker domains in the offcut).

Plagioclase forms medium-grained subhedral crystals (up to 3 mm long), which are randomly oriented and are intergrown with the quartz. Very fine- to fine-grained flakes of white mica weakly to moderately altered the plagioclase, which I interpret as the relic of a magmatic rock, likely a tonalite. In the fine-grained granoblastic domains, fine-grained plagioclase is associated with quartz and chlorite. These domains are probably derived from the deformation of a magmatic rock similar to the tonalite relic occurring in the central part of the section.

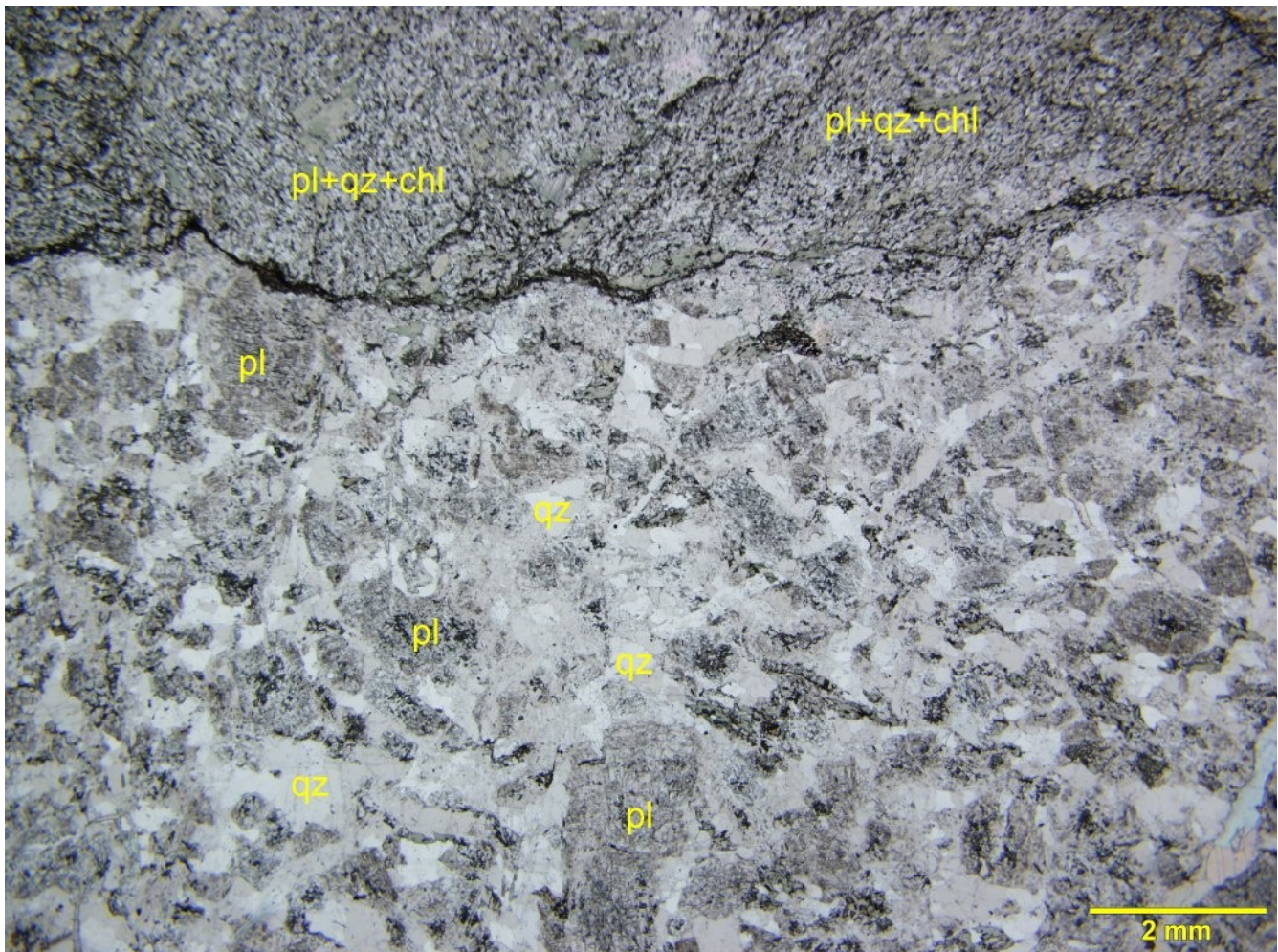
Chlorite forms fine-grained flakes intergrown with the granoblastic quartz in the upper and lower part

of the section. In these domains, the chlorite defines a rough foliation. In the granular domain, the chlorite completely and epitaxially replaced magmatic biotite.

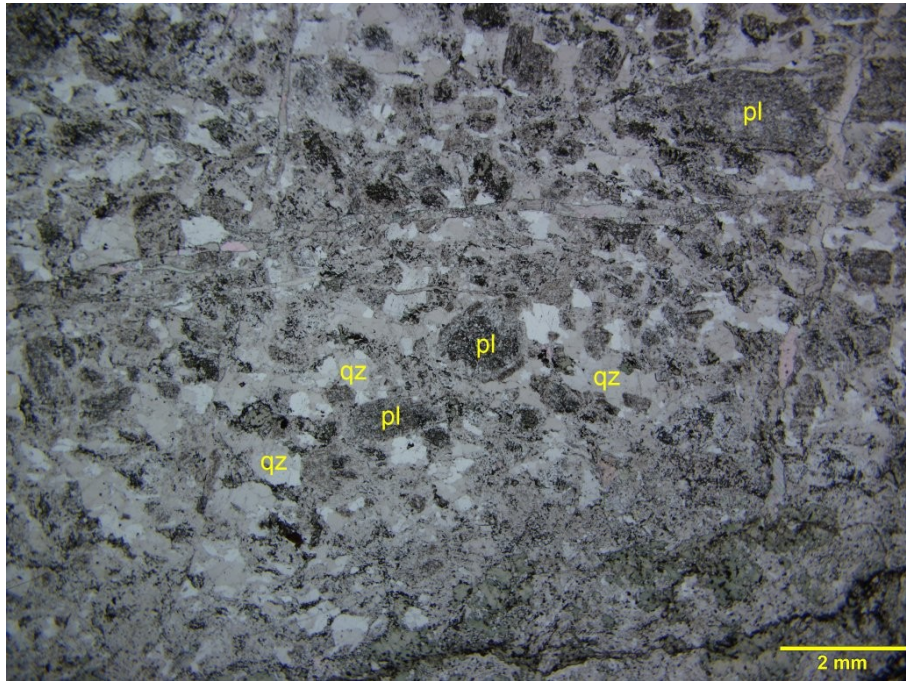
Calcite is heterogeneously disseminated as fine-grained xenoblastic crystals in the two domains, and forms irregular veinlets crosscutting the section.

Very fine-grained **titanite** are disseminated in the schist, likely derived from the replacement of the biotite.

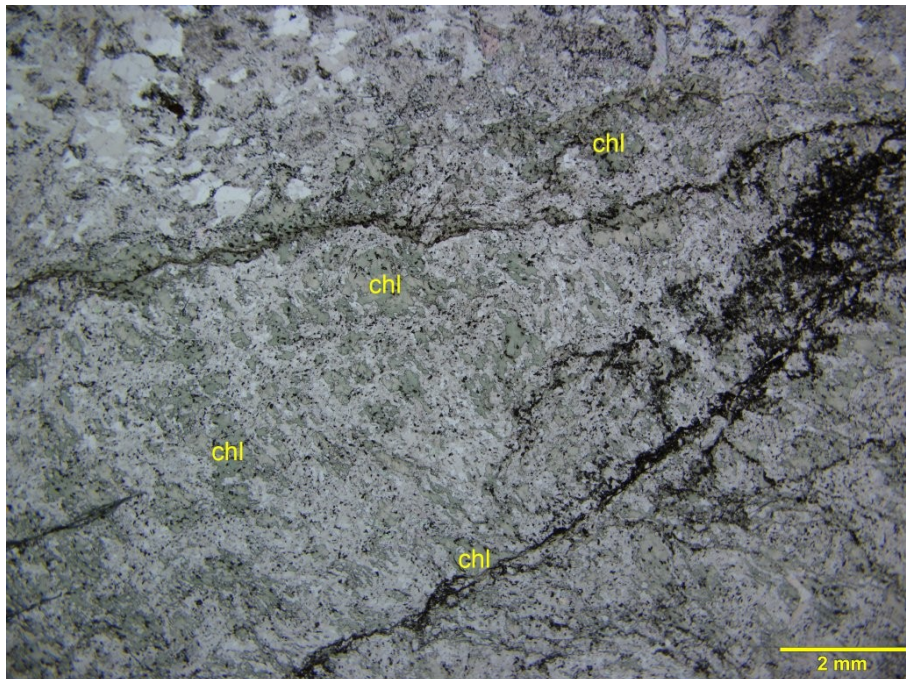
Very rare and xenoblastic **pyrite** is dispersed within the granular texture.



Photomicrograph 24a: Two main domains are distinguished: a granular domain comprising subhedral plagioclase (pl) and anhedral quartz (qz) and chlorite in the lower part of this photomicrograph, and a fine-grained granoblastic domain, in which the chlorite define a weak schistosity in the granoblastic aggregate of plagioclase and quartz (in the upper part). Plane-polarized transmitted light.



Photomicrograph 24b: In the granular domain, the altered plagioclase (pl) is easily distinguished from the quartz (qz) under plane-polarized transmitted light.

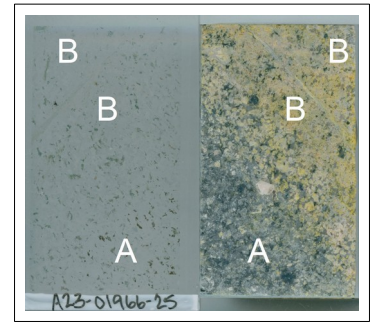


Photomicrograph 24c: Chlorite altered clusters and fine-grained pseudomorphs of chlorite define a rough schistosity in the fine-grained granoblastic domains. Plane-polarized transmitted light.

Sample 25: A23-01966-25-IG_BH04_MG075

Microquartz-diorite

Epidote-chlorite-sericite-altered microgranodiorite/microquartz-monzodiorite



This section comprises two different domains: Domain A, the less altered domain, comprises subhedral and weakly altered plagioclase associated with anhedral quartz and randomly oriented biotite. Domain B is probably generated by the alteration surrounding an irregular epidote veinlet and comprises moderately altered plagioclase, chlorite-altered biotite, and quartz.

Alteration: Chlorite>titanite: strong after biotite in Domain B; subtle to weak in Domain A; **K-feldspar:** weak to moderate in Domain B; **sericite-epidote:** weak after plagioclase in Domain A; moderate to strong in Domain B

Mineral	Alteration/Weathering Mineral	Modal %	Size Range (mm)
Domain A: microquartz-diorite (~45% of PTS)			
plagioclase	sericite-epidote	30- 31	up to 2
quartz		12- 13	up to 0.5
biotite	Fe-chlorite-titanite	2- 3	up to 0.4 long
zircon		tr	0.02
Domain B altered microgranodiorite (~54% of PTS)			
plagioclase	sericite-epidote	34- 35	up to 2
quartz		14- 15	up to 0.5
biotite	Fe-chlorite-titanite	2- 3	0.02
	K-feldspar	2- 3	up to 0.2
zircon		tr	up to 0.02
epidote-clay veinlet (~1% of PTS)			
clay(?)		0.5	0.01
epidote		0.5	0.01

Plagioclase forms inequigranular (up to 2.5 mm long) subhedral and randomly oriented crystals, which in Domain A are weakly altered. The alteration is mostly concentrated within the subhedral crystal cores and consists of a very fine-grained and mostly unresolved aggregate of epidote and sericite (Photomicrograph 25a). In Domain B, the plagioclase is moderately altered by very fine-grained

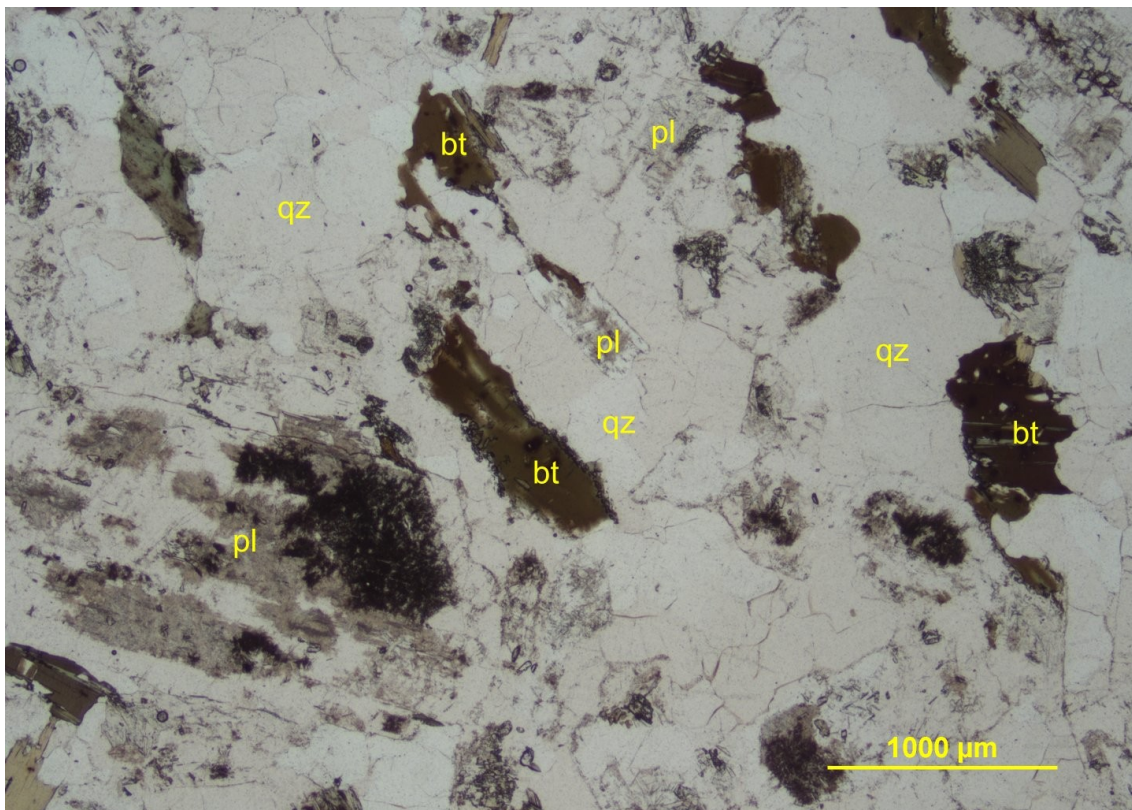
sericite and sparse replacement patches of K-feldspar. K-feldspar occurs as irregular patches (Photomicrograph 25c) near the epidote-rich veinlet. I interpret the alteration as being generated by the veinlet, and the veinlet mineralogy probably represent a further evolution of the earliest K-feldspar-bearing assemblage as it is now comprising very fine-grained epidote and a very fine-grained unresolved aggregate of probable clay?

Quartz forms anhedral crystals occupying the interstices between the subhedral plagioclase crystals.

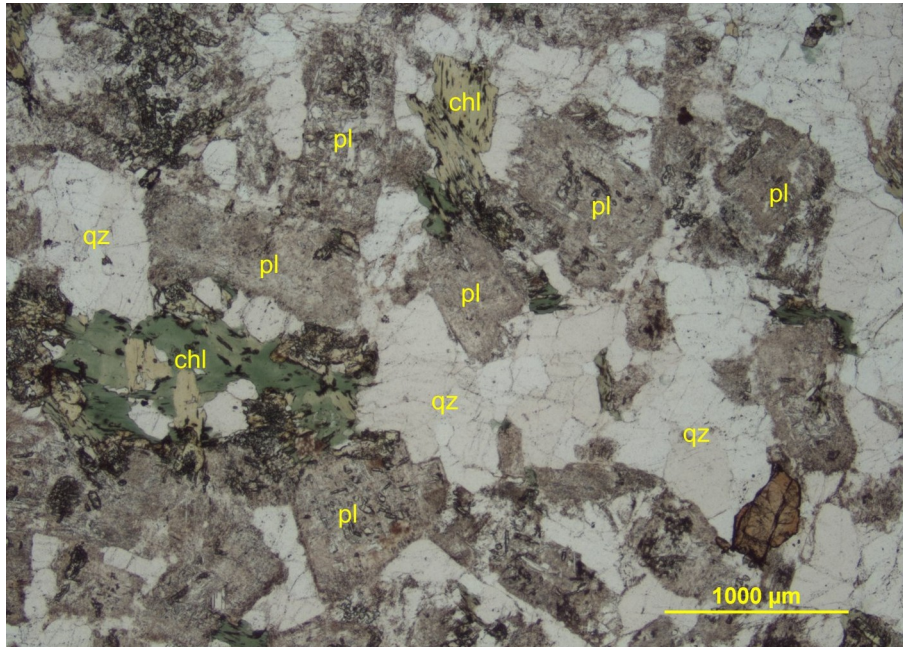
Biotite occurs in Domain A as fine- to medium-grained (up to 1 mm long) and randomly oriented lamellae (Photomicrograph 25 A). In Domain B, Fe-chlorite and subordinate titanite completely and epitaxially replaced the biotite crystals (Photomicrographs 25b and 25c).

K-feldspar is heterogeneously dispersed within Domain B, and is particularly abundant around the epidote and clay(?) veinlet triggering the alteration (Photomicrograph 52c).

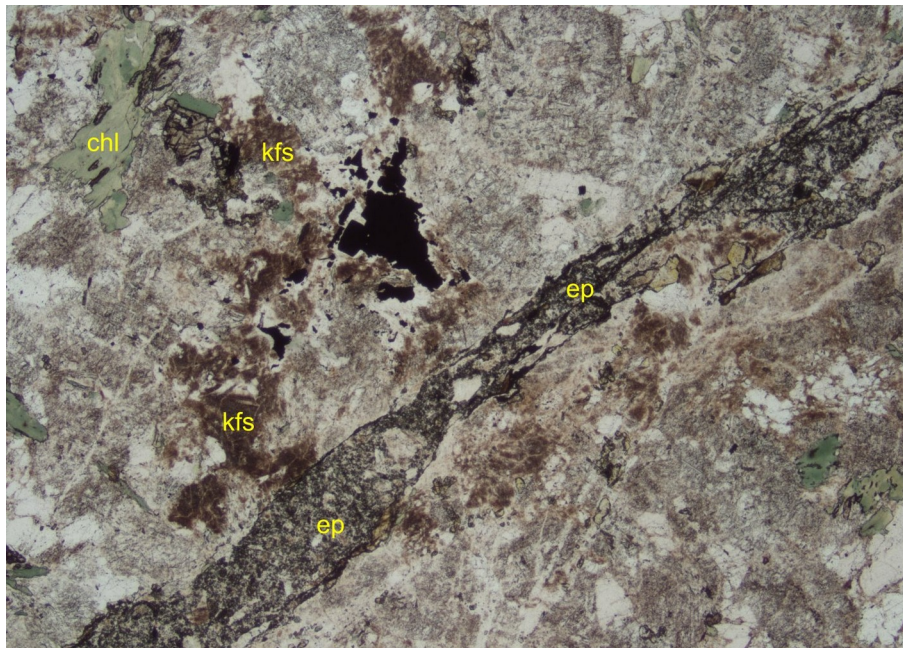
Very rare **pyrite** forms subhedral and fractured crystals in Domain B near the epidote-bearing veinlet.



Photomicrograph 25a: Domain A—Weakly altered plagioclase (pl), quartz (qz) and randomly oriented biotite define a granular texture. Plane-polarized transmitted light



Photomicrograph 25b: Domain B—The plagioclase is moderately altered (pl) and together with the quartz and chlorite-altered biotite (chl) define a granular texture. Plane-polarized transmitted light

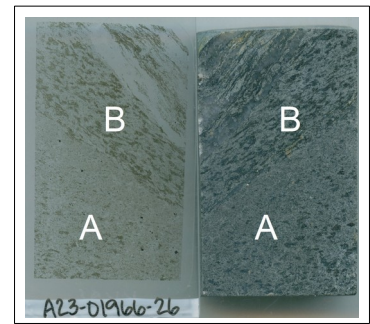


Photomicrograph 25c: Domain B—Within the veinlet very fine-grained epidote (ep) and unresolved material (clay?) occur. Sparse patches of K-feldspar (kfs) occur near the veinlet in the host Domain B. Plane-polarized transmitted light.

Sample 26: A23-01966-26-IG_BH04_MG076

Epidote-albite-biotite granofels

Biotite schist



Two domains occur in this section. A fine-grained xenoblastic and relatively homogeneous and isotropic aggregate of albite, epidote and biotite (Domain A), and a roughly schistose Domain B comprising clusters of biotite, fine-grained and xenoblastic albite and epidote, and vein-like domains of calcite and subordinate quartz and biotite.

Mineral	Alteration/Weathering Mineral	Modal %	Size Range (mm)
Domain A: granofels (~50% of PTS)			
biotite		22- 23	up to 0.2
plagioclase (albite?)		19- 20	up to 0.1
epidote		7- 8	up to 0.1
pyrite		0.2- 0.3	up to 0.4
zircon		tr	0.01
Domain B: schist (~50% of PTS)			
biotite		20- 21	up to 1 long
plagioclase (albite?)		15- 16	up to 0.1
calcite		7- 8	up to 1
epidote		6- 8	up to 0.2
quartz		0.5- 1	up to 0.1
zircon		tr	0.01

Biotite is fine-grained (up to 0.2 mm long) and its lamellae are randomly oriented in Domain A (Photomicrograph 26d). In Domain B, the biotite crystals are up to 1 mm long and forms irregular clusters, which are roughly iso-oriented and define a weak schistosity (Photomicrographs 26b and 26e). Biotite hosts very fine-grained zircon crystals.

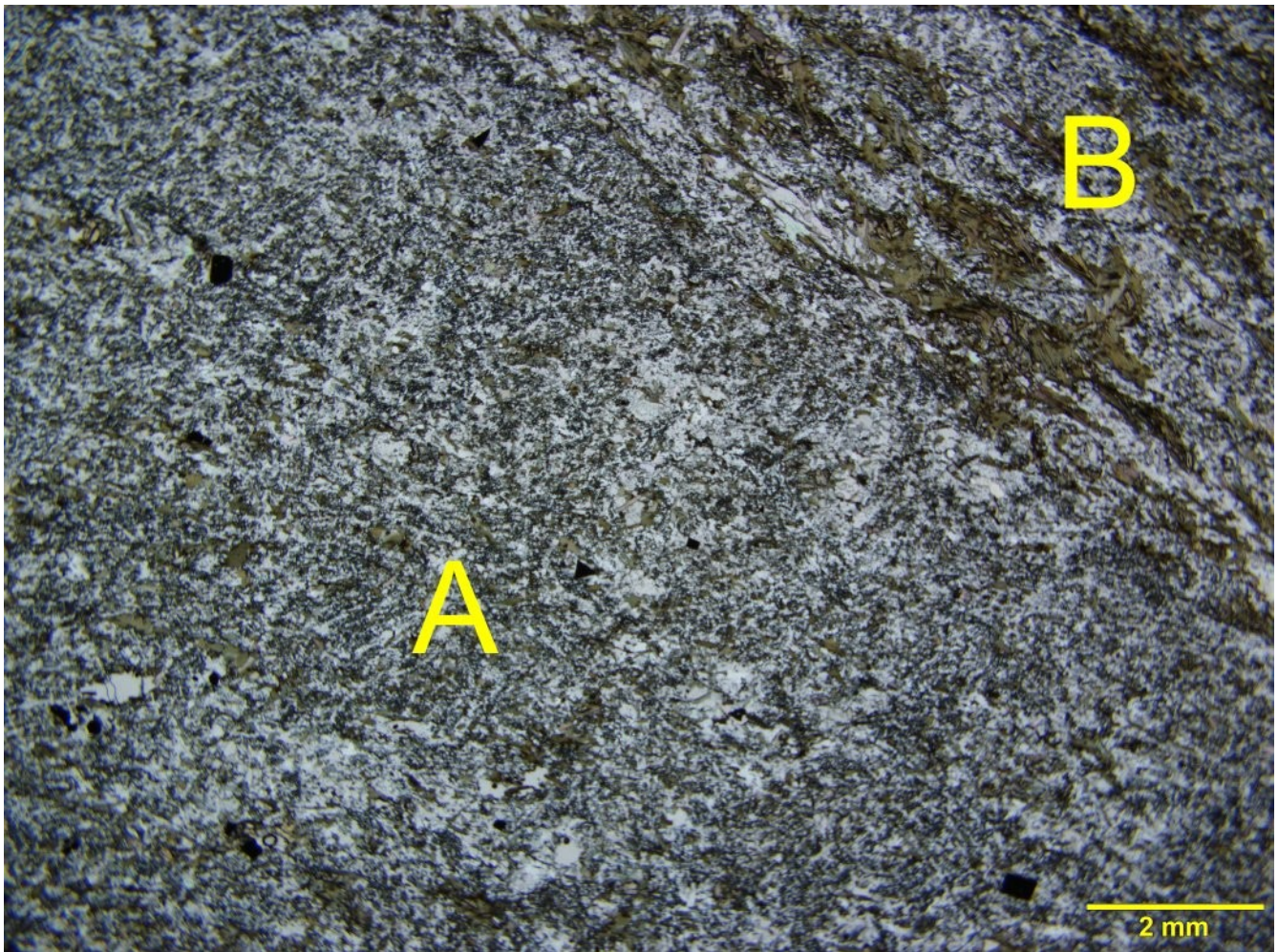
Plagioclase is xenoblastic and forms fine-grained crystals in Domain A and Domain B. Most albite crystals host very fine- to fine-grained epidote inclusions. The lack of quartz in contact with the plagioclase does not allow me to test the plagioclase’s refractive indexes, and the only clue to the plagioclase nature is the low birefringence of the crystals associated with the lack of staining on the

offcut (see image above).

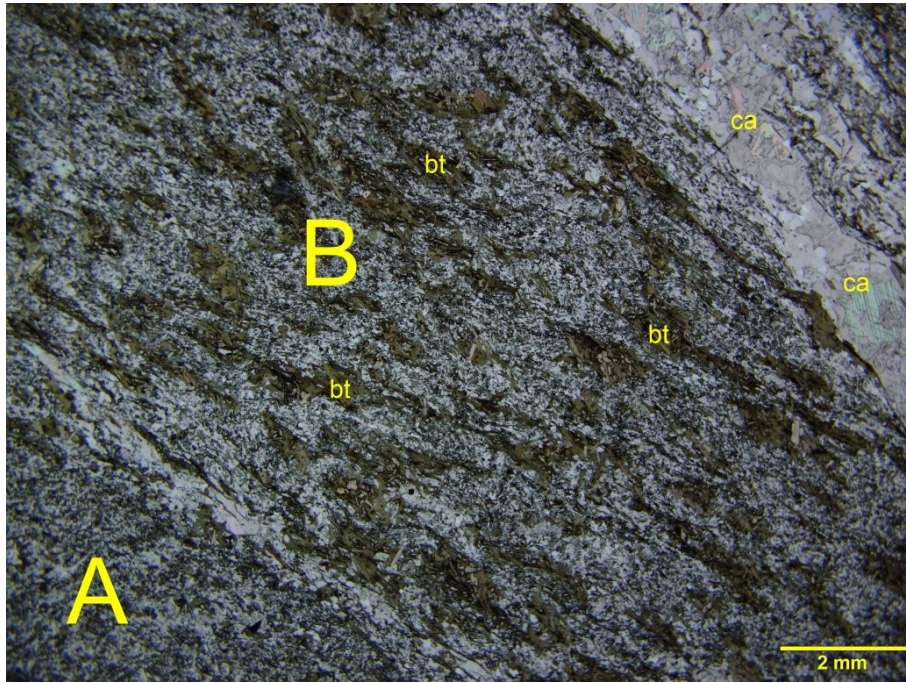
Epidote is very fine- to fine-grained and its xenoblastic crystals are disseminated within the plagioclase and the biotite. Fine-grained xenoblastic epidote is spatially associated with the biotite clusters in Domain B.

Calcite is concentrated within sub-parallel and up to 4.5 mm thick veins or vein-like domains, in which the xenoblastic and up to 1 mm across calcite crystals are associated with subordinate and fine-grained quartz crystals (Photomicrograph 26c). The calcite briskly reacted to cold dilute (10%) HCl.

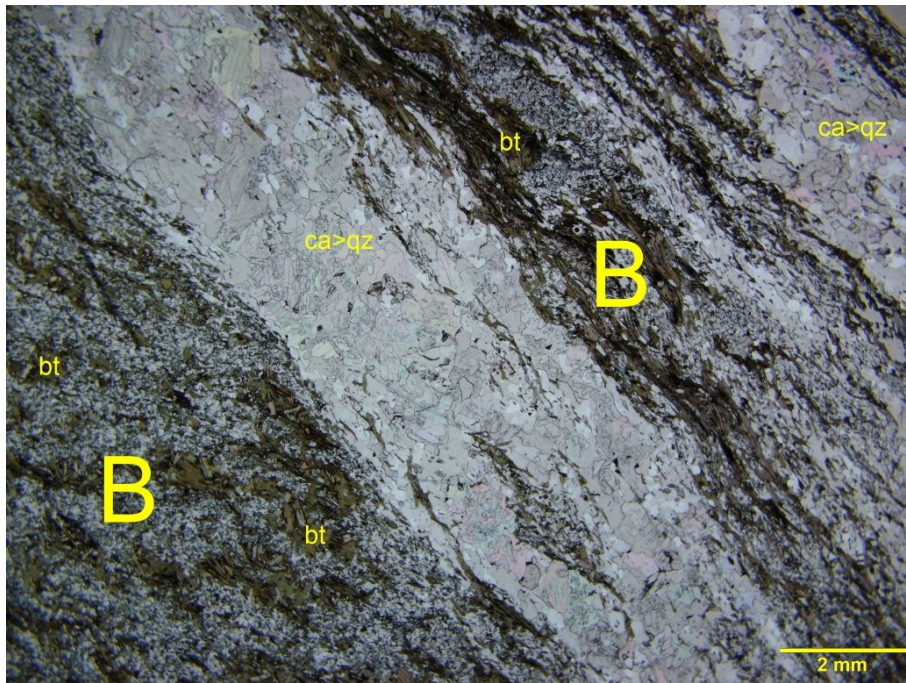
Pyrite forms idiomorphic crystals (up to 0.4 mm across), which are homogeneously disseminated in Domain A.



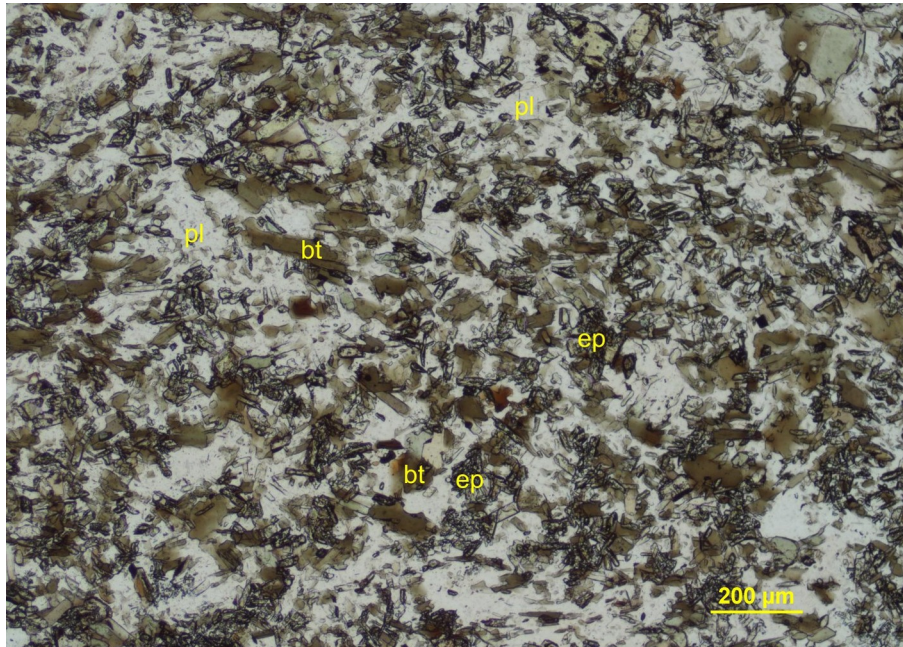
Photomicrograph 26a: A fine-grained xenoblastic and isotropic Domain A (A) is in contact with a schistose Domain B (B). Plane-polarized transmitted light.



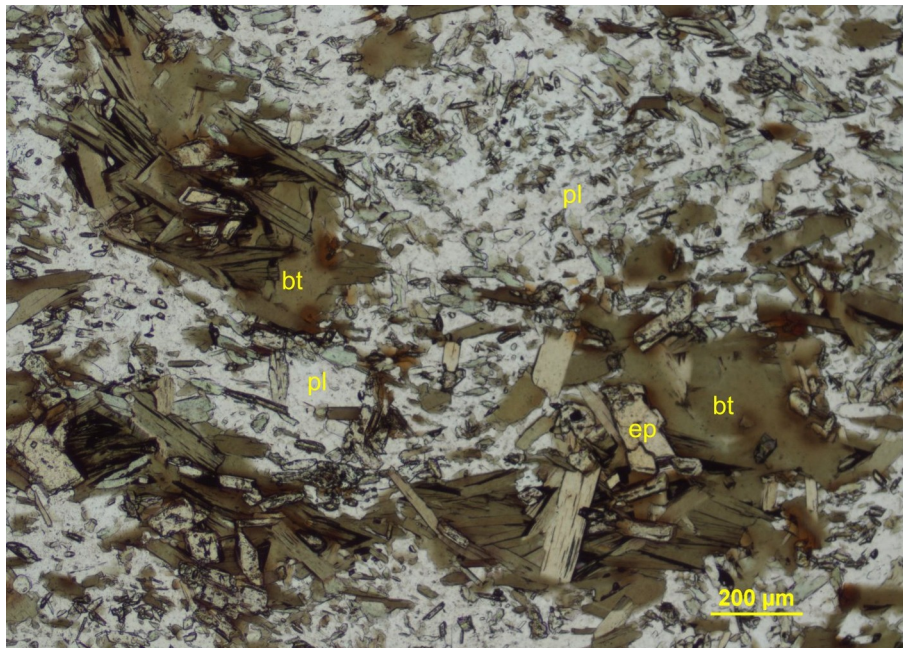
Photomicrograph 26b: Domain B—Biotite clusters (bt) define the schistosity. Plane-polarized transmitted light.



Photomicrograph 26c: Calcite-rich (ca>qz) vein-like domains crosscut Domain B parallel to the schistosity defined by the biotite clusters (bt). Plane-polarized transmitted light.



Photomicrograph 26d: Domain A—Fine-grained and randomly oriented biotite (bt), plagioclase (pl) and epidote define a fine-grained xenoblastic and isotropic texture. Plane-polarized transmitted light.



Photomicrograph 26e: Biotite forms irregular clusters (bt) defining a rough schistosity. Plane-polarized transmitted light.

Sample 27: A23-01966-27-IG_BH04_MG077



Calcite-epidote-biotite schist

Iso-oriented and medium-grained lamellae of biotite, subordinate xenoblasts of calcite, epidote, and fine-grained plagioclase and quartz define a continuous schistosity in this relatively homogeneous section.

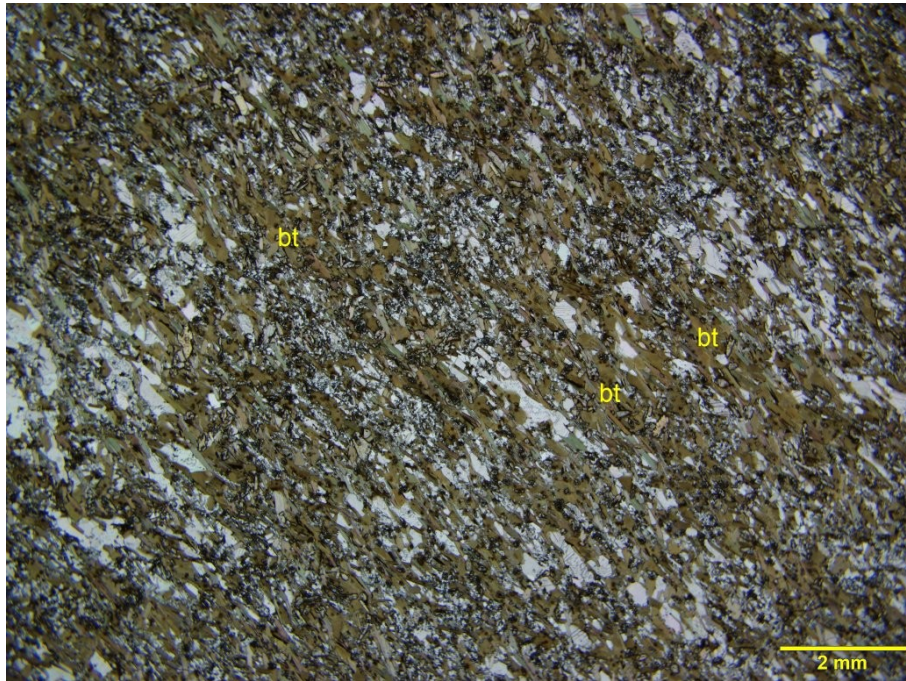
Mineral	Alteration/Weathering Mineral	Modal %	Size Range (mm)
biotite		68- 70	up to 1 long
epidote		15- 20	0.01 to 0.5 long
calcite		8- 9	up to 0.5 long
quartz		3- 4	up to 0.2
plagioclase		2- 2.5	up to 0.1
zircon		tr	up to 0.02

Biotite forms abundant and up to 1 mm long lamellae and xenoblasts, which are preferentially iso-oriented and define a continuous schistosity. The biotite hosts very fine-grained inclusions of zircon.

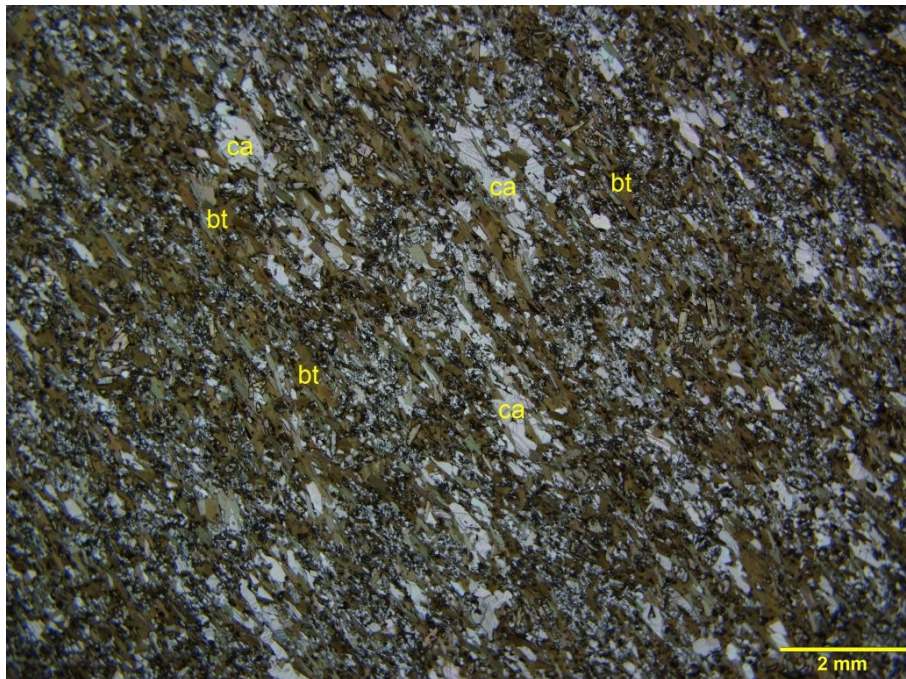
Epidote forms inequigranular xenoblasts ranging from 0.01 to 0.5 mm long, and rare subidioblastic crystals. The finer-grained crystals are disseminated within the biotite, plagioclase, and quartz. The fine-grained subidioblastic crystals are spatially associated with the biotite lamellae. The larger epidote crystals are randomly oriented and likely crystallized after the tectonometamorphic event.

Calcite forms xenoblastic crystals (up to 0.5 mm long), which are intergrown with the biotite and are iso-oriented parallel to the schistosity.

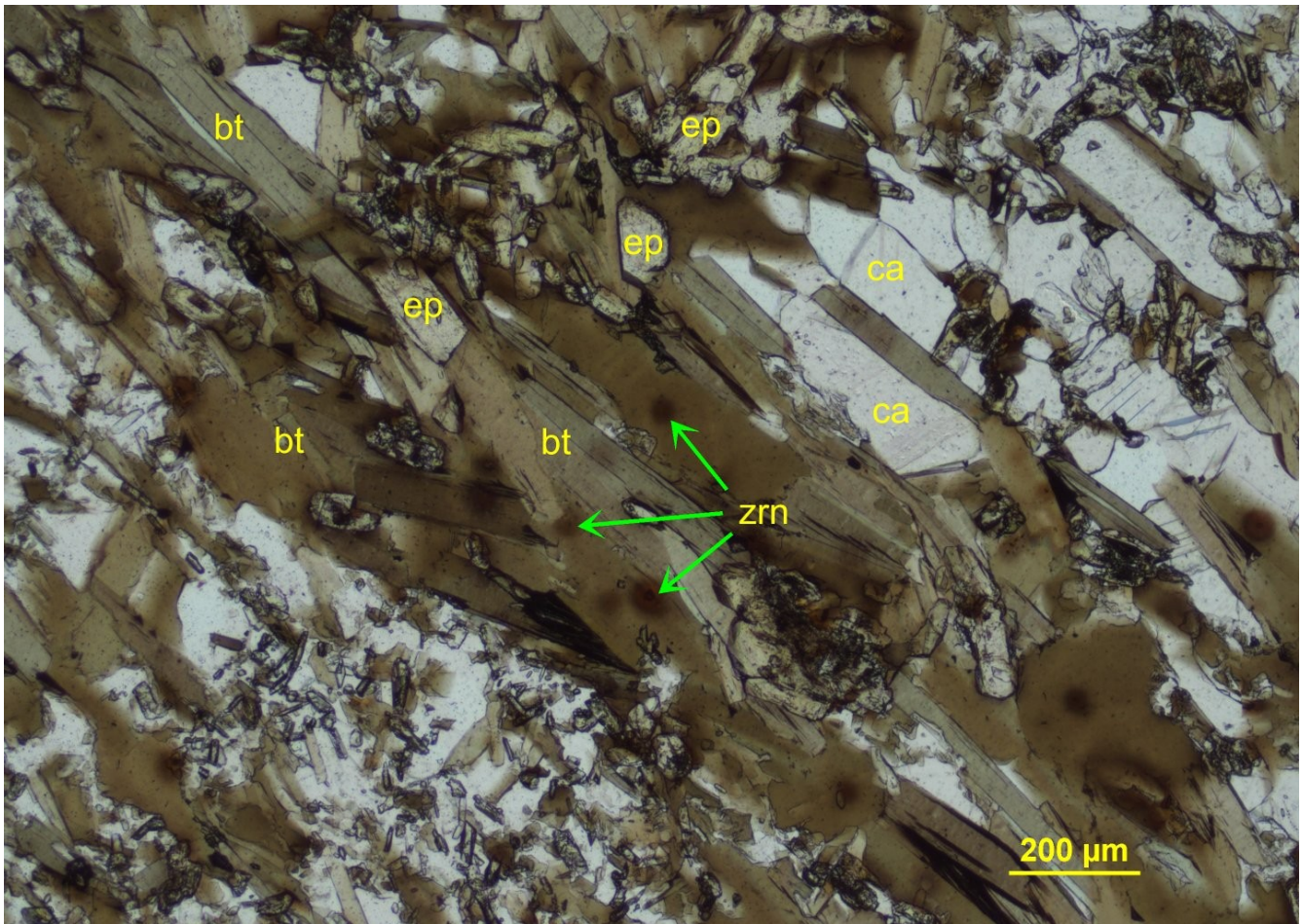
Plagioclase and **quartz** are very fine- to fine grained and forms interlobate aggregate associated with the biotite, epidote, and calcite. The quartz forms sparse blocky crystals. The fine-grained plagioclase is distinguished by very rare Albite twinnings.



Photomicrograph 27a: Preferentially iso-oriented biotite (bt) and subordinate epidote and calcite define a continuous schistosity. Plane-polarized transmitted light.



Photomicrograph 27b: The biotite (bt) is associated with subordinate epidote and preferentially iso-oriented calcite crystals (ca). Plane-polarized transmitted light.



Photomicrograph 27c: The biotite (bt) forms irregular clusters oriented roughly parallel to the schistosity, and hosts very fine-grained zircon (zrn). Xenoblastic epidote (ep) overprinted the biotite and the quartzofeldspathic aggregate. Plane-polarized transmitted light.

Sample 28: A23-01966-28-IG_BH04_MG078



Meta-tonalite(?)

Inequigranular plagioclase crystals are intergrown with fine-grained and subordinate crystals of quartz, epidote, chlorite, biotite, and titanite. The epidote and chlorite define irregular clusters imparting a subtle anisotropy to the granular texture.

Alteration/Metamorphism: **epidote:** moderate; **Fe-chlorite:** weak to moderate after biotite; **white mica:** subtle after plagioclase; **titanite:** subtle

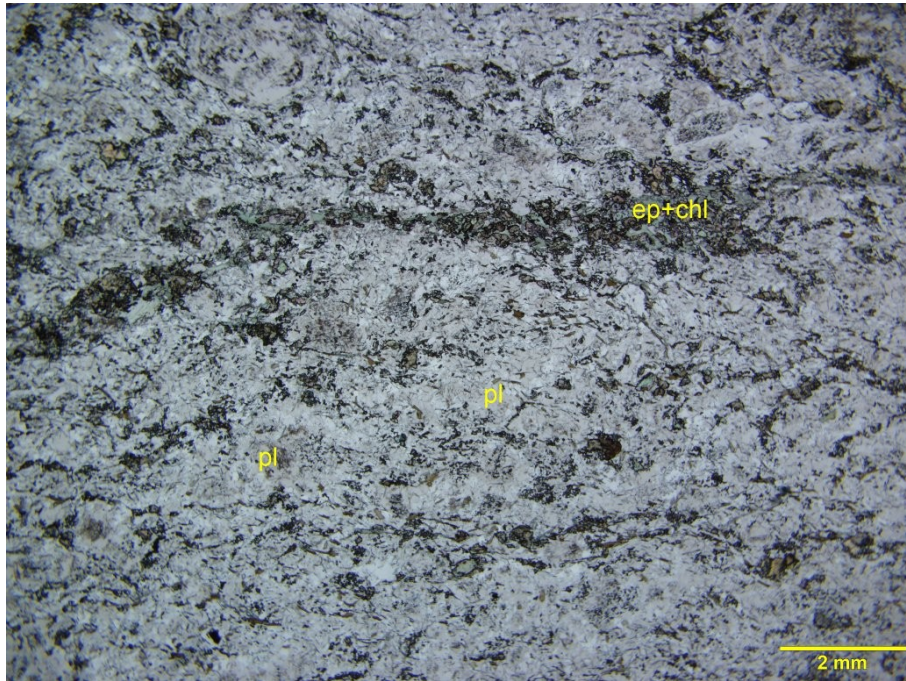
Mineral	Alteration/Metamorphism Mineral	Modal %	Size Range (mm)
plagioclase	epidote-white mica	78- 79	up to 2
	epidote	15- 17	up to 0.4
quartz		2- 4	up to 0.25
[biotite]	chlorite	1- 1.5	up to 0.3
	titanite	tr	up to 0.2

Plagioclase forms inequigranular (up to 2 mm across) crystals. Most of the crystals show xenoblastic shape, only the coarse-grained crystals show relic of subhedral shape, likely derived from the probable magmatic protolith. The plagioclase crystals show Albite twinnings. The plagioclase is albite, as indicated by its refractive indexes lower than those of the quartz.

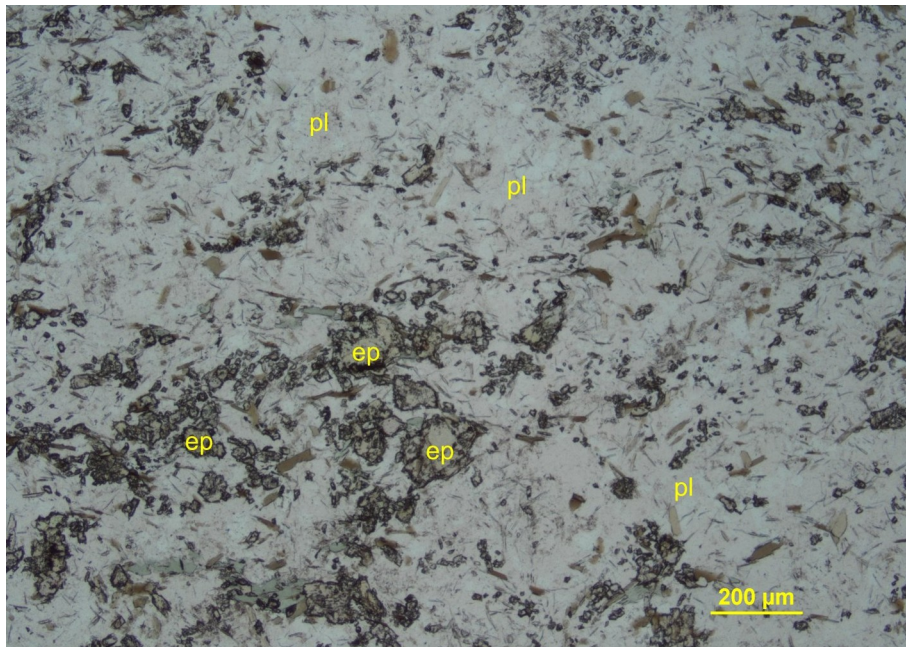
Epidote is the second most abundant mineral in this section, and occurs as fine-grained xenoblastic crystals overprinting the plagioclase and quartz. The epidote is up to 0.4 mm across and shows its typical high relief, pleochroic and mottled high birefringence. The epidote and chlorite forms irregular clusters and crystal trains defining a weak and rough anisotropy.

Quartz is subordinate to the plagioclase and occurs as fine-grained granoblastic crystals intergrown with the plagioclase. The quartzofeldspathic aggregate likely formed by the deformation and recrystallization of a magmatic (tonalitic?) rock.

Biotite is disseminated within the quartzofeldspathic aggregate and it is weakly to moderately altered to Fe-chlorite. Most biotite lamellae are randomly oriented.



Photomicrograph 28a: Epidote and chlorite define the anisotropy in the mostly granular and xenoblastic texture of this sample. Plane-polarized transmitted light.



Photomicrograph 28b: Xenoblastic epidote (ep) and subordinate biotite (bt) is dispersed within the plagioclase-rich (pl) rock. Plane-polarized transmitted light.

Sample 29: A23-01966-29-IG_BH04_MG079



Chlorite-sericite-altered microtonalite

Subhedral and anhedral plagioclase prevails over interstitial quartz and K-feldspar, and together with chlorite-rich pseudomorphs after biotite define a relatively homogeneous granular texture.

Alteration: sericite-epidote: moderate after plagioclase; **Fe-chlorite-epidote-titanite:** subtle to strong after biotite

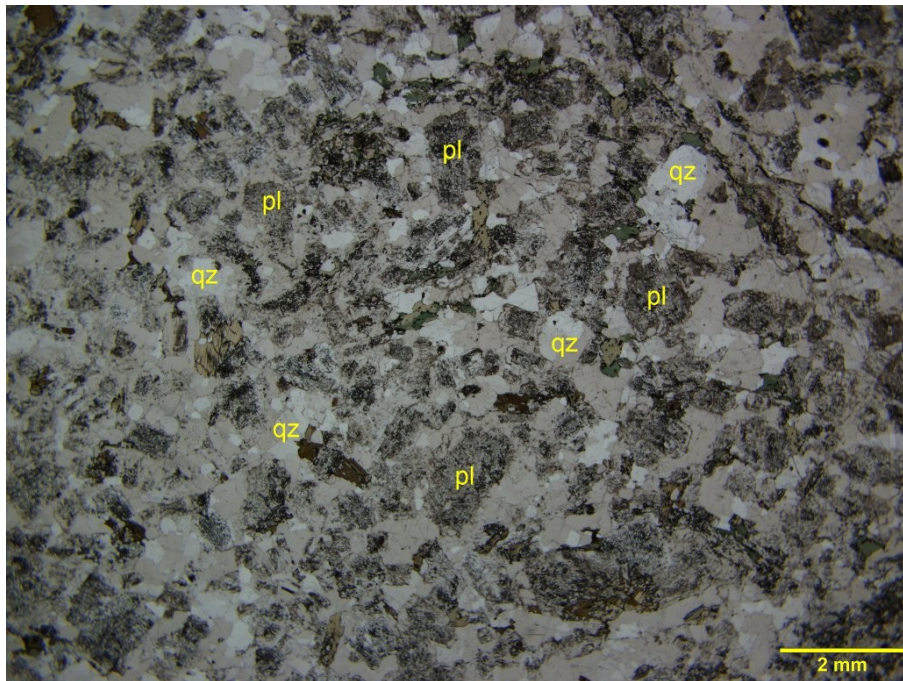
Mineral	Alteration/Weathering Mineral	Modal %	Size Range (mm)
plagioclase	sericite-epidote	65- 67	up to 2.5
quartz		26- 28	up to 0.5
[biotite]	Fe-chlorite-titanite	5- 7	[up to 0.6]
K-feldspar (microcline)		2- 4	up to 0.2
	calcite	tr	0.2
zircon		tr	0.01

Plagioclase is inequigranular (up to 2 mm across), and its crystals are moderately altered to very fine-grained **sericite** and subordinate **epidote** (Photomicrograph 29c). The heterogeneous alteration of the plagioclase define a subtle heterogeneity in this section. Some crystals are euhedral and strongly altered to sericite and epidote, other crystals are moderately altered to sericite (Photomicrograph 29b). This heterogeneity is not detected in the offcuts’ image above and would be extremely difficult to detect in the field.

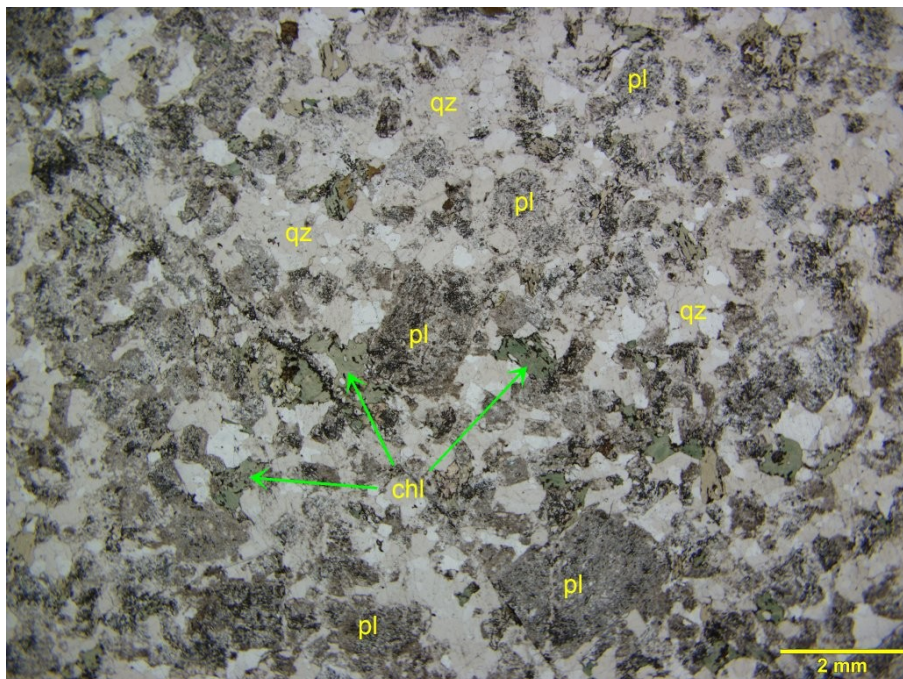
Quartz forms fine- to medium-grained crystals subordinate to the plagioclase (Photomicrograph 29a, 29b, and 29c).

Fe-chlorite, epidote, and **titanite** (Photomicrograph 29a and 29b) completely replaced fine- to medium-grained and randomly oriented biotite crystals.

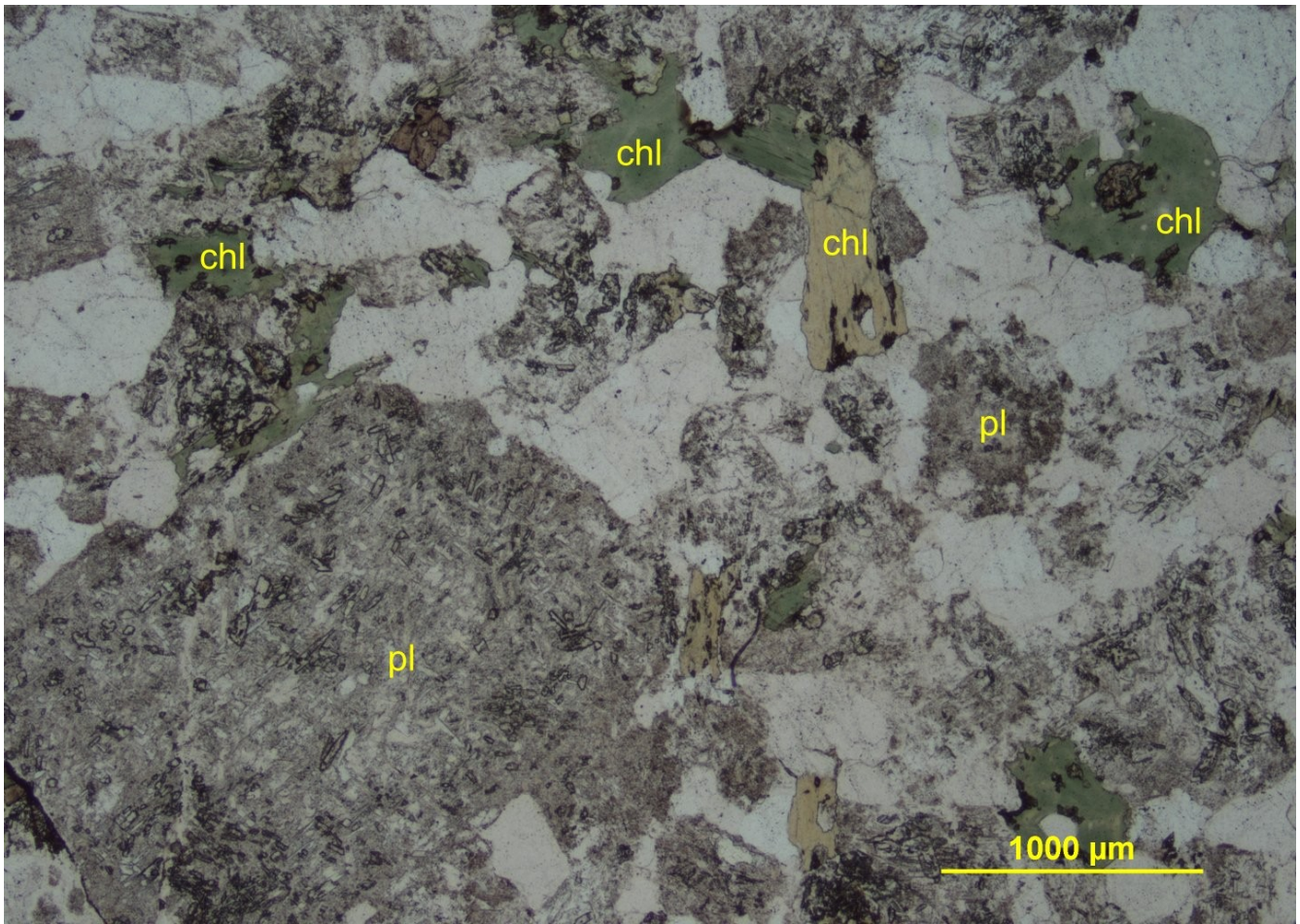
K-feldspar is fine-grained and interstitial and shows Albite-Pericline twinnings in most of its occurrences. K-feldspar is a primary magmatic mineral in this section.



Photomicrograph 29a: Moderately altered plagioclase (pl), quartz (qz), and Fe-chlorite-rich pseudomorphs after biotite defines a granular texture. Plane-polarized transmitted light.



Photomicrograph 29b: The plagioclase alteration is subtly heterogeneous. Some crystals are strongly altered to sericite and epidote (the darker plagioclase crystals) and others are moderately altered to sericite. Plane-polarized transmitted light.



Photomicrograph 29c: Fe-chlorite (chl) and titanite completely replaced biotite lamellae. Sericite and subordinate epidote moderately altered the plagioclase (pl). Plane-polarized transmitted light.

Sample 30: A23-01966-30-IG_BH04_MG080



Fe-chlorite-sericite-altered microgranodiorite

In this section, subhedral plagioclase crystals are intergrown with quartz, interstitial K-feldspar and randomly oriented biotite. The biotite is heterogeneously altered in different parts of the section.

Alteration: sericite-epidote: subtle to moderate after plagioclase; **Fe-chlorite-titanite:** subtle to strong after biotite

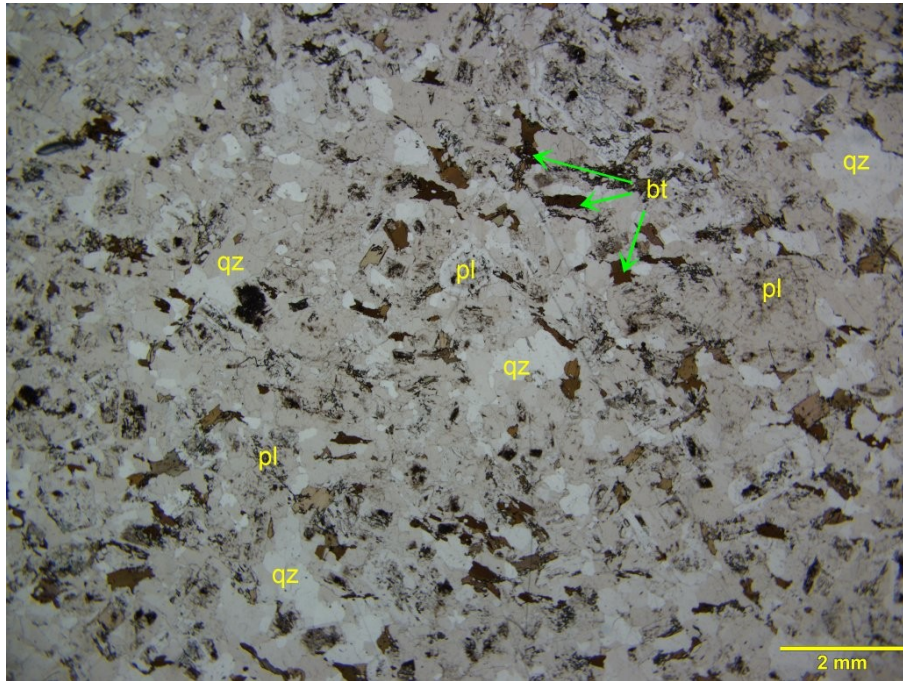
Mineral	Alteration/Weathering Mineral	Modal %	Size Range (mm)
plagioclase	sericite-epidote	51- 52	up to 1.5, rare up to 2.5
quartz		35- 37	0.2 to 1
K-feldspar (microcline)		10- 12	up to 0.2
[biotite]	Fe-chlorite-epidote-titanite	6- 8	up to 1 long
zircon		tr	0.01

Plagioclase is inequigranular (up to 2 mm across), and its subhedral crystals are moderately altered to very fine-grained **sericite** and subordinate **epidote** (Photomicrograph 29c). The heterogeneous alteration of the plagioclase defines a subtle heterogeneity in this section. Some crystals are moderately altered to sericite and epidote, other crystals are subtly to weakly altered to sericite. This heterogeneity is not detected in the offcuts' image above and would be extremely difficult to detect in the field. The less altered plagioclase crystals show refractive indexes lower than those of the quartz; therefore, the plagioclase is **albite**.

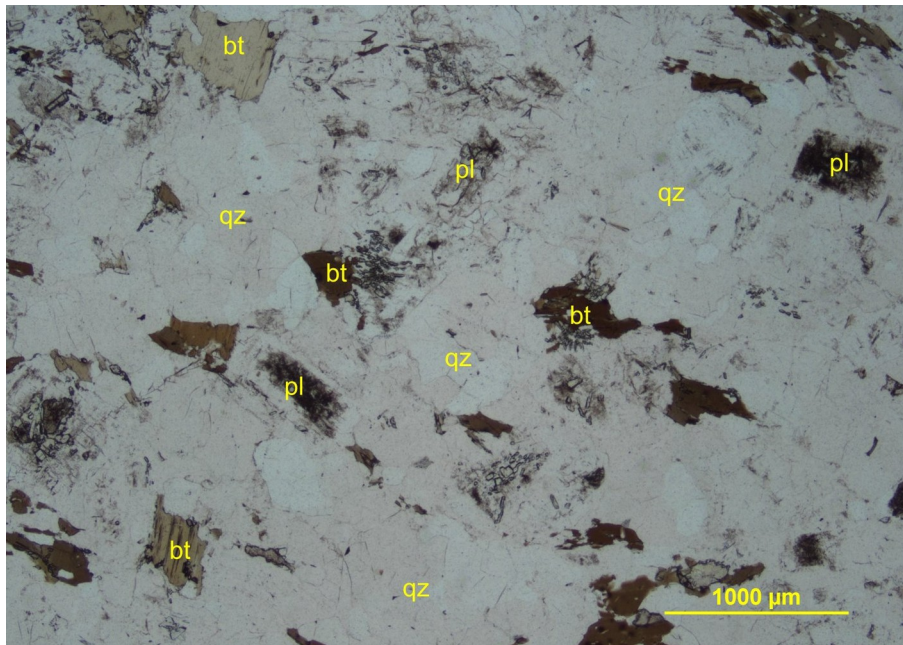
Quartz forms fine- to medium-grained crystals associated with subhedral plagioclase.

Fe-chlorite, epidote, and **titanite** (Photomicrograph 29a and 29b) completely replaced fine- to medium-grained and randomly oriented biotite crystals. Some fresh biotite crystals are disseminated within the section near the completely altered biotite (e.g., Photomicrograph 30c and 30d).

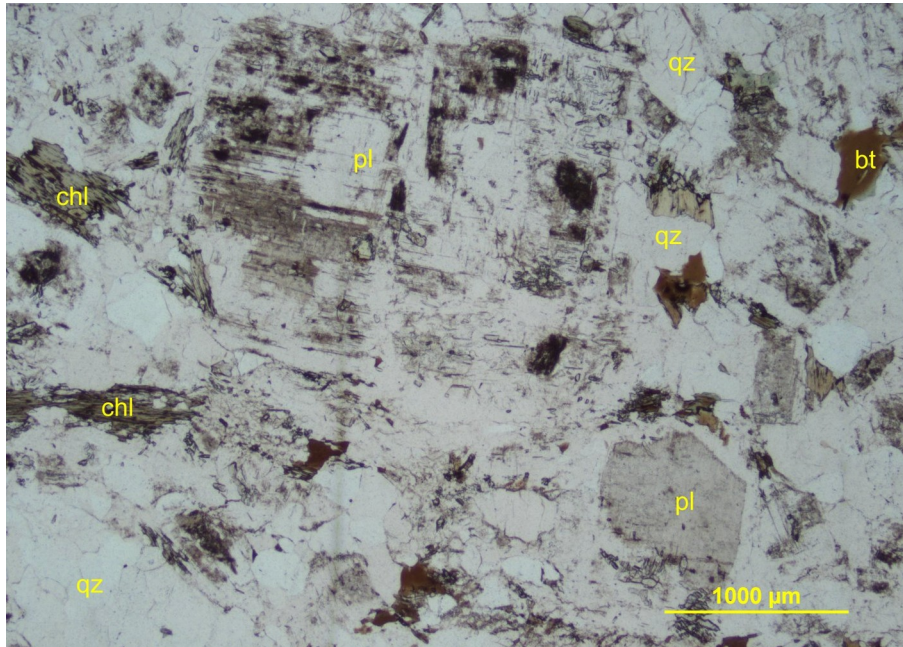
K-feldspar is fine-grained and interstitial and shows Albite-Pericline twinnings in most of its occurrences. I interpret the K-feldspar as a primary magmatic mineral in this section.



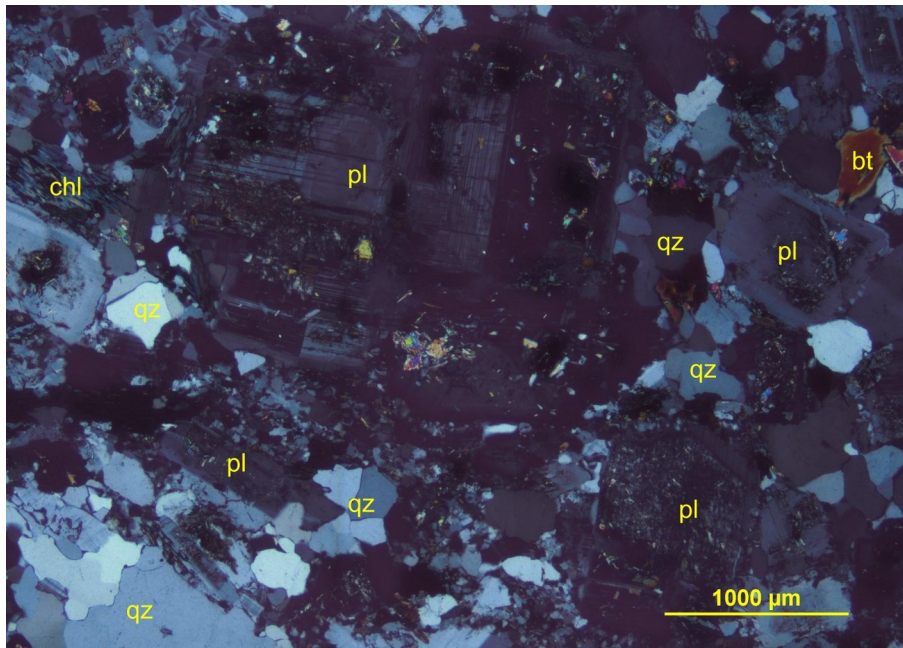
Photomicrograph 30a: Plagioclase (pl), quartz (qz), and randomly oriented biotite define a granular texture. Plane-polarized transmitted light.



Photomicrograph 30b: Fresh biotite is randomly oriented within relatively fresh plagioclase (pl) and quartz (qz). Plane-polarized transmitted light.

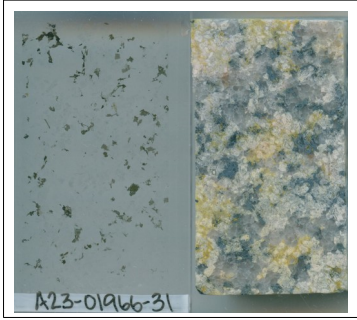


Photomicrograph 30c: Fresh biotite occurs on the right of the weakly altered plagioclase crystal. Fe-chlorite (chl) completely altered the biotite on the left of the plagioclase. Plane-polarized transmitted light.



Photomicrograph 30d: Same area as shown in Photomicrograph 30c. The plagioclase is only subtly altered and shows Albite twinnings under crossed polarizers transmitted light.

Sample 31: A23-01966-31-IG_BH04_MG081



Tonalite

Subhedral and inequigranular plagioclase crystals, anhedral crystals of quartz, randomly oriented and anhedral biotite and poikilitic K-feldspar define a granular texture.

Alteration: white mica-epidote: weak after plagioclase; **epidote:** subtle

Mineral	Alteration/Weathering Mineral	Modal %	Size Range (mm)
plagioclase (albite)	white mica-epidote	45- 47	up to 2.5 long
quartz		35- 37	up to 3.5 long
K-feldspar (microcline)		9- 10	up to 7.5 long
biotite		7- 9	up to 1.5 long, rare up to 2 long
	epidote	0.1- 0.3	up to 0.6 long
zircon		tr	up to 0.05

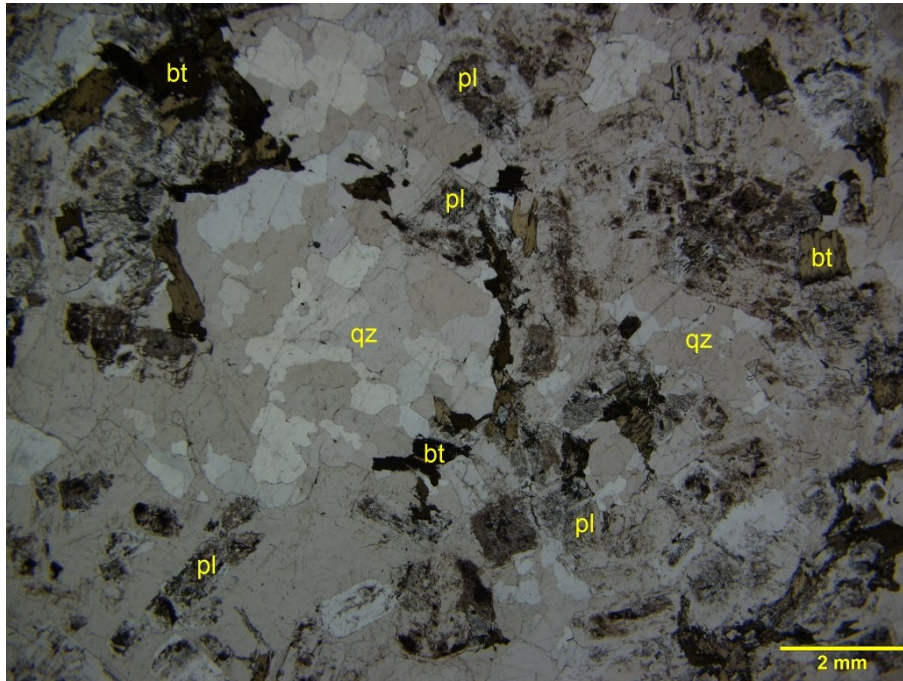
Plagioclase is the prevailing mineral and forms subhedral crystals up to 2.5 mm long. The plagioclase shows Albite twinings and its refractive indexes are lower than those of the quartz, thus indicating that its composition is albitic. Fine-grained white mica flakes and anhedral epidote weakly altered the plagioclase. Some plagioclase crystals show a subhedral growth zoning.

Quartz forms medium-grained anhedral crystals (up to 3.5 mm long), which in some cases form monomineralic domains, likely the result of recrystallized quartz phenocrysts. Most crystals show a moderate undulose extinction.

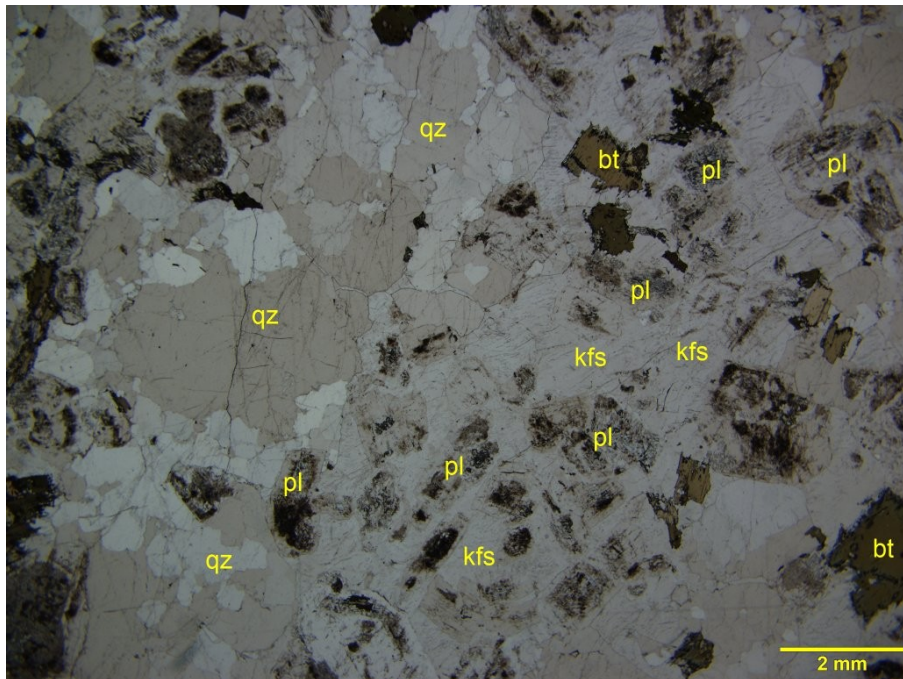
Biotite is randomly oriented and occurs as fine to medium-grained (up to 2 mm long) subhedral and anhedral lamellae. The biotite hosts very fine-grained zircon, which generates the typical pleochroic halo within the biotite host.

Epidote crystals preferentially overprinted the biotite and are dispersed, together with the white mica, as fine-grained alteration products within the plagioclase.

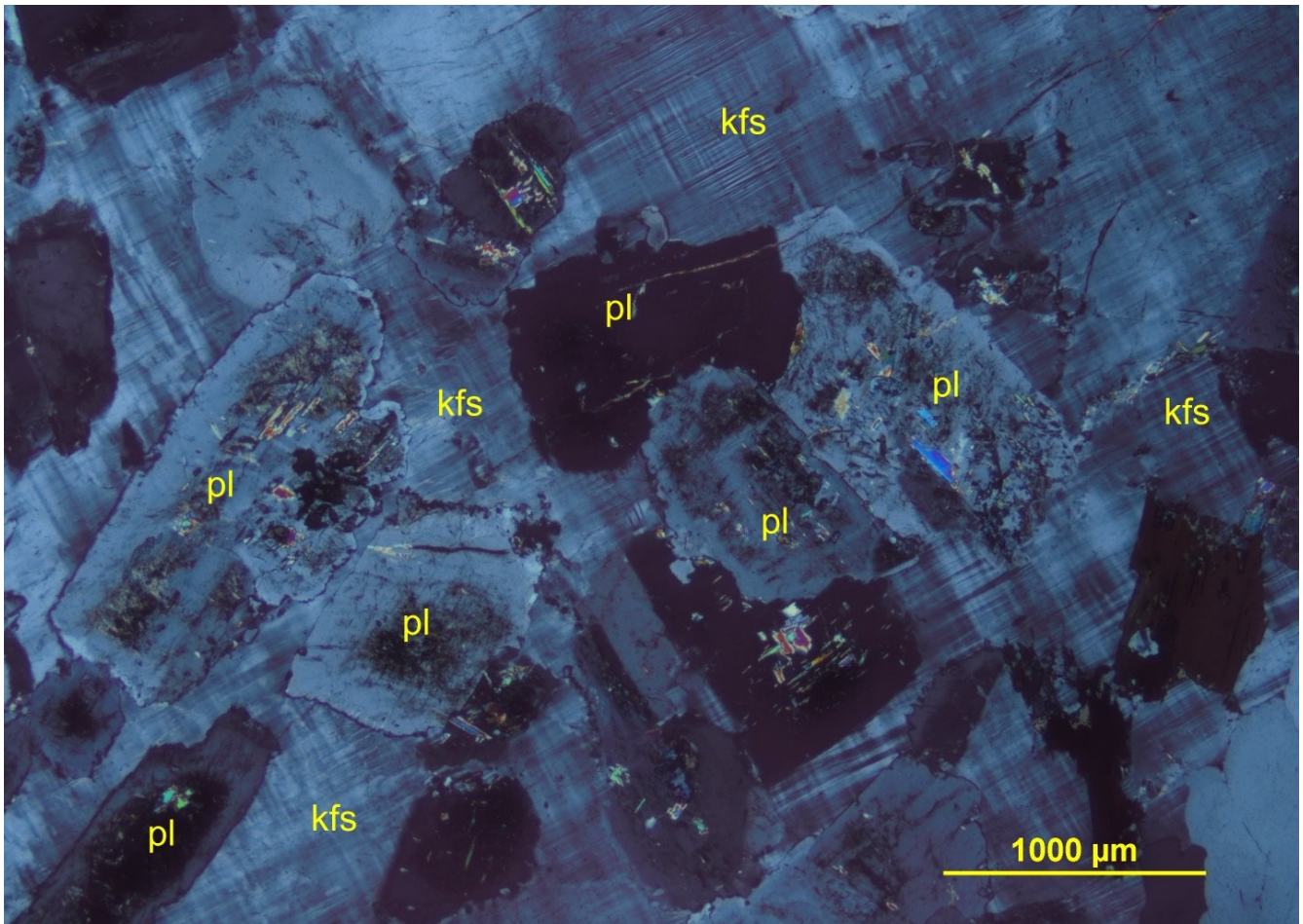
K-feldspar occurs as sparse patches (see yellow staining spots in the offcut’s image above), which under the microscope are poikilitic crystals (up to 5 mm across) including subhedral plagioclase (Photomicrograph 31c). Because of the Albite-Pericline (tartan) twinings, the K-feldspar is **microcline**.



Photomicrograph 31a: Subhedral and weakly altered plagioclase (pl) anhedral quartz (qz) and randomly oriented biotite define a granular texture. Plane-polarized transmitted light.



Photomicrograph 31b: The quartz (qz) forms monomineralic domains, likely the result of recrystallized phenocrysts. Plane-polarized transmitted light.



Photomicrograph 31c: Poikilitic K-feldspar (kfs) encloses subhedral plagioclase (pl) and biotite (bt). Crossed polarizers transmitted light.

Sample 32: A23-01966-32-IG_BH04_MG082

Tonalite

Subhedral and inequigranular plagioclase crystals, anhedral crystals of quartz, randomly oriented and anhedral biotite and poikilitic K-feldspar define a granular texture.



Alteration: white mica-epidote: weak after plagioclase; **epidote:** subtle

Mineral	Alteration/Weathering Mineral	Modal %	Size Range (mm)
plagioclase (albite)	white mica-epidote	44- 45	up to 3 long
quartz		40- 42	up to 2.5 long
K-feldspar (microcline)		7- 9	up to 5 across
biotite		5- 6	up to 1.5 long, rare up to 2 long
	epidote	tr	up to 0.6 long
zircon		tr	up to 0.05
	iron oxides	tr	0.02

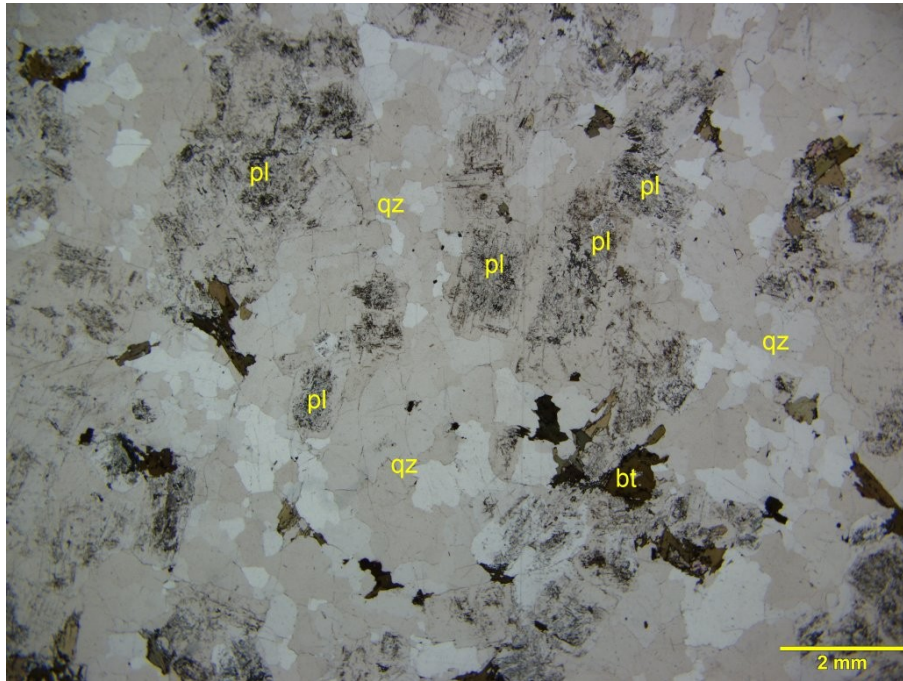
Plagioclase is the prevailing mineral and forms subhedral crystals up to 3 mm long. The plagioclase shows Albite twinings and its refractive indexes are lower than those of the quartz, thus indicating that its composition is albitic. Fine-grained white mica flakes and anhedral epidote weakly altered the plagioclase. Some plagioclase crystals show a subhedral growth zoning (Photomicrograph 32d).

Quartz forms medium-grained anhedral crystals (up to 2.5 mm long), which in some cases form monomineralic domains (Photomicrograph 32c). Most crystals show a moderate undulose extinction.

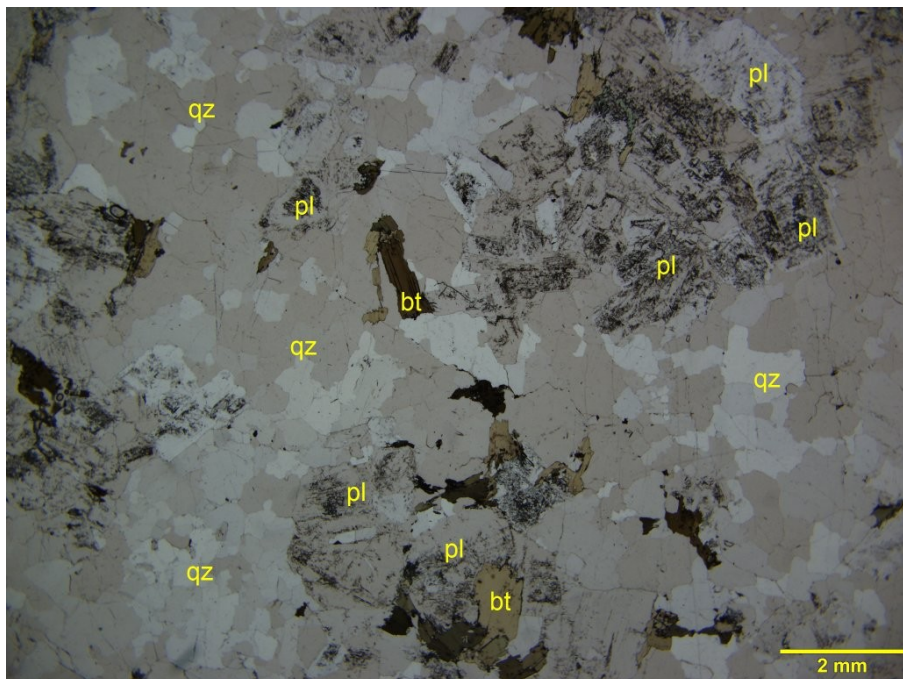
Biotite is randomly oriented and occurs as fine to medium-grained (up to 2 mm long) subhedral and anhedral lamellae. The biotite hosts very fine-grained zircon, which generates the typical pleochroic halo within the biotite host.

K-feldspar occurs as sparse patches (see yellow staining spots in the offcut's image above), which under the microscope are poikilitic crystals (up to 5 mm across) including subhedral plagioclase (Photomicrograph 32d). Because of the Albite-Pericline (tartan) twinings, the K-feldspar is **microcline**. Some crystals host fine-grained perthitic stringlets (Photomicrograph 32d).

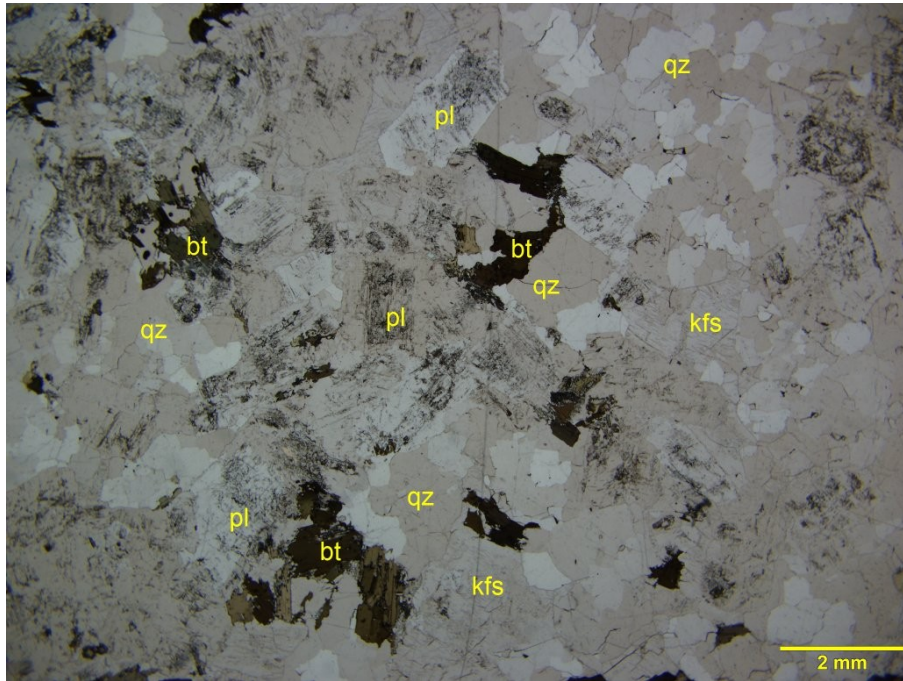
Epidote crystals preferentially overprinted the biotite and are dispersed, together with the white mica, as fine-grained alteration products within the plagioclase.



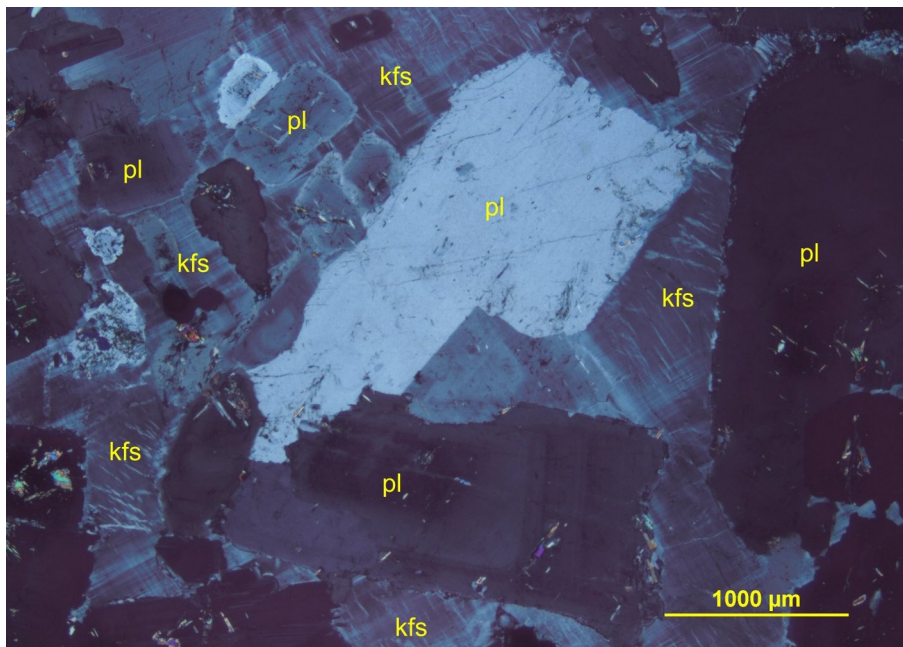
Photomicrograph 32a: Subhedral and weakly altered plagioclase (pl) anhedral quartz (qz) and randomly oriented biotite define a granular texture. Plane-polarized transmitted light.



Photomicrograph 32b: The quartz (qz) forms monomineralic domains, likely the result of recrystallized phenocrysts. Plane-polarized transmitted light.



Photomicrograph 32c: The quartz (qz) forms monomineralic domains, and is associated with subhedral plagioclase (pl) and anhedral K-feldspar (kfs). Plane-polarized transmitted light.



Photomicrograph 32d: Poikilitic K-feldspar (kfs) encloses subhedral plagioclase (pl) . Crossed polarizers transmitted light.

Sample 33: A23-01966-33-IG_BH04_MG083



Sericite-altered tonalite

Subhedral and anhedral crystals of plagioclase, anhedral quartz, and subhedral biotite define a granular texture, in which very fine-grained sericite weakly to moderately altered the plagioclase.

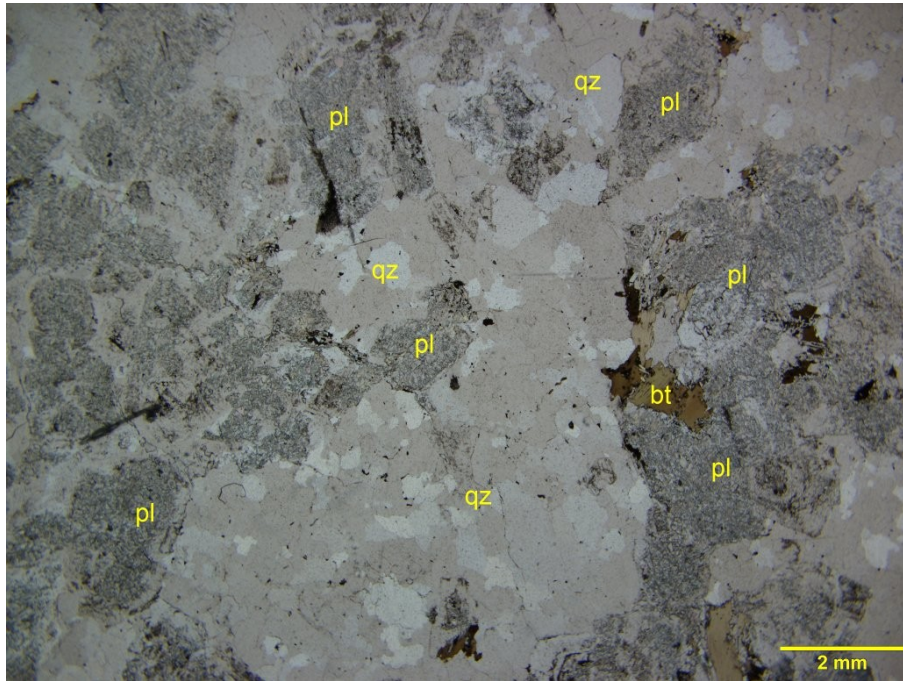
Alteration: white mica: weak to moderate after plagioclase; **pyrite:** subtle; **iron oxides:** strong after pyrite

Mineral	Alteration/Weathering Mineral	Modal %	Size Range (mm)
plagioclase (albite)	sericite	58- 60	up to 2.5
quartz		36- 38	up to 1.5 long
biotite		2- 2.5	up to 1
	[pyrite]→iron oxides	tr	[up to 0.1]
zircon		tr	0.01

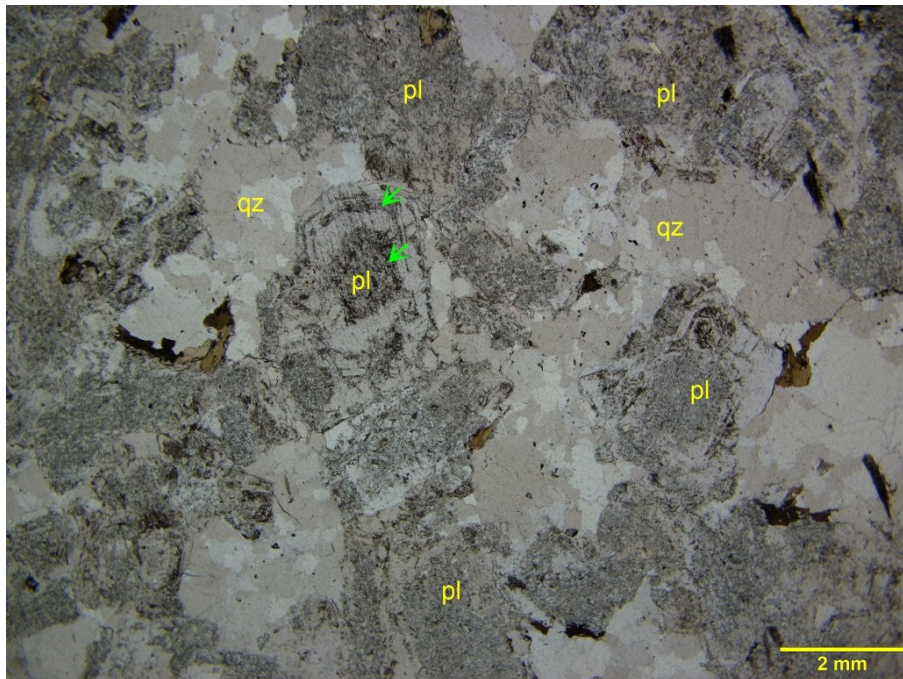
Plagioclase (albite) forms subhedral crystals up to 2.5 mm across. The plagioclase shows Albite twinnings and its refractive indexes are lower than those of the quartz, thus indicating that its composition is albitic. Fine-grained white mica flakes weakly to moderately altered the plagioclase. Some plagioclase crystals show a euhedral growth zoning (see yellow arrows in Photomicrograph 33b).

Quartz forms medium-grained anhedral crystals (up to 2.5 mm long), which in most cases form monomineralic domains. Most crystals show a moderate undulose extinction.

Biotite is randomly oriented and occurs as fine to medium-grained (up to 1 mm long) subhedral and anhedral lamellae. The biotite hosts very fine-grained zircon, which generates the typical pleochroic halo within the biotite host.

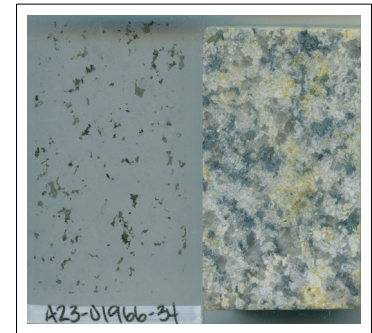


Photomicrograph 33a: Anhedral and subhedral plagioclase (pl), quartz (qz), and randomly oriented lamellae of biotite (bt) define a granular isotropic texture. Plane-polarized transmitted light.



Photomicrograph 33b: Another example of the granular texture defined by plagioclase (pl), quartz (qz), and biotite (bt). The yellow arrows show the euhedral growth zoning in one plagioclase crystal. Plane-polarized transmitted light.

Sample 34: A23-01966-34-IG_BH04_MG084



Tonalite

Subhedral and inequigranular plagioclase crystals, anhedral crystals of quartz, randomly oriented and anhedral biotite define a granular texture.

Alteration: white mica-epidote: weak to strong after plagioclase; **chlorite:** weak after the biotite; **epidote>>iron oxides:** subtle

Mineral	Alteration/Weathering Mineral	Modal %	Size Range (mm)
plagioclase (albite)	white mica-epidote	49- 50	up to 3 long
quartz		39- 40	up to 2.5 long
biotite		6- 7	up to 1.5 long, rare up to 2 long
K-feldspar (microcline)		2- 2.5	up to 3 across
	epidote	tr	up to 0.5
zircon		tr	up to 0.05
	iron oxides	tr	0.02

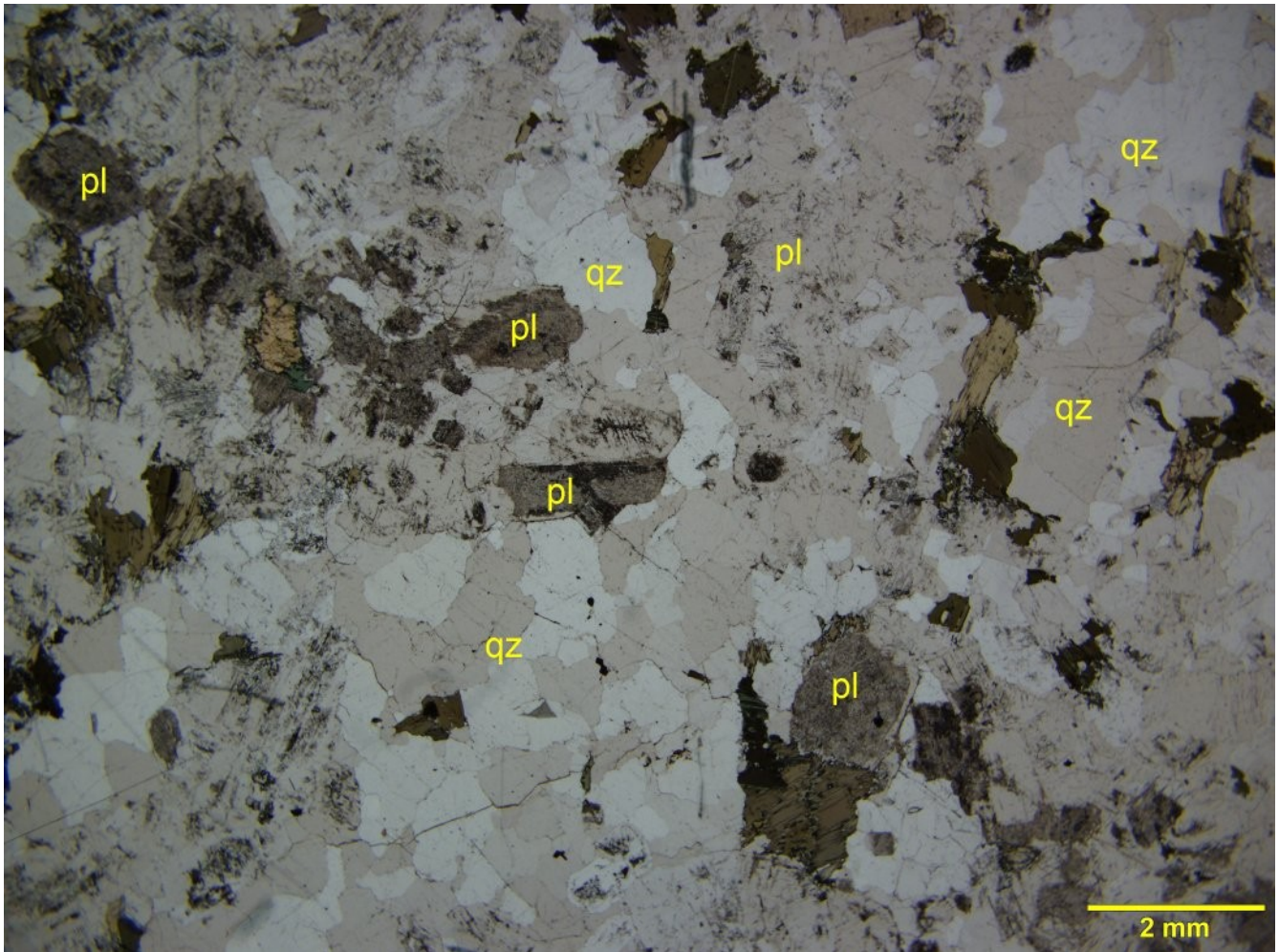
Plagioclase is the prevailing mineral and forms subhedral crystals up to 3 mm long. The plagioclase shows Albite twinnings and its refractive indexes are lower than those of the quartz, thus indicating that the plagioclase is albite. Fine-grained white mica flakes and anhedral epidote weakly to strongly altered the plagioclase. Some plagioclase crystals show a subhedral growth zoning (Photomicrograph 32d), and some others (Photomicrograph 34a) are strongly altered

Quartz forms medium-grained anhedral crystals (up to 2.5 mm long), which in some cases form monomineralic domains. Most crystals show a moderate undulose extinction.

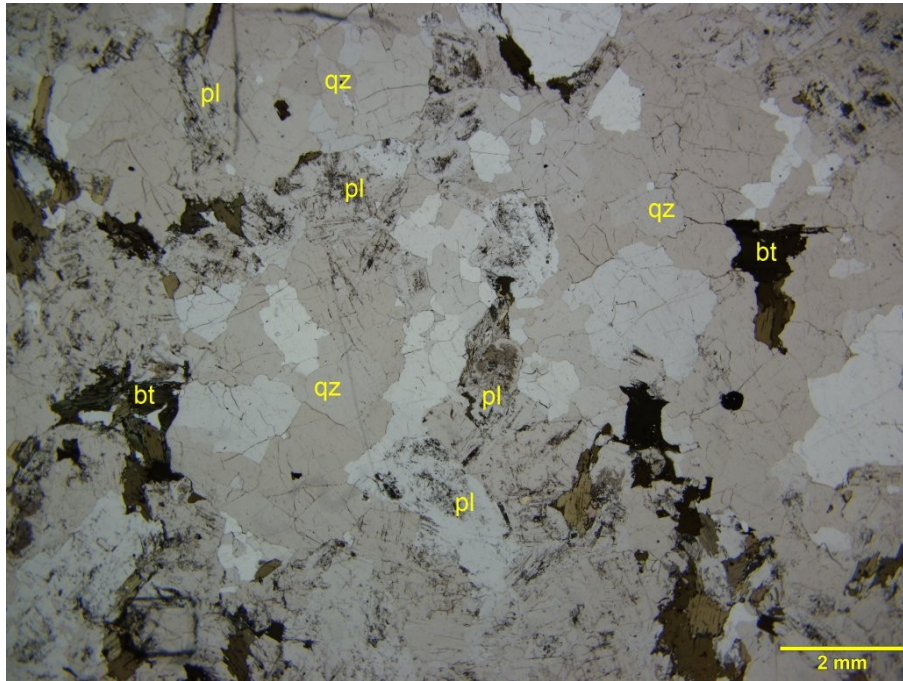
Biotite is randomly oriented and occurs as fine to medium-grained (up to 2 mm long) subhedral and anhedral lamellae. The biotite hosts very fine-grained zircon, which generates the typical pleochroic halo within the biotite host. Chlorite epitaxially and weakly altered some of the biotite crystals.

K-feldspar occurs as sparse patches (see yellow staining spots in the offcut’s image above), and the patches are roughly aligned along an irregular line parallel to the longer side of the section. The medium-grained K-feldspar crystals are less abundant than in the tonalite described above (e.g., Samples 6, 9, 10, 31, and 32); however, it forms rare poikilitic crystals up to 3 mm across hosting subhedral inclusions of plagioclase and biotite (Photomicrograph 34c). This feature reinforces the similarity and co-magmatic nature of this sample and the tonalite listed above. Like in the other tonalite samples, the K-feldspar displays Albite-Pericline twinnings indicating it is microcline.

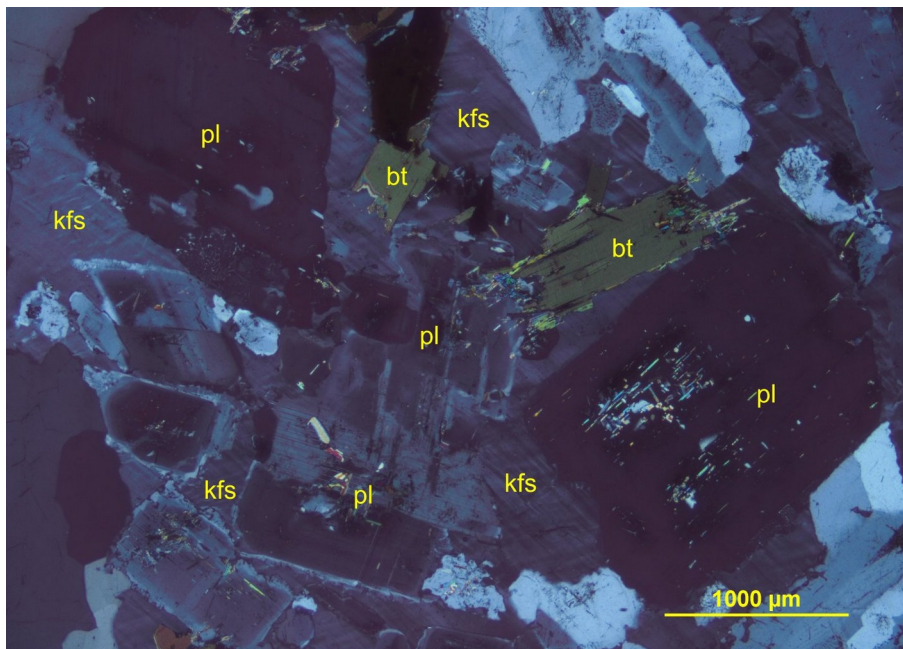
Epidote crystals preferentially overprinted the biotite and are dispersed, together with the white mica, as fine-grained alteration products within the plagioclase.



Photomicrograph 34a: Subhedral and altered plagioclase (pl) anhedral quartz (qz) and randomly oriented biotite define a granular texture. Plane-polarized transmitted light.



Photomicrograph 34b: Most plagioclase crystals (pl) are weakly altered and are associated with monomineralic domains of quartz (qz). Plane-polarized transmitted light.



Photomicrograph 34c: Poikilitic K-feldspar (kfs) encloses subhedral plagioclase (pl). Crossed polarizers transmitted light.

Sample 35: A23-01966-35-IG_BH04_MG085



Fe-chlorite-K-feldspar-altered tonalite

Epidote-K-feldspar veinlet

Euhedral and subhedral crystals of plagioclase and quartz define a granular texture associated with randomly oriented pseudomorphs of chlorite after biotite. The concentration of K-feldspar alteration around an irregular epidote-K-feldspar veinlet defines a second compositional sub-domain in the lower part of this granular rock.

Alteration: **Fe-chlorite:** strong after biotite; **K-feldspar:** weak to moderate after plagioclase in the lower part; **saussurite (epidote+sericite):** weak to moderate after the plagioclase in the upper part

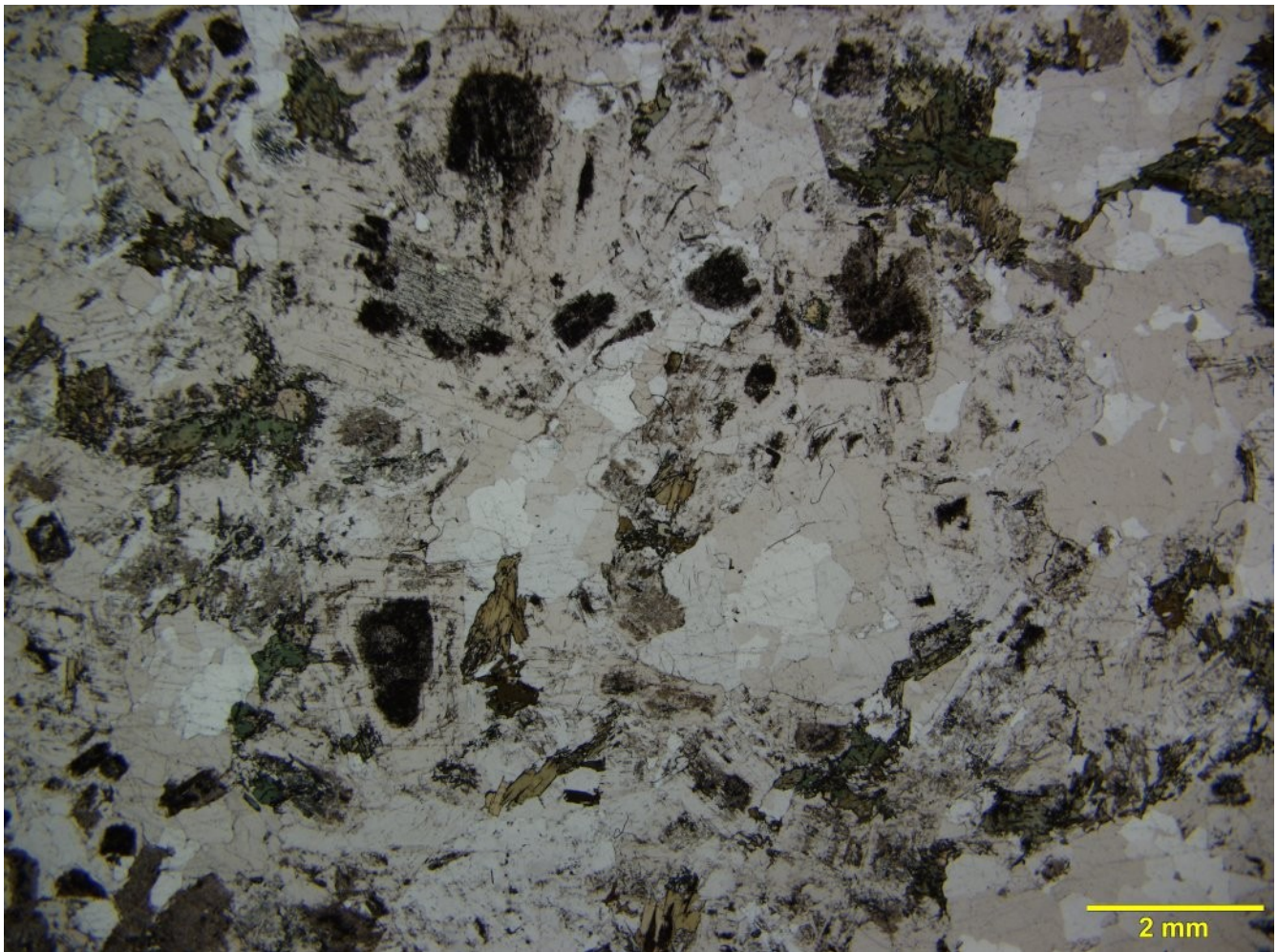
Mineral	Alteration/Weathering Mineral	Modal %	Size Range (mm)
altered tonalite (~99% of PTS)			
plagioclase	epidote+sericite±K-feldspar	53- 55	up to 3 long
quartz		30- 32	up to 1.5
K-feldspar	K-feldspar	12- 15	up to 4
biotite	Fe-chlorite	2- 3	up to 1
zircon		tr	0.01
epidote-K-feldspar veinlet (~1% of PTS)			
K-feldspar		1	up to 0.1
epidote		tr	up to 0.1

Plagioclase forms subhedral and anhedral crystals up to 3 mm long. The plagioclase crystals are altered mostly in the core in the upper part of the section (Photomicrograph 35a). In this case, the very fine-grained earthy alteration product is unresolved and I tentatively interpret it as a mixture of very fine-grained epidote and phyllosilicates (saussurite?). In the lower part of the section and around the epidote-K-feldspar veinlet, the plagioclase is moderately altered by a very fine-grained unresolved material, which display a pale-yellow colour on the stained surface (see image above), and I interpret this as a partial replacement of the plagioclase by **K-feldspar**.

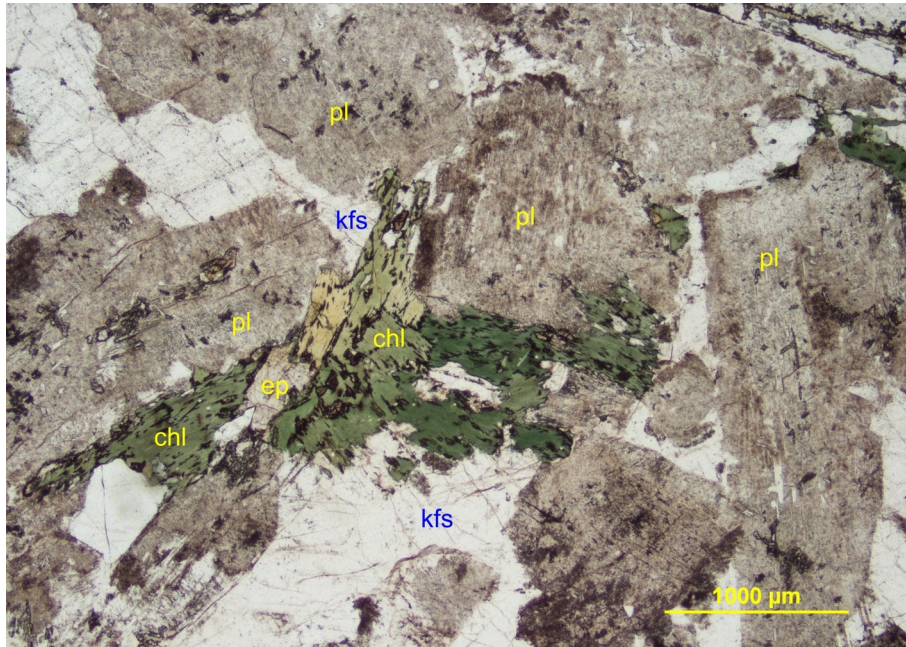
Quartz forms inequigranular and anhedral crystals forming monomineralic and interstitial aggregates associated with the plagioclase, biotite, and K-feldspar (Photomicrograph 35a).

K-feldspar occurs as very fine-grained crystals concentrated within the epidote-K-feldspar veinlet and it forms heterogeneous replacement patches overprinting the plagioclase in the the lower part of the section, and to a lesser extent, in the upper part. Because of its distribution. I interpret most of the K-feldspar as an alteration mineral. Rare poikilitic and interstitial K-feldspar crystals (Photomicrograph 35b and 35c) are magmatic.

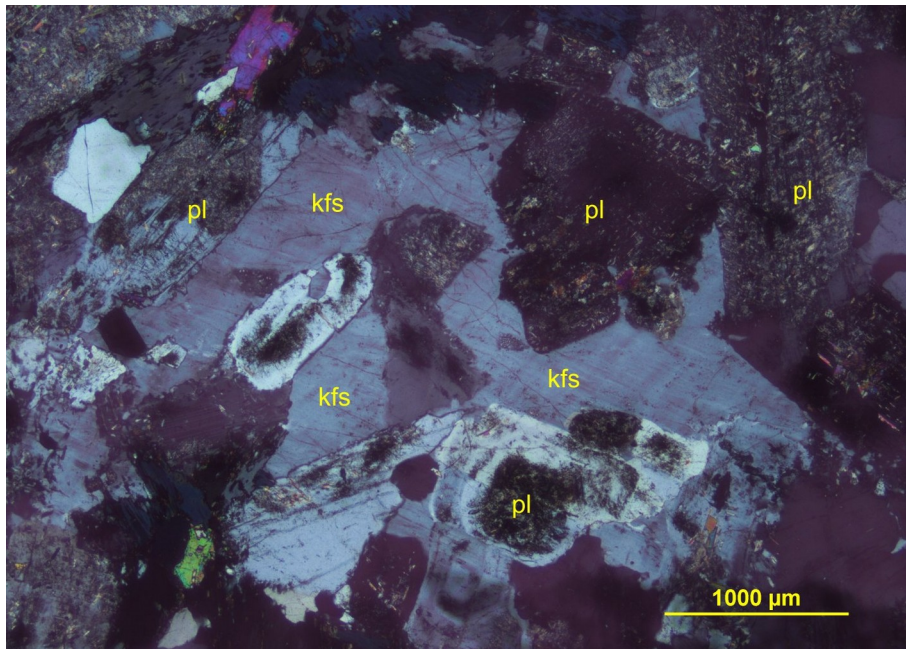
Biotite forms anhedral lamellae (up to 1 mm across), which only in rare instances show their typical pleochroism. In most cases, the Fe-chlorite completely replaced the biotite, and near the epidote-K-feldspar veinlet, epidote overprinted the Fe-chlorite-rich pseudomorph (Photomicrograph 35d).



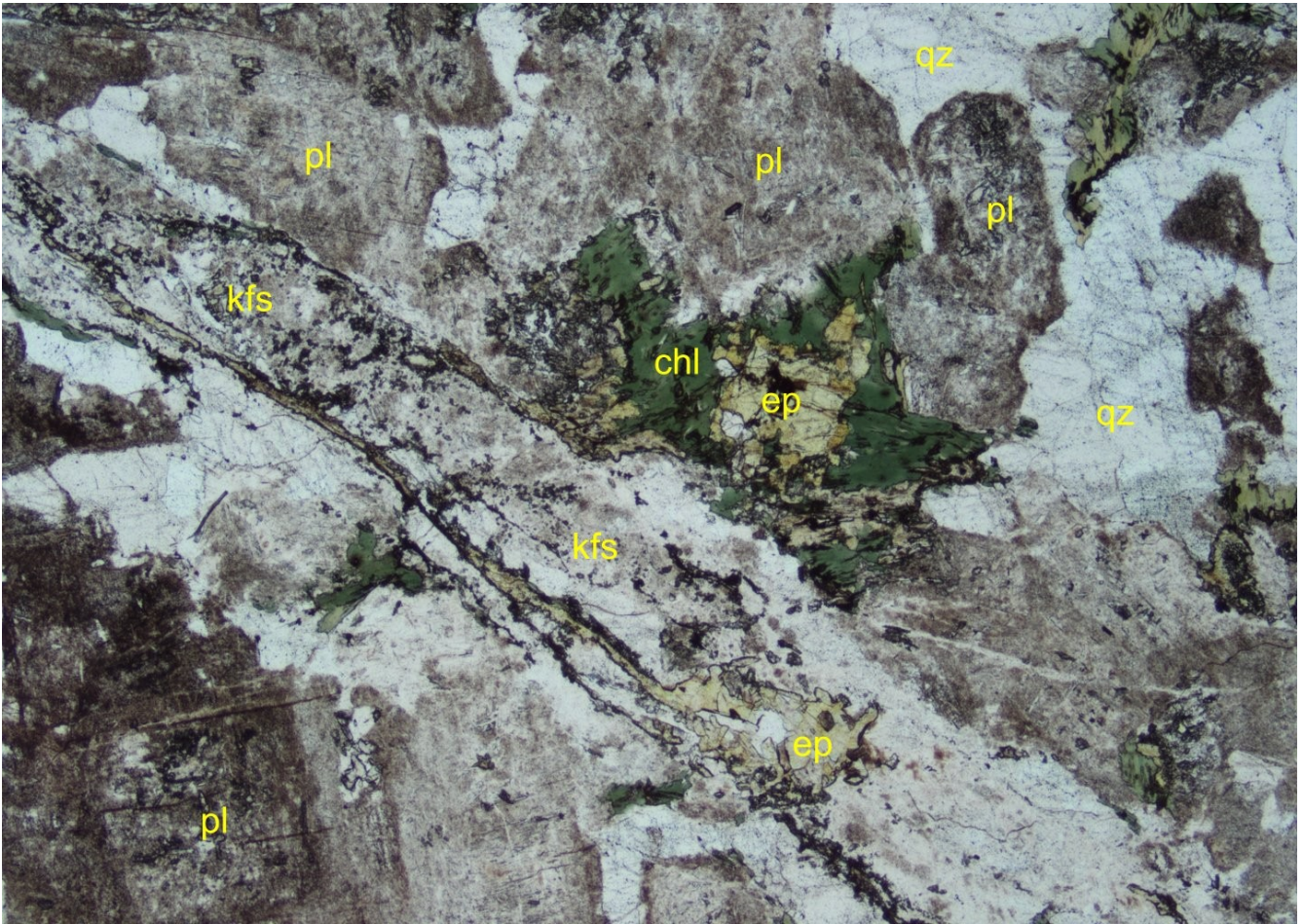
Photomicrograph 35a: The plagioclase is strongly altered in the core of its crystals and, together with quartz and sparse chlorite-altered biotite, defines a granular texture in the upper part of the section. Plane-polarized transmitted light.



Photomicrograph 35b: In the lower part of the section, the plagioclase shows a cloudy appearance, which is probably imparted by replacement patches of K-feldspar. Interstitial K-feldspar (kfs) occur between the altered plagioclase (pl). Plane-polarized transmitted light.



Photomicrograph 35c: Poikilitic K-feldspar (kfs) host inclusions of subhedral plagioclase (pl). This type of K-feldspar is magmatic. Crossed polarizers transmitted light.



Photomicrograph 35d: Near the epidote-K-feldspar veinlet ((kfs and ep) chlorite (chl) and epidote (ep) completely replaced the biotite. Crossed polarizers transmitted light. FOV 4 mm.

Sample 36: A23-01966-36-IG_BH01_LG046

Sericite-altered tonalite

Subhedral plagioclase crystals are immersed within a medium-grained anhedral aggregate of quartz and, together with randomly oriented lamellae of biotite, define a granular texture.



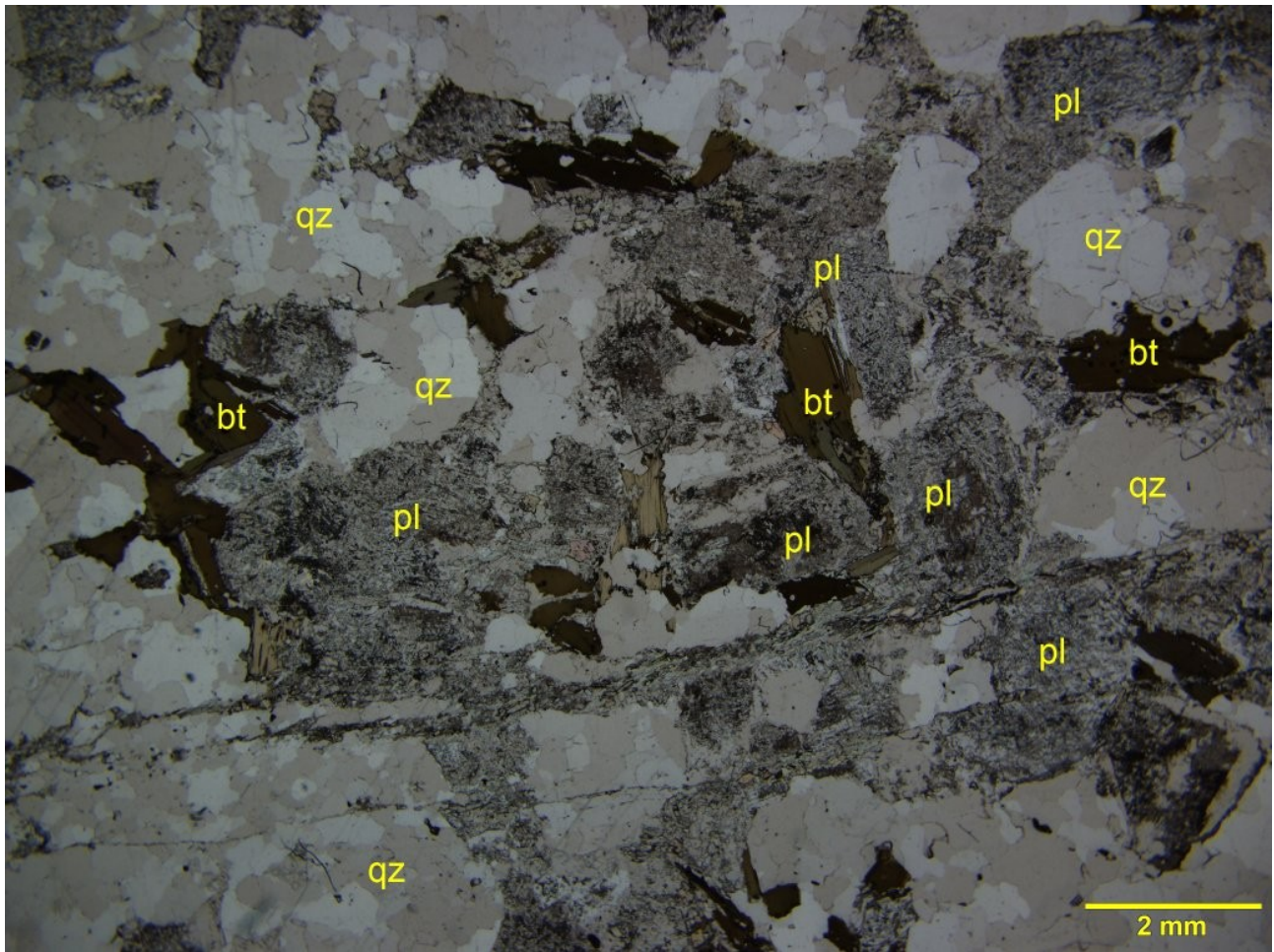
Alteration: white mica>>epidote: weak to moderate after plagioclase

Mineral	Alteration/Weathering Mineral	Modal %	Size Range (mm)
plagioclase	white mica-epidote	45- 47	up to 2.5
quartz		44- 46	0.1 to 1
biotite	epidote	7- 8	up to 2 long
K-feldspar		1- 1.5	up to 0.5
zircon		tr	0.02

Plagioclase forms subhedral crystals up to 2.5 mm across. The plagioclase crystals are randomly oriented and define a granular isotropic texture. Fine-grained flakes of **white mica** and subordinate **epidote** weakly to moderately altered the plagioclase crystals, which under plane-polarized transmitted light are easily distinguished from the inclusion-free quartz (Photomicrograph 36). The granular texture is crosscut by intersecting micro-shear zones filled in by iso-oriented flakes of white mica. These texture indicate that the tonalite was crosscut by brittle fractures and shears during the sericite-alteration event after the magmatic crystallization.

Quartz forms monomineralic and irregularly shaped aggregates, which may be derived from the re-crystallization of quartz phenocrysts. The quartz crystals range from 0.1 mm to 1 mm across and show interlobate shape.

Biotite is dispersed as randomly oriented anhedral lamellae ranging from 0.4 mm long to 2 mm long. The biotite is relatively fresh and hosts very fine-grained crystals of **zircon**. Some biotite crystals are in contact with the plagioclase, and these crystals are rimmed and partially replaced by very fine-grained flakes of sericite.



Photomicrograph 36: Subhedral plagioclase (pl) randomly oriented biotite (bt) and monomineralic domains of quartz define a granular texture. Plane-polarized transmitted light.

Sample 37: A23-01966-37-IG_BH02_LG027



Chlorite-white mica-altered felsitic rock

Inequigranular and anhedral crystals of quartz, plagioclase, and randomly oriented lamellae of white mica define a granular texture. A quartz-vein crosscut the fragmental texture and is fractured and filled in by chlorite and white mica.

Alteration: chlorite: strong after biotite; white mica: weak; limonite: weak; rutile-pyrite: subtle

Mineral	Alteration/Weathering Mineral	Modal %	Size Range (mm)
quartz		53- 55	up to 2.5, rare up to 4.5 long
plagioclase (albite)		40- 42	up to 2
	white mica	3- 4	up to 3.5
	limonitic material	0.8- 1	<0.01
[biotite]	chlorite	0.2- 0.4	up to 1 long
titanite		tr	up to 0.2
	rutile	tr	0.01
	pyrite	tr	0.01

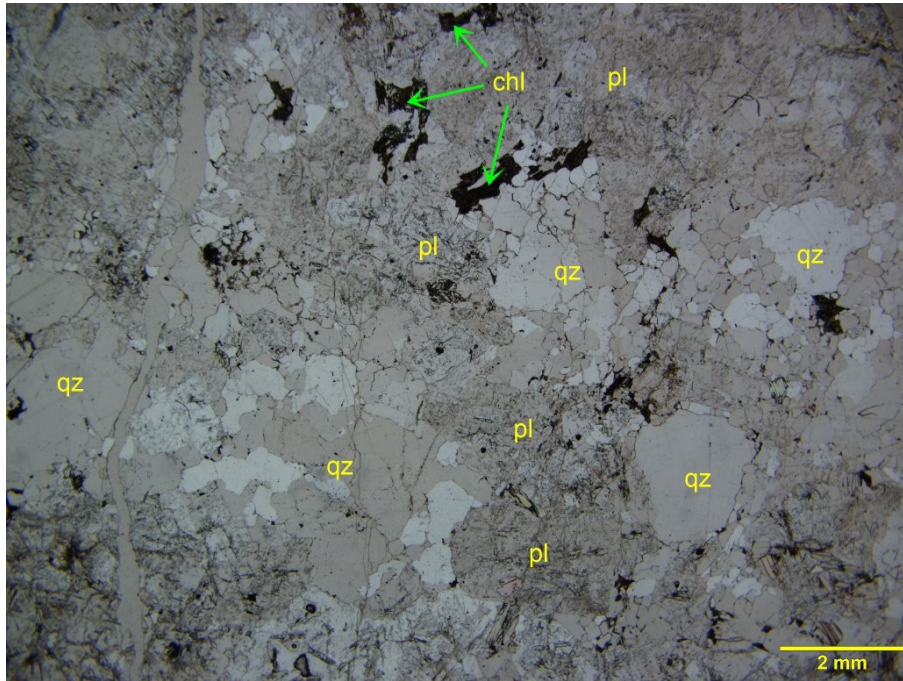
Quartz occurs as inequigranular and anhedral crystals ranging from 0.05 mm to 2.5 mm across, and in rare cases up to 4.5 mm long. The quartz is concentrated within an irregular and up to 7.5 mm thick vein. The vein is fractured and filled in by chlorite and white mica.

Plagioclase is dispersed within the section as xenoblastic crystals (up to 2 mm across) showing Albite twinnings. The plagioclase’s refractive indexes are lower than those of the quartz; therefore, the plagioclase is **albite**. Fine-grained lamellae of white mica weakly to moderately altered the plagioclase crystals.

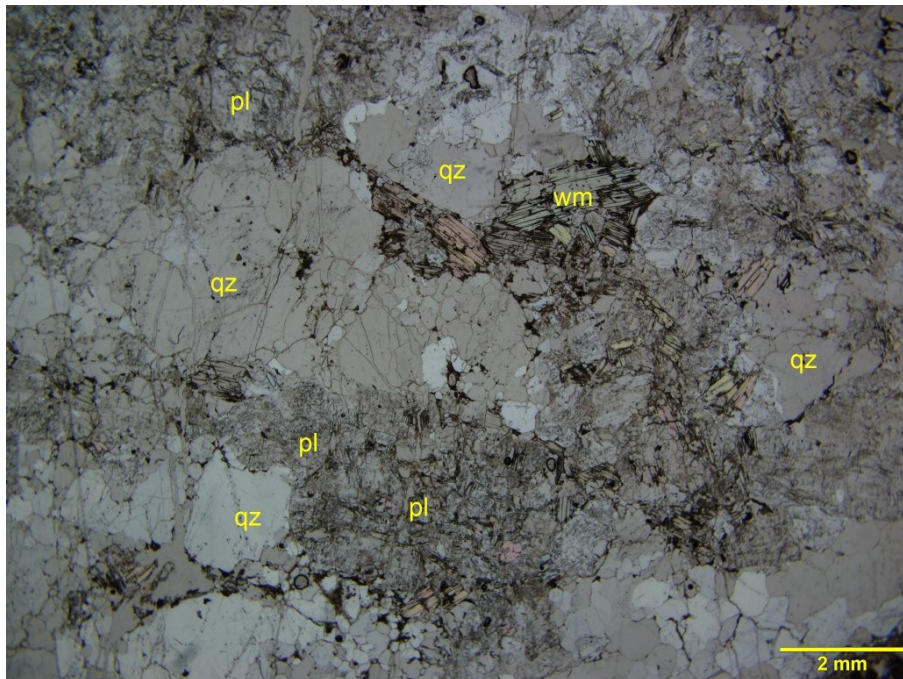
White mica overprinted the plagioclase and forms medium-grained lamellae concentrated within the crack of the quartz vein and disseminated within the granular texture (Photomicrograph 37b).

Titanite is rare and heterogeneously disseminated within the granular texture.

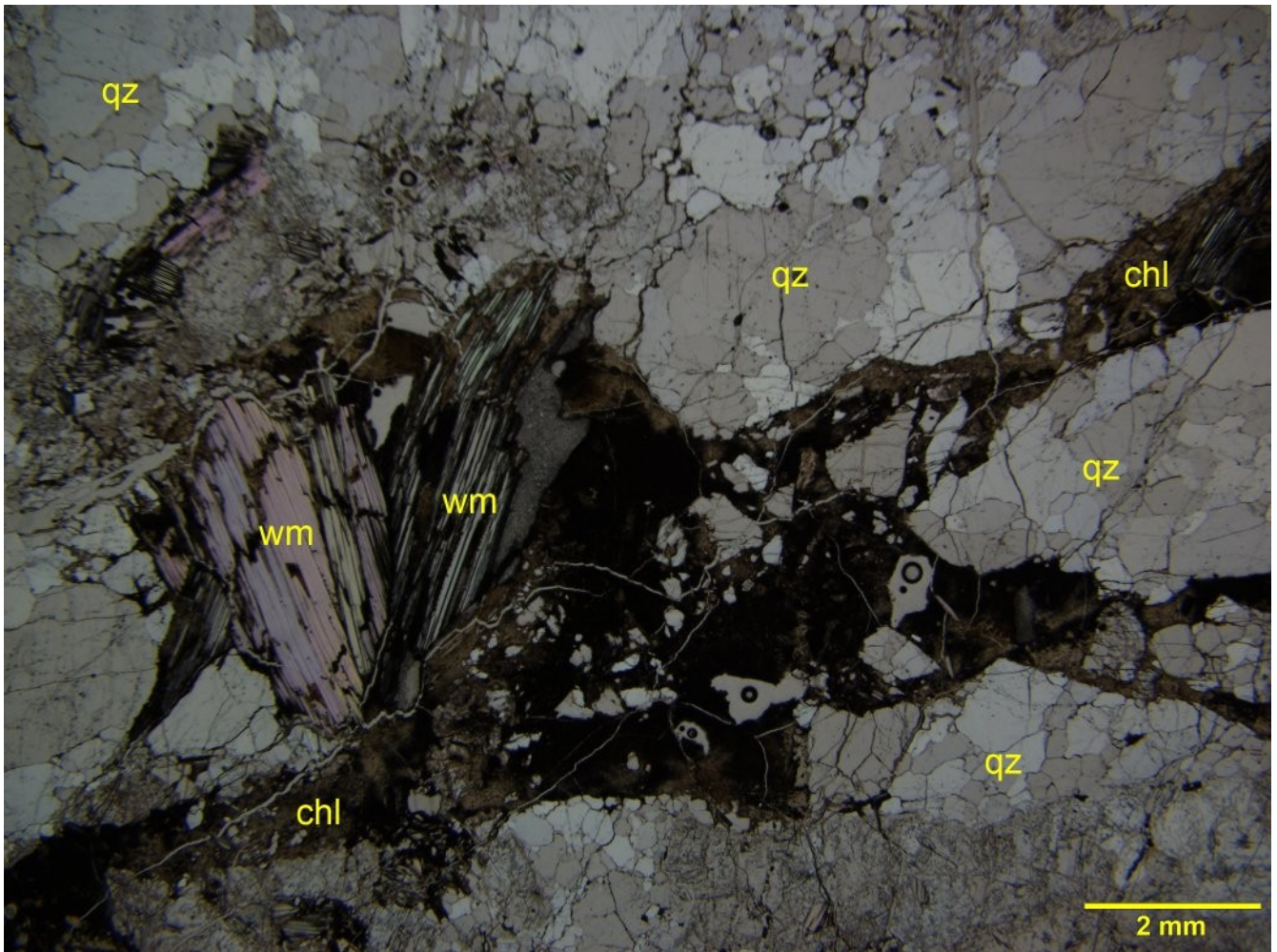
Fine-grained **chlorite** filled in an irregular crack, which reactivated the quartz-vein. The chlorite epitaxially replaced euhedral lamellae of **biotite** in the host rock (Photomicrograph 37c).



Photomicrograph 37a: Anhedronal plagioclase (pl), quartz (qz) and chlorite replacing biotite (chl) define a fragmental texture. Plane-polarized transmitted light.



Photomicrograph 37b: Anhedronal plagioclase (pl) and quartz (qz) are associated with clusters of white mica lamellae (wm). Plane-polarized transmitted light.

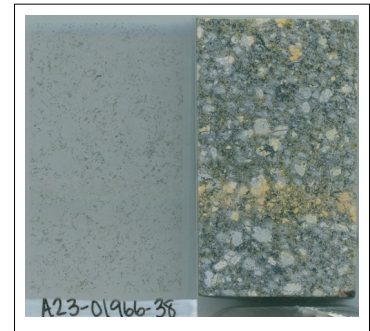


Photomicrograph 37c: The quartz vein (qz) is fractured and filled in by chlorite (chl), limonitic material. Plane-polarized transmitted light.

Sample 38: A23-01966-38-IG_BH02_LG028

Chlorite-altered plagioclase-phyric quartz-diorite

K-feldspar-quartz veinlet



Subhedral phenocrysts of plagioclase are randomly oriented within a fine-grained granophyric aggregate of plagioclase and quartz hosting anhedral biotite. A K-feldspar-quartz veinlet crosscut the porphyritic section.

Alteration: K-feldspar: weak; sericite-earthy and unresolved: weak to moderate after plagioclase; **chlorite:** moderate to strong after biotite

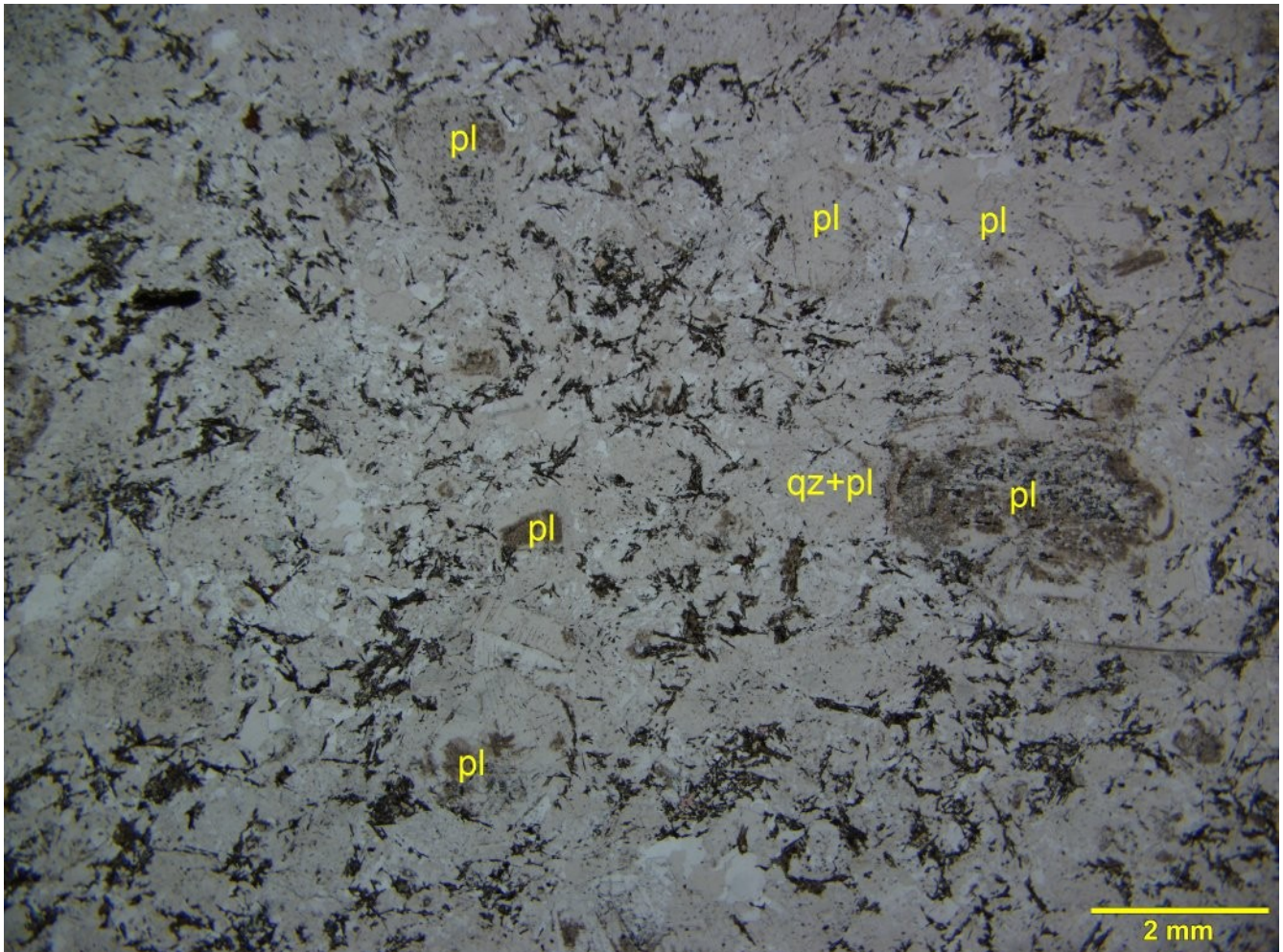
Mineral	Alteration/Weathering Mineral	Modal %	Size Range (mm)
porphyritic rock (~99% of PTS)			
plagioclase (albite)	sericite-earthy and unresolved	72- 74	up to 3 long
quartz		18- 20	up to 1
biotite	chlorite	4- 5	up to 0.2
K-feldspar	K-feldspar	2- 3	up to 0.2
	iron oxides	tr	<0.01
K-feldspar-quartz veinlet (~1% of PTS)			
quartz		0.7	0.1
K-feldspar		0.3	0.1

Plagioclase forms subhedral phenocrysts (up to 3 mm long). Very fine-grained sericite and earthy and unresolved aggregate weakly to moderately altered some of the phenocrysts. The alteration products help to distinguish the phenocrysts from the relatively fresh plagioclase-quartz granophyric aggregate under plane-polarized transmitted light (Photomicrographs 38a and 38c). Plagioclase and quartz form granophyric aggregates (up to 1 mm across) surrounding the phenocrysts (Photomicrograph 38b). Anhedral and fine-grained plagioclase, quartz, biotite, and K-feldspar complete the mineralogy of this porphyritic section. Most of the plagioclase is **albitic**.

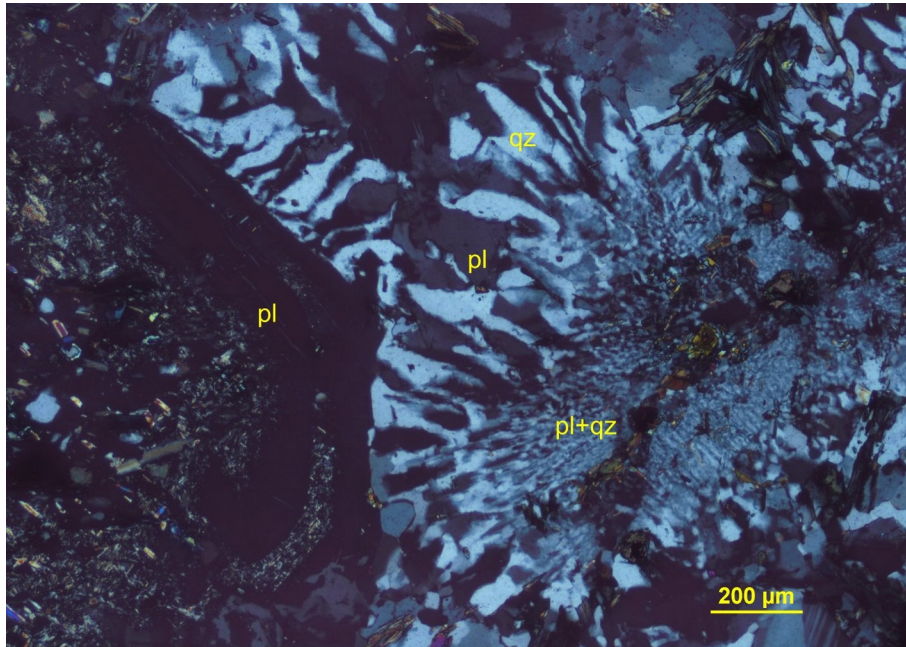
Quartz is subordinate to the plagioclase and mostly occurs as granophyric intergrowths with the prevailing plagioclase. In some cases, the plagioclase and quartz are associated with fine-grained anhedral crystals of K-feldspar. Fine-grained and anhedral crystals are dispersed within the interstitial positions between the granophyric domains surrounding the plagioclase phenocrysts.

Biotite is homogeneously dispersed as anhedral flakes and lamellae. **Chlorite** moderately to strongly altered the biotite.

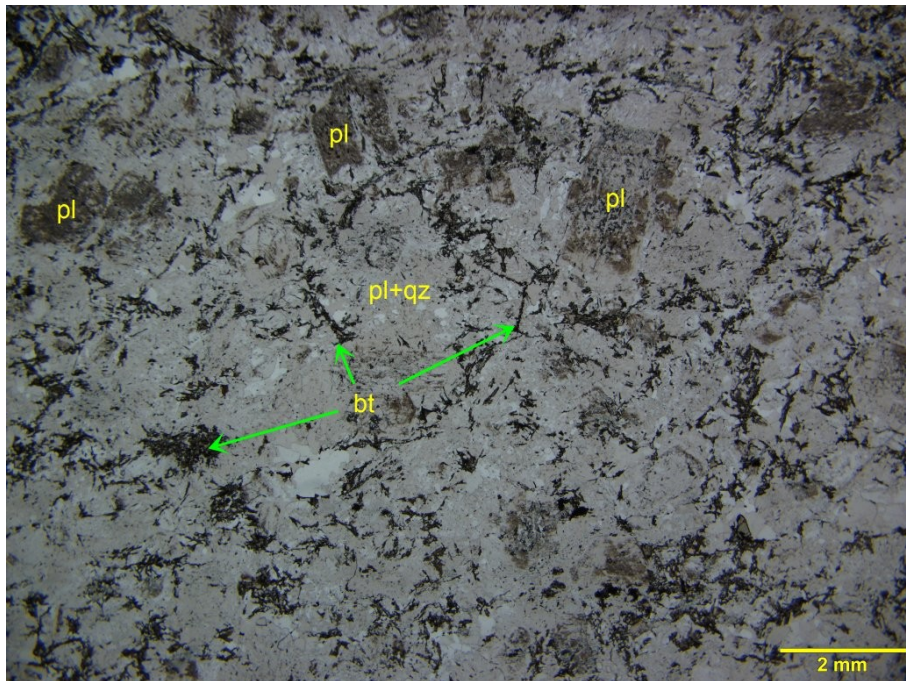
K-feldspar is homogeneously dispersed within the plagioclase and quartz granophyric aggregate, and it is concentrated around a thin veinlet crosscutting the porphyritic section in the mid-lower part (see offcut's image above). The K-feldspar distribution indicate its crystallization occurred during the final stages of the granophyric crystallization and continued, in a smaller amount of this section, after the end of the magmatic crystallization.



Photomicrograph 38a: Plagioclase phenocrysts (pl) are immersed within a fine-grained aggregate of quartz and plagioclase (qz+pl) and biotite aggregate. Plane-polarized transmitted light.



Photomicrograph 38b: Granophyric plagioclase (pl) and quartz (qz) and (pl+qz) surround plagioclase phenocrysts. Crossed polarizers transmitted light.



Photomicrograph 38c: The random orientation of the partially altered biotite flakes and clusters define an isotropic texture. Plane-polarized transmitted light.

Sample 39: A23-01966-39-IG_BH02_LG029



Sericite-epidote-altered plagioclase-phyric microtonalite

Subhedral and anhedral plagioclase phenocrysts are randomly oriented within a fine-grained groundmass of quartz, biotite, and plagioclase. Anhedral crystals of epidote and white mica overprinted the porphyritic texture.

Alteration: white mica: weak to moderate after plagioclase; subtle to weak after the groundmass;
epidote: weak in the groundmass

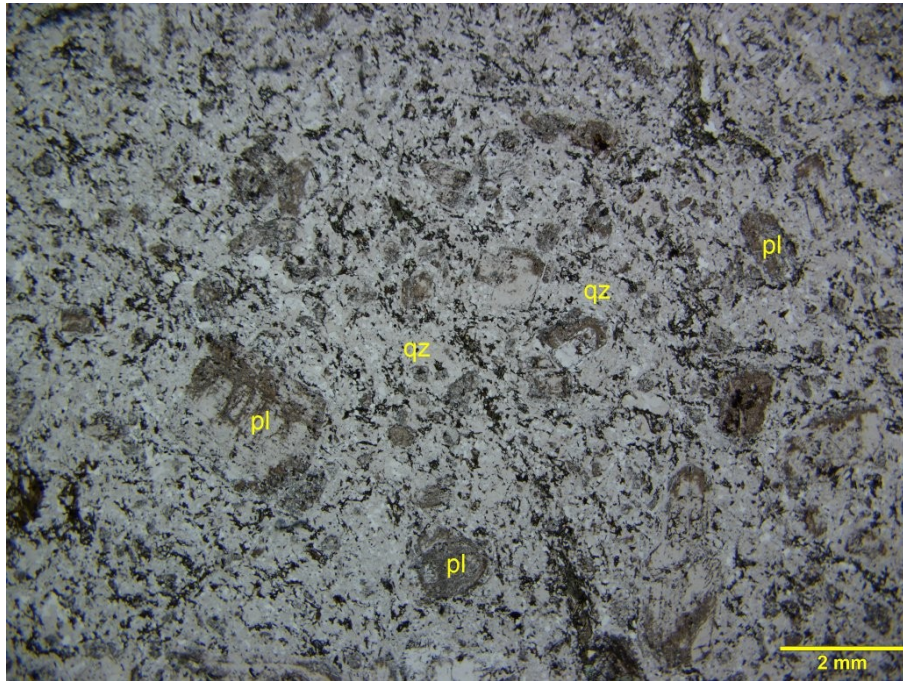
Mineral	Alteration/Weathering Mineral	Modal %	Size Range (mm)
<i>phenocrysts</i>			
plagioclase		10- 12	up to 2
<i>groundmass</i>			
quartz		53- 55	up to 0.2
plagioclase (albite)		20- 22	up to 0.2
biotite		10- 12	up to 0.6
	epidote	3- 4	up to 0.3
	white mica	tr	up to
	iron oxides	tr	<0.01
zircon		tr	0.01

Quartz dominates the composition of the groundmass as fine-grained blocky to interlobate crystals. The quartz is intergrown with plagioclase, randomly oriented biotite, and epidote.

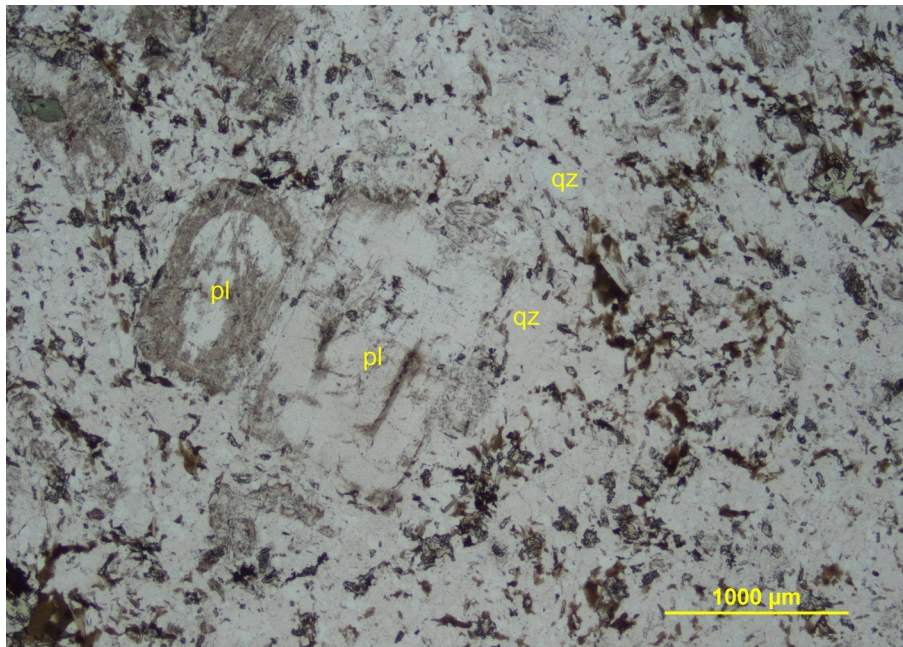
Plagioclase occurs as medium-grained euhedral and subhedral phenocrysts (up to 2 mm long). The plagioclase shows Albite twinings and euhedral growth zoning, which are highlighted by the concentration of very fine-grained flakes of sericite. Fine-grained albite is intergrown with the quartz in the groundmass.

Biotite forms fine- to medium-grained lamellae (up to 0.6 mm long), which are randomly oriented and define an isotropic texture in the groundmass. The biotite hosts very fine-grained inclusions of zircon and is overprinted by fine-grained epidote crystals.

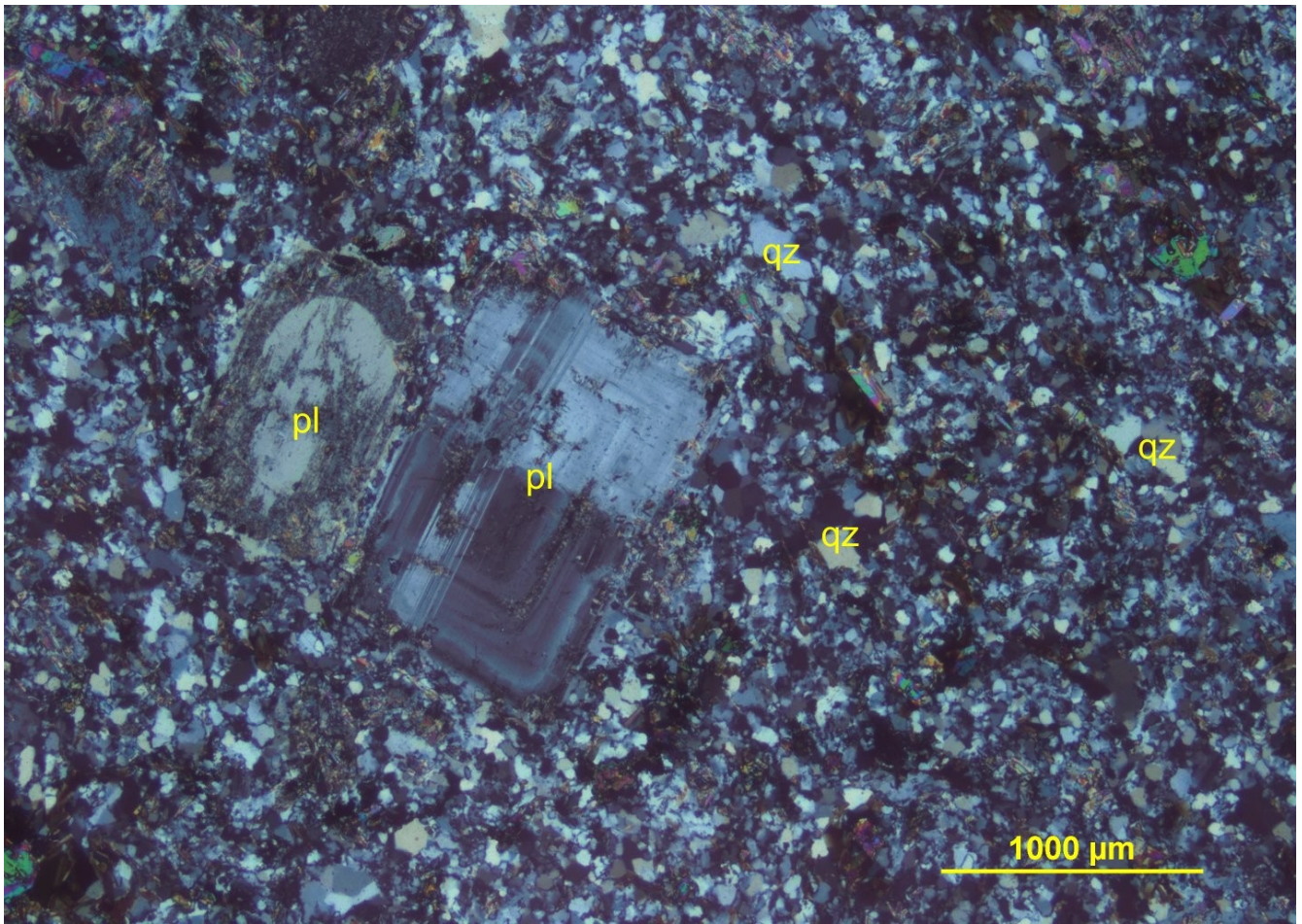
Fine-grained **epidote** and subordinate **white mica** overprinted the groundmass. The epidote is spatially associated with the biotite, the white mica preferentially overprinted the plagioclase.



Photomicrograph 39a: Phenocrysts of plagioclase (pl) are immersed within a fine-grained groundmass dominated by quartz. Plane-polarized transmitted light.



Photomicrograph 39b: Euhedral plagioclase phenocrysts are immersed within a fine-grained groundmass of quartz (qz), biotite, and plagioclase. Plane-polarized transmitted light.



Photomicrograph 39c: . Same area as shown in Photomicrograph 39b. Under crossed polarizers transmitted light, the plagioclase phenocrysts show a euhedral growth zoning.

Sample 40: A23-01966-40-IG_BH02_LG030

Fe-chlorite-plagioclase-calcite granofels

Inequigranular and xenoblastic crystals of calcite, plagioclase, and irregularly shaped patches of fine-grained Fe-chlorite define a granular, xenoblastic, and relatively homogeneous texture.



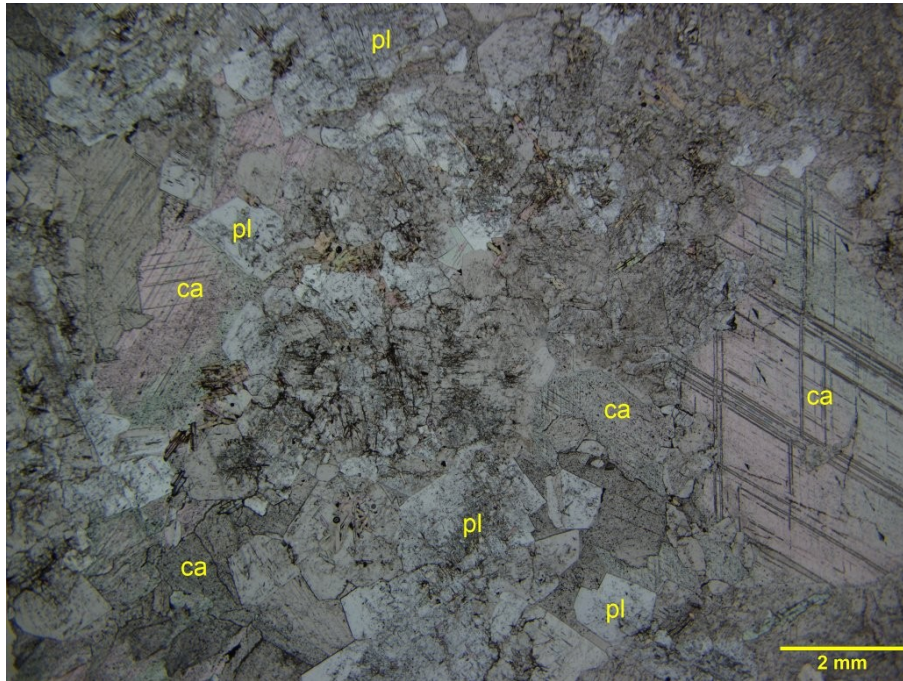
Alteration/Metamorphism: Calcite-plagioclase: strong; chlorite: weak; white mica: weak after plagioclase

Mineral	Alteration/Weathering Mineral	Modal %	Size Range (mm)
calcite		50- 52	up to 6
plagioclase (albite)	white mica	44- 45	up to 3, rare up to 7 long
	Fe-chlorite	3- 4	up to 0.2

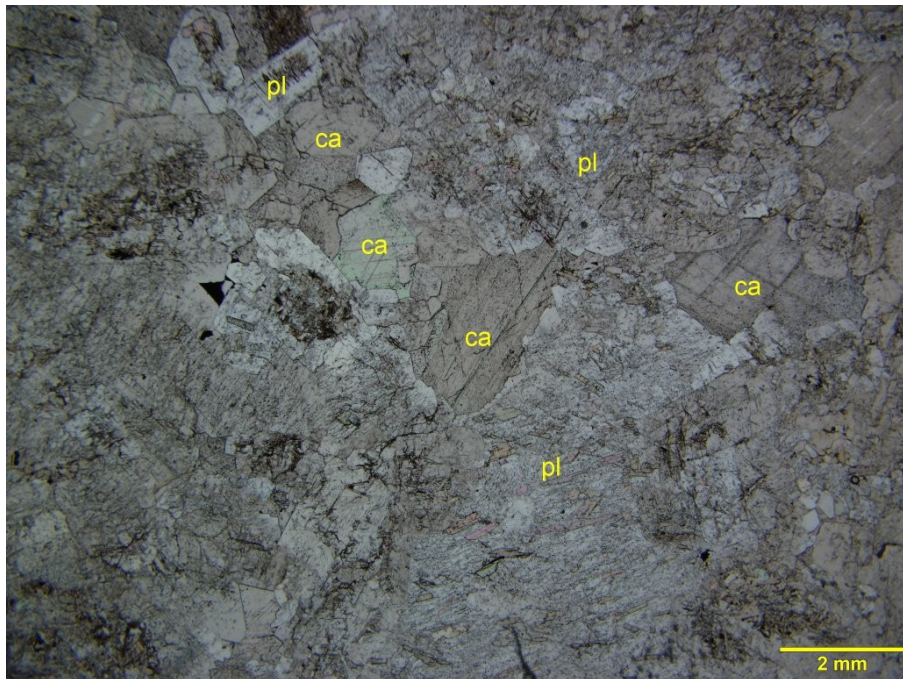
Calcite forms xenoblastic to polygonal crystals up to 6 mm across. The calcite slightly prevails over the plagioclase and, in some cases, forms polygonal crystals intergrown with the plagioclase. These textures suggest that the calcite and the plagioclase crystallized together during a strain-free contact metamorphic event. The calcite briskly reacts to cold dilute (10%) HCl.

Plagioclase crystals are inequigranular (up to 3 mm across, and in one case up to 7 mm long) and their crystals show xenoblastic, subidioblastic (Photomicrographs 40a and 40c) and polygonal grain shape. Fine-grained flakes of white mica weakly altered the plagioclase crystals, which show Albite twinning lamellae.

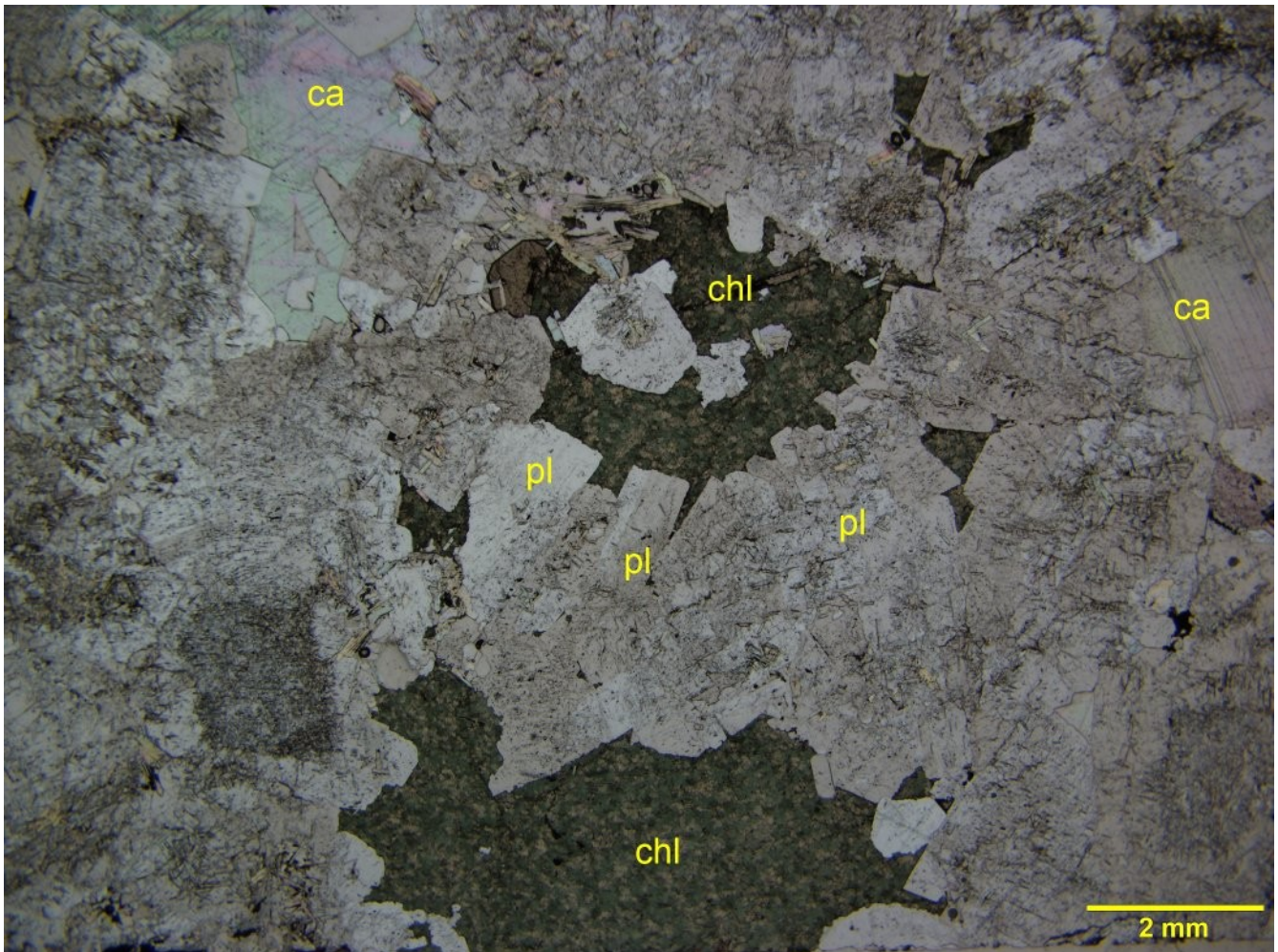
Fe-chlorite forms irregular replacement patches (up to 5 mm across) filling in the interstitial positions between the calcite and the plagioclase.



Photomicrograph 40a: Xenoblastic calcite (ca) is intergrown with xenoblastic to subidioblastic plagioclase (pl). Plane-polarized /Crossed polarizers transmitted /reflected light.

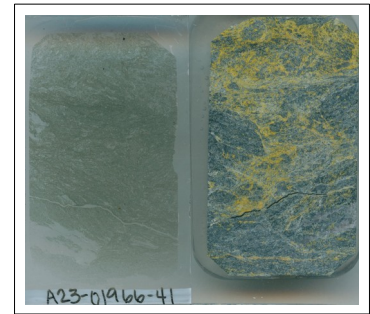


Photomicrograph 40b: Xenoblastic crystals of calcite (ca) and plagioclase (pl) define a granular and xenoblastic texture. Plane-polarized /Crossed polarizers transmitted /reflected light.



Photomicrograph 40c: Patches of fine-grained chlorite (chl) filled in the interstitial positions between the plagioclase (pl) and the calcite (ca). Plane-polarized transmitted light.

Sample 41: A23-01966-41-IG_BH03_LG023



Epidote-Fe-chlorite-retrogressed schist

This section shows a heterogeneous composition and texture. In the upper part, fine-grained K-feldspar crystals are mixed with fine-grained flakes of chlorite and xenoblastic epidote. In most of the mid to lower part of the section, abundant Fe-chlorite define a rough continuous schistosity, which wraps angular fragments of fine-grained chlorite, epidote, and quartz.

Alteration/Metamorphism: Fe-chlorite: strong; epidote-K-feldspar: moderate; quartz-calcite-earthy and unresolved: weak

Mineral	Alteration/Metamorphic Mineral	Modal %	Size Range (mm)
	Fe-chlorite	45- 47	up to 0.2
	epidote	15- 20	up to 0.1
	K-feldspar	15- 17	up to 0.1
	earthy and unresolved	12- 15	<0.01
	quartz	5- 10	up to 0.1
	calcite	5- 10	up to 0.1

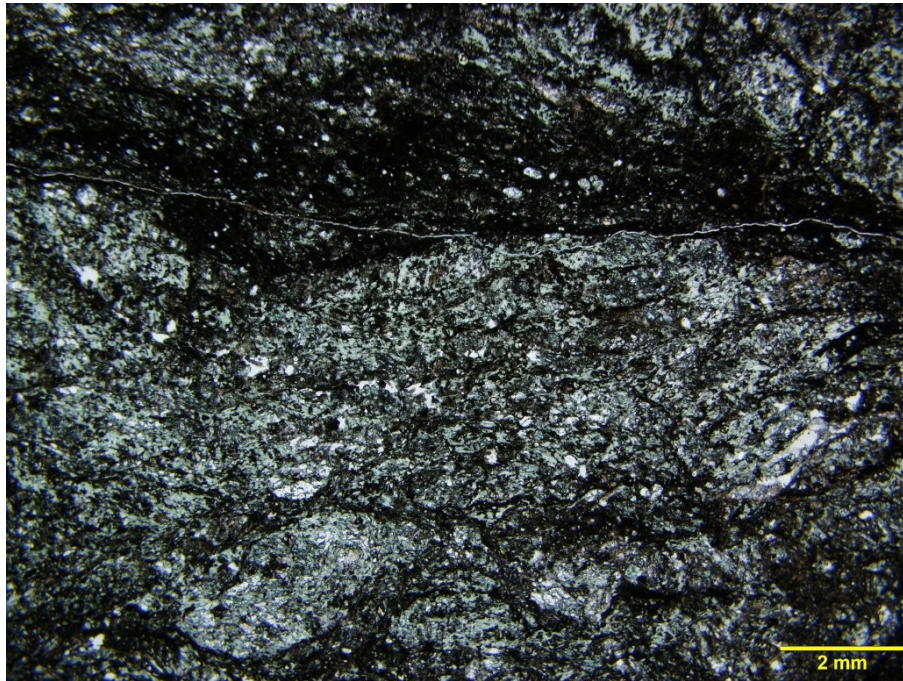
Fe-chlorite is fine-grained, and it is concentrated in the darker part of the section (see the offcut's image above), in which it is preferentially iso-oriented and defines a continuous, and rough schistosity. In some areas of the section the schistosity is folded. In other parts wraps angular fragments of fine-grained chlorite, epidote, and quartz. Very fine- to fine-grained and xenoblastic epidote overprinted the chlorite.

Epidote is disseminated within the chlorite-rich domains as very fine- to fine-grained xenoblastic crystals.

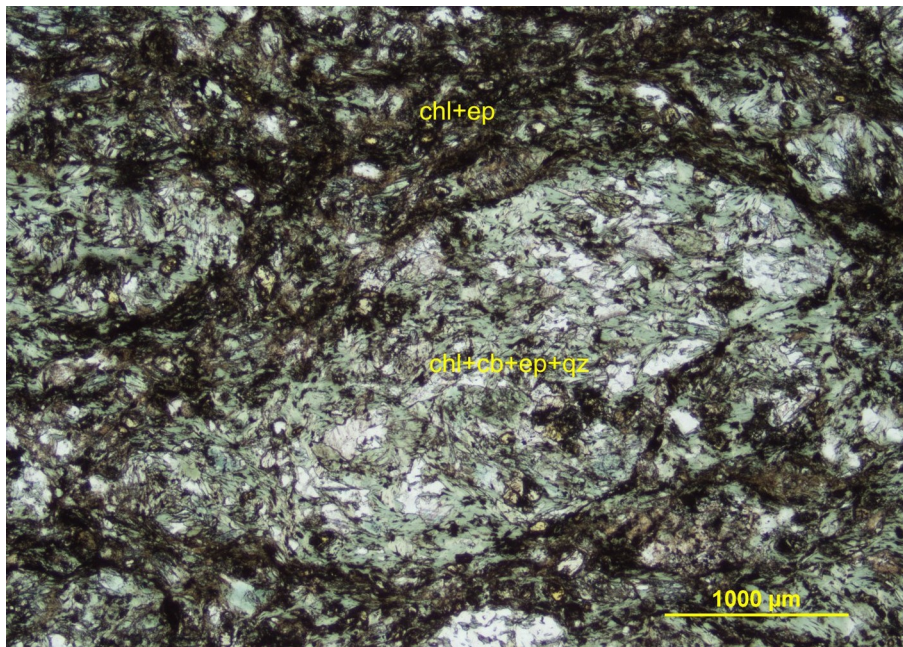
K-feldspar is concentrated within the fragmental texture in the upper part of the section. The crystals are fine-grained and are distinguished by their low birefringence. Plagioclase and quartz may be associated with the K-feldspar. The occurrence and distribution of the K-feldspar is shown in the yellow-stained domain in the offcut's image above.

Quartz and **calcite** are heterogeneously dispersed within the angular fragments (e.g., Photomicrograph 41b) wrapped by the schistosity.

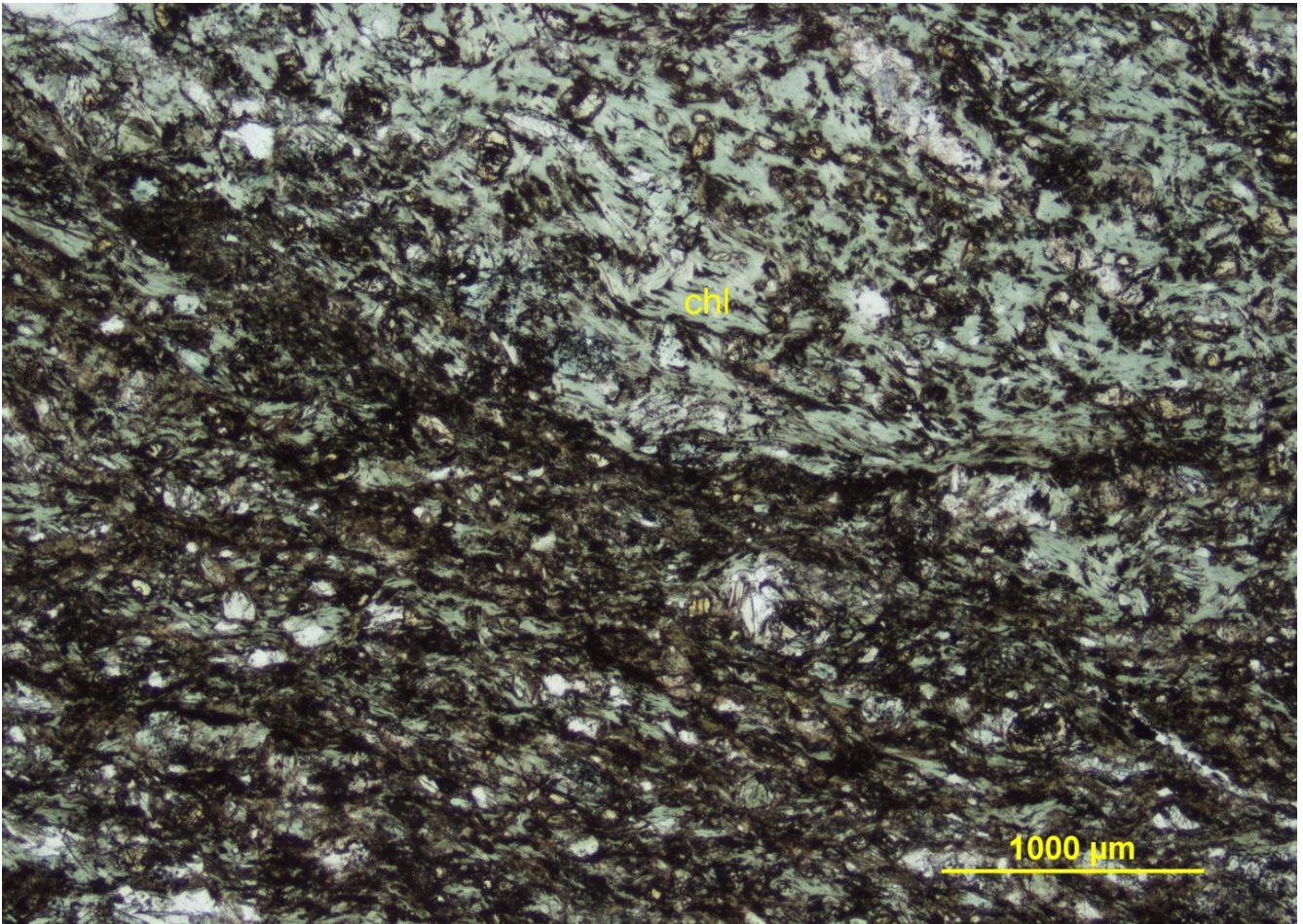
Very fine-grained crushed and unresolved material is concentrated within irregular domains associated with the chlorite (see the lower part of Photomicrograph 41c).



Photomicrograph 41a: Angular fragments (light domains) of chlorite-bearing rock (see detail in Photomicrograph 41b) are wrapped by the continuous schistosity defined by the chlorite and by the crushed material (dark domains). Plane-polarized transmitted light.



Photomicrograph 41b: The angular fragments comprise fine-grained chlorite, carbonate, epidote, and quartz (chl+cb+ep+qz). Plane-polarized transmitted light.



Photomicrograph 41c: Chlorite (chl) defines a continuous schistosity in the upper part of this photomicrographs and it is overprinted by abundant epidote. Very fine-grained crushed and unresolved material is dispersed within the chlorite in the lower part. Plane-polarized transmitted light.

Sample 42: A23-01966-42-IG_BH04_MG086



White mica-chlorite-retrogressed biotite schist

Lenticular and irregular microlithons of plagioclase, quartz, and biotite are wrapped by cleavage domains of chlorite and subordinate white mica.

The chlorite and white mica replaced iso-oriented biotite and all the phyllosilicates define a spaced and rough schistosity.

Alteration/Metamorphism: chlorite: strong after biotite; white mica: weak; earthy and unresolved: moderate to strong after plagioclase; rutile: subtle

Mineral	Alteration/Weathering Mineral	Modal %	Size Range (mm)
quartz		43- 45	up to 0.2
[biotite]	chlorite-white mica	25- 30	up to 0.4 long
plagioclase		20- 22	up to 0.6
biotite		8- 10	up to 0.3 long
	rutile	tr	0.02

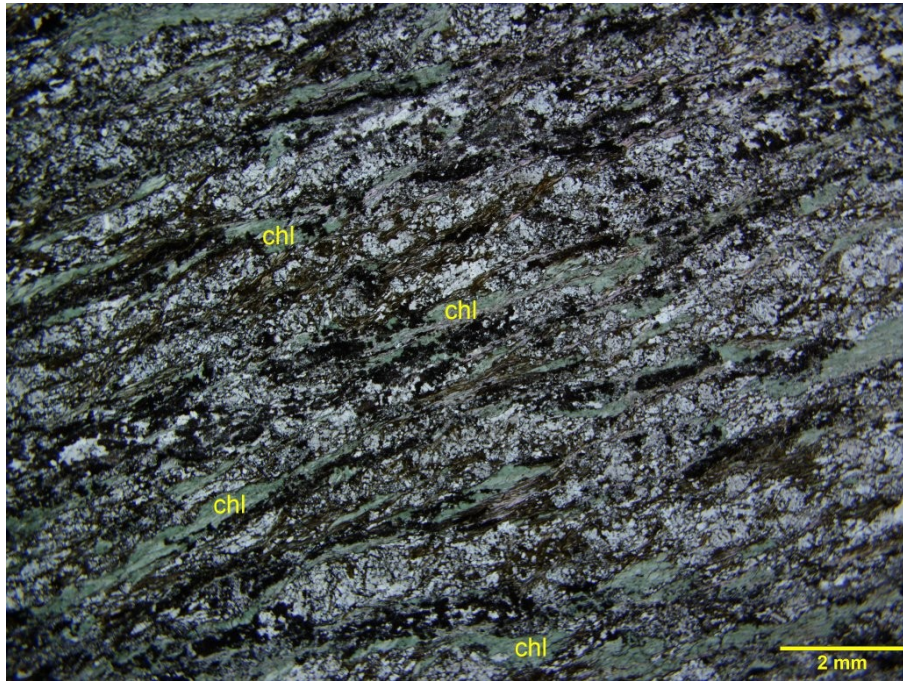
Chlorite is concentrated as iso-oriented lamellae within irregular cleavage domains. The cleavage domains wrap fine-grained granular microlithons and define a spaced and rough schistosity. The chlorite moderately to strongly replaced biotite crystals, which I interpret as having crystallized during the schistogenic metamorphic event.

Biotite occurs as randomly oriented lamellae and flakes within some microlithons and as a relic within the cleavage domains. Subordinate **white mica** is intergrown with the chlorite in some cleavage domains.

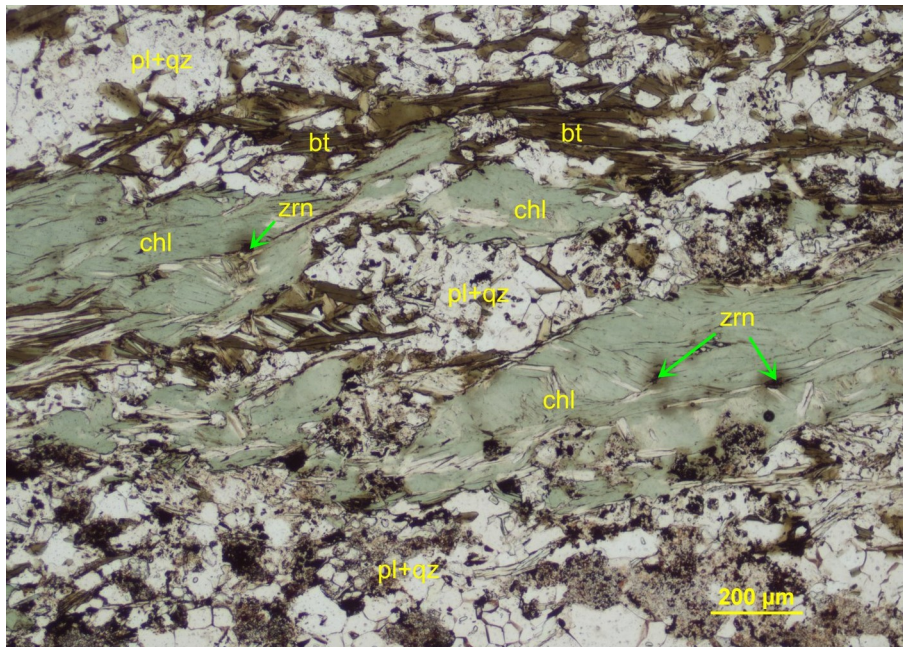
Quartz forms xenoblastic crystals prevailing over the plagioclase and the biotite in the irregular and lenticular microlithons.

Plagioclase is subordinate to the quartz within the fine-grained and granoblastic microlithons (Photomicrographs 42b and 42c). In some cases, the plagioclase is strongly altered and is easily distinguished from the fresh quartz (Photomicrograph 42c).

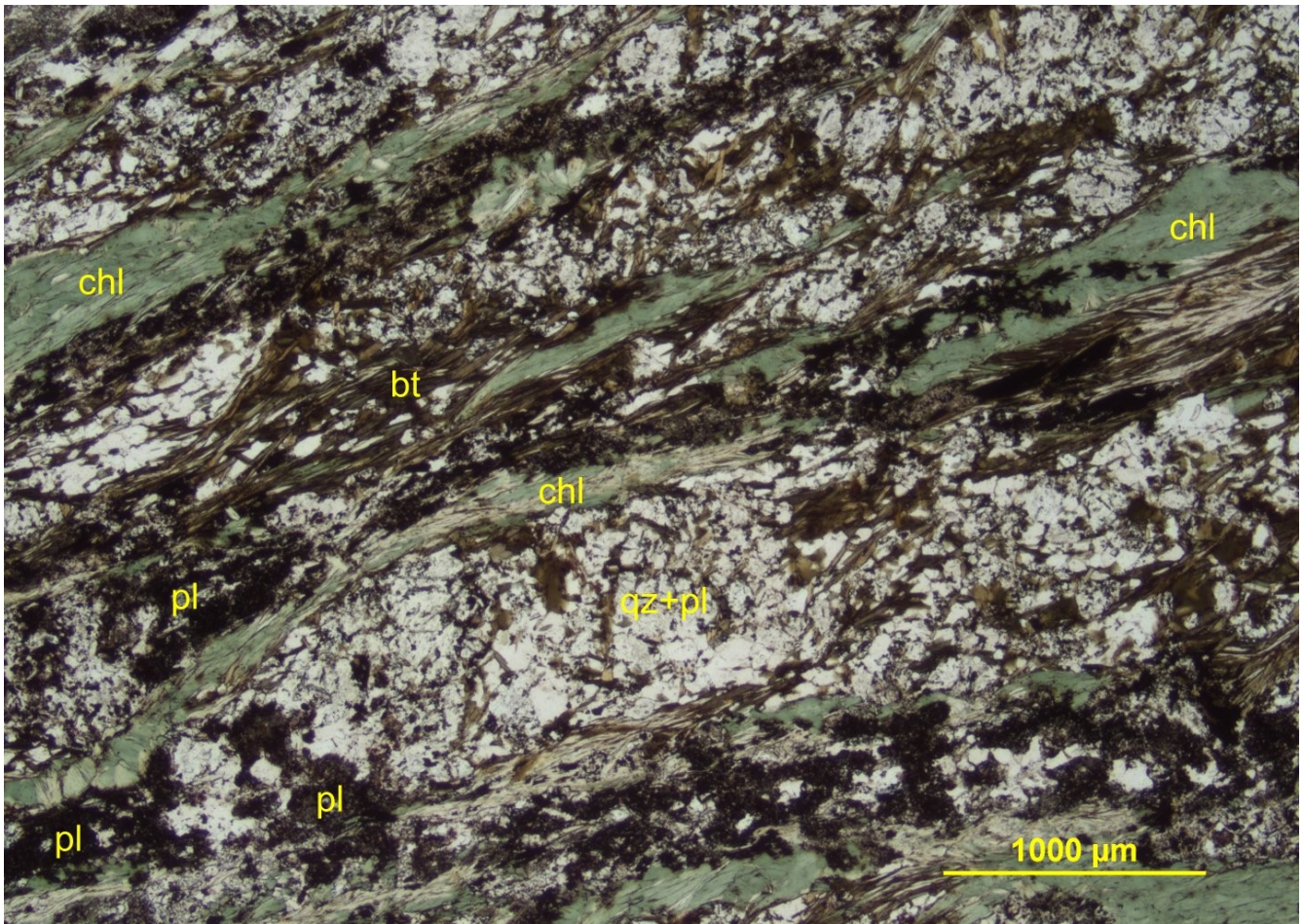
Rutile is very rare and forms crystal clusters disseminated within the schistose section.



Photomicrograph 42a: Chlorite-rich cleavage domains define the spaced schistosity in this section. Plane-polarized transmitted light.



Photomicrograph 42b: The chlorite (chl) epitaxially replaced the iso-oriented biotite within the cleavage domains. Very fine-grained inclusions of zircon (zrn) occur within the epitaxial chlorite. Plane-polarized transmitted light.



Photomicrograph 42c: Biotite occurs as a relic within the chlorite-rich (chl) cleavage domains, which wrap the granoblastic microlithons of quartz (qz) and plagioclase (pl). Plane-polarized transmitted light.

Sample 43: A23-01966-43-IG_BH04_MG087

Chlorite-calcite-white mica-altered albitite

Anhedral and subhedral plagioclase, subordinate patches of fine-grained Fe-chlorite and interstitial calcite define a granular xenomorphic texture.



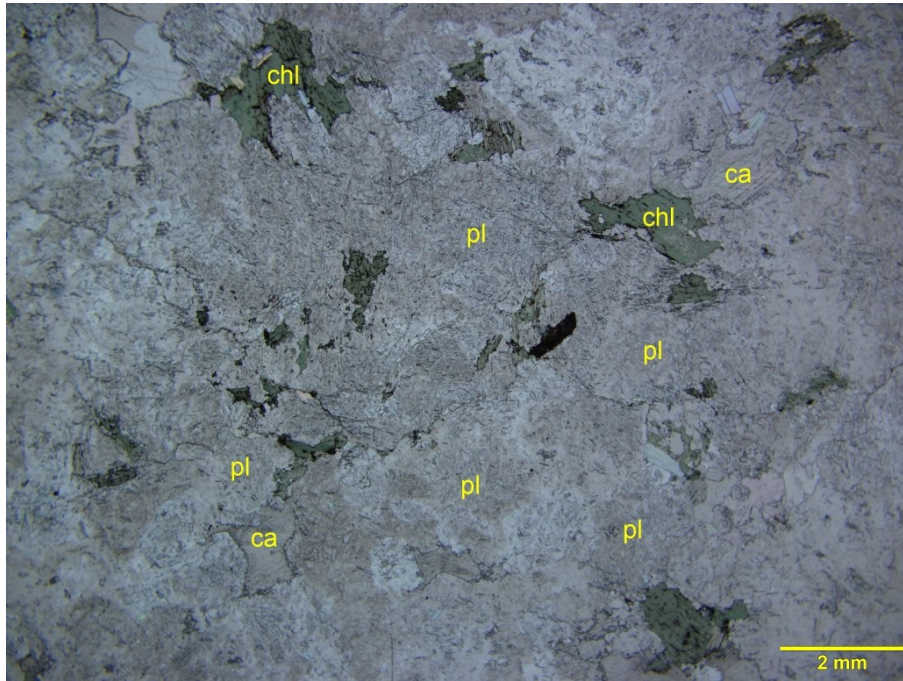
Alteration: white mica: weak after plagioclase; **Fe-chlorite-calcite:** weak

Mineral	Alteration/Weathering Mineral	Modal %	Size Range (mm)
plagioclase		52- 53	up to 7.5 long
[biotite]	Fe-chlorite	3- 4	[up to 2 long]
	calcite	0.5- 0.6	up to 4.5
	white mica	tr	up to 0.6
	iron oxides	tr	up to 0.01
zircon		tr	0.01

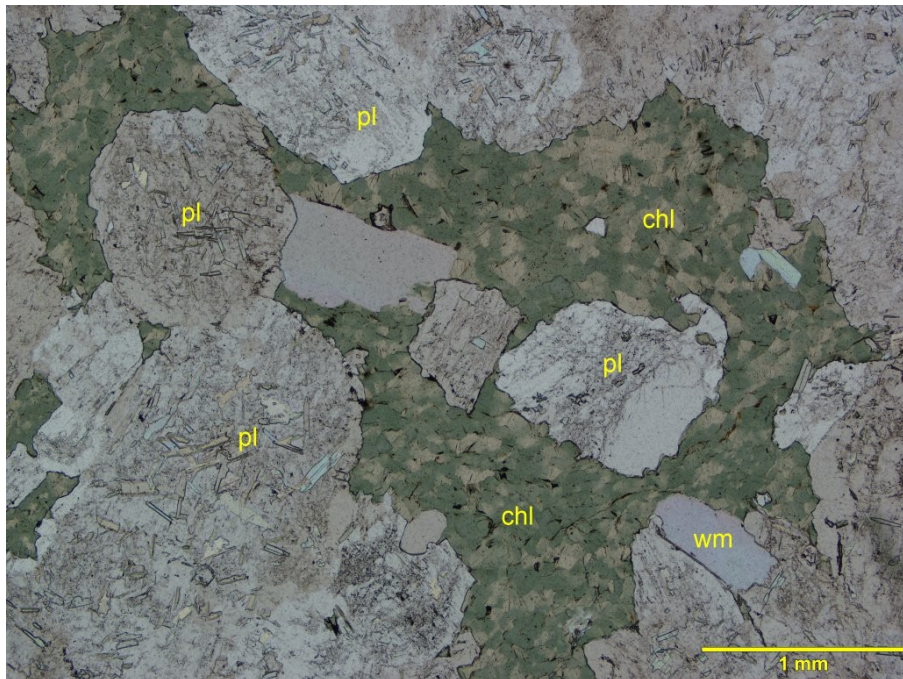
Plagioclase (albite) dominates the composition of this section as anhedral and subhedral crystals ranging from 0.4 mm to 2.5 mm long. The plagioclase crystals are randomly oriented and are in reciprocal contact (Photomicrograph 43c). Very fine-grained flakes of **white mica** weakly altered the plagioclase, which in some instances, shows Albite twinnings. Rare lamellae of white mica (up to 0.6 mm) are dispersed within the chlorite patches (Photomicrograph 43b).

Chlorite completely replaced anhedral biotite lamellae up to 2 mm long (e.g., the upper part of Photomicrograph 43a) and in these pseudomorphs relic **zircon** crystals occur. In some cases, the chlorite is fine-grained and forms interstitial patches between the anhedral and subhedral plagioclase crystals (Photomicrographs 43b and 43c).

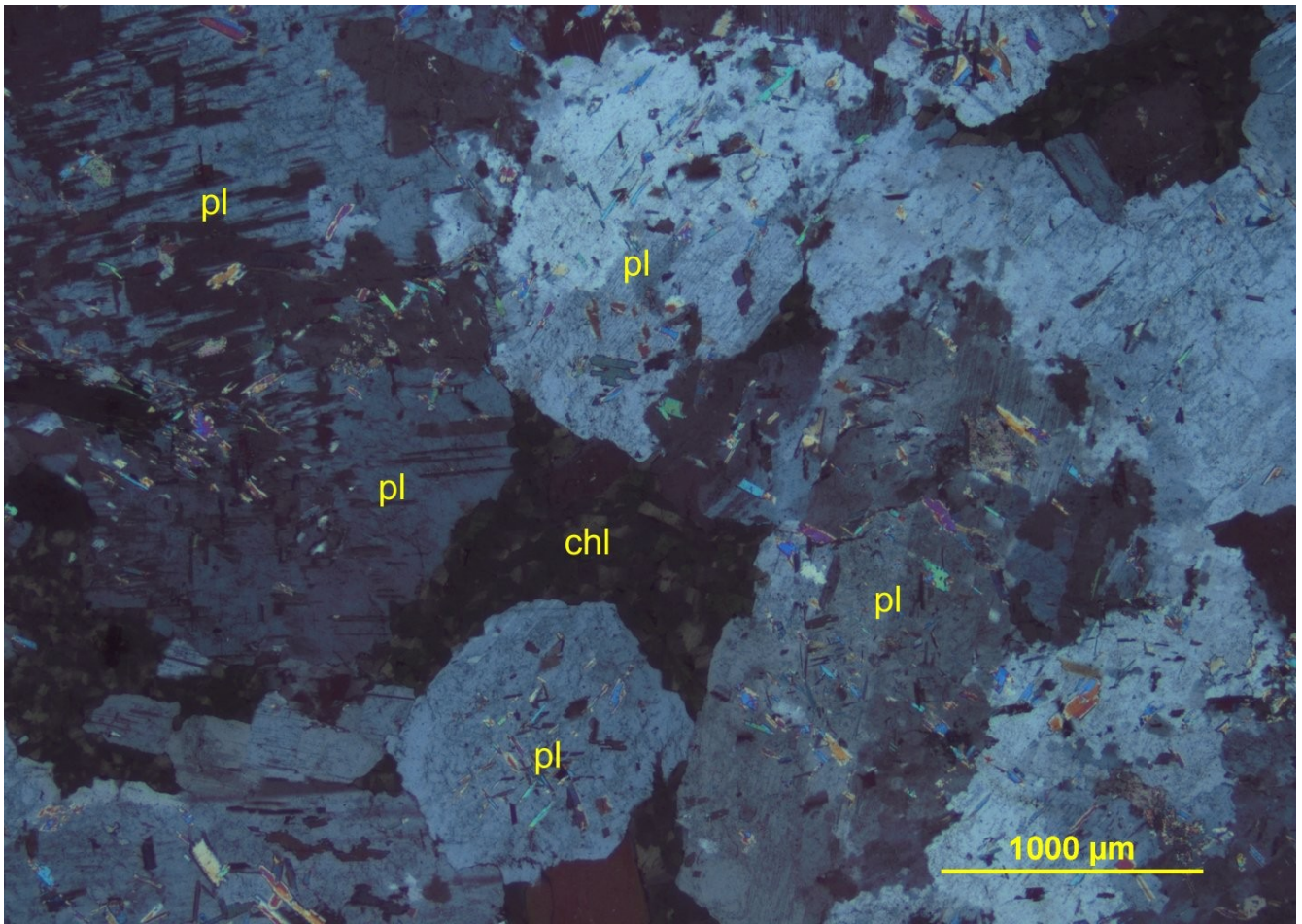
Calcite forms medium-grained crystals filling in some of the interstitial positions between the plagioclase. The calcite is distinguished by its high relief and extreme birefringence under the microscope and its brisk reaction to cold dilute (10%) HCl.



Photomicrograph 43a: Abundant plagioclase (pl) is associated with interstitial patches of chlorite (chl). In the upper part of the section, the chlorite replaced biotite crystals. Plane-polarized transmitted light.



Photomicrograph 43b: Fine-grained chlorite (chl) defines interstitial patches between the plagioclase crystals (pl). Plane-polarized transmitted light.



Photomicrograph 43c: The plagioclase crystals (pl) are in reciprocal contact and are weakly altered to white mica. Crossed polarizers transmitted light.

Sample 44: A23-01966-44-IG_BH04_MG088



Chlorite-sericite-altered tonalite

Sheared iron oxides-white mica-calcite veins

Subhedral plagioclase crystals are immersed within a medium-grained anhedral aggregate of quartz and, together with randomly oriented lamellae of biotite, define a granular texture, which is crosscut by 1 mm thick micro-shear zone filled in by iso-oriented flakes of white mica and calcite.

Alteration: white mica>>**epidote**: weak to moderate after plagioclase; **chlorite**: moderate to strong after biotite; **iron oxides**: subtle

Mineral	Alteration/Weathering Mineral	Modal %	Size Range (mm)
tonalite (~99% of PTS)			
plagioclase	white mica-epidote	67- 69	up to 2.5
quartz		25- 30	0.1- 1
biotite	epidote	4- 5	0.4- 2
K-feldspar		tr	up to 0.4
[orthite/allanite?]		tr	up to 1.2 long
	iron oxides	tr	up to 0.05
zircon		tr	0.02
iron oxides-white mica-calcite veins (~1% of PTS)			
calcite		0.6	up to 1
white mica		0.4	up to 1.2 long
iron oxides		tr	up to 1.5

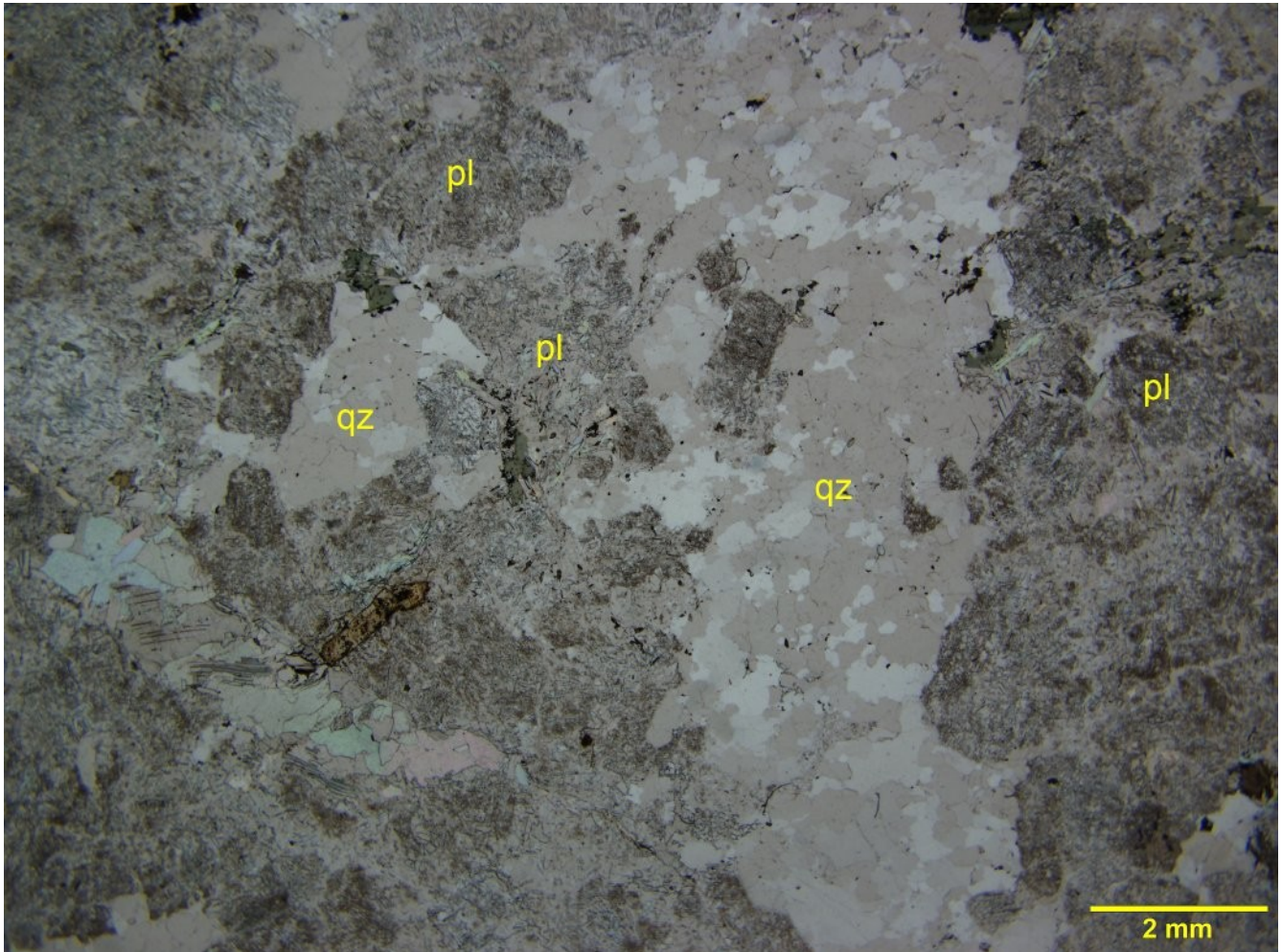
Plagioclase forms anhedral and subhedral crystals up to 2.5 mm across. The plagioclase crystals are randomly oriented and define a granular isotropic texture. Fine-grained flakes of **white mica** and subordinate **epidote** weakly to moderately altered the plagioclase crystals, which under plane-polarized transmitted light are easily distinguished from the inclusion-free quartz (Photomicrographs 44a and 44b).

Quartz forms monomineralic and irregularly shaped aggregates, which may be derived from the re-crystallization of quartz phenocrysts. The quartz crystals range from 0.1 mm to 1 mm across and show interlobate shape.

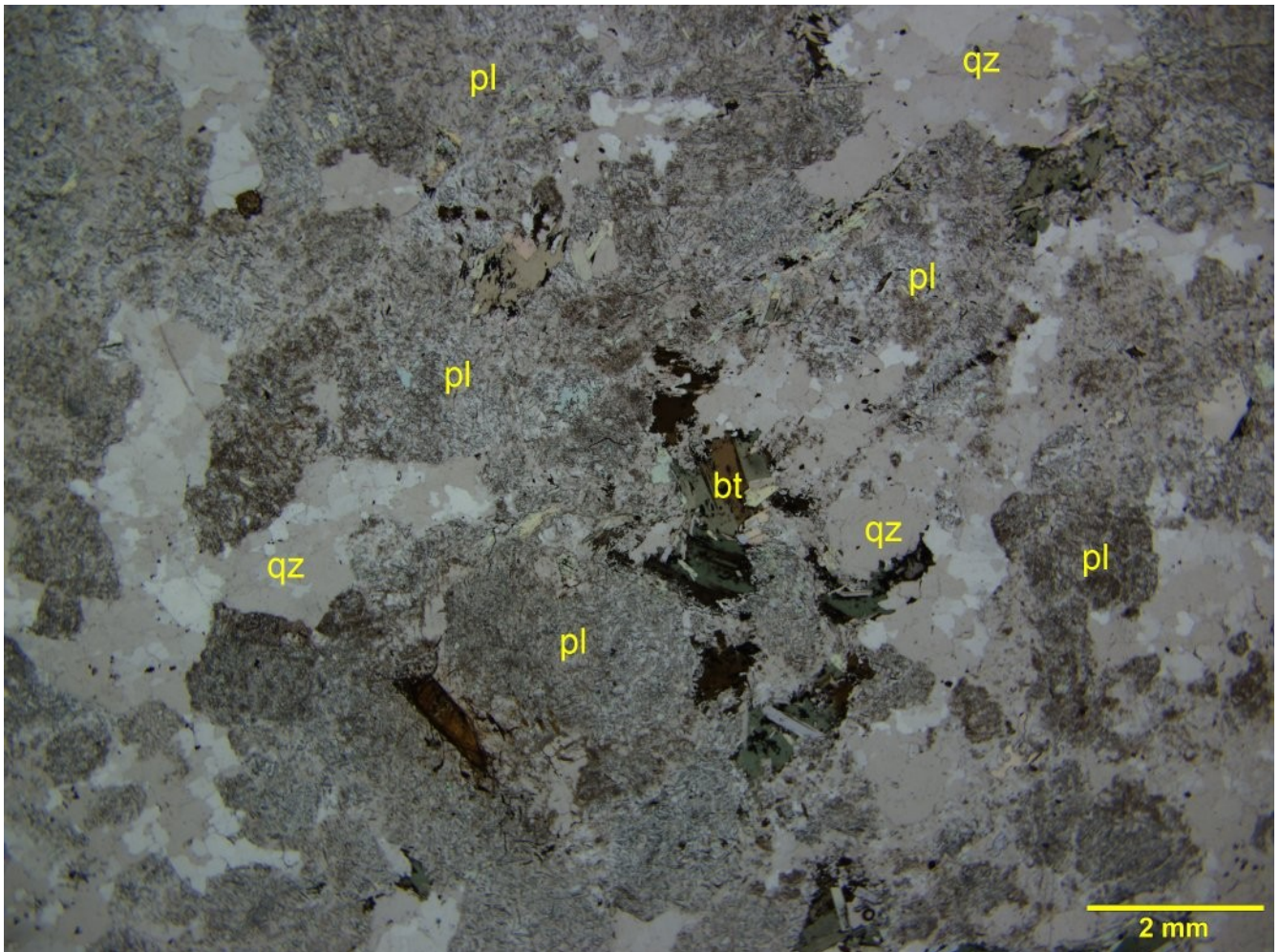
Biotite is dispersed as randomly oriented anhedral lamellae ranging from 0.4 mm long to 2 mm long. The biotite is relatively fresh and host very fine-grained crystals of **zircon**.

Chlorite moderately to strongly altered some biotite crystals.

An unresolved prismatic mineral (up to 1.2 mm long) forms rare and strongly altered crystals dispersed within the plagioclase interstices. The alteration products comprises limonitic material, which completely mask the optical features of the crystals. I tentatively interpret the mineral as **orthite/allanite**. This interpretation would need to be confirmed by SEM-EDS analysis.

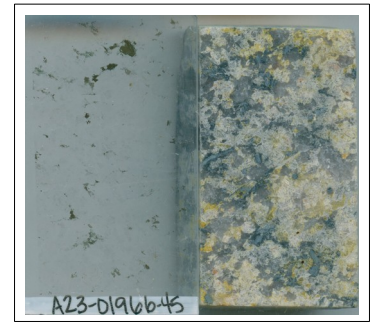


Photomicrograph 44a: Anhedral and subhedral crystals of plagioclase (pl) and irregularly shaped monomineralic aggregates of quartz (qz) define a granular texture. Plane-polarized transmitted light.



Photomicrograph 44b: Anhedral and subhedral crystals of plagioclase (pl), quartz (qz), and randomly oriented biotite (bt) define an isotropic and granular texture. Plane-polarized transmitted light.

Sample 45: A23-01966-45-IG_BH04_MG089



Chlorite-epidote-white mica-altered tonalite

This section comprises inequigranular and anhedral crystals of plagioclase, quartz, biotite, and subordinate K-feldspar. The composition is similar to other tonalitic samples (e.g., Samples 6, 9, 10, 31, 32, and 34). Texturally, this sample shows a finer-grained nature, probably due to the post- or late-magmatic re-crystallization of the quartzofeldspathic minerals.

Alteration: white mica-titanite-chlorite-epidote: weak to moderate after plagioclase; **chlorite:** weak after the biotite; **epidote > iron oxides:** subtle

Mineral	Alteration/Weathering Mineral	Modal %	Size Range (mm)
plagioclase (albite)	white mica-epidote	49- 50	up to 3.5 long
quartz		39- 40	up to 2.5 long
biotite	titanite-white mica-chlorite-epidote	6- 7	up to 1.5 long
K-feldspar (microcline)		2- 2.5	up to 3 across
	epidote	0.2- 0.4	up to 0.5
zircon		tr	up to 0.05
	iron oxides	tr	0.02

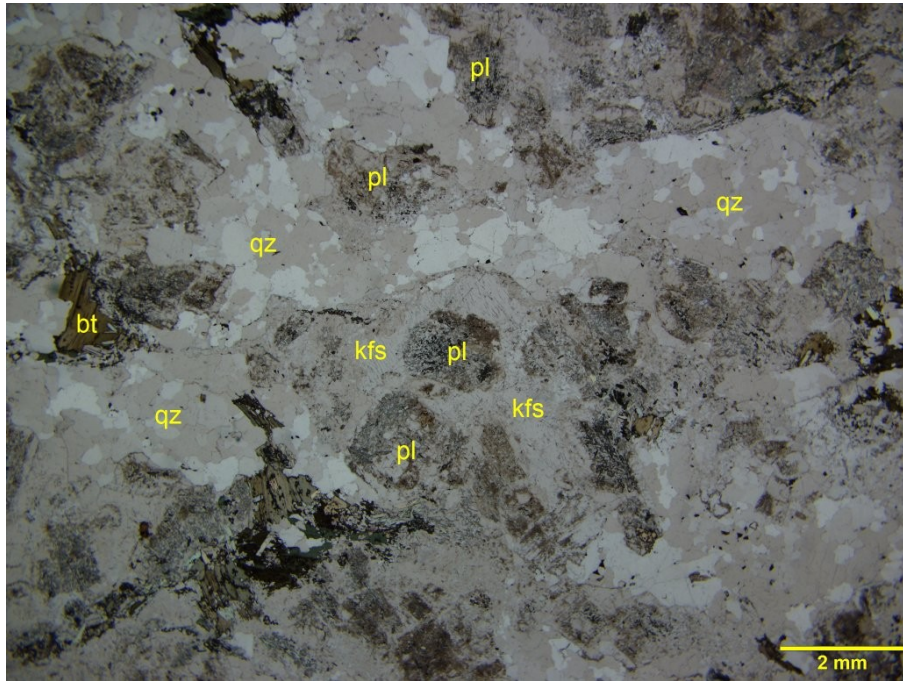
Plagioclase forms inequigranular and mostly anhedral crystals up to 3.5 mm long. The anhedral shape is probably due to post- or late-magmatic re-crystallization of its boundaries (stress or thermal event?). Fine-grained flakes of **white mica** and fine-grained anhedral crystals of epidote weakly to moderately altered some plagioclase crystals (Photomicrograph 45b); however, most of the crystals are subtly to weakly altered and show Albite twinnings and relic growth zoning.

Quartz forms fine- to medium-grained monomineralic domains, likely recrystallized from larger quartz crystals or phenocrysts. Most quartz crystals show a moderate undulose extinction.

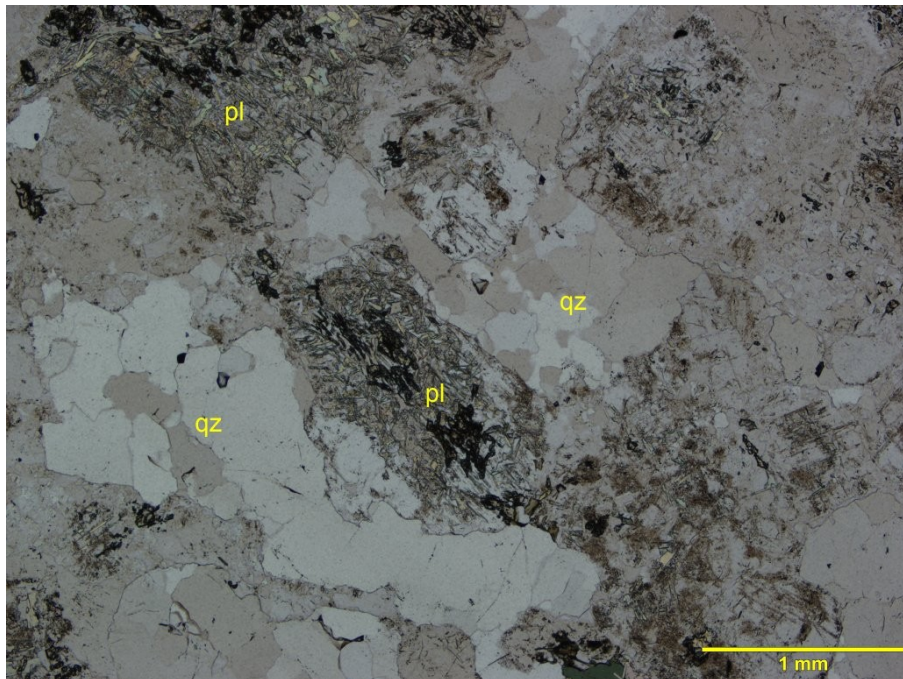
Biotite is fine- to medium-grained and its anhedral crystals (up to 1.5 mm long) are finely intergrown with the feldspars, and are weakly altered to fine-grained **titanite**, white mica and epitaxial **chlorite**.

K-feldspar forms sparse interstitial and poikilitic crystals up to 3 mm across hosting anhedral and subhedral inclusions of plagioclase and biotite (Photomicrograph 45c).

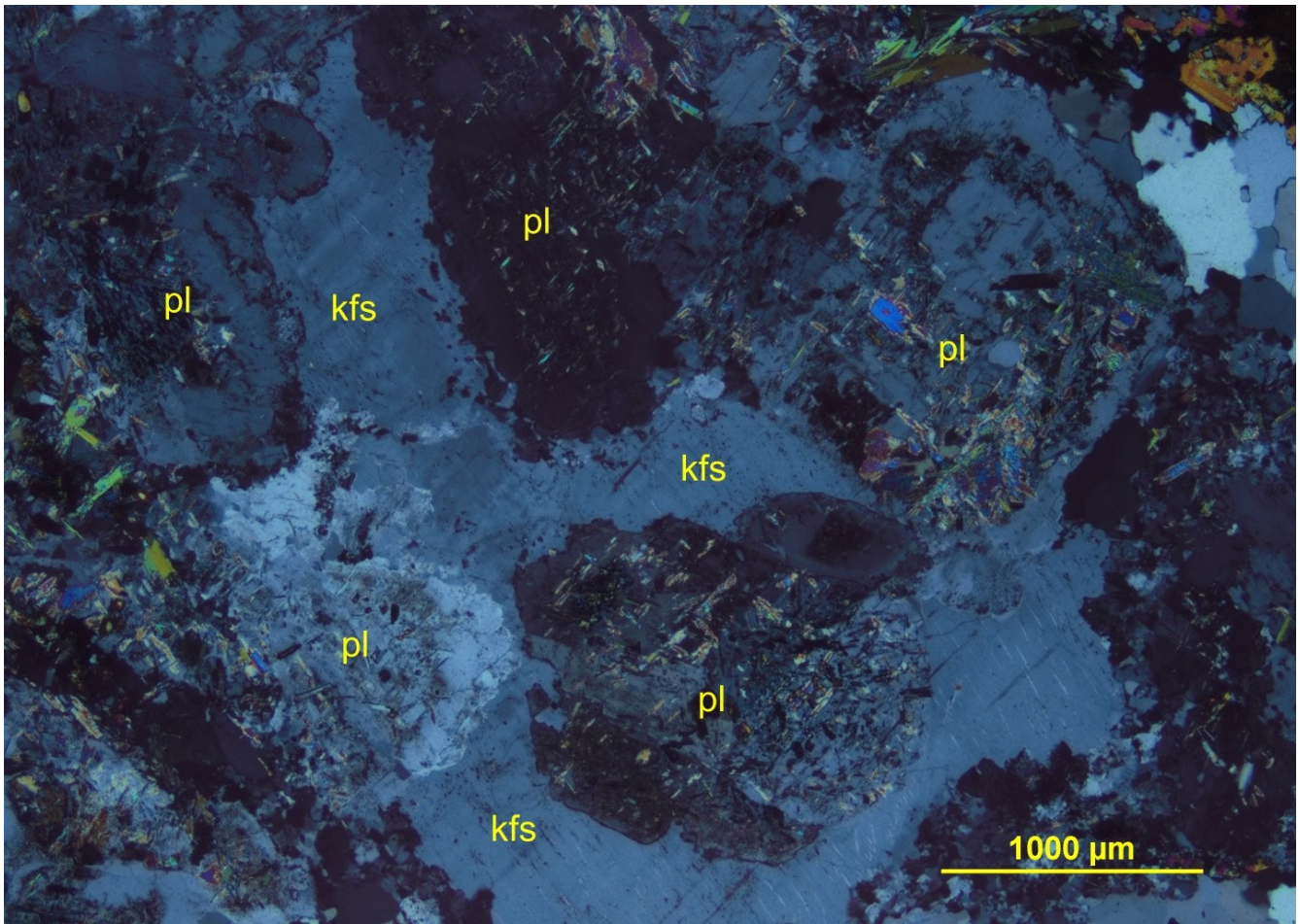
Fine-grained anhedral **epidote** forms irregular clusters dispersed within the quartzofeldspathic domains.



Photomicrograph 45a: Some plagioclase crystals are moderately altered and are distinguished from the inclusion-free quartz and K-feldspar (kfs). Plane-polarized transmitted light.

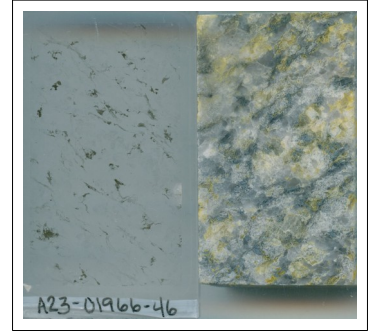


Photomicrograph 45b: Detail of the alteration (white mica-epidote) affecting the plagioclase (pl). Plane-polarized transmitted light.



Photomicrograph 45c: Poikilitic K-feldspar host anhedral plagioclase (pl) and biotite (bt) crystals. Crossed polarizers transmitted light.

Sample 46: A23-01966-46-IG_BH02_LG031



Orthogneiss

This section is compositionally similar to Sample 45. In some domains of this section, the plagioclase and subordinate K-feldspar define porphyroclastic domains immersed within a fine-grained matrix of quartz and the epidote and the white mica, which partially to completely replaced randomly oriented lamellae of biotite, define discontinuous sub-parallel cleavage domains imparting a gneissose texture.

Alteration: white mica-epidote: weak after plagioclase, and weak to strong after biotite

Mineral	Alteration/Weathering Mineral	Modal %	Size Range (mm)
plagioclase (albite)	white mica-epidote	47- 49	up to 2.5 long
quartz		38- 40	up to 0.5 long
biotite	white mica-epidote	6- 7	up to 1 long
K-feldspar (microcline)		5- 6	up to 3 across
	epidote	1- 2	up to 0.5
zircon		tr	up to 0.05

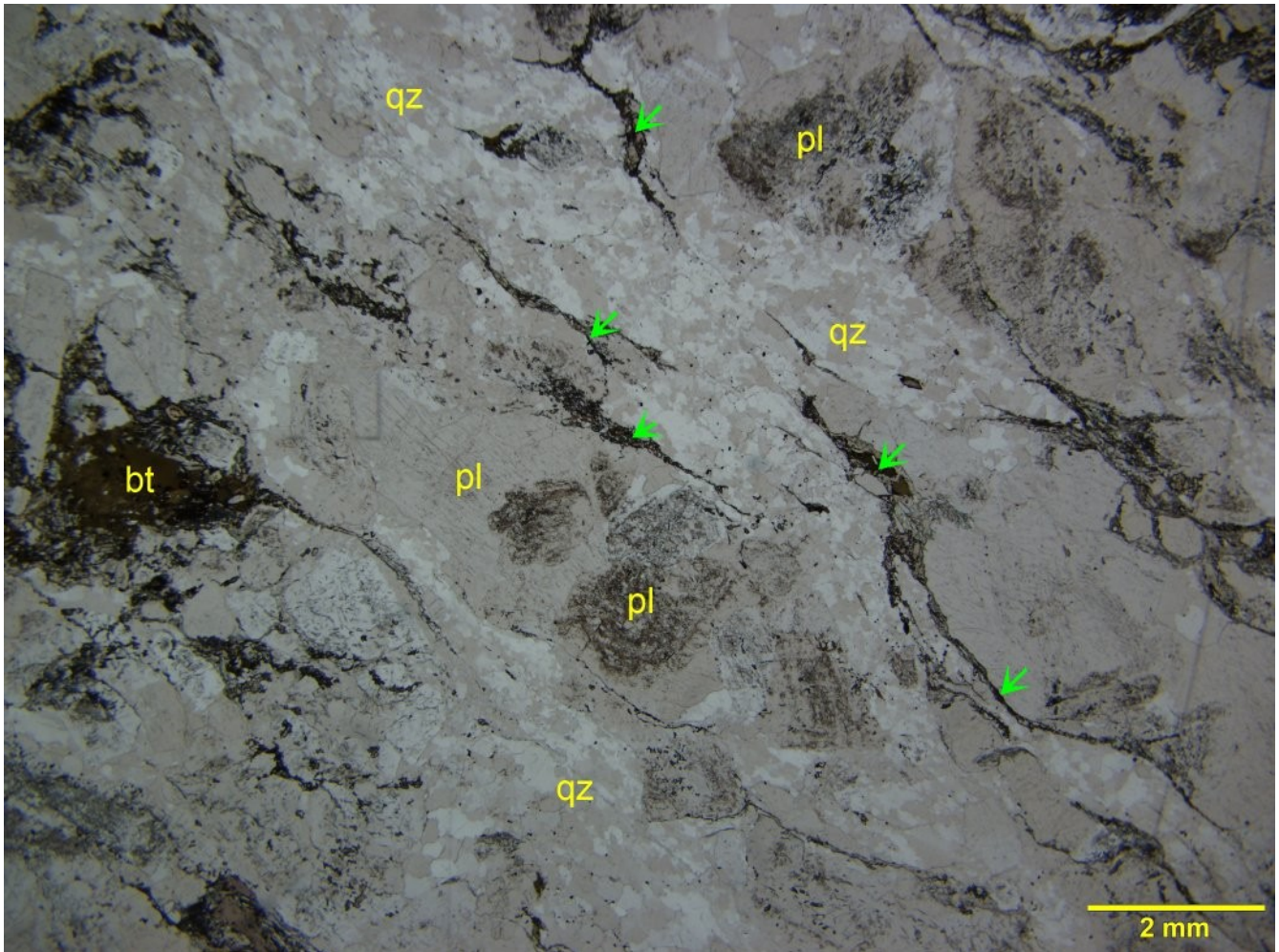
Plagioclase forms inequigranular anhedral and subhedral crystals up to 3.5 mm long. In most of its occurrences, the plagioclase define a granular texture associated with interstitial K-feldspar and quartz (e.g., Photomicrograph 46c and 46d). Some more deformed domains comprise porphyroclastic plagioclase immersed within a fine-grained matrix of quartz (Photomicrographs 46a and 46b). In these domains, discontinuous cleavage domains of white mica and epidote wrap the porphyroclastic plagioclase. Fine-grained flakes of **white mica** and fine-grained anhedral crystals of **epidote**, probably derived by the complete replacement of biotite, weakly to moderately altered some plagioclase crystals.

Quartz forms fine- to medium-grained monomineralic domains. Most quartz crystals show a moderate undulose extinction. Most of the quartz is concentrated within monomineralic domains, in which the inequigranular crystals show interlobate crystal boundaries.

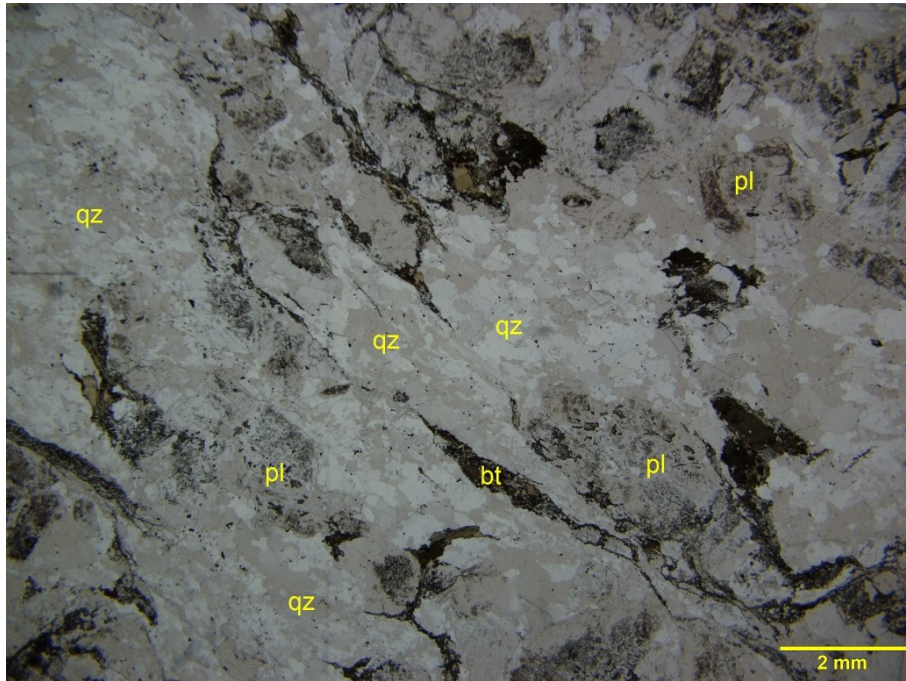
Biotite is fine- to medium-grained and its anhedral crystals (up to 1 mm long) are randomly oriented within the less deformed domains. White mica and epidote partially replaced the biotite, and define discontinuous and sub-parallel cleavage domains, which I interpret as the product of the complete replacement of biotite in the sheared domains.

K-feldspar forms sparse interstitial and subhedral crystals up to 3 mm across. The K-feldspar is

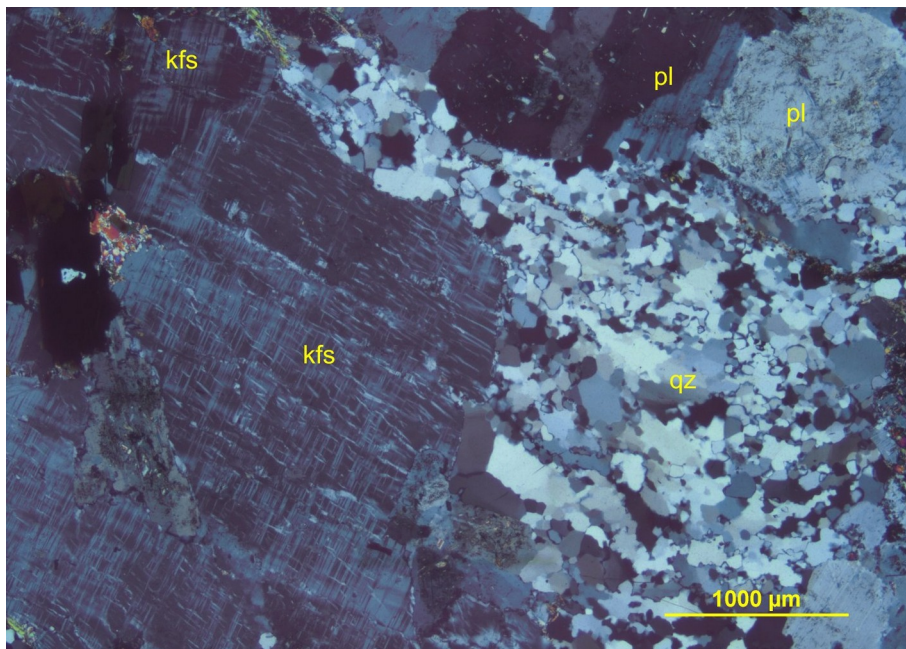
relatively fresh and display Albite-Pericline twinnings indicating its triclinic symmetry; therefore it is **microcline**.



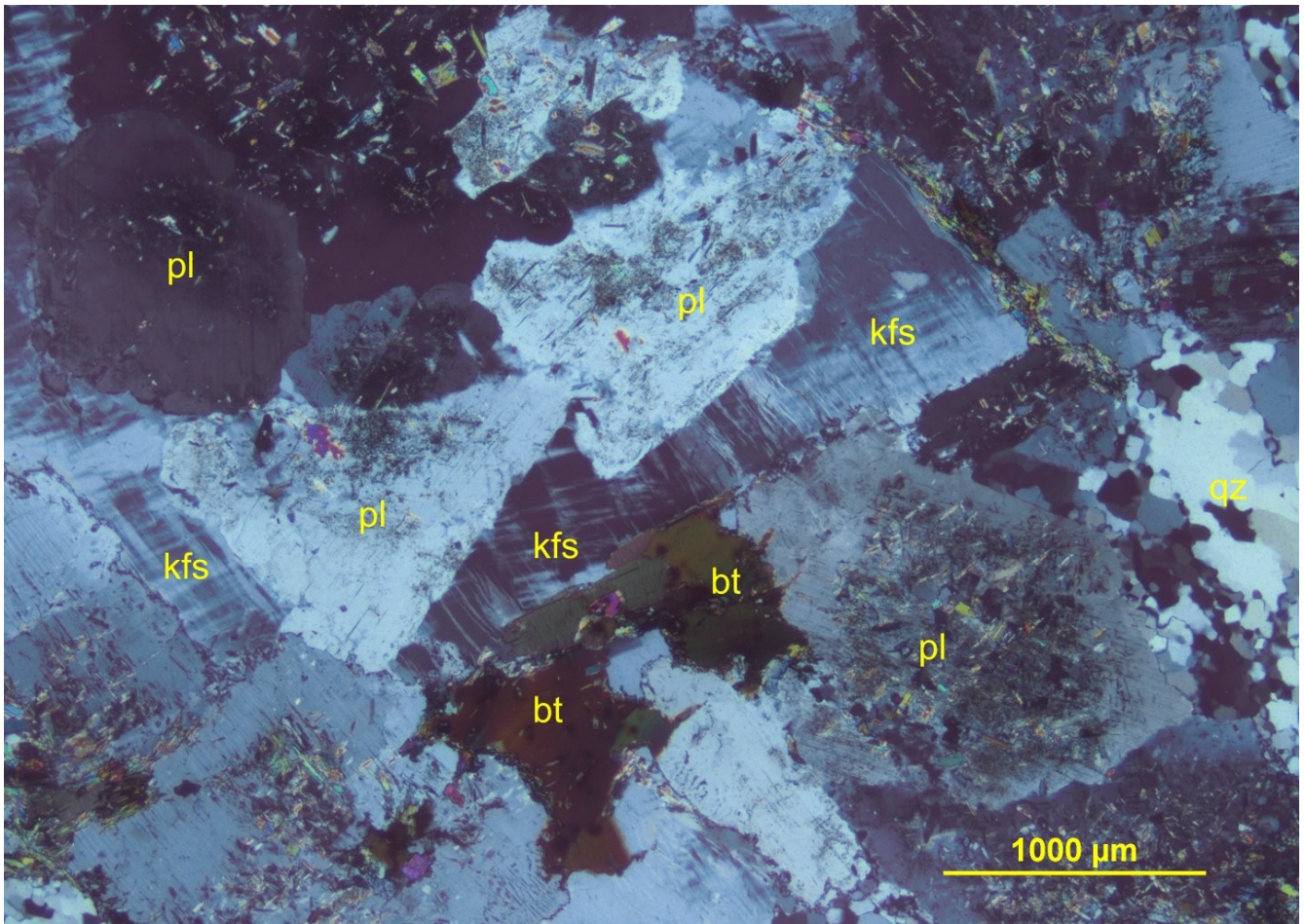
Photomicrograph 46a: Thin and discontinuous cleavage domains of white mica and epidote (yellow arrows) wrap porphyroclastic domains of plagioclase (pl) immersed within a quartz matrix (qz). Plane-polarized transmitted light.



Photomicrograph 46b: The cleavage domains define a gneissic texture, in which the porphyroclastic domains of plagioclase (pl) are rotated and immersed within the quartz-rich matrix (qz). Plane-polarized transmitted light.



Photomicrograph 46c: Fine-grained quartz (qz) filled in the strain shadow surrounding the subhedral K-feldspar (kfs). Crossed polarizers transmitted light.



Photomicrograph 46d: In the least deformed domains, plagioclase (pl) shows subhedral shape and is associated with interstitial K-feldspar (kfs) and subordinate biotite (bt). Crossed polarizers transmitted light.

Sample 47: A23-01966-47-IG_BH02_LG032

Chlorite-sericite-altered tonalite

Sheared calcite-K-feldspar-quartz vein(?)



This section comprises 2 domains. Subhedral plagioclase, and anhedral quartz, K-feldspar, and biotite define the granular texture in Domain A. A fine-grained tabular and sheared Domain B is made up to fine-grained quartz, K-feldspar, calcite and white mica crosscut the granular Domain A.

Alteration: sericite-epidote: weak to moderate after the plagioclase; **Fe-chlorite>epidote:** strong after biotite; **pyrite:** subtle; **iron oxides:** strong after pyrite

Mineral	Alteration/Weathering Mineral	Modal %	Size Range (mm)
Domain A: tonalite (~78% of PTS)			
plagioclase (albite)	white mica-epidote	40- 50	up to 3.5 long
quartz		32- 34	up to 2.5 long
K-feldspar (microcline)		3- 4	up to 3 across
biotite	chlorite-epidote	1- 2	up to 1.5 long
zircon		tr	up to 0.05
[pyrite]	iron oxides	tr	0.02
Domain B: sheared calcite-K-feldspar-quartz vein(?) (~22% of PTS)			
quartz		10	up to 0.1, rare up to 0.5
K-feldspar		10	up to 0.1
calcite		2	up to 0.1
plagioclase (albite)		tr	up to 0.1
white mica		tr	up to 0.15 long

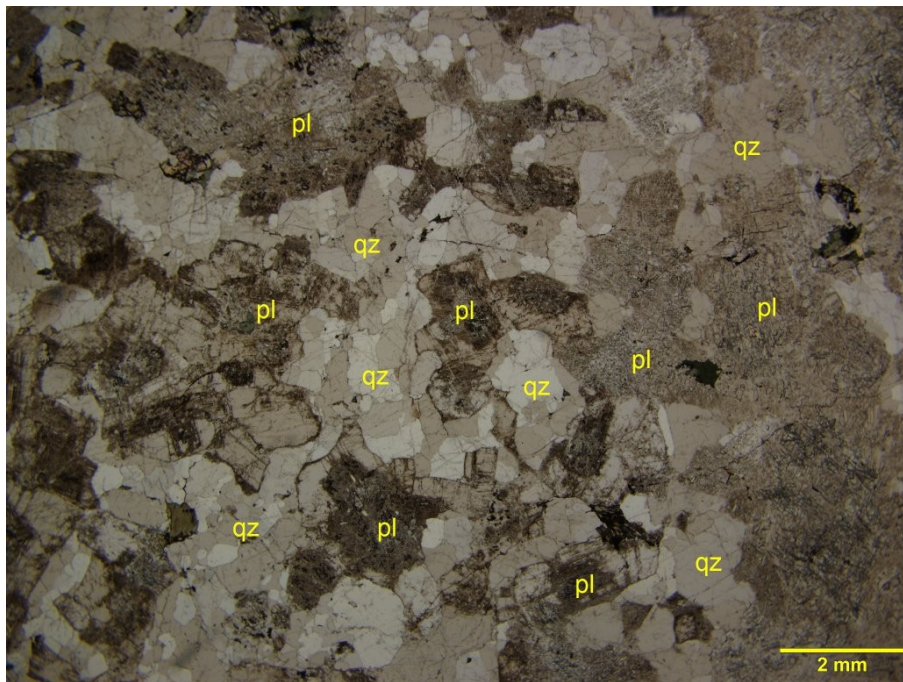
Plagioclase (albite) forms subhedral and anhedral crystals ranging from 0.5 mm to 2 mm across. The plagioclase prevails over the quartz and defines a granular texture. Very fine-grained dispersions of sericite and earthy and unresolved material (epidote?) weakly altered the plagioclase crystals and help distinguish the plagioclase from the quartz under plane-polarized transmitted light (Photomicrograph 47a and 47b). The plagioclase's refractive indexes are lower than those of the quartz, thus indicating the plagioclase is **albite**.

Quartz forms fine- to medium-grained monomineralic aggregates in Domain A. In Domain B, the quartz is fine-grained and it is finely intergrown with fine-grained K-feldspar, subordinate calcite, and rare white mica within a sheared tabular domain ~6 mm thick (see Domain B in the image above).

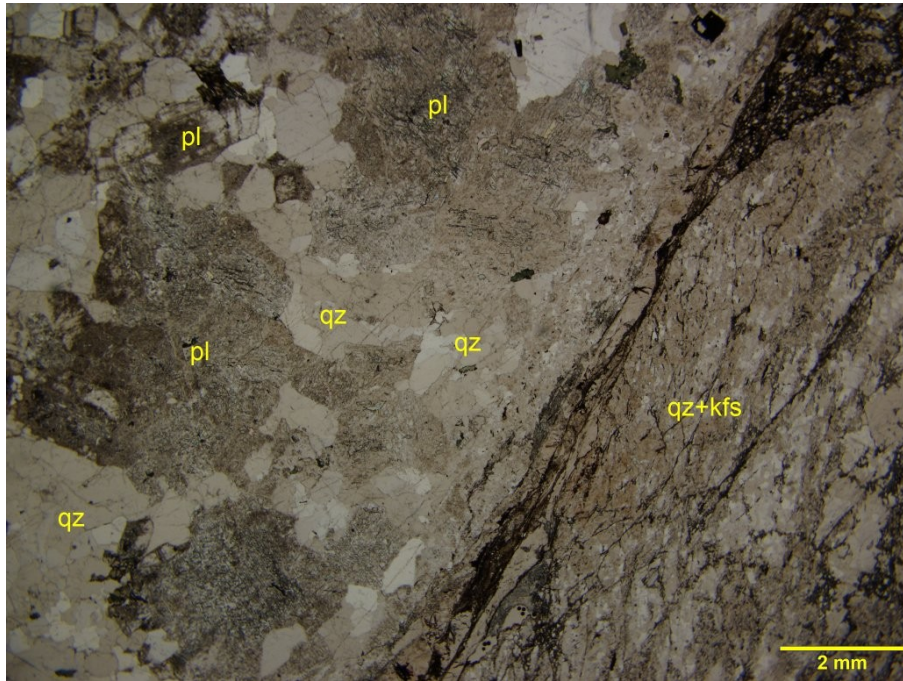
K-feldspar is concentrated as fine-grained anhedral crystals within the sheared Domain B. Its abundance and distribution is visible in the stained offcut's image above. Fine- to medium-grained anhedral K-feldspar is subordinate to the plagioclase and quartz in Domain A.

Fe-chlorite strongly altered most of the biotite crystals (up to 1 mm long). The Fe-chlorite is distinguished by its strong green pleochroism and anomalous birefringence colours, which distinguish the chlorite from the rare and highly birefringent **biotite** lamellae. Fine-grained crystals of epidote and relic of zircon inclusions are associated with the chlorite within the epitaxial pseudomorphs after biotite.

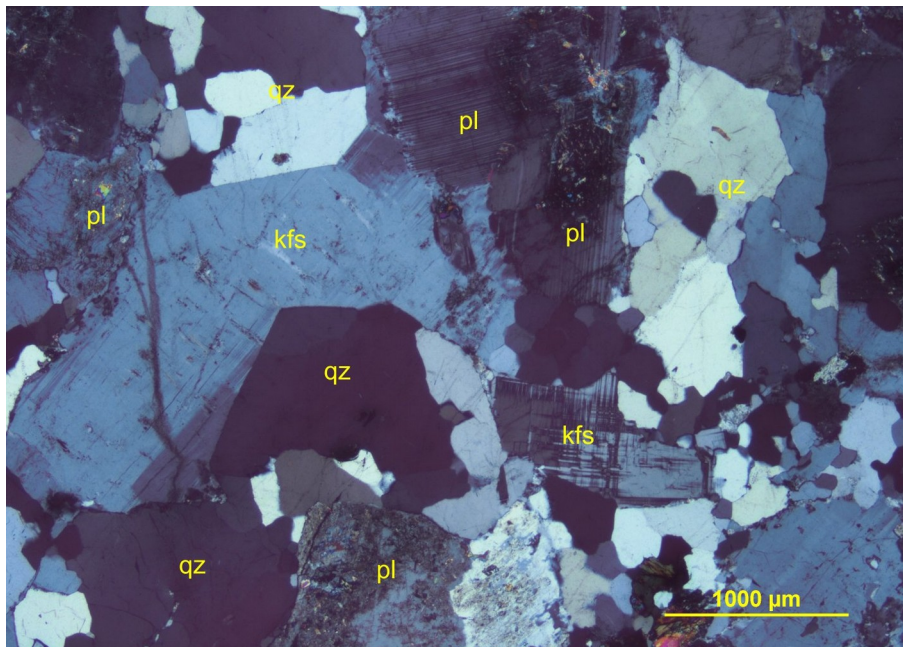
One crystal of **pyrite** (~0.4 mm across) occur near the contact with Domain B and it is completely replaced by iron oxides-rich boxwork textures



Photomicrograph 47a: Subhedral and heterogeneously altered plagioclase (pl) and anhedral quartz (qz) define a granular texture. Plane-polarized transmitted light.



Photomicrograph 47b: The granular texture defined by the plagioclase (pl) and quartz (qz) is very little deformed at the contact with the quartz and K-feldspar sheared domain (qz+kfs). Plane-polarized transmitted light.

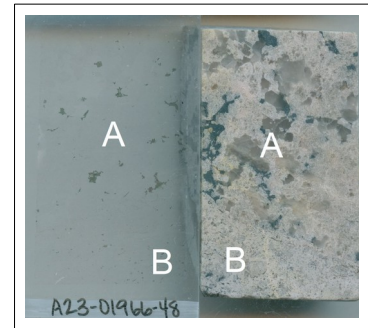


Photomicrograph 47c: Interstitial K-feldspar (kfs) shows Albite-Pericline twinnings and occupy the interstices between the plagioclase (pl) and quartz crystals (qz). Crossed polarizers transmitted light.

Sample 48: A23-01966-48-IG_BH02_LG033

Fe-chlorite-calcite-altered tonalite

Plagioclase-phyric andesite(?)



This section comprises two Domains. In the upper part of the section (Domain A), anhedral and subhedral plagioclase and quartz, patches of calcite and pseudomorphs of Fe-chlorite after biotite define a granular texture. In the lower part (Domain B), anhedral and subhedral phenocrysts of plagioclase are immersed within a very fine-grained groundmass of plagioclase and subordinate quartz.

Alteration: white mica-epidote: weak after plagioclase; **Fe-chlorite:** strong after biotite; **calcite:** weak in Domain A

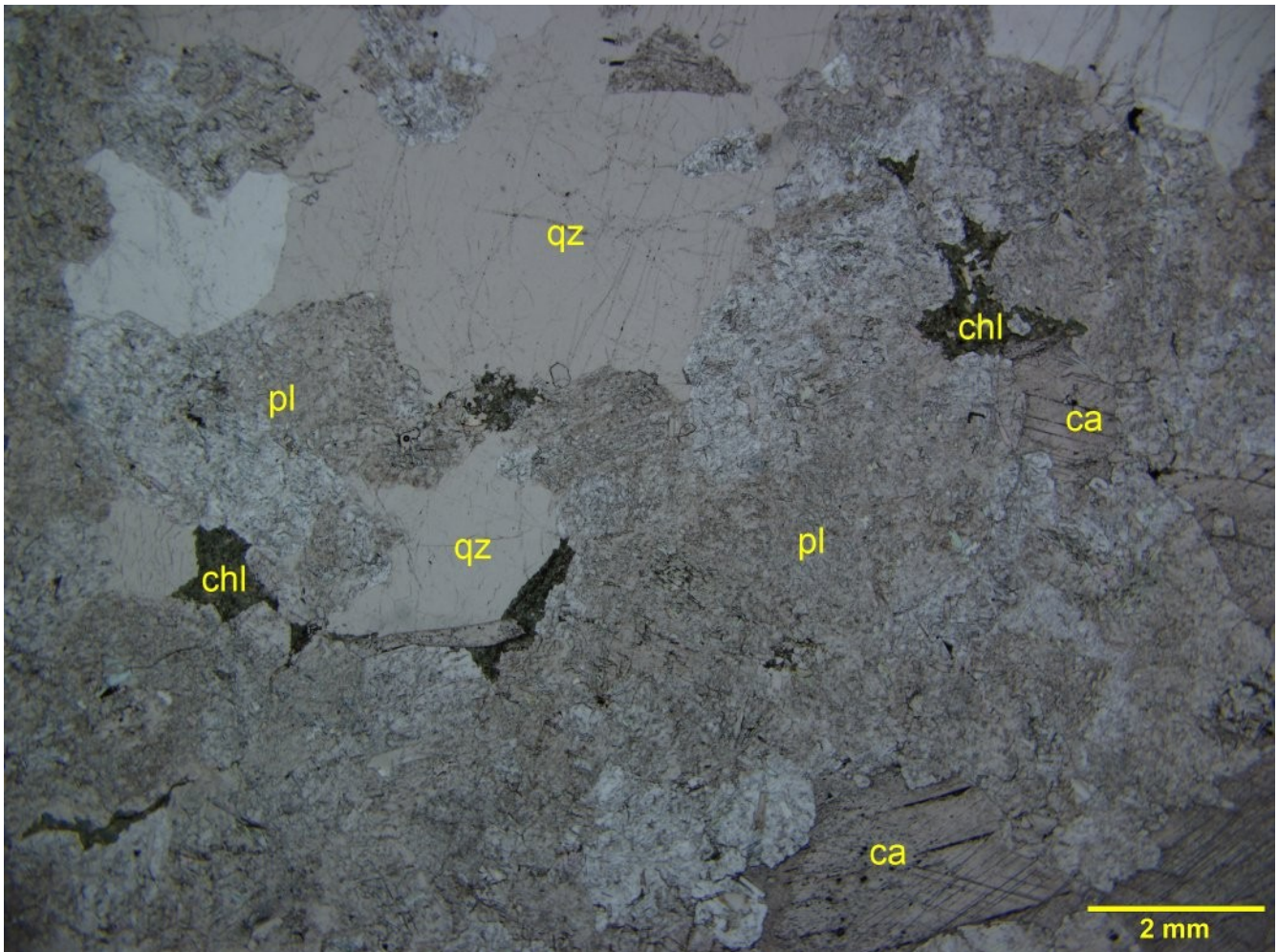
Mineral	Alteration/Weathering Mineral	Modal %	Size Range (mm)
Domain A: tonalite (~75% of PTS)			
plagioclase		52- 53	up to 7.5 long
quartz		19- 21	up to 9 long
	calcite	2- 3	up to 4.5
[biotite]	Fe-chlorite	1- 1.5	[up to 1 mm across]
	iron oxides	tr	up to 0.01
Domain B (~25% of pTS) plagioclase-phyric andesite(?)			
<i>phenocrysts</i>			
plagioclase		2- 3	up to 1.5 long, rare up to 3.5 long
<i>groundmass</i>			
plagioclase		19- 20	up to 0.02
quartz		2- 3	up to 0.02
[?]	Fe-chlorite	0.2- 0.5	up to 0.4 long
	rutile	tr	up to 0.02

Plagioclase prevails in both domains. In Domain A, the plagioclase crystals are anhedral and subhedral and ranges from 0.5 mm to 7.5 mm long. The plagioclase crystals are randomly oriented and show refractive indexes lower than those of the quartz, thus indicating the plagioclase is albite. Very fine-grained flakes of white mica and earthy and unresolved dispersions (likely epidote) weakly altered the

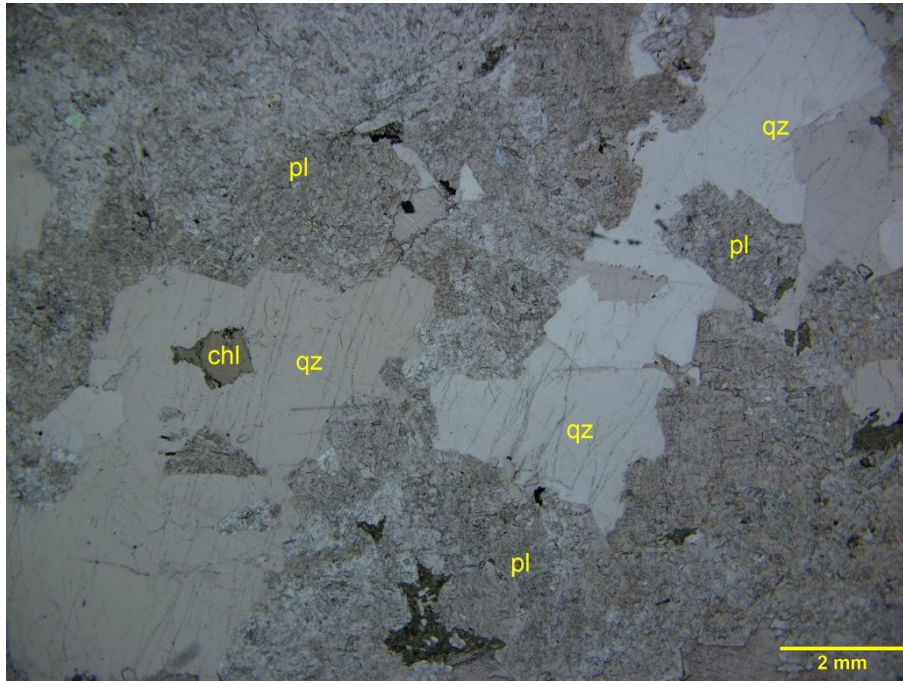
plagioclase. In Domain B, the plagioclase forms anhedral and subhedral phenocrysts (up to 1.5 mm long, and in rare cases up to 3.5 mm long) immersed within a very fine-grained groundmass, in which the plagioclase forms interlobate and anhedral crystals intergrown with subordinate quartz.

Quartz forms coarse- (up to 7.5 mm long) and medium-grained anhedral crystals in Domain A. In most quartz crystal a moderate undulose extinction occurs. Within Domain B, the quartz is very fine-grained and it is subordinate to the plagioclase in the groundmass.

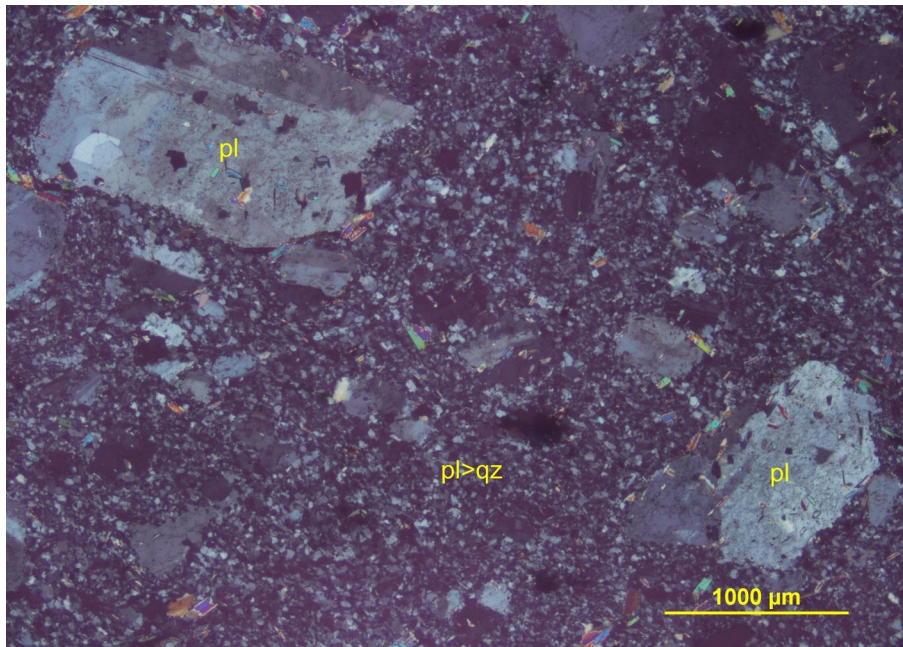
Fe-chlorite completely replaced biotite crystals up to 1 mm across in Domain A, and up to 0.4 mm long in Domain B.



Photomicrograph 48a: Domain A—Subhedral and anhedral crystals of plagioclase (pl) and quartz (qz) define a granular texture hosting sparse pseudomorphs of chlorite (chl) and calcite replacement patches (ca). Plane-polarized transmitted light.

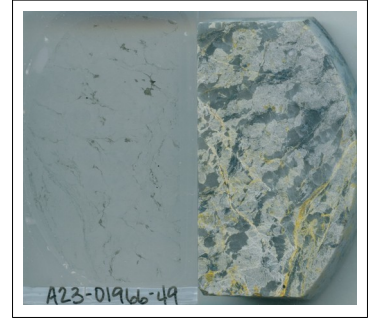


Photomicrograph 48b: Domain A—Another example of the granular texture defined by abundant and weakly altered plagioclase (pl) and quartz (qz). Plane-polarized transmitted light.



Photomicrograph 48c: Domain B—Plagioclase phenocrysts (pl) are immersed within a very fine-grained groundmass, in which plagioclase prevails over the quartz (pl>qz). Crossed polarizers transmitted light.

Sample 49: A23-01966-49-IG_BH02_LG034



Brecciated chlorite-sericite-altered tonalite

Subhedral plagioclase, and anhedral quartz, K-feldspar, and biotite define the granular texture, which is crosscut by intersecting fractures filled in by white mica, chlorite and limonitic material.

Alteration: sericite: moderate after the plagioclase; **Fe-chlorite:** strong after biotite; **pyrite:** subtle; **iron oxides:** weak after pyrite

Mineral	Alteration/Weathering Mineral	Modal %	Size Range (mm)
plagioclase (albite)	white mica	43- 45	up to 2.5 long
quartz		38- 40	up to 1.2
	white mica	10- 12	0.1
K-feldspar (microcline)		4- 5	up to 1.2
[biotite]	chlorite	1- 2	up to 0.75
	chlorite	0.8- 1.2	0.02
zircon		tr	0.01
[pyrite]	iron oxides	tr	up to 0.2

Plagioclase (albite) forms subhedral and anhedral crystals ranging from 0.5 mm to 2 mm across. The plagioclase prevails over the quartz and defines a granular texture. Very fine-grained dispersions of sericite moderately altered the plagioclase crystals and help distinguish the plagioclase from the quartz under plane-polarized transmitted light (Photomicrograph 49a, 49b, and 49c). The plagioclase’s refractive indexes are lower than those of the quartz, thus indicating the plagioclase is **albite**.

Quartz forms fine- to medium-grained monomineralic aggregates in Domain A. In Domain B, the quartz is fine-grained and it is finely intergrown with fine-grained K-feldspar, subordinate calcite, and rare white mica within a sheared tabular domain ~6 mm thick (see Domain B in the image above).

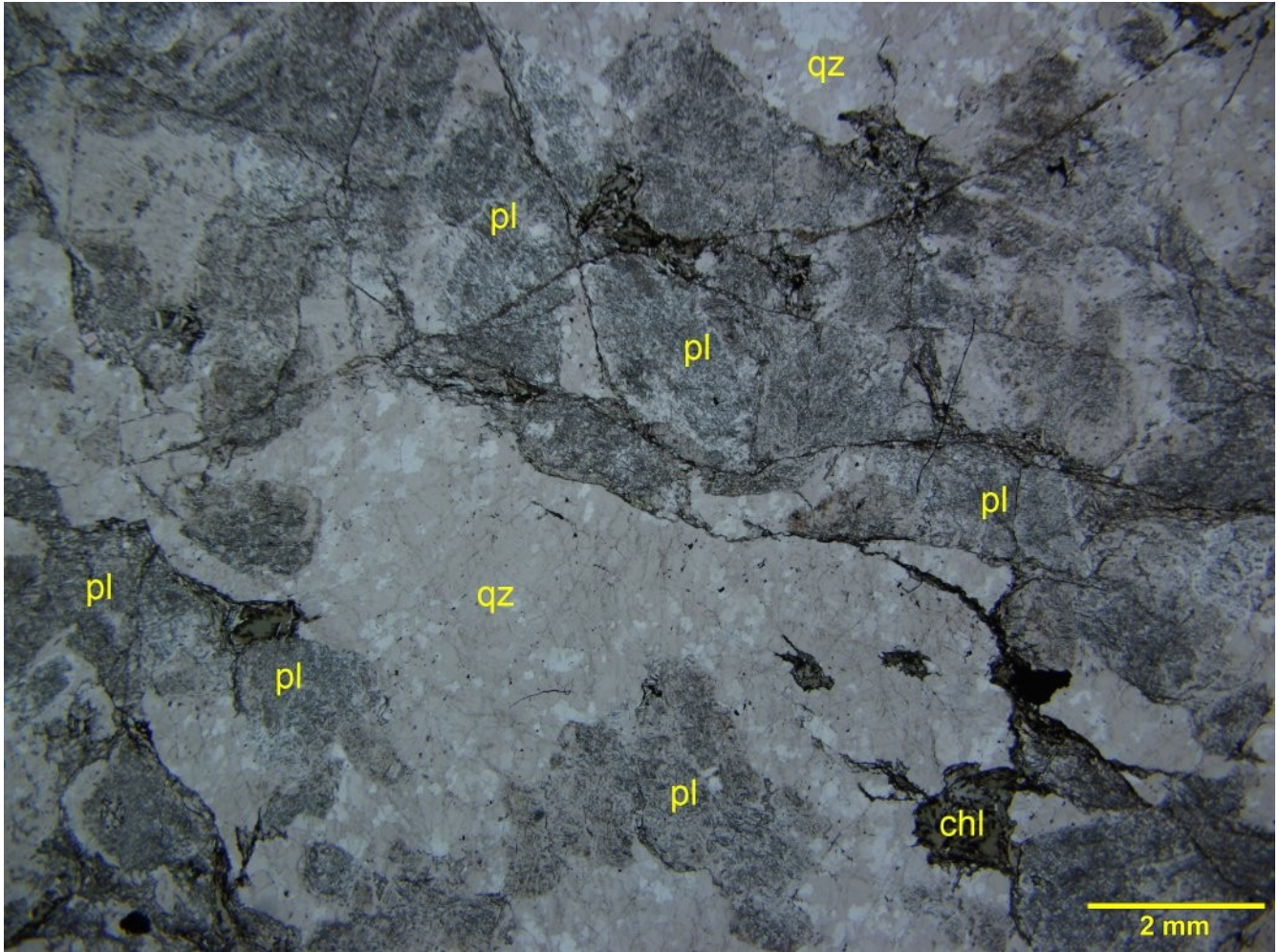
White mica occurs as very fine-grained alteration products replacing the plagioclase and as fine-grained flakes filling in the intersecting fractures brecciating the granular texture (Photomicrographs 49a, 49b, and 49c). Within the fractures, the white mica is associated with subordinate chlorite and iron oxides.

K-feldspar (microcline) is fine- to medium-grained and occupies interstitial positions between the plagioclase crystals (Photomicrograph 49d). The Albite-Pericline twinnings indicate the K-feldspar is microcline.

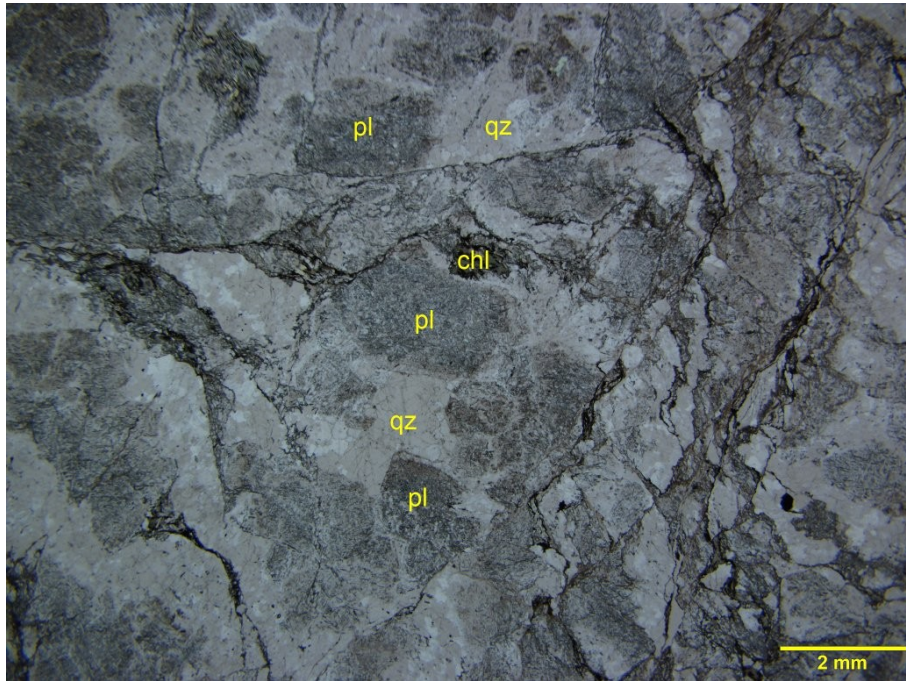
Fe-chlorite completely altered most of the biotite crystals (up to 0.75 mm long). The Fe-chlorite is

distinguished by its strong green pleochroism and anomalous birefringence colours.

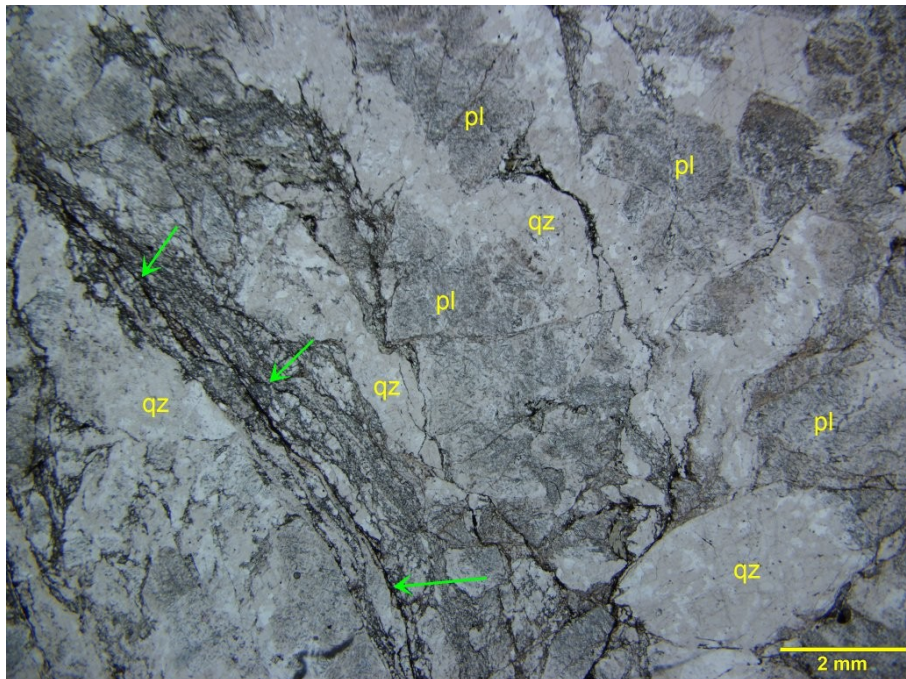
Pyrite is rare and is disseminated within the granular texture as fine-grained subhedral crystals up to 0.2 mm across. Iron oxides subtly to weakly altered the pyrite.



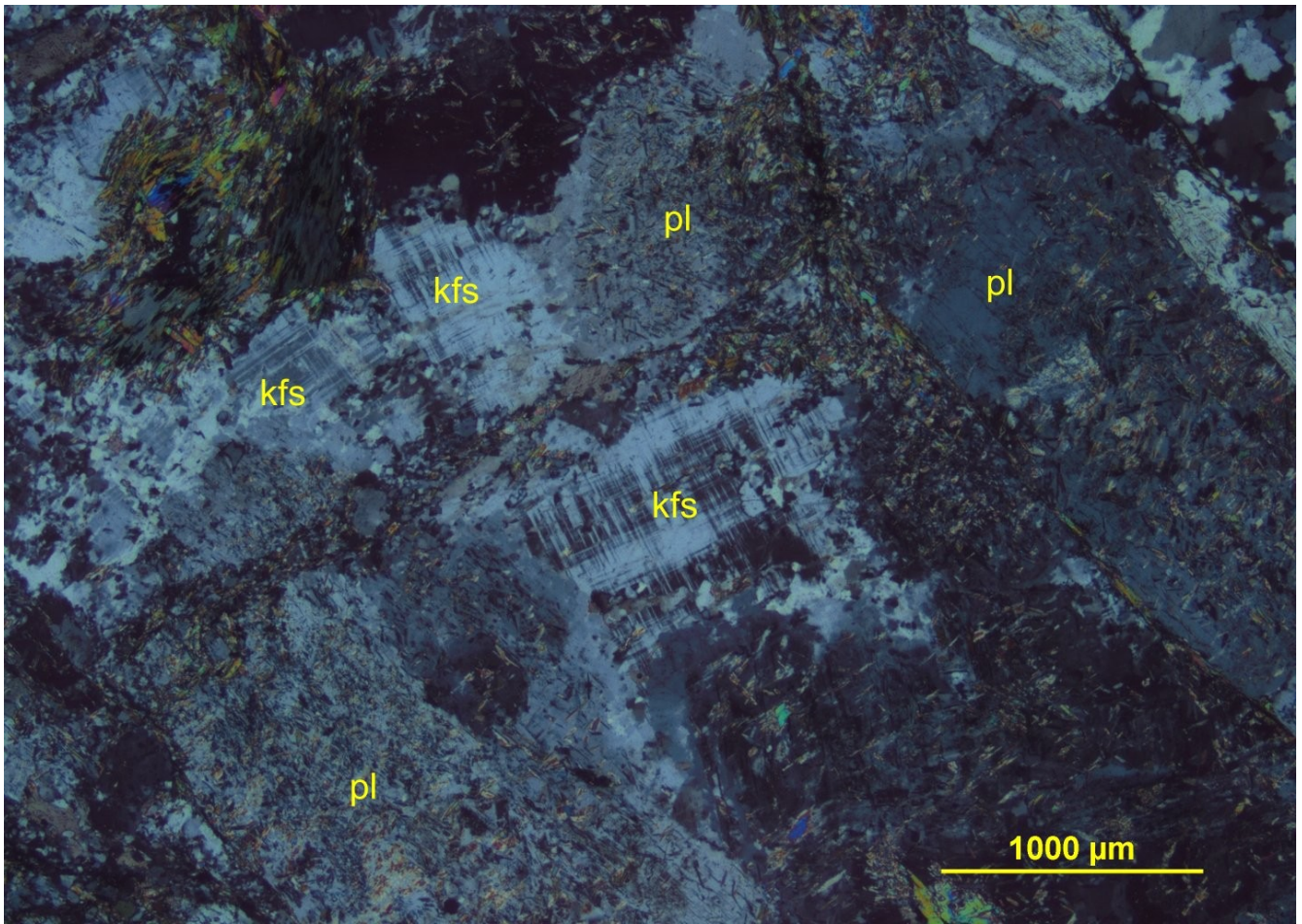
Photomicrograph 49a: Mostly anhedral plagioclase (pl) and quartz define a granular texture crosscut by irregular fractures. Plane-polarized transmitted light.



Photomicrograph 49b: Another example of the irregular fractures crosscutting the granular texture defined by plagioclase (pl) and quartz (qz). Plane-polarized transmitted light.



Photomicrograph 49c: In some cases, the fractures are concentrated within brittle shear zones (yellow arrows). Plane-polarized transmitted light.

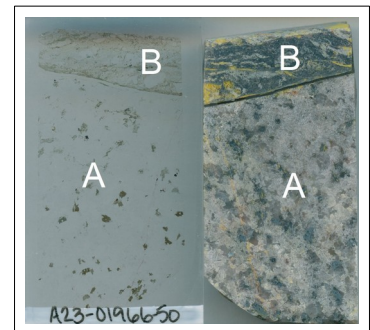


Photomicrograph 49d: Interstitial K-feldspar (kfs) occurs between anhedral crystals of plagioclase (pl). Crossed polarizers transmitted light.

Sample 50: A23-01966-50-IG_BH01_LG047

Chlorite-white mica-altered tonalite

White mica-orthoschist



Most of this section comprises anhedral crystals of plagioclase, anhedral quartz, and randomly oriented biotite (Domain A). These minerals define a relatively homogeneous and isotropic granular texture. In the upper part of the section (Domain B), porphyroclasts of plagioclase and K-feldspar are immersed within a schistose matrix of fine-grained plagioclase and white mica.

Alteration: white mica: weak after plagioclase in Domain A; weak to moderate after biotite in Domain A; **chlorite:** weak to strong after biotite in Domain A; **iron oxides:** strong after unknown mineral

Mineral	Alteration/Metamorphism Mineral	Modal %	Size Range (mm)
Domain A: tonalite (~82% of PTS)			
plagioclase (albite)	white mica	58- 60	up to 2.5 long
quartz		18- 20	up to 3 long
biotite	chlorite-clay(?) -white mica	4- 5	up to 1.5
[?]	iron oxides	tr	[up to 0.4]
zircon		tr	
Domain B: orthoschist (~18% of PTS)			
<i>porphyroclasts</i>			
plagioclase (albite)		1- 1.5	up to 2
K-feldspar (microcline)		1- 1.5	up to 3 long
<i>matrix</i>			
	white mica	9- 10	up to 0.1
	plagioclase	6- 7	up to 0.1
	iron oxides-limonite	tr	<0.01

Plagioclase forms inequigranular and mostly anhedral crystals up to 2.5 mm long. Fine-grained flakes of **white mica** weakly altered the plagioclase crystals in Domain A. In the schistose Domain B, the plagioclase occurs as anhedral porphyroclasts (up to 2 mm across) and is fine-grained within the matrix.

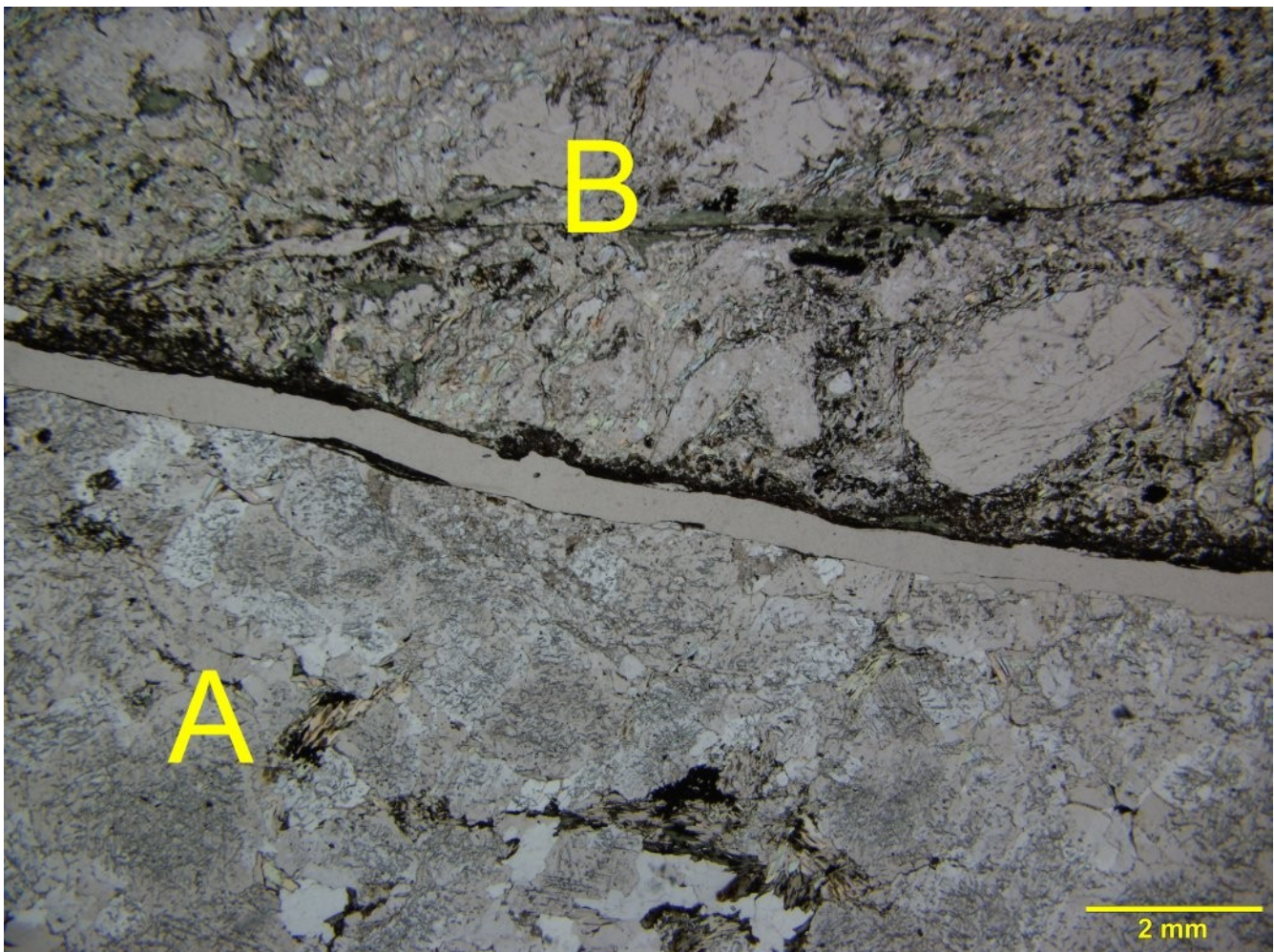
White mica is abundant in the sheared matrix of the domain in the upper part of the section (Domain B) which the lamellae are preferentially iso-oriented and define a continuous schistosity in which

anhedral porphyroclasts of plagioclase and K-feldspar are immersed (Photomicrographs 50a and 50d). White mica partially overprinted some of the biotite crystals. The white mica replacement after biotite occurs near the boundary with the white mica-rich Domain B.

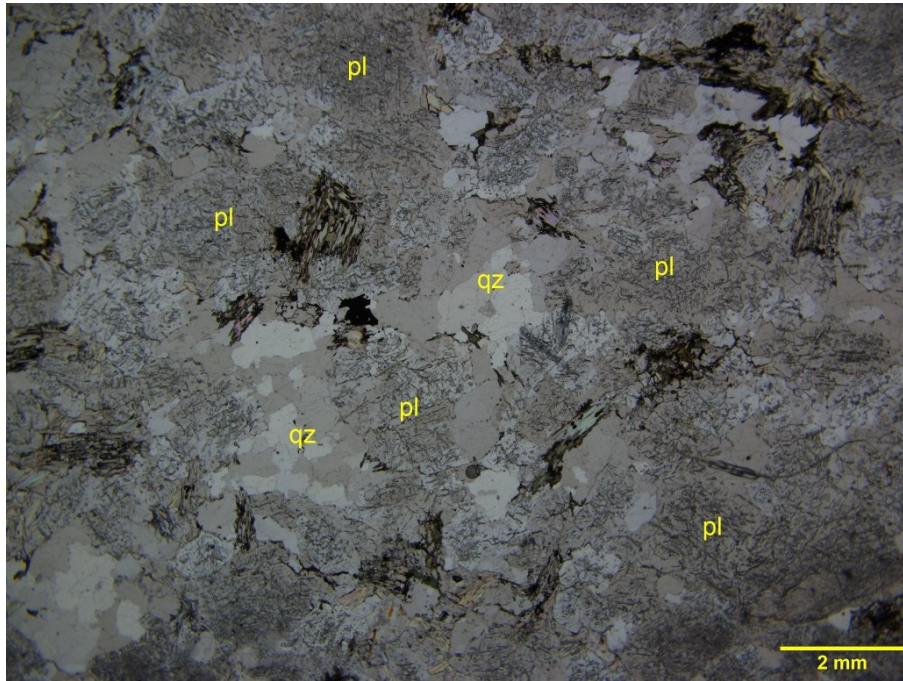
Quartz forms fine- to medium-grained monomineralic domains (Photomicrographs 50b and 50c). Most quartz crystals show a moderate undulose extinction.

Biotite is fine- to medium-grained and its anhedral crystals (up to 1.5 mm long) are finely intergrown with the feldspars, and are weakly altered to epitaxial **chlorite**. Near the boundary with Domain B, the biotite is overprinted by white mica.

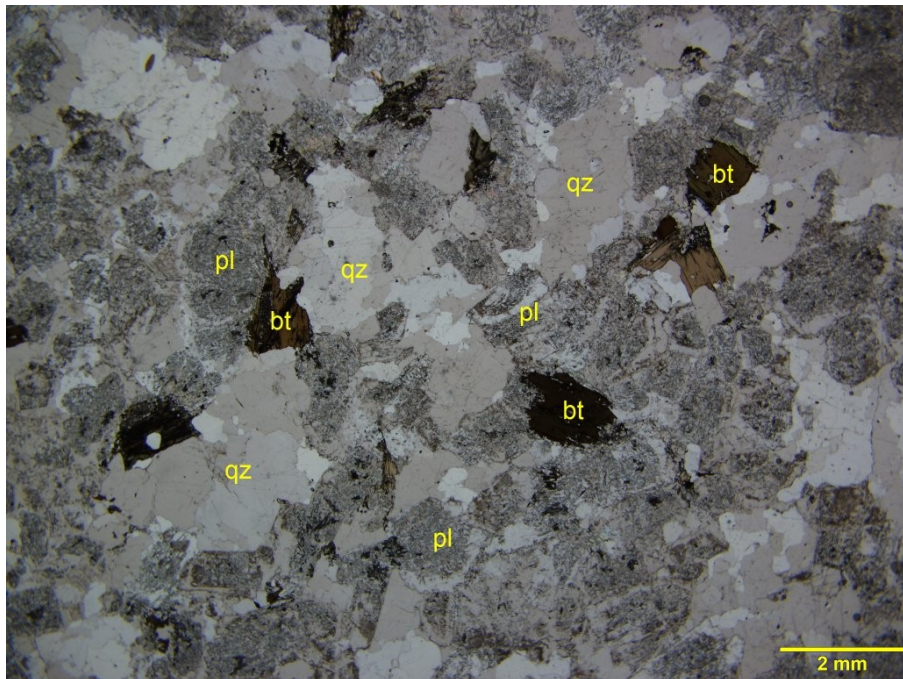
K-feldspar forms anhedral porphyroclasts immersed within the fine-grained and schistose matrix of white mica and plagioclase (Photomicrograph 50d).



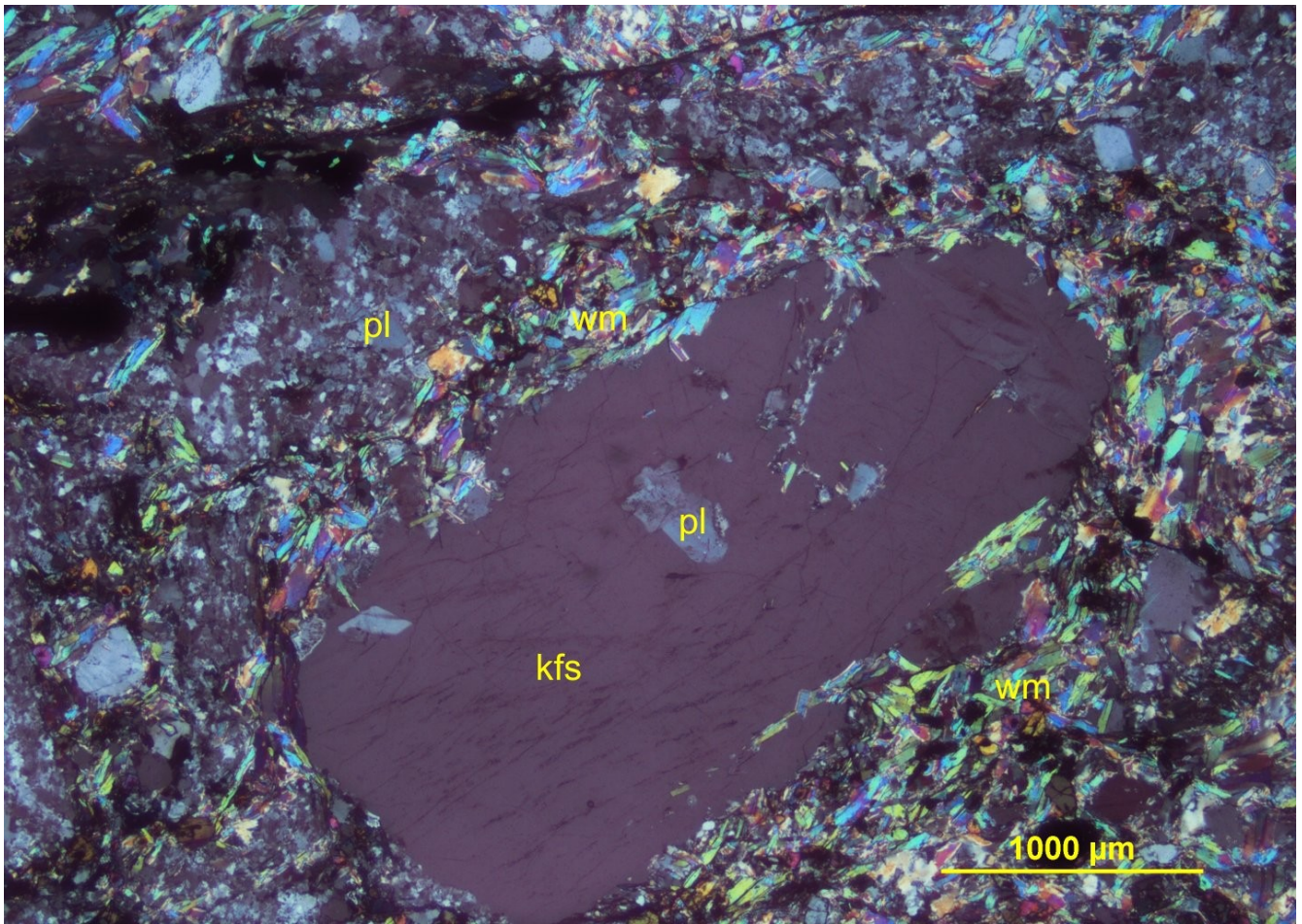
Photomicrograph 50a: The disjunct boundary between the schistose Domain B (B) and the granular Domain A (A) is shown under plane-polarized transmitted /reflected light.



Photomicrograph 50b: Domain A—Plagioclase (pl), quartz (qz) and biotite (bt) define a granular texture. Plane-polarized transmitted light.

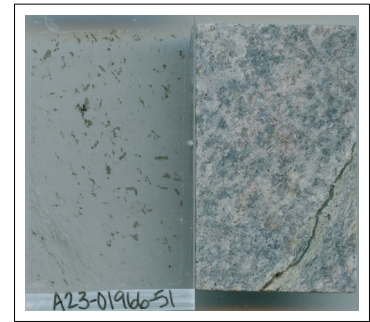


Photomicrograph 50c: Domain A—Another example of the granular texture. The quartz forms irregularly shaped monomineralic aggregates (qz), and the biotite is relatively fresh (bt). Plane-polarized transmitted light.



Photomicrograph 50d: Domain B—A K-feldspar porphyroblast (kfs) host plagioclase inclusions (pl) and is immersed within a fine-grained matrix of white mica (wm) and plagioclase (pl). Plane-polarized transmitted light.

Sample 51: A23-01966-51-IG_BH01_LG048



White mica-altered tonalite

White mica-quartz schist

Anhedral and white mica-altered plagioclase crystals are associated with anhedral quartz and randomly oriented biotite and define a relatively homogeneous and isotropic granular texture. In the lower left part of the section, a sheared domain comprises cleavage domains of white mica, lenticular microlithons of quartz, and subordinate fine-grained plagioclase.

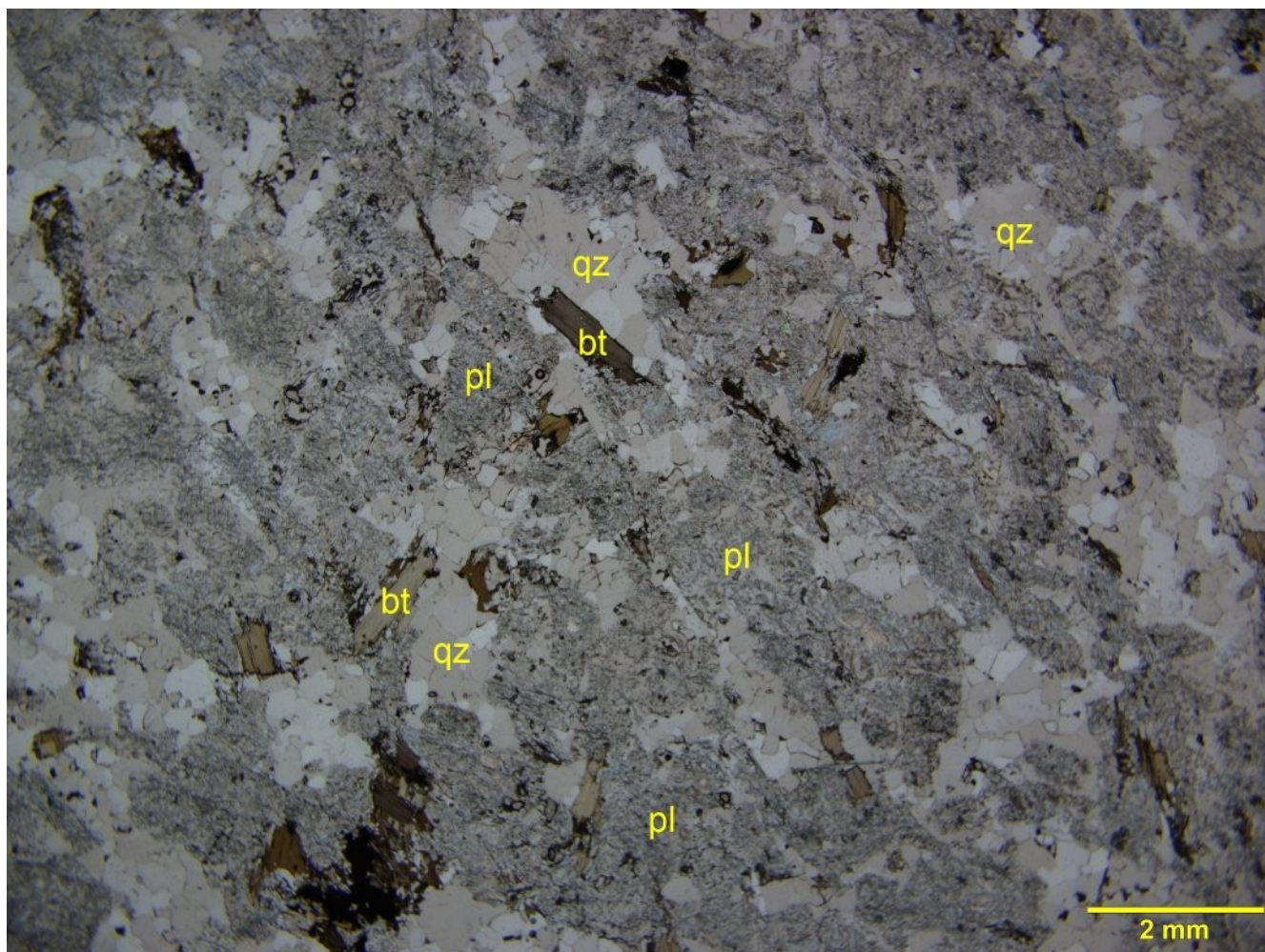
Alteration: white mica: moderate after plagioclase; weak after biotite; titanite: subtle after biotite

Mineral	Alteration/Metamorphic Mineral	Modal %	Size Range (mm)
tonalite (~85% of PTS)			
plagioclase (albite)	white mica	58- 60	up to 2.5 long
quartz		18- 20	up to 3 long
biotite	white mica-titanite	4- 5	up to 1 long
[?]	iron oxides	tr	[up to 0.4]
zircon		tr	
schist (~15% of PTS)			
	white mica	8	up to 0.2, rare up to 0.5 long
	quartz	6	up to 1
plagioclase		1	up to 1
	titanite	tr	up to 0.05

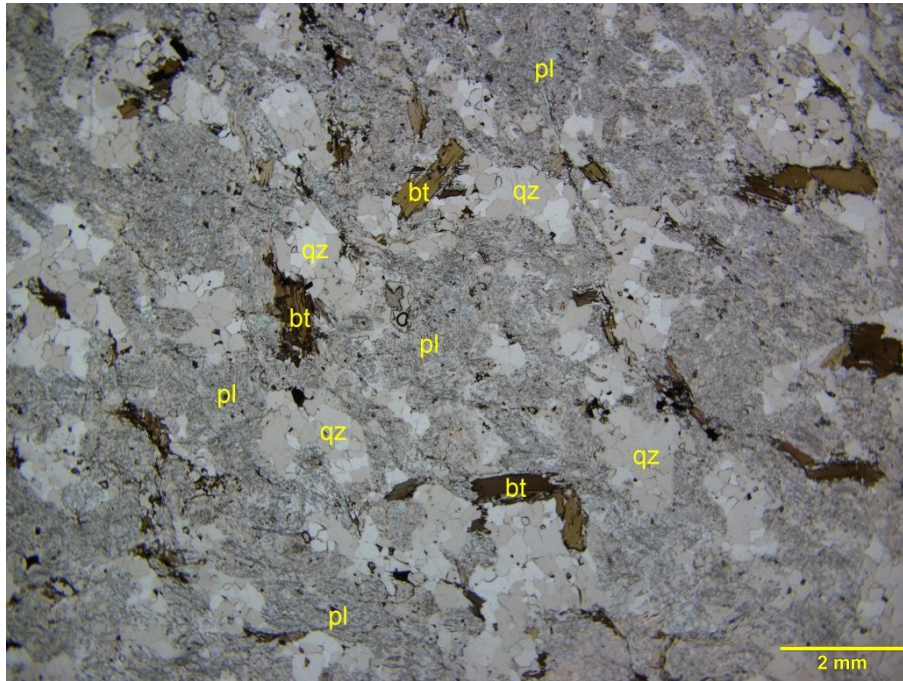
Plagioclase forms anhedral and subhedral crystals up to 2.5 mm long. Fine-grained flakes of white mica moderately altered the plagioclase crystals, which are randomly oriented in the granular texture. The plagioclase's refractive indexes are lower than those of the quartz; therefore, the plagioclase is **albite**.

Quartz forms fine- to medium-grained crystals defining irregularly shaped monomineralic domains (Photomicrographs 51a and 51b). Within the schistose domain in the lower left part of the section, quartz forms lenticular domains alternating with the irregular white mica-rich cleavage domains (Photomicrograph 51c). I interpret the schist as generated by the deformation, mechanical wearing and replacement of white mica after plagioclase during a brittle-ductile deformation event partitioned into this schistose domain.

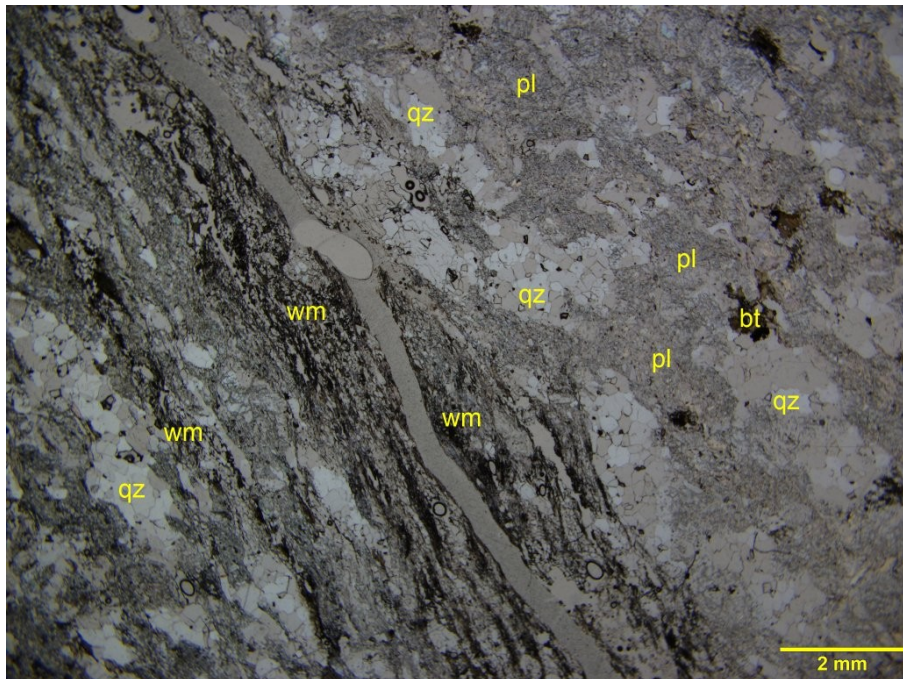
Biotite is fine- to medium-grained (up to 1 mm long) and its lamellae are randomly oriented and define an isotropic granular texture. The biotite hosts very fine-grained zircon inclusions. Some biotite crystals are deformed and partially replaced by fine-grained flakes of white mica and fine-grained **titanite**.



Photomicrograph 51a: Anhedra and subhedra of plagioclase (pl), quartz (qz), and randomly oriented biotite (bt) define a granular texture. Plane-polarized transmitted light.



Photomicrograph 51b: Another example of the granular texture. In this photomicrograph, the biotite lamellae (bt) are randomly oriented and fresh. Plane-polarized transmitted light.



Photomicrograph 51c: A schistose domain comprise sub-parallel and discontinuous cleavage domains of white mica associated with lenticular microlithons of quartz (qz). The granular texture defined by the plagioclase (pl) and quartz (qz) is shown in the upper right part of this photomicrograph. Plane-polarized transmitted light.

Appendix 1. Glossary of Microstructural and Petrologic Terms Used in the Text

a, b, c: Symbols used to describe the crystallographic axes of the crystals.

alteromorph: Mineral or group of minerals developed by partial to complete alteration or weathering of a primary mineral. An alteromorph does not always preserve the shape, size, and volume of the mineral that it has replaced.

amoeboid: With strongly curved and lobate interlocking grain boundaries; like an amoeba.

anhedral: Describes irregular grains showing no crystal-face boundaries.

cleavage domain: Layer or lens with a relatively high content of elongate grains (such as micas or amphiboles) and low content of equidimensional grains (such as quartz, feldspar, or carbonate). Together with microlithons they make up a spaced foliation. Micas in cleavage domains commonly have a preferred orientation parallel to or at a small angle to the domain.

euhedral: Describes a mineral with crystal faces.

foliation: Planar microstructural element that occurs penetratively on a mesoscopic scale in a rock. Primary foliation includes bedding and igneous layering; secondary foliations are formed by deformation-induced processes.

groundmass: Aggregate that is distinctly finer-grained than the phenocrysts in an igneous rock.

interlobate: With irregular lobate grain boundaries.

interstitial: Describes a mineral occupying angular cavities or interspace fillings between other minerals.

limonite: a very fine-grained mass of amorphous hydrated iron oxides, quartz, and manganese oxides. Among the iron oxides hematite, goethite and lepidocrocite may occur.

matrix: Aggregate that is distinctly finer-grained than the crystals, clasts, and lithic fragments in a metamorphic and volcanoclastic rock. The usage is similar to that of “groundmass” in an igneous rock.

microlithon: Layer or lens with a relatively small degree of preferred orientation compared to cleavage domains. A crenulated older foliation may be present in microlithons. Together with cleavage domains, microlithons make up a spaced foliation.

phenocryst: Crystal (commonly euhedral) that is distinctly larger than the other minerals around it.

pleochroism: A property of certain crystals of absorbing light to an extent that depends on the orientation of the vector of the light with respect to the optic axes of the crystal.

poikilitic: Describes a crystal with numerous, randomly oriented inclusions of other minerals.

pseudomorph: Mineral or group of minerals developed by partial to complete alteration or weathering of a primary mineral. The pseudomorph preserves the shape, size, and volume of the mineral that it has replaced.

relic (residual structure): Structure remaining after a deformation or metamorphic event, such as a porphyroclast in a mylonite, a phenocryst in a metamorphosed volcanic rock, or a partially replaced porphyroblast in a retrograde metamorphic rock. “Relict” is sometimes used as a synonym for “residual.”

strain shadow: Region adjacent to a clast or porphyroblast that is protected from deformation, such that it may preserve earlier microstructures that have been obliterated from the rest of the matrix.

undulose (undulatory) **extinction**: Wavy, nonuniform extinction in a single grain, owing to slight bending of the crystal. Patchy, irregular undulose extinction can be due to submicroscopic fractures, kinks, and dislocation angles.

X, Y, Z: symbols used to describe the optical indicatrix of the crystals.

Appendix 2. Bibliography

- Deer WA, Howie RA, Zussmann J (2013) An introduction to the rock-forming minerals. 3rd The Mineralogical Society, London
- Delvigne JE (1998) Atlas of micromorphology of mineral alteration and weathering. The Canadian mineralogist, special publication 3. Mineralogical Association of Canada, Ottawa
- Gifkins C, Herrmann W, Large R (2005) Altered volcanic rocks, A guide to description and interpretation, Centre for Ore Deposits Research University of Tasmania, Australia
- Gillespie MR, Barnes RP, Milodowski A (2011) British Geological Survey scheme for classifying discontinuities and fillings. In: British Geological Survey research report RR/10/05. <https://www.bgs.ac.uk/technologies/bgs-rock-classification-scheme/#download> Accessed July 2023
- Gillespie MR, Styles MT (1999) Classification of igneous rocks. British Geological Survey research report RR 99/06 (2nd edn), vol 1. <https://www.bgs.ac.uk/technologies/bgs-rock-classification-scheme/#download> Accessed July 2023
- Hallsworth CR, Knox RWO'B (1999) Classification of sediments and sedimentary rocks. British Geological Survey research report (2nd edn), vol 3. <https://www.bgs.ac.uk/technologies/bgs-rock-classification-scheme/#download> Accessed July 2023
- Parmenter A., Waffle L., and DesRoches (2020) Bedrock Geology of the Revell Batholith and Surrounding Greenstone Belts. Nuclear Waste Management Organization Unpublished Report.
- Passchier CW, Trouw RAJ (2005) Microtectonics (2nd edn). Springer, Heidelberg
- Ramdohr P (1980) The ore minerals and their intergrowths (2nd edn), vol 1/2. Pergamon Press, Oxford
- Robertson S (1999) Classification of metamorphic rocks. British Geological Survey Research Report RR 99/02, vol 2. <https://www.bgs.ac.uk/technologies/bgs-rock-classification-scheme/#download> Accessed July 2023
- Tröger WE (1979) Optical determination of rock-forming minerals, part 1: determinative tables. Schweizerbart Science Publishers, Stuttgart
- Vernon RH (2004) A practical guide to rock microstructure. Cambridge University Press, Cambridge

B) Lithogeochemical Analysis



Report No.: A23-01966
 Report Date: 12-Apr-23
 Date Submitted: 10-Feb-23
 Your Reference: APM-REF-01913-301925

Nuclear Waste Management Organization
 22 St. Clair Ave. East
 3rd Floor
 Toronto ON M4T 2S3
 Canada

ATTN: Stefan Markovic

CERTIFICATE OF ANALYSIS

51 Core samples were submitted for analysis.

The following analytical package(s) were requested:		Testing Date:
4B-INAA(Lithores)	QOP INAAGEO (INAA)	
4F-C, S	Infrared	
4LITHORES + 4B1 (11+)	QOP WRA/ QOP WRA 4B2/QOP Total (/Major/Trace Elements Fusion ICPOES/ICPMS/Total Digestion ICPOES)	2023-04-03 14:52:50

REPORT A23-01966

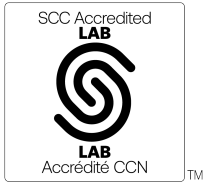
This report may be reproduced without our consent. If only selected portions of the report are reproduced, permission must be obtained. If no instructions were given at time of sample submittal regarding excess material, it will be discarded within 90 days of this report. Our liability is limited solely to the analytical cost of these analyses. Test results are representative only of material submitted for analysis.

Notes:

Values which exceed the upper limit should be assayed for most accurate values.

We recommend using option 4B1 for accurate levels of the base metals Cu, Pb, Zn, Ni and Ag. Option 4B-INAA for As, Sb, high W >100ppm, Cr >1000ppm and Sn >50ppm by Code 5D. Values for these elements provided by Fusion ICP/MS, are order of magnitude only and are provided for general information. Mineralized samples should have the Quant option selected or request assays for values which exceed the range of option 4B1. Total includes all elements in % oxide to the left of total. Zr is now being reported from FUS-ICP instead of FUS-MS.

Footnote: INAA data may be suppressed due to high concentrations of some analytes.



LabID: 266

ACTIVATION LABORATORIES LTD.
41 Bittern Street, Ancaster, Ontario, Canada, L9G 4V5
TELEPHONE +905 648-9611 or +1.888.228.5227 FAX +1.905.648.9613
E-MAIL Ancaster@actlabs.com ACTLABS GROUP WEBSITE www.actlabs.com

CERTIFIED BY:

Mark Vandergeest
Quality Control Coordinator

Results

Activation Laboratories Ltd.

Report: A23-01966

Analyte Symbol	Au	As	Br	Cr	Ir	Sc	Se	Sb	Mass	C-Total	Total S	SiO2	Al2O3	Fe2O3(T)	MnO	MgO	CaO	Na2O	K2O	TiO2	P2O5	LOI	Total
Unit Symbol	ppb	ppm	ppm	ppm	ppb	ppm	ppm	ppm	g	%	%	%	%	%	%	%	%	%	%	%	%	%	%
Lower Limit	2	0.5	0.5	5	5	0.1	3	0.2		0.01	0.01	0.01	0.01	0.01	0.005	0.01	0.01	0.01	0.01	0.001	0.01		0.01
Method Code	INAA	INAA	INAA	INAA	INAA	INAA	INAA	INAA	INAA	CS	CS	FUS-ICP	FUS-ICP	FUS-ICP	FUS-ICP	FUS-ICP	FUS-ICP	FUS-ICP	FUS-ICP	FUS-ICP	FUS-ICP	GRAV	FUS-ICP
IG_BH04_MG051	< 2	< 0.5	10.3	16	< 5	2.3	< 3	< 0.2	27.7	0.04	< 0.01	73.37	14.57	2.26	0.038	0.44	2.20	4.19	2.60	0.171	0.05	0.45	100.3
IG_BH04_MG052	< 2	< 0.5	< 0.5	45	< 5	5.2	< 3	< 0.2	30.3	0.28	0.05	69.84	14.14	3.05	0.044	1.61	3.14	4.21	1.89	0.294	0.10	1.68	99.99
IG_BH04_MG053	< 2	< 0.5	< 0.5	334	< 5	18.9	< 3	< 0.2	24.4	0.90	< 0.01	48.28	15.03	8.99	0.139	8.48	6.96	2.44	3.95	0.850	0.21	4.89	100.2
IG_BH04_MG054	< 2	< 0.5	< 0.5	162	< 5	15.1	< 3	< 0.2	26.2	0.77	0.05	52.43	14.05	8.25	0.120	7.12	7.77	3.37	2.64	0.936	0.32	3.95	101.0
IG_BH04_MG055	< 2	< 0.5	< 0.5	130	< 5	14.4	59	< 0.2	23.5	0.69	0.02	51.92	14.30	8.50	0.114	7.75	6.65	2.36	1.76	0.872	0.32	5.83	100.4
IG_BH04_MG056	< 2	< 0.5	7.1	11	< 5	2.4	< 3	< 0.2	28.2	< 0.01	< 0.01	71.94	15.09	2.63	0.030	0.63	2.82	4.34	1.81	0.282	0.08	0.42	100.1
IG_BH04_MG057	< 2	< 0.5	< 0.5	21	< 5	2.3	< 3	< 0.2	28.4	0.02	< 0.01	72.52	14.86	2.87	0.035	0.64	2.75	4.29	1.82	0.279	0.08	0.40	100.6
IG_BH04_MG058	< 2	< 0.5	5.2	21	< 5	3.6	< 3	< 0.2	29.3	< 0.01	< 0.01	70.63	14.76	3.36	0.039	0.84	3.18	3.99	1.88	0.419	0.12	0.38	99.59
IG_BH04_MG059	< 2	< 0.5	< 0.5	23	< 5	2.6	< 3	< 0.2	27.0	< 0.01	< 0.01	70.97	15.10	3.16	0.030	0.85	3.23	4.52	1.69	0.369	0.10	0.33	100.3
IG_BH04_MG060	< 2	< 0.5	< 0.5	16	< 5	2.6	< 3	< 0.2	26.2	< 0.01	< 0.01	70.02	14.78	3.23	0.030	0.80	3.11	4.37	1.71	0.347	0.11	0.31	98.81
IG_BH04_MG061	< 2	< 0.5	11.5	17	< 5	2.6	< 3	0.3	27.1	< 0.01	< 0.01	71.92	14.44	3.09	0.041	0.63	2.79	4.42	1.93	0.266	0.07	0.26	99.86
IG_BH04_MG062	< 2	< 0.5	9.9	16	< 5	4.1	< 3	< 0.2	29.3	< 0.01	< 0.01	69.35	15.12	3.37	0.040	1.01	3.46	4.41	1.53	0.362	0.08	0.52	99.26
IG_BH04_MG063	< 2	< 0.5	15.3	14	< 5	3.6	< 3	< 0.2	27.7	0.01	< 0.01	70.11	14.54	3.05	0.040	0.79	2.75	4.32	2.57	0.297	0.07	0.55	99.06
IG_BH04_MG064	< 2	< 0.5	7.2	12	< 5	3.5	< 3	< 0.2	29.2	< 0.01	< 0.01	71.18	14.98	3.29	0.040	0.88	3.08	4.49	1.85	0.327	0.08	0.19	100.4
IG_BH04_MG065	< 2	< 0.5	< 0.5	642	< 5	26.7	< 3	0.3	30.2	0.10	0.24	50.03	13.28	9.99	0.169	9.75	10.86	2.57	1.14	0.726	0.22	1.98	100.7
IG_BH04_MG066	7	< 0.5	< 0.5	754	< 5	18.1	< 3	0.5	25.8	1.35	< 0.01	47.63	11.89	8.08	0.134	11.37	8.62	2.06	1.91	0.495	0.16	7.97	100.3
IG_BH04_MG067	< 2	< 0.5	< 0.5	1100	< 5	21.4	< 3	< 0.2	22.4	1.06	< 0.01	46.41	11.87	10.12	0.124	14.08	5.30	0.37	2.70	0.670	0.17	8.71	100.5
IG_BH04_MG068	< 2	< 0.5	15.3	18	< 5	3.3	< 3	< 0.2	30.5	0.01	0.03	70.29	14.50	2.64	0.035	0.79	2.53	4.26	2.55	0.273	0.08	0.65	98.60
IG_BH04_MG069	< 2	1.1	< 0.5	17	< 5	3.4	< 3	< 0.2	24.1	0.39	< 0.01	69.99	13.85	2.86	0.037	0.78	2.69	3.97	2.32	0.266	0.07	2.21	99.04
IG_BH04_MG070	< 2	< 0.5	3.4	37	< 5	16.5	< 3	< 0.2	29.3	1.23	< 0.01	44.49	16.34	9.76	0.133	4.60	7.74	3.72	3.07	1.108	0.43	7.00	98.37
IG_BH04_MG071	< 2	< 0.5	1.8	34	< 5	8.8	< 3	< 0.2	25.2	0.57	0.32	61.90	14.04	5.79	0.085	2.55	4.90	4.55	1.05	0.559	0.23	3.30	98.95
IG_BH04_MG072	< 2	< 0.5	< 0.5	49	< 5	18.1	< 3	< 0.2	25.2	0.93	0.22	49.06	14.74	10.17	0.180	5.73	7.56	3.89	0.80	0.995	0.50	6.04	99.66
IG_BH04_MG073	< 2	< 0.5	< 0.5	18	< 5	3.7	< 3	< 0.2	28.7	0.01	< 0.01	70.65	14.79	2.82	0.036	0.85	2.91	4.15	2.28	0.300	0.07	0.60	99.46
IG_BH04_MG074	< 2	5.0	1.7	95	< 5	16.4	< 3	< 0.2	24.6	0.81	< 0.01	51.39	14.60	8.91	0.131	5.11	6.17	4.42	0.83	0.919	0.44	5.46	98.38
IG_BH04_MG075	< 2	< 0.5	8.9	23	< 5	4.2	< 3	< 0.2	27.9	< 0.01	< 0.01	70.49	14.98	3.45	0.042	1.01	2.92	4.53	2.16	0.329	0.08	0.80	100.8
IG_BH04_MG076	4	< 0.5	< 0.5	252	< 5	14.1	< 3	< 0.2	29.1	0.49	0.17	50.25	16.18	7.51	0.120	7.28	7.60	3.82	3.13	0.736	0.51	2.72	99.85
IG_BH04_MG077	< 2	0.6	< 0.5	320	< 5	18.4	< 3	< 0.2	27.3	0.86	< 0.01	41.90	16.56	9.58	0.150	8.73	8.95	2.34	4.83	0.862	0.60	4.60	99.08
IG_BH04_MG078	< 2	< 0.5	1.5	161	< 5	11.5	< 3	0.3	25.5	0.10	< 0.01	52.20	20.89	5.80	0.077	3.91	6.09	5.36	2.18	0.579	0.12	1.82	99.04
IG_BH04_MG079	< 2	2.1	11.0	21	< 5	3.5	< 3	< 0.2	27.8	0.02	< 0.01	69.78	14.84	3.29	0.040	0.90	3.20	4.41	1.67	0.320	0.07	0.78	99.31
IG_BH04_MG080	< 2	1.2	6.4	22	< 5	3.4	< 3	< 0.2	28.0	< 0.01	< 0.01	70.60	15.10	3.09	0.041	0.90	2.87	4.44	1.87	0.326	0.08	0.70	100.0
IG_BH04_MG081	< 2	1.2	3.3	33	< 5	2.3	< 3	< 0.2	27.5	< 0.01	< 0.01	72.19	14.48	2.57	0.035	0.58	2.35	4.25	2.28	0.242	0.07	0.36	99.41
IG_BH04_MG082	< 2	2.4	< 0.5	22	< 5	2.5	< 3	< 0.2	27.4	< 0.01	< 0.01	72.22	15.13	2.68	0.035	0.60	2.53	4.44	2.39	0.268	0.08	0.24	100.6
IG_BH04_MG083	< 2	< 0.5	< 0.5	21	< 5	2.1	< 3	< 0.2	26.9	0.38	0.06	72.73	14.06	2.43	0.031	0.53	2.31	4.39	2.08	0.234	0.06	1.92	100.8
IG_BH04_MG084	< 2	1.1	8.3	17	< 5	2.3	< 3	< 0.2	28.2	< 0.01	< 0.01	71.03	15.31	3.09	0.030	0.71	2.90	4.37	1.86	0.320	0.09	0.43	100.1
IG_BH04_MG085	< 2	< 0.5	7.8	16	< 5	2.8	< 3	< 0.2	29.9	< 0.01	< 0.01	71.14	14.69	2.89	0.047	0.73	2.93	4.25	2.03	0.280	0.10	0.43	99.52
IG_BH01_LG046	< 2	< 0.5	< 0.5	23	< 5	2.1	< 3	< 0.2	28.6	0.02	< 0.01	76.78	12.24	3.14	0.038	0.67	2.24	3.34	1.79	0.269	0.07	0.28	100.9
IG_BH02_LG027	< 2	< 0.5	1.7	22	< 5	1.7	< 3	< 0.2	25.8	0.03	< 0.01	74.30	13.24	1.95	0.016	0.75	0.43	4.52	2.43	0.136	0.05	1.19	99.01
IG_BH02_LG028	< 2	< 0.5	< 0.5	28	< 5	3.8	< 3	< 0.2	28.9	0.03	< 0.01	70.88	14.28	3.63	0.055	0.98	2.96	4.13	1.69	0.405	0.12	0.77	99.90
IG_BH02_LG029	< 2	< 0.5	< 0.5	28	< 5	3.7	< 3	< 0.2	27.5	0.09	< 0.01	70.66	14.15	3.03	0.037	0.92	2.87	4.56	1.53	0.287	0.08	0.75	98.87
IG_BH02_LG030	< 2	< 0.5	14.4	< 5	< 5	2.9	< 3	< 0.2	28.7	2.10	0.01	50.90	17.41	1.57	0.063	0.40	10.19	7.22	1.87	0.243	0.07	8.33	98.28
IG_BH03_LG023	< 2	2.8	3.6	652	< 5	27.1	< 3	< 0.2	24.4	1.18	0.14	39.80	11.57	11.05	0.204	13.37	11.37	0.13	1.57	0.914	0.46	8.44	98.89
IG_BH04_MG086	< 2	1.6	< 0.5	586	< 5	19.6	< 3	< 0.2	24.0	0.79	< 0.01	53.02	13.66	8.05	0.042	7.25	4.08	1.62	3.55	0.771	0.21	6.36	98.61
IG_BH04_MG087	< 2	2.2	< 0.5	14	< 5	2.5	< 3	< 0.2	26.9	0.64	< 0.01	60.24	19.25	1.67	0.028	0.82	3.35	8.31	1.90	0.145	0.08	2.94	98.75
IG_BH04_MG088	< 2	< 0.5	< 0.5	28	< 5	2.3	< 3	< 0.2	27.3	0.29	< 0.01	73.04	13.88	2.23	0.028	0.53	2.33	4.45	1.96	0.189	0.06	1.61	100.3
IG_BH04_MG089	< 2	< 0.5	< 0.5	18	< 5	2.6	< 3	< 0.2	27.9	0.04	< 0.01	74.06	13.93	2.29	0.040	0.54	2.18	3.97	2.66	0.183	0.05	0.61	100.5
IG_BH02_LG031	< 2	< 0.5	< 0.5	25	< 5	1.9	< 3	< 0.2	26.6	0.01	< 0.01	74.88	13.81	2.01	0.032	0.35	1.81	4.25	3.02	0.157	0.05	0.23	100.6
IG_BH02_LG032	< 2	< 0.5	6.5	12	< 5	2.0	< 3	0.2	26.6	0.04	< 0.01	75.22	14.05	1.88	0.030	0.36	1.87	4.34	2.64	0.156	0.04	0.39	101.0
IG_BH02_LG033	< 2	< 0.5	10.2	21	< 5	2.8	< 3	< 0.2	26.9	0.35	< 0.01	70.96	15.25	1.81	0.020	0.48	1.89	6.67	1.10	0.216	0.06	1.62	100.1
IG_BH02_LG034	< 2	< 0.5	12.3	22	< 5	2.1	< 3																

Results

Activation Laboratories Ltd.

Report: A23-01966

Analyte Symbol	Au	As	Br	Cr	Ir	Sc	Se	Sb	Mass	C-Total	Total S	SiO2	Al2O3	Fe2O3(T)	MnO	MgO	CaO	Na2O	K2O	TiO2	P2O5	LOI	Total
Unit Symbol	ppb	ppm	ppm	ppm	ppb	ppm	ppm	ppm	g	%	%	%	%	%	%	%	%	%	%	%	%	%	%
Lower Limit	2	0.5	0.5	5	5	0.1	3	0.2		0.01	0.01	0.01	0.01	0.01	0.005	0.01	0.01	0.01	0.01	0.001	0.01		0.01
Method Code	INAA	INAA	INAA	INAA	INAA	INAA	INAA	INAA	INAA	CS	CS	FUS-ICP	FUS-ICP	FUS-ICP	FUS-ICP	FUS-ICP	FUS-ICP	FUS-ICP	FUS-ICP	FUS-ICP	FUS-ICP	GRAV	FUS-ICP
IG_BH01_LG047	< 2	< 0.5	4.8	29	< 5	3.1	< 3	< 0.2	26.4	0.12	< 0.01	68.46	15.47	3.67	0.040	0.93	1.59	4.52	2.53	0.297	0.08	1.39	98.97
IG_BH01_LG048	< 2	< 0.5	< 0.5	17	< 5	4.1	< 3	< 0.2	28.2	0.10	< 0.01	68.96	15.41	3.38	0.029	0.88	1.82	3.79	2.82	0.343	0.09	1.40	98.94

Results

Activation Laboratories Ltd.

Report: A23-01966

Analyte Symbol	Sc	Be	V	Cr	Co	Ni	Cu	Zn	Cd	S	Ga	Ge	As	Rb	Sr	Y	Zr	Nb	Mo	Ag	In	Sn	Sb
Unit Symbol	ppm	ppm	ppm	ppm	ppm	ppm	ppm	ppm	ppm	%	ppm	ppm	ppm	ppm	ppm	ppm	ppm	ppm	ppm	ppm	ppm	ppm	ppm
Lower Limit	1	1	5	20	1	1	1	1	0.5	0.001	1	0.5	5	1	2	1	1	0.2	2	0.3	0.1	1	0.2
Method Code	FUS-ICP	FUS-ICP	FUS-ICP	FUS-MS	FUS-MS	TD-ICP	TD-ICP	TD-ICP	TD-ICP	TD-ICP	FUS-MS	FUS-MS	FUS-MS	FUS-MS	FUS-ICP	FUS-ICP	FUS-MS	FUS-MS	TD-ICP	FUS-MS	FUS-MS	FUS-MS	
IG_BH04_MG051	2	1	15	20	3	4	8	43	< 0.5	0.008	22	1.2	< 5	95	200	6	78	4.4	< 2	< 0.3	< 0.1	2	< 0.2
IG_BH04_MG052	5	1	40	50	8	35	34	49	< 0.5	0.053	20	1.0	< 5	63	396	8	91	3.8	< 2	0.4	< 0.1	1	< 0.2
IG_BH04_MG053	20	1	179	410	39	151	5	102	< 0.5	0.005	23	1.0	< 5	121	592	13	114	3.8	< 2	0.4	< 0.1	1	< 0.2
IG_BH04_MG054	17	2	151	210	33	145	35	86	< 0.5	0.060	21	1.3	< 5	75	903	19	175	4.6	< 2	0.3	< 0.1	1	< 0.2
IG_BH04_MG055	15	2	141	160	36	122	90	85	< 0.5	0.021	22	1.5	< 5	93	940	19	159	5.1	< 2	0.9	< 0.1	1	0.8
IG_BH04_MG056	2	< 1	23	< 20	4	3	10	64	< 0.5	0.007	22	0.8	< 5	59	317	3	147	3.3	2	0.4	< 0.1	1	< 0.2
IG_BH04_MG057	3	1	21	20	4	3	13	68	< 0.5	0.003	22	0.9	< 5	57	294	5	156	4.2	< 2	0.4	< 0.1	1	< 0.2
IG_BH04_MG058	4	1	31	20	6	5	17	72	< 0.5	0.007	22	0.9	< 5	58	263	6	154	5.3	< 2	0.4	< 0.1	1	< 0.2
IG_BH04_MG059	3	< 1	30	< 20	5	3	18	75	< 0.5	0.004	22	0.7	< 5	73	359	5	186	3.4	< 2	0.5	< 0.1	1	< 0.2
IG_BH04_MG060	2	< 1	29	< 20	5	3	20	67	< 0.5	0.005	22	0.8	< 5	65	346	4	173	3.8	< 2	0.4	< 0.1	1	< 0.2
IG_BH04_MG061	3	1	26	< 20	4	5	15	57	< 0.5	0.010	19	0.8	< 5	59	270	5	123	4.1	< 2	0.3	< 0.1	1	< 0.2
IG_BH04_MG062	4	< 1	37	< 20	7	6	9	66	< 0.5	0.007	21	0.7	< 5	52	374	4	139	2.6	3	< 0.3	< 0.1	1	< 0.2
IG_BH04_MG063	4	< 1	30	< 20	5	4	8	49	< 0.5	0.003	20	0.8	< 5	72	317	4	111	2.3	< 2	< 0.3	< 0.1	1	< 0.2
IG_BH04_MG064	4	1	32	< 20	6	5	10	60	< 0.5	0.003	21	0.9	< 5	58	324	5	127	2.7	< 2	< 0.3	< 0.1	1	< 0.2
IG_BH04_MG065	31	1	224	830	42	112	87	69	< 0.5	0.226	17	1.5	< 5	33	741	17	94	3.0	< 2	< 0.3	< 0.1	1	0.2
IG_BH04_MG066	20	< 1	151	920	38	241	144	66	< 0.5	0.019	14	0.9	< 5	51	325	11	69	3.6	< 2	< 0.3	< 0.1	< 1	< 0.2
IG_BH04_MG067	23	1	185	1290	52	344	35	89	< 0.5	0.010	17	1.1	< 5	84	71	11	103	3.9	< 2	< 0.3	< 0.1	1	< 0.2
IG_BH04_MG068	4	< 1	29	< 20	6	5	13	45	< 0.5	0.036	20	0.7	< 5	65	283	4	102	2.2	< 2	< 0.3	< 0.1	< 1	< 0.2
IG_BH04_MG069	4	< 1	29	< 20	5	4	11	56	< 0.5	0.015	19	0.8	< 5	55	234	3	107	2.5	< 2	0.3	< 0.1	< 1	< 0.2
IG_BH04_MG070	18	2	152	30	25	21	84	122	< 0.5	0.014	30	1.2	< 5	88	407	25	181	10.7	< 2	< 0.3	0.1	2	< 0.2
IG_BH04_MG071	9	2	74	30	21	15	27	64	< 0.5	0.306	20	1.0	< 5	28	527	12	125	4.8	< 2	< 0.3	< 0.1	1	< 0.2
IG_BH04_MG072	20	2	174	60	31	32	73	114	< 0.5	0.198	20	1.0	< 5	32	721	25	165	8.2	< 2	0.3	0.1	2	< 0.2
IG_BH04_MG073	4	< 1	31	< 20	6	5	9	62	< 0.5	0.006	21	0.8	< 5	58	306	5	116	2.7	< 2	< 0.3	< 0.1	1	< 0.2
IG_BH04_MG074	18	1	143	80	28	35	8	140	< 0.5	0.011	24	0.8	< 5	29	300	17	159	7.3	< 2	< 0.3	< 0.1	1	< 0.2
IG_BH04_MG075	5	< 1	36	< 20	7	5	9	46	< 0.5	0.005	22	0.8	< 5	69	319	5	123	3.1	< 2	< 0.3	< 0.1	1	< 0.2
IG_BH04_MG076	16	2	145	210	29	96	32	94	< 0.5	0.180	20	0.9	< 5	102	1318	22	229	8.2	< 2	< 0.3	< 0.1	1	< 0.2
IG_BH04_MG077	20	1	175	270	33	112	2	129	< 0.5	0.008	29	1.2	< 5	143	1300	23	246	6.7	8	0.3	0.1	1	< 0.2
IG_BH04_MG078	12	2	95	150	18	62	1	75	< 0.5	0.004	28	1.3	< 5	62	1208	12	245	5.0	< 2	< 0.3	< 0.1	1	< 0.2
IG_BH04_MG079	4	< 1	32	< 20	6	5	8	60	< 0.5	0.009	21	0.8	< 5	42	329	4	130	2.8	2	< 0.3	< 0.1	1	< 0.2
IG_BH04_MG080	4	< 1	32	< 20	6	5	9	68	< 0.5	0.008	21	0.8	< 5	59	313	5	120	2.8	12	< 0.3	< 0.1	1	< 0.2
IG_BH04_MG081	2	< 1	19	< 20	4	3	8	59	< 0.5	0.002	21	0.9	< 5	66	264	4	125	3.7	< 2	0.4	< 0.1	1	< 0.2
IG_BH04_MG082	3	< 1	21	< 20	4	4	11	63	< 0.5	0.003	22	0.8	< 5	66	288	4	148	4.1	< 2	0.4	< 0.1	1	< 0.2
IG_BH04_MG083	2	< 1	17	30	3	2	17	51	< 0.5	0.068	21	0.7	< 5	60	207	4	135	3.7	< 2	0.4	< 0.1	1	< 0.2
IG_BH04_MG084	2	< 1	26	< 20	5	4	18	62	< 0.5	0.005	22	0.7	< 5	60	331	4	171	3.8	< 2	0.5	< 0.1	1	< 0.2
IG_BH04_MG085	3	< 1	24	< 20	4	3	14	70	< 0.5	0.004	22	0.9	< 5	65	319	3	170	4.1	< 2	0.4	< 0.1	1	< 0.2
IG_BH01_LG046	2	< 1	19	< 20	5	3	9	56	< 0.5	0.004	17	0.9	< 5	58	221	3	153	3.7	< 2	0.3	< 0.1	1	< 0.2
IG_BH02_LG027	2	1	15	< 20	2	5	39	62	< 0.5	0.005	20	1.3	< 5	60	89	4	83	4.0	2	0.4	< 0.1	1	< 0.2
IG_BH02_LG028	4	1	31	30	7	7	9	90	< 0.5	0.002	21	0.9	< 5	53	265	6	160	6.4	< 2	0.4	< 0.1	1	< 0.2
IG_BH02_LG029	4	1	33	20	6	6	16	57	< 0.5	0.003	21	0.9	< 5	67	280	5	129	4.3	< 2	< 0.3	< 0.1	1	< 0.2
IG_BH02_LG030	3	1	33	< 20	1	3	11	20	< 0.5	0.004	23	1.0	< 5	47	509	10	122	7.9	< 2	0.7	< 0.1	1	< 0.2
IG_BH03_LG023	28	2	219	590	51	291	18	176	< 0.5	0.119	18	1.3	< 5	64	574	17	138	8.2	< 2	< 0.3	< 0.1	1	< 0.2
IG_BH04_MG086	21	1	148	560	45	236	20	174	< 0.5	0.004	25	1.6	< 5	135	118	14	112	4.8	< 2	< 0.3	< 0.1	1	< 0.2
IG_BH04_MG087	3	1	19	< 20	3	15	4	26	< 0.5	0.001	18	1.0	< 5	47	625	5	113	2.4	< 2	< 0.3	< 0.1	< 1	< 0.2
IG_BH04_MG088	2	1	19	< 20	4	4	16	37	< 0.5	0.002	21	1.0	< 5	61	245	5	109	5.0	< 2	< 0.3	< 0.1	1	< 0.2
IG_BH04_MG089	3	1	16	20	4	4	7	47	< 0.5	0.003	21	1.1	< 5	79	197	6	103	5.2	< 2	< 0.3	< 0.1	1	< 0.2
IG_BH02_LG031	2	1	12	< 20	3	2	8	46	< 0.5	0.002	21	0.9	< 5	96	192	4	94	4.7	< 2	< 0.3	< 0.1	1	< 0.2
IG_BH02_LG032	2	1	12	< 20	3	2	7	43	< 0.5	0.003	21	1.0	< 5	78	195	4	92	4.0	< 2	< 0.3	< 0.1	1	< 0.2
IG_BH02_LG033	3	1	19	< 20	3	5	13	30	< 0.5	0.003	19	1.0	< 5	32	358	5	125	7.9	< 2	< 0.3	< 0.1	1	< 0.2
IG_BH02_LG034	2	1	13	< 20	2	2	12	27	< 0.5	0.021	21	0.9	< 5	81	190	5	94	4.3	< 2	0.4	< 0.1	1	< 0.2
IG_BH01_LG047	3	< 1	29	< 20	5	5	66	52	< 0.5	0.002	21	1.0	< 5	70	234	5	121	2.6	< 2	< 0.3	< 0.1	1	< 0.2

Results

Activation Laboratories Ltd.

Report: A23-01966

Analyte Symbol	Sc	Be	V	Cr	Co	Ni	Cu	Zn	Cd	S	Ga	Ge	As	Rb	Sr	Y	Zr	Nb	Mo	Ag	In	Sn	Sb
Unit Symbol	ppm	ppm	ppm	ppm	ppm	ppm	ppm	ppm	ppm	%	ppm	ppm	ppm	ppm	ppm	ppm	ppm	ppm	ppm	ppm	ppm	ppm	ppm
Lower Limit	1	1	5	20	1	1	1	1	0.5	0.001	1	0.5	5	1	2	1	1	0.2	2	0.3	0.1	1	0.2
Method Code	FUS-ICP	FUS-ICP	FUS-ICP	FUS-MS	FUS-MS	TD-ICP	TD-ICP	TD-ICP	TD-ICP	TD-ICP	FUS-MS	FUS-MS	FUS-MS	FUS-MS	FUS-ICP	FUS-ICP	FUS-ICP	FUS-MS	FUS-MS	TD-ICP	FUS-MS	FUS-MS	FUS-MS
IG_BH01_LG048	4	< 1	32	< 20	5	4	13	76	< 0.5	0.004	22	0.8	< 5	73	274	5	131	2.7	< 2	0.4	< 0.1	1	< 0.2

Results

Activation Laboratories Ltd.

Report: A23-01966

Analyte Symbol	Cs	Ba	La	Ce	Pr	Nd	Sm	Eu	Gd	Tb	Dy	Ho	Er	Tm	Yb	Lu	Hf	Ta	W	Tl	Pb	Bi	Th
Unit Symbol	ppm	ppm	ppm	ppm	ppm	ppm	ppm	ppm	ppm	ppm	ppm	ppm	ppm	ppm	ppm	ppm	ppm	ppm	ppm	ppm	ppm	ppm	ppm
Lower Limit	0.1	2	0.05	0.05	0.01	0.05	0.01	0.005	0.01	0.01	0.01	0.01	0.01	0.005	0.01	0.002	0.1	0.01	0.5	0.05	5	0.1	0.05
Method Code	FUS-MS	FUS-ICP	FUS-MS	TD-ICP	FUS-MS	FUS-MS																	
IG_BH04_MG051	1.7	565	13.4	23.8	2.59	9.32	1.96	0.469	1.55	0.21	1.06	0.20	0.52	0.075	0.47	0.069	2.7	0.97	0.9	0.51	11	< 0.1	5.36
IG_BH04_MG052	1.4	804	17.6	34.9	3.86	14.4	2.93	0.783	2.21	0.29	1.50	0.26	0.70	0.098	0.63	0.098	2.7	0.61	0.7	0.40	7	0.1	4.60
IG_BH04_MG053	6.3	1167	34.0	69.1	7.85	30.7	5.39	1.36	3.91	0.48	2.53	0.48	1.25	0.162	1.04	0.168	3.1	0.29	1.9	0.69	7	0.1	4.67
IG_BH04_MG054	2.7	747	51.3	107	12.8	52.0	9.15	2.40	6.64	0.81	4.14	0.74	1.97	0.252	1.46	0.217	4.7	0.48	2.1	0.45	7	< 0.1	7.52
IG_BH04_MG055	6.4	401	59.1	112	12.8	50.0	8.70	2.24	6.36	0.76	3.88	0.71	1.88	0.248	1.47	0.214	4.5	0.40	0.7	0.81	20	0.2	7.95
IG_BH04_MG056	1.6	516	31.0	52.8	5.13	16.8	2.43	0.664	1.41	0.15	0.73	0.12	0.28	0.039	0.26	0.041	3.7	0.44	1.3	0.34	6	< 0.1	5.85
IG_BH04_MG057	1.8	534	26.7	46.8	4.70	15.8	2.70	0.709	1.68	0.21	0.99	0.16	0.39	0.050	0.30	0.047	3.8	0.49	< 0.5	0.30	< 5	< 0.1	5.10
IG_BH04_MG058	1.5	521	25.4	44.0	4.51	15.6	2.73	0.734	2.04	0.23	1.10	0.19	0.49	0.062	0.38	0.057	3.8	0.59	< 0.5	0.31	< 5	< 0.1	5.10
IG_BH04_MG059	2.2	470	33.0	54.7	5.17	17.0	2.41	0.624	1.58	0.17	0.88	0.15	0.42	0.056	0.38	0.059	3.8	0.61	< 0.5	0.41	6	< 0.1	5.58
IG_BH04_MG060	1.6	410	31.3	51.1	4.89	15.5	2.13	0.618	1.53	0.17	0.79	0.14	0.36	0.049	0.33	0.053	4.0	0.46	< 0.5	0.37	5	< 0.1	5.68
IG_BH04_MG061	1.8	503	18.7	33.1	3.37	11.0	1.79	0.483	1.28	0.15	0.78	0.13	0.38	0.050	0.32	0.050	2.7	0.64	< 0.5	0.29	8	< 0.1	4.03
IG_BH04_MG062	1.1	504	19.2	33.2	3.35	11.4	1.74	0.543	1.14	0.14	0.69	0.12	0.32	0.043	0.28	0.046	2.9	0.20	< 0.5	0.33	< 5	< 0.1	2.46
IG_BH04_MG063	0.9	636	16.5	28.9	2.98	10.3	1.63	0.482	1.14	0.13	0.73	0.13	0.33	0.047	0.33	0.050	2.5	0.26	< 0.5	0.38	6	< 0.1	3.21
IG_BH04_MG064	1.2	435	18.1	31.6	3.21	11.1	1.74	0.509	1.25	0.14	0.75	0.14	0.37	0.053	0.35	0.053	2.9	0.29	< 0.5	0.34	6	< 0.1	3.54
IG_BH04_MG065	1.1	407	28.8	60.2	7.27	29.5	5.57	1.46	4.26	0.53	2.88	0.56	1.55	0.211	1.33	0.205	2.2	0.17	< 0.5	0.19	7	< 0.1	3.55
IG_BH04_MG066	3.1	1924	18.8	38.8	4.73	18.9	3.48	0.982	2.75	0.34	1.89	0.38	1.05	0.140	0.89	0.139	1.7	0.18	< 0.5	0.31	< 5	< 0.1	2.58
IG_BH04_MG067	5.6	455	11.1	24.1	2.92	12.0	2.95	0.703	2.61	0.35	1.93	0.36	1.05	0.142	0.84	0.129	2.4	0.21	< 0.5	0.51	< 5	< 0.1	4.03
IG_BH04_MG068	0.7	645	14.7	26.4	2.82	9.79	1.61	0.479	1.26	0.15	0.81	0.14	0.39	0.055	0.35	0.055	2.5	0.30	< 0.5	0.27	7	< 0.1	2.97
IG_BH04_MG069	1.5	552	14.6	25.9	2.71	9.16	1.51	0.419	1.15	0.13	0.68	0.12	0.32	0.044	0.28	0.047	2.5	0.28	< 0.5	0.28	5	0.1	2.74
IG_BH04_MG070	1.4	808	41.5	84.3	10.2	42.4	8.46	2.14	6.87	0.87	4.55	0.86	2.25	0.303	1.90	0.299	4.5	0.87	1.5	0.46	< 5	< 0.1	6.93
IG_BH04_MG071	1.4	480	22.5	46.8	5.57	21.9	4.44	1.17	3.34	0.40	2.05	0.39	1.01	0.142	0.89	0.142	3.1	0.44	0.8	0.14	6	0.1	3.93
IG_BH04_MG072	2.5	180	40.7	89.1	11.3	48.7	9.63	2.56	7.38	0.89	4.76	0.88	2.38	0.322	2.12	0.326	4.1	0.47	0.6	0.17	8	0.2	6.54
IG_BH04_MG073	1.4	653	16.0	28.7	2.97	10.3	1.82	0.537	1.47	0.17	0.96	0.16	0.42	0.054	0.33	0.052	2.7	0.33	< 0.5	0.34	7	< 0.1	2.82
IG_BH04_MG074	0.4	88	37.4	73.4	8.67	35.3	6.50	1.29	4.49	0.57	3.10	0.60	1.82	0.264	1.68	0.260	3.8	0.46	< 0.5	0.19	< 5	0.1	5.95
IG_BH04_MG075	0.7	519	17.9	31.7	3.33	11.2	1.90	0.551	1.53	0.19	0.93	0.19	0.47	0.062	0.38	0.059	3.0	0.36	0.6	0.40	5	< 0.1	3.39
IG_BH04_MG076	8.6	1079	100	192	21.7	82.9	12.7	3.07	7.96	0.85	4.15	0.69	1.73	0.214	1.36	0.212	4.6	0.44	2.1	0.65	12	0.1	12.3
IG_BH04_MG077	7.1	1028	105	206	23.9	90.0	14.2	3.55	9.05	1.00	4.72	0.79	1.94	0.242	1.46	0.229	5.2	0.41	< 0.5	0.97	13	0.3	12.4
IG_BH04_MG078	2.6	712	58.0	111	12.3	45.1	6.97	1.78	4.41	0.50	2.39	0.41	1.03	0.129	0.80	0.127	5.8	0.37	1.8	0.37	10	0.2	8.85
IG_BH04_MG079	0.7	464	19.1	34.1	3.52	12.1	1.95	0.525	1.36	0.15	0.80	0.14	0.38	0.051	0.33	0.051	3.0	0.23	< 0.5	0.22	6	< 0.1	3.56
IG_BH04_MG080	1.0	472	17.9	31.2	3.25	10.8	1.78	0.496	1.25	0.15	0.79	0.14	0.38	0.053	0.34	0.054	2.8	0.32	< 0.5	0.31	< 5	< 0.1	3.29
IG_BH04_MG081	1.1	607	23.9	40.5	4.04	12.9	2.08	0.548	1.37	0.15	0.67	0.12	0.28	0.038	0.23	0.035	2.8	0.47	< 0.5	0.33	6	< 0.1	5.38
IG_BH04_MG082	1.1	715	22.6	38.3	3.81	12.6	1.88	0.564	1.34	0.15	0.69	0.12	0.28	0.037	0.24	0.036	3.4	0.43	< 0.5	0.37	6	< 0.1	4.66
IG_BH04_MG083	1.5	471	21.9	36.2	3.57	11.9	1.69	0.470	1.20	0.12	0.57	0.10	0.26	0.035	0.23	0.034	3.2	0.39	1.1	0.29	5	0.2	4.27
IG_BH04_MG084	1.1	490	29.2	48.3	4.58	14.8	2.04	0.597	1.35	0.13	0.66	0.12	0.29	0.037	0.24	0.037	3.8	0.38	< 0.5	0.32	< 5	< 0.1	5.32
IG_BH04_MG085	1.4	667	27.7	46.3	4.42	14.1	1.86	0.590	1.19	0.13	0.59	0.09	0.25	0.032	0.20	0.033	3.7	0.32	< 0.5	0.35	< 5	< 0.1	4.64
IG_BH01_LG046	1.6	500	24.6	39.6	3.67	11.0	1.31	0.498	0.85	0.09	0.48	0.09	0.24	0.038	0.28	0.046	3.6	0.63	< 0.5	0.33	< 5	< 0.1	5.06
IG_BH02_LG027	1.6	416	9.38	17.2	1.86	6.11	1.31	0.285	1.12	0.14	0.77	0.12	0.32	0.042	0.25	0.038	2.3	0.61	1.0	0.31	< 5	< 0.1	5.12
IG_BH02_LG028	0.9	543	22.5	41.4	4.29	15.0	2.61	0.747	1.98	0.22	1.14	0.19	0.51	0.067	0.41	0.059	3.8	0.59	< 0.5	0.28	7	< 0.1	4.90
IG_BH02_LG029	2.6	541	19.4	34.2	3.49	11.9	2.05	0.539	1.44	0.17	0.86	0.15	0.39	0.054	0.34	0.054	3.4	0.53	0.6	0.34	7	0.1	4.97
IG_BH02_LG030	0.6	580	3.56	7.60	0.98	4.63	1.85	0.799	2.27	0.30	1.61	0.29	0.76	0.100	0.64	0.105	3.5	1.46	1.5	0.20	14	0.1	6.41
IG_BH03_LG023	1.4	190	43.0	94.9	11.5	45.0	8.04	1.76	5.63	0.70	3.67	0.67	1.78	0.242	1.50	0.238	3.1	0.44	1.3	0.31	< 5	< 0.1	5.45
IG_BH04_MG086	5.6	442	55.9	96.8	11.2	43.1	7.27	1.71	5.31	0.61	3.01	0.52	1.31	0.162	0.99	0.160	3.1	0.29	1.4	0.89	< 5	< 0.1	4.54
IG_BH04_MG087	0.5	612	17.3	32.1	3.37	12.3	2.01	0.580	1.49	0.16	0.78	0.13	0.32	0.042	0.27	0.042	3.1	0.20	0.6	0.22	< 5	< 0.1	5.11
IG_BH04_MG088	1.3	566	11.8	23.1	2.39	8.40	1.61	0.422	1.50	0.18	0.96	0.17	0.47	0.062	0.39	0.064	3.2	0.86	1.7	0.29	8	0.2	4.43
IG_BH04_MG089	1.8	500	12.8	24.5	2.48	9.04	1.72	0.431	1.43	0.18	1.00	0.17	0.48	0.065	0.42	0.069	3.0	1.09	0.6	0.42	6	< 0.1	4.70
IG_BH02_LG031	3.3	648	16.5	29.3	3.00	10.5	1.88	0.466	1.43	0.16	0.78	0.12	0.30	0.039	0.25	0.040	2.6	0.62	2.1	0.54	10	< 0.1	5.96
IG_BH02_LG032	1.7	578	20.6	36.5	3.80	13.0	2.23	0.486	1.64	0.17	0.76	0.12	0.31	0.040	0.25	0.038	2.8	0.42	1.2	0.40	8	0.2	7.55
IG_BH02_LG033	0.4	492	4.41	9.99	1.10	4.46	1.17	0.316	1.18	0.16	0.92	0.16	0.41	0.058	0.39	0.063	3.7	1.19	1.0	0.13	< 5	< 0.1	6.68
IG_BH02_LG034	2.7	503	16.8	28.6	2.96	10.4	1.74	0.352	1.33	0.17	0.76	0.13	0.35	0.043	0.28	0.047	2.3	0.98	1.0	0.36	< 5	< 0.1	5.56
IG_BH01_LG047	1.3	634	14.4	24.4	2.60	8.74	1.48	0.390	1.15	0.14	0.73	0.14	0.37	0.054	0.37	0.059	2.8	0.20	1.3	0.38	10	0.1	3.66

Results

Activation Laboratories Ltd.

Report: A23-01966

Analyte Symbol	Cs	Ba	La	Ce	Pr	Nd	Sm	Eu	Gd	Tb	Dy	Ho	Er	Tm	Yb	Lu	Hf	Ta	W	Tl	Pb	Bi	Th
Unit Symbol	ppm	ppm	ppm	ppm	ppm	ppm	ppm	ppm	ppm	ppm	ppm	ppm	ppm	ppm	ppm	ppm	ppm	ppm	ppm	ppm	ppm	ppm	ppm
Lower Limit	0.1	2	0.05	0.05	0.01	0.05	0.01	0.005	0.01	0.01	0.01	0.01	0.01	0.005	0.01	0.002	0.1	0.01	0.5	0.05	5	0.1	0.05
Method Code	FUS-MS	FUS-ICP	FUS-MS	TD-ICP	FUS-MS	FUS-MS																	
IG_BH01_LG048	2.1	659	20.0	29.4	3.45	11.9	1.76	0.492	1.31	0.15	0.78	0.14	0.38	0.050	0.32	0.051	3.1	0.34	0.9	0.39	9	0.1	3.48

Analyte Symbol	U
Unit Symbol	ppm
Lower Limit	0.01
Method Code	FUS-MS
IG_BH04_MG051	3.95
IG_BH04_MG052	14.9
IG_BH04_MG053	1.78
IG_BH04_MG054	1.93
IG_BH04_MG055	24.8
IG_BH04_MG056	1.26
IG_BH04_MG057	1.29
IG_BH04_MG058	1.30
IG_BH04_MG059	1.45
IG_BH04_MG060	1.89
IG_BH04_MG061	1.52
IG_BH04_MG062	0.60
IG_BH04_MG063	1.01
IG_BH04_MG064	0.89
IG_BH04_MG065	0.90
IG_BH04_MG066	0.64
IG_BH04_MG067	0.90
IG_BH04_MG068	0.71
IG_BH04_MG069	0.68
IG_BH04_MG070	2.56
IG_BH04_MG071	1.22
IG_BH04_MG072	1.96
IG_BH04_MG073	0.62
IG_BH04_MG074	1.66
IG_BH04_MG075	1.05
IG_BH04_MG076	2.74
IG_BH04_MG077	2.80
IG_BH04_MG078	1.69
IG_BH04_MG079	0.78
IG_BH04_MG080	0.83
IG_BH04_MG081	0.97
IG_BH04_MG082	0.96
IG_BH04_MG083	1.16
IG_BH04_MG084	1.15
IG_BH04_MG085	0.63
IG_BH01_LG046	1.65
IG_BH02_LG027	1.45
IG_BH02_LG028	1.14
IG_BH02_LG029	1.55
IG_BH02_LG030	1.73
IG_BH03_LG023	1.08
IG_BH04_MG086	3.53
IG_BH04_MG087	1.06
IG_BH04_MG088	1.62
IG_BH04_MG089	1.11
IG_BH02_LG031	1.41
IG_BH02_LG032	1.51
IG_BH02_LG033	1.62
IG_BH02_LG034	2.41
IG_BH01_LG047	0.81

Analyte Symbol	U
Unit Symbol	ppm
Lower Limit	0.01
Method Code	FUS-MS
IG_BH01_LG048	0.90

Analyte Symbol	Au	As	Br	Cr	Ir	Sc	Se	Sb	Mass	C-Total	Total S	SiO2	Al2O3	Fe2O3(T)	MnO	MgO	CaO	Na2O	K2O	TiO2	P2O5	LOI	Total
Unit Symbol	ppb	ppm	ppm	ppm	ppb	ppm	ppm	ppm	g	%	%	%	%	%	%	%	%	%	%	%	%	%	%
Lower Limit	2	0.5	0.5	5	5	0.1	3	0.2		0.01	0.01	0.01	0.01	0.01	0.005	0.01	0.01	0.01	0.01	0.001	0.01		0.01
Method Code	INAA	CS	CS	FUS-ICP	FUS-ICP	FUS-ICP	FUS-ICP	FUS-ICP	FUS-ICP	FUS-ICP	FUS-ICP	FUS-ICP	FUS-ICP	GRAV	FUS-ICP								
NIST 694 Meas												10.89	1.91	0.76	0.013	0.39	42.82	0.86	0.54	0.116	30.24		
NIST 694 Cert												11.2	1.80	0.790	0.0116	0.330	43.6	0.860	0.510	0.110	30.2		
GBW 07113 Meas												69.82	12.66	3.22	0.139	0.15	0.58	2.46	5.37	0.271	0.04		
GBW 07113 Cert												72.8	13.0	3.21	0.140	0.160	0.590	2.57	5.43	0.300	0.0500		
BaSO4 Meas											14.1												
BaSO4 Cert											14.0												
BaSO4 Meas											13.6												
BaSO4 Cert											14.0												
BaSO4 Meas											14.3												
BaSO4 Cert											14.0												
NIST 696 Meas												3.88	53.62	8.64	0.009	0.01	0.04		< 0.01	2.619	0.06		
NIST 696 Cert												3.79	54.5	8.70	0.00400	0.0120	0.0180		0.00900	2.64	0.0500		
SY-4 Meas												49.25	20.34	6.05	0.107	0.56	8.05	6.87	1.65	0.282	0.14		
SY-4 Cert												49.9	20.69	6.21	0.108	0.54	8.05	7.10	1.66	0.287	0.131		
BIR-1a Meas												48.30	15.73	11.35	0.173	10.84	13.51	1.82	0.01	0.977	0.02		
BIR-1a Cert												47.96	15.50	11.30	0.175	9.700	13.30	1.82	0.030	0.96	0.021		
ZW-C Meas																							
ZW-C Cert																							
OREAS 101b (Fusion) Meas																							
OREAS 101b (Fusion) Cert																							
OREAS 101b (4 Acid) Meas																							
OREAS 101b (4 Acid) Cert																							
OREAS 98 (4 Acid) Meas																							
OREAS 98 (4 Acid) Cert																							
NCS DC86318 Meas																							
NCS DC86318 Cert																							
USZ 25-2006 Meas																							
USZ 25-2006 Cert																							
DNC-1a Meas												47.43	18.69	9.78	0.147	11.46	11.48	1.91	0.22	0.485	0.07		
DNC-1a Cert												47.15	18.34	9.97	0.150	10.13	11.49	1.890	0.234	0.480	0.07		
BCR-2 Meas												53.75	13.48	13.76	0.198	3.99	7.14	3.05	1.79	2.246	0.35		
BCR-2 Cert												54.1	13.5	13.8	0.196	3.59	7.12	3.16	1.79	2.26	0.35		
USZ 42-2006 Meas																							
USZ 42-2006 Cert																							
GS311-4 Meas											1.11	0.53											
GS311-4 Cert											1.11	0.54											
GS311-4 Meas											1.12	0.54											
GS311-4 Cert											1.11	0.54											
GS311-4 Meas											1.12	0.54											
GS311-4 Cert											1.11	0.54											
OREAS 903 (4 Acid) Meas																							

Analyte Symbol	Au	As	Br	Cr	Ir	Sc	Se	Sb	Mass	C-Total	Total S	SiO2	Al2O3	Fe2O3(T)	MnO	MgO	CaO	Na2O	K2O	TiO2	P2O5	LOI	Total
Unit Symbol	ppb	ppm	ppm	ppm	ppb	ppm	ppm	ppm	g	%	%	%	%	%	%	%	%	%	%	%	%	%	%
Lower Limit	2	0.5	0.5	5	5	0.1	3	0.2		0.01	0.01	0.01	0.01	0.01	0.005	0.01	0.01	0.01	0.01	0.001	0.01		0.01
Method Code	INAA	CS	CS	FUS-ICP	FUS-ICP	FUS-ICP	FUS-ICP	FUS-ICP	FUS-ICP	FUS-ICP	FUS-ICP	FUS-ICP	FUS-ICP	GRAV	FUS-ICP								
OREAS 903 (4 Acid) Cert																							
SiO2 Meas											< 0.01	< 0.01											
SiO2 Cert																							
SiO2 Meas											< 0.01	< 0.01											
SiO2 Cert																							
SiO2 Meas											< 0.01	< 0.01											
SiO2 Cert																							
OREAS 45d (4-Acid) Meas																							
OREAS 45d (4-Acid) Cert																							
REE-1 Meas																							
REE-1 Cert																							
OREAS 96 (4 Acid) Meas																							
OREAS 96 (4 Acid) Cert																							
Oreas 72b (4 Acid) Meas																							
Oreas 72b (4 Acid) Cert																							
GS316-3 Meas										0.06	0.34												
GS316-3 Cert										0.0600	0.340												
W-2b Meas												52.43	15.25	10.73	0.165	7.12	11.02	2.23	0.62	1.076	0.13		
W-2b Cert												52.4	15.4	10.7	0.163	6.37	10.9	2.14	0.626	1.06	0.140		
OREAS 681 (4 Acid) Meas																							
OREAS 681 (4 Acid) Cert																							
OREAS 147 (4 Acid) Meas																							
OREAS 147 (4 Acid) Cert																							
Oreas 521 (4 Acid) Meas																							
Oreas 521 (4 Acid) Cert																							
GS317-5 Meas										8.27	14.9												
GS317-5 Cert										8.46	15.5												
GS317-5 Meas										8.13	14.8												
GS317-5 Cert										8.46	15.5												
GS317-5 Meas										8.13	14.7												
GS317-5 Cert										8.46	15.5												
OREAS 70b (4 Acid) Meas																							
OREAS 70b (4 Acid) Cert																							
OREAS 620 (4 Acid) Meas																							
OREAS 620 (4 Acid) Cert																							
DMMAS 125 Meas	1400	1580		80		8.6	< 3	4.7															

Analyte Symbol	Au	As	Br	Cr	Ir	Sc	Se	Sb	Mass	C-Total	Total S	SiO2	Al2O3	Fe2O3(T)	MnO	MgO	CaO	Na2O	K2O	TiO2	P2O5	LOI	Total
Unit Symbol	ppb	ppm	ppm	ppm	ppb	ppm	ppm	ppm	g	%	%	%	%	%	%	%	%	%	%	%	%	%	%
Lower Limit	2	0.5	0.5	5	5	0.1	3	0.2		0.01	0.01	0.01	0.01	0.01	0.005	0.01	0.01	0.01	0.01	0.001	0.01		0.01
Method Code	INAA	INAA	INAA	INAA	INAA	INAA	INAA	INAA	INAA	CS	CS	FUS-ICP	FUS-ICP	FUS-ICP	FUS-ICP	FUS-ICP	FUS-ICP	FUS-ICP	FUS-ICP	FUS-ICP	FUS-ICP	GRAV	FUS-ICP
DMMAS 125 Cert	1410	1560		86.0		8.94	4.79	4.68															
IG_BH04_MG060 Orig										< 0.01	< 0.01												
IG_BH04_MG060 Dup										< 0.01	< 0.01												
IG_BH04_MG064 Orig																							
IG_BH04_MG064 Dup																							
IG_BH04_MG065 Orig												50.04	13.18	9.89	0.167	9.73	10.84	2.59	1.15	0.722	0.22		100.5
IG_BH04_MG065 Dup												50.03	13.38	10.10	0.171	9.78	10.88	2.56	1.14	0.730	0.22		101.0
IG_BH04_MG071 Orig										0.58	0.34												
IG_BH04_MG071 Dup										0.57	0.30												
IG_BH04_MG074 Orig																							
IG_BH04_MG074 Dup																							
IG_BH04_MG081 Orig										< 0.01	< 0.01												
IG_BH04_MG081 Dup										< 0.01	< 0.01												
IG_BH04_MG082 Orig	< 2	1.5	< 0.5	22	< 5	2.5	< 3	< 0.2	29.5			72.20	15.19	2.68	0.035	0.60	2.53	4.43	2.39	0.272	0.08		100.6
IG_BH04_MG082 Dup	< 2	3.2	< 0.5	22	< 5	2.5	< 3	< 0.2	25.4			72.24	15.07	2.68	0.035	0.60	2.53	4.45	2.40	0.265	0.07		100.6
IG_BH04_MG085 Orig																							
IG_BH04_MG085 Dup																							
IG_BH04_MG086 Orig										0.79	< 0.01												
IG_BH04_MG086 Dup										0.79	< 0.01												
IG_BH02_LG033 Orig																							
IG_BH02_LG033 Dup																							
IG_BH01_LG047 Orig										0.12	< 0.01												
IG_BH01_LG047 Dup										0.11	< 0.01												
IG_BH01_LG048 Orig	< 2	< 0.5	< 0.5	17	< 5	4.1	< 3	< 0.2	28.2	0.10	< 0.01											1.40	
IG_BH01_LG048 Split PREP DUP																							
Method Blank																							
Method Blank																							
Method Blank																							
Method Blank																							
Method Blank																							
Method Blank																							
Method Blank																							

Analyte Symbol	Au	As	Br	Cr	Ir	Sc	Se	Sb	Mass	C-Total	Total S	SiO2	Al2O3	Fe2O3(T)	MnO	MgO	CaO	Na2O	K2O	TiO2	P2O5	LOI	Total
Unit Symbol	ppb	ppm	ppm	ppm	ppb	ppm	ppm	ppm	g	%	%	%	%	%	%	%	%	%	%	%	%	%	%
Lower Limit	2	0.5	0.5	5	5	0.1	3	0.2		0.01	0.01	0.01	0.01	0.01	0.005	0.01	0.01	0.01	0.01	0.001	0.01		0.01
Method Code	INAA	INAA	INAA	INAA	INAA	INAA	INAA	INAA	INAA	CS	CS	FUS-ICP	FUS-ICP	FUS-ICP	FUS-ICP	FUS-ICP	FUS-ICP	FUS-ICP	FUS-ICP	FUS-ICP	FUS-ICP	GRAV	FUS-ICP
Method Blank																							
Method Blank																							
Method Blank																							
Method Blank	< 2	< 0.5	< 0.5	< 5	< 5	< 0.1	< 3	< 0.2	30.0														
Method Blank												0.01	< 0.01	0.01	< 0.005	< 0.01	0.01	< 0.01	< 0.01	< 0.001	0.01		

Analyte Symbol	Sc	Be	V	Cr	Co	Ni	Cu	Zn	Cd	S	Ga	Ge	As	Rb	Sr	Y	Zr	Nb	Mo	Ag	In	Sn	Sb
Unit Symbol	ppm	ppm	ppm	ppm	ppm	ppm	ppm	ppm	ppm	%	ppm	ppm	ppm	ppm	ppm	ppm	ppm	ppm	ppm	ppm	ppm	ppm	ppm
Lower Limit	1	1	5	20	1	1	1	1	0.5	0.001	1	0.5	5	1	2	1	1	0.2	2	0.3	0.1	1	0.2
Method Code	FUS-ICP	FUS-ICP	FUS-ICP	FUS-MS	FUS-MS	TD-ICP	TD-ICP	TD-ICP	TD-ICP	TD-ICP	FUS-MS	FUS-MS	FUS-MS	FUS-MS	FUS-ICP	FUS-ICP	FUS-ICP	FUS-MS	FUS-MS	TD-ICP	FUS-MS	FUS-MS	FUS-MS
NIST 694 Meas			1613																				
NIST 694 Cert			1740																				
GBW 07113 Meas	5	4	< 5												41	46	399						
GBW 07113 Cert	5.00	4.00	5.00												43.0	43.0	403						
BaSO4 Meas																							
BaSO4 Cert																							
BaSO4 Meas																							
BaSO4 Cert																							
BaSO4 Meas																							
BaSO4 Cert																							
NIST 696 Meas			389														1058						
NIST 696 Cert			403.00 00														1037.0 000						
SY-4 Meas	1	3	7												1178	121	559						
SY-4 Cert	1.1	2.6	8.0												1191	119	517						
BIR-1a Meas	43	< 1	327	390	52						16				110	16	15						
BIR-1a Cert	44	0.58	310	370	52						16				110	16	18						
ZW-C Meas				60							99			> 1000				215				> 1000	4.4
ZW-C Cert				56.0							99			8500				198				1300	4.2
OREAS 101b (Fusion) Meas					46														20				
OREAS 101b (Fusion) Cert					47														21				
OREAS 101b (4 Acid) Meas						9	424																
OREAS 101b (4 Acid) Cert						8.2	412																
OREAS 98 (4 Acid) Meas								> 10000	1270		16.6									42.4			
OREAS 98 (4 Acid) Cert								14800 0.0	1360		15.5									45.1			
NCS DC86318 Meas															380								
NCS DC86318 Cert														369.42									
USZ 25-2006 Meas					35																		
USZ 25-2006 Cert					32.5																		
DNC-1a Meas	31		151												147	17	36						
DNC-1a Cert	31		148												144	18.0	38.0						
BCR-2 Meas	33		424												348	34	178						
BCR-2 Cert	33		416												346	37	188						
USZ 42-2006 Meas													238					35.0	35				
USZ 42-2006 Cert													224					31.00	34.40				
GS311-4 Meas																							
GS311-4 Cert																							
GS311-4 Meas																							
GS311-4 Cert																							
GS311-4 Meas																							
GS311-4 Cert																							
OREAS 903 (4 Acid) Meas						59	6780	30	< 0.5	0.515										0.8			

Analyte Symbol	Sc	Be	V	Cr	Co	Ni	Cu	Zn	Cd	S	Ga	Ge	As	Rb	Sr	Y	Zr	Nb	Mo	Ag	In	Sn	Sb
Unit Symbol	ppm	ppm	ppm	ppm	ppm	ppm	ppm	ppm	ppm	%	ppm	ppm	ppm	ppm	ppm	ppm	ppm	ppm	ppm	ppm	ppm	ppm	ppm
Lower Limit	1	1	5	20	1	1	1	1	0.5	0.001	1	0.5	5	1	2	1	1	0.2	2	0.3	0.1	1	0.2
Method Code	FUS-ICP	FUS-ICP	FUS-ICP	FUS-MS	FUS-MS	TD-ICP	TD-ICP	TD-ICP	TD-ICP	TD-ICP	FUS-MS	FUS-MS	FUS-MS	FUS-MS	FUS-ICP	FUS-ICP	FUS-ICP	FUS-MS	FUS-MS	TD-ICP	FUS-MS	FUS-MS	FUS-MS
OREAS 903 (4 Acid) Cert						54.0	6520	24.3	0.200	0.500										0.432			
SiO2 Meas																							
SiO2 Cert																							
SiO2 Meas																							
SiO2 Cert																							
SiO2 Meas																							
SiO2 Cert																							
OREAS 45d (4-Acid) Meas						236	392	46		0.045													
OREAS 45d (4-Acid) Cert						231.0	371	45.7		0.049													
REE-1 Meas				290									115	> 1000				> 1000				505	
REE-1 Cert				277									124	1050				4050				498	
OREAS 96 (4 Acid) Meas							> 10000	444		4.36										11.6			
OREAS 96 (4 Acid) Cert							39300	457		4.19										11.5			
Oreas 72b (4 Acid) Meas						6400	219	91	< 0.5	1.45										0.4			
Oreas 72b (4 Acid) Cert						6860	222	99.0	0.310	1.49										0.230			
GS316-3 Meas																							
GS316-3 Cert																							
W-2b Meas	35	< 1	267	90	44						18			20	198	20	89	7.4					0.8
W-2b Cert	36.0	1.30	262	92.0	43.0						17.0			21.0	190	24.0	94.0	7.90					0.790
OREAS 681 (4 Acid) Meas						461	271	77		0.104										< 0.3			
OREAS 681 (4 Acid) Cert						503	264	88.0		0.109										0.118			
OREAS 147 (4 Acid) Meas						24	300	147		0.020													
OREAS 147 (4 Acid) Cert						21.2	298	138		0.0300													
Oreas 521 (4 Acid) Meas						66	5880	23		1.74										1.2			
Oreas 521 (4 Acid) Cert						73	6070	24		1.80										0.89			
GS317-5 Meas																							
GS317-5 Cert																							
GS317-5 Meas																							
GS317-5 Cert																							
GS317-5 Meas																							
GS317-5 Cert																							
OREAS 70b (4 Acid) Meas						2030	51	98	< 0.5	0.291										< 0.3			
OREAS 70b (4 Acid) Cert						2180	52	110	0.4	0.309										0.2			
OREAS 620 (4 Acid) Meas						16	1830	> 10000	165	2.64										40.6			
OREAS 620 (4 Acid) Cert						15	1730	31500	163	2.47										38.5			
DMMAS 125 Meas																							
DMMAS 125 Cert																							

Analyte Symbol	Sc	Be	V	Cr	Co	Ni	Cu	Zn	Cd	S	Ga	Ge	As	Rb	Sr	Y	Zr	Nb	Mo	Ag	In	Sn	Sb
Unit Symbol	ppm	ppm	ppm	ppm	ppm	ppm	ppm	ppm	ppm	%	ppm	ppm	ppm	ppm	ppm	ppm	ppm	ppm	ppm	ppm	ppm	ppm	ppm
Lower Limit	1	1	5	20	1	1	1	1	0.5	0.001	1	0.5	5	1	2	1	1	0.2	2	0.3	0.1	1	0.2
Method Code	FUS-ICP	FUS-ICP	FUS-ICP	FUS-MS	FUS-MS	TD-ICP	TD-ICP	TD-ICP	TD-ICP	TD-ICP	FUS-MS	FUS-MS	FUS-MS	FUS-MS	FUS-ICP	FUS-ICP	FUS-ICP	FUS-MS	FUS-MS	TD-ICP	FUS-MS	FUS-MS	FUS-MS
IG_BH04_MG060 Orig																							
IG_BH04_MG060 Dup																							
IG_BH04_MG064 Orig							5	10	61	< 0.5	0.003									< 0.3			
IG_BH04_MG064 Dup							5	9	60	< 0.5	0.002									< 0.3			
IG_BH04_MG065 Orig	31	1	224	820	41						17	1.4	< 5	33	744	17	94	3.0	< 2		< 0.1	1	0.2
IG_BH04_MG065 Dup	31	1	224	830	42						17	1.5	< 5	33	739	16	94	3.1	< 2		< 0.1	1	0.2
IG_BH04_MG071 Orig																							
IG_BH04_MG071 Dup																							
IG_BH04_MG074 Orig							34	7	138	< 0.5	0.012										< 0.3		
IG_BH04_MG074 Dup							36	8	141	< 0.5	0.011										< 0.3		
IG_BH04_MG081 Orig																							
IG_BH04_MG081 Dup																							
IG_BH04_MG082 Orig	3	< 1	21	< 20	4						22	0.7	< 5	65	288	4	145	4.1	< 2		< 0.1	1	< 0.2
IG_BH04_MG082 Dup	3	< 1	21	< 20	4						22	0.9	< 5	67	289	4	151	4.2	2		< 0.1	1	< 0.2
IG_BH04_MG085 Orig							3	14	69	< 0.5	0.004										0.4		
IG_BH04_MG085 Dup							3	14	71	< 0.5	0.005										0.4		
IG_BH04_MG086 Orig																							
IG_BH04_MG086 Dup																							
IG_BH02_LG033 Orig							5	12	30	< 0.5	0.003										0.3		
IG_BH02_LG033 Dup							5	13	29	< 0.5	0.004										< 0.3		
IG_BH01_LG047 Orig																							
IG_BH01_LG047 Dup																							
IG_BH01_LG048 Orig				< 20	5	4	13	76	< 0.5	0.004	22	0.8	< 5	73				2.7	< 2	0.4	< 0.1	1	< 0.2
IG_BH01_LG048 Split PREP DUP				< 20	6						22	0.8	< 5	72				2.2	4		< 0.1	1	< 0.2
Method Blank						< 1	< 1	< 1	< 0.5	< 0.001											< 0.3		
Method Blank						< 1	< 1	< 1	< 0.5	0.001											< 0.3		
Method Blank						< 1	< 1	< 1	< 0.5	0.004											< 0.3		
Method Blank						< 1	< 1	< 1	< 0.5	0.002											< 0.3		
Method Blank						< 1	< 1	< 1	< 0.5	0.002											< 0.3		
Method Blank						< 1	< 1	< 1	< 0.5	0.001											< 0.3		
Method Blank						< 1	< 1	< 1	< 0.5	0.005											< 0.3		
Method Blank						< 1	< 1	< 1	< 0.5	0.002											< 0.3		

Analyte Symbol	Sc	Be	V	Cr	Co	Ni	Cu	Zn	Cd	S	Ga	Ge	As	Rb	Sr	Y	Zr	Nb	Mo	Ag	In	Sn	Sb
Unit Symbol	ppm	ppm	ppm	ppm	ppm	ppm	ppm	ppm	ppm	%	ppm	ppm	ppm	ppm	ppm	ppm	ppm	ppm	ppm	ppm	ppm	ppm	ppm
Lower Limit	1	1	5	20	1	1	1	1	0.5	0.001	1	0.5	5	1	2	1	1	0.2	2	0.3	0.1	1	0.2
Method Code	FUS-ICP	FUS-ICP	FUS-ICP	FUS-MS	FUS-MS	TD-ICP	TD-ICP	TD-ICP	TD-ICP	TD-ICP	FUS-MS	FUS-MS	FUS-MS	FUS-MS	FUS-ICP	FUS-ICP	FUS-ICP	FUS-MS	FUS-MS	TD-ICP	FUS-MS	FUS-MS	FUS-MS
Method Blank						< 1	< 1	< 1	< 0.5	< 0.001										< 0.3			
Method Blank				< 20	< 1						< 1	< 0.5	< 5	< 1				< 0.2	< 2		< 0.1	< 1	< 0.2
Method Blank																							
Method Blank	< 1	< 1	< 5												< 2	< 1	1						

Analyte Symbol	Cs	Ba	La	Ce	Pr	Nd	Sm	Eu	Gd	Tb	Dy	Ho	Er	Tm	Yb	Lu	Hf	Ta	W	Tl	Pb	Bi	Th
Unit Symbol	ppm	ppm	ppm	ppm	ppm	ppm	ppm	ppm	ppm	ppm	ppm	ppm	ppm	ppm	ppm	ppm	ppm	ppm	ppm	ppm	ppm	ppm	ppm
Lower Limit	0.1	2	0.05	0.05	0.01	0.05	0.01	0.005	0.01	0.01	0.01	0.01	0.01	0.005	0.01	0.002	0.1	0.01	0.5	0.05	5	0.1	0.05
Method Code	FUS-MS	FUS-ICP	FUS-MS	TD-ICP	FUS-MS	FUS-MS																	
NIST 694 Meas																							
NIST 694 Cert																							
GBW 07113 Meas		504																					
GBW 07113 Cert		506																					
BaSO4 Meas																							
BaSO4 Cert																							
BaSO4 Meas																							
BaSO4 Cert																							
BaSO4 Meas																							
BaSO4 Cert																							
NIST 696 Meas																							
NIST 696 Cert																							
SY-4 Meas		350																					
SY-4 Cert		340																					
BIR-1a Meas		8	0.60	1.90		2.30	1.10	0.510	1.90						1.50	0.270	0.6						
BIR-1a Cert		6	0.63	1.9		2.5	1.1	0.55	2.0						1.7	0.3	0.60						
ZW-C Meas	262		29.0	97.6	9.10	24.5	6.60		4.40			1.90		1.60	14.1	2.21	9.9	80.9	309	32.8			43.5
ZW-C Cert	260		30.0	97	9.5	25.0	6.6		4.70			2.0		1.60	14	2.20	9.7	82	320	34			43
OREAS 101b (Fusion) Meas			784	1330	127	384	50.0	7.82		5.18	31.4	6.24	18.6	2.63	17.5	2.61							36.6
OREAS 101b (Fusion) Cert			789	1331	127	378	48	7.77		5.37	32.1	6.34	18.7	2.66	17.6	2.58							37.1
OREAS 101b (4 Acid) Meas																						19	
OREAS 101b (4 Acid) Cert																						23	
OREAS 98 (4 Acid) Meas																						269	
OREAS 98 (4 Acid) Cert																						345	
NCS DC86318 Meas	10.9		1900	401	710	> 2000	> 1000	18.4	> 1000	468	> 1000	574	> 1000	262	> 1000	253							65.1
NCS DC86318 Cert	11.88		1960	432	737	3429	1725	18.91	2168	468	3224	560	1750	271	1844	264							67.0
USZ 25-2006 Meas			> 2000	> 3000	> 1000																		
USZ 25-2006 Cert			19300	29000	2800																		
DNC-1a Meas		108																					
DNC-1a Cert		118																					
BCR-2 Meas		708																					
BCR-2 Cert		683																					
USZ 42-2006 Meas			> 2000	> 3000	> 1000	> 2000	501	85.0				7.19											944
USZ 42-2006 Cert			21100	27600	2300	6500	539	87.22				7.86											946
GS311-4 Meas																							
GS311-4 Cert																							
GS311-4 Meas																							
GS311-4 Cert																							
GS311-4 Meas																							
GS311-4 Cert																							
OREAS 903 (4 Acid) Meas																						10	
OREAS 903 (4																						11.3	

Analyte Symbol	Cs	Ba	La	Ce	Pr	Nd	Sm	Eu	Gd	Tb	Dy	Ho	Er	Tm	Yb	Lu	Hf	Ta	W	Tl	Pb	Bi	Th
Unit Symbol	ppm	ppm	ppm	ppm	ppm	ppm	ppm	ppm	ppm	ppm	ppm	ppm	ppm	ppm	ppm	ppm	ppm	ppm	ppm	ppm	ppm	ppm	ppm
Lower Limit	0.1	2	0.05	0.05	0.01	0.05	0.01	0.005	0.01	0.01	0.01	0.01	0.01	0.005	0.01	0.002	0.1	0.01	0.5	0.05	5	0.1	0.05
Method Code	FUS-MS	FUS-ICP	FUS-MS	TD-ICP	FUS-MS	FUS-MS																	
Acid) Cert																							
SiO2 Meas																							
SiO2 Cert																							
SiO2 Meas																							
SiO2 Cert																							
SiO2 Meas																							
SiO2 Cert																							
SiO2 Meas																							
OREAS 45d (4-Acid) Meas																						14	
OREAS 45d (4-Acid) Cert																						21.8	
REE-1 Meas	1.0		1660	> 3000	427	1460	387	23.8	427	109	861	208	702	108	690		497						747
REE-1 Cert	1.07		1661	3960	435	1456	381	23.5	433	106	847	208	701	106	678		479						719
OREAS 96 (4 Acid) Meas																						85	
OREAS 96 (4 Acid) Cert																						101	
Oreas 72b (4 Acid) Meas																						10	
Oreas 72b (4 Acid) Cert																						14.9	
GS316-3 Meas																							
GS316-3 Cert																							
W-2b Meas	0.8	181	10.8	22.9		12.7	3.20	1.10		0.58	3.70	0.76			1.90	0.310	2.5	0.51					
W-2b Cert	0.990	182	10.0	23.0		13.0	3.30	1.00		0.630	3.60	0.760			2.10	0.330	2.60	0.500					
OREAS 681 (4 Acid) Meas																						< 5	
OREAS 681 (4 Acid) Cert																						10.2	
OREAS 147 (4 Acid) Meas																						27	
OREAS 147 (4 Acid) Cert																						27.8	
Oreas 521 (4 Acid) Meas																						7	
Oreas 521 (4 Acid) Cert																						9	
GS317-5 Meas																							
GS317-5 Cert																							
GS317-5 Meas																							
GS317-5 Cert																							
GS317-5 Meas																							
GS317-5 Cert																							
OREAS 70b (4 Acid) Meas																						11	
OREAS 70b (4 Acid) Cert																						14	
OREAS 620 (4 Acid) Meas																						> 5000	
OREAS 620 (4 Acid) Cert																						7740	
DMMAS 125 Meas																							
DMMAS 125 Cert																							
IG_BH04_MG060																							

Analyte Symbol	Cs	Ba	La	Ce	Pr	Nd	Sm	Eu	Gd	Tb	Dy	Ho	Er	Tm	Yb	Lu	Hf	Ta	W	Tl	Pb	Bi	Th
Unit Symbol	ppm	ppm	ppm	ppm	ppm	ppm	ppm	ppm	ppm	ppm	ppm	ppm	ppm	ppm	ppm	ppm	ppm	ppm	ppm	ppm	ppm	ppm	ppm
Lower Limit	0.1	2	0.05	0.05	0.01	0.05	0.01	0.005	0.01	0.01	0.01	0.01	0.01	0.005	0.01	0.002	0.1	0.01	0.5	0.05	5	0.1	0.05
Method Code	FUS-MS	FUS-ICP	FUS-MS	TD-ICP	FUS-MS	FUS-MS																	
Orig																							
IG_BH04_MG060 Dup																							
IG_BH04_MG064 Orig																						6	
IG_BH04_MG064 Dup																						6	
IG_BH04_MG065 Orig	1.1	408	28.7	60.2	7.27	29.6	5.54	1.46	4.25	0.53	2.90	0.56	1.54	0.209	1.32	0.203	2.2	0.17	20.8	0.17		< 0.1	3.62
IG_BH04_MG065 Dup	1.1	405	29.0	60.2	7.26	29.3	5.60	1.47	4.27	0.53	2.87	0.55	1.56	0.213	1.33	0.207	2.2	0.17	< 0.5	0.20		0.1	3.48
IG_BH04_MG071 Orig																							
IG_BH04_MG071 Dup																							
IG_BH04_MG074 Orig																						< 5	
IG_BH04_MG074 Dup																						< 5	
IG_BH04_MG081 Orig																							
IG_BH04_MG081 Dup																							
IG_BH04_MG082 Orig	1.1	712	22.0	37.5	3.71	12.3	1.86	0.555	1.29	0.14	0.68	0.12	0.28	0.035	0.22	0.034	3.3	0.42	< 0.5	0.36		< 0.1	4.53
IG_BH04_MG082 Dup	1.1	717	23.2	39.2	3.91	12.9	1.91	0.572	1.39	0.15	0.70	0.12	0.29	0.039	0.26	0.038	3.6	0.44	< 0.5	0.37		< 0.1	4.79
IG_BH04_MG085 Orig																						< 5	
IG_BH04_MG085 Dup																						5	
IG_BH04_MG086 Orig																							
IG_BH04_MG086 Dup																							
IG_BH02_LG033 Orig																						6	
IG_BH02_LG033 Dup																						< 5	
IG_BH01_LG047 Orig																							
IG_BH01_LG047 Dup																							
IG_BH01_LG048 Orig	2.1		20.0	29.4	3.45	11.9	1.76	0.492	1.31	0.15	0.78	0.14	0.38	0.050	0.32	0.051	3.1	0.34	0.9	0.39	9	0.1	3.48
IG_BH01_LG048 Split PREP DUP	2.2		19.0	28.1	3.31	11.3	1.79	0.480	1.18	0.16	0.78	0.14	0.36	0.052	0.34	0.057	2.8	0.33	1.8	0.41		0.2	3.15
Method Blank																						< 5	
Method Blank																						< 5	
Method Blank																						< 5	
Method Blank																						< 5	
Method Blank																						< 5	
Method Blank																						< 5	
Method Blank																						< 5	
Method Blank																						< 5	
Method Blank																						< 5	

Analyte Symbol	Cs	Ba	La	Ce	Pr	Nd	Sm	Eu	Gd	Tb	Dy	Ho	Er	Tm	Yb	Lu	Hf	Ta	W	Tl	Pb	Bi	Th
Unit Symbol	ppm	ppm	ppm	ppm	ppm	ppm	ppm	ppm	ppm	ppm	ppm	ppm	ppm	ppm	ppm	ppm	ppm	ppm	ppm	ppm	ppm	ppm	ppm
Lower Limit	0.1	2	0.05	0.05	0.01	0.05	0.01	0.005	0.01	0.01	0.01	0.01	0.01	0.005	0.01	0.002	0.1	0.01	0.5	0.05	5	0.1	0.05
Method Code	FUS-MS	FUS-ICP	FUS-MS	FUS-MS	FUS-MS	FUS-MS	FUS-MS	FUS-MS	FUS-MS	FUS-MS	FUS-MS	FUS-MS	FUS-MS	FUS-MS	FUS-MS	FUS-MS	FUS-MS	FUS-MS	FUS-MS	FUS-MS	TD-ICP	FUS-MS	FUS-MS
Method Blank	< 0.1		< 0.05	< 0.05	< 0.01	< 0.05	< 0.01	< 0.005	< 0.01	< 0.01	< 0.01	< 0.01	< 0.01	< 0.005	< 0.01	< 0.002	< 0.1	< 0.01	< 0.5	< 0.05		< 0.1	< 0.05
Method Blank																							
Method Blank		< 2																					

Analyte Symbol	U
Unit Symbol	ppm
Lower Limit	0.01
Method Code	FUS-MS
NIST 694 Meas	
NIST 694 Cert	
GBW 07113 Meas	
GBW 07113 Cert	
BaSO4 Meas	
BaSO4 Cert	
BaSO4 Meas	
BaSO4 Cert	
BaSO4 Meas	
BaSO4 Cert	
NIST 696 Meas	
NIST 696 Cert	
SY-4 Meas	
SY-4 Cert	
BIR-1a Meas	
BIR-1a Cert	
ZW-C Meas	18.7
ZW-C Cert	20.0
OREAS 101b (Fusion) Meas	406
OREAS 101b (Fusion) Cert	396
OREAS 101b (4 Acid) Meas	
OREAS 101b (4 Acid) Cert	
OREAS 98 (4 Acid) Meas	
OREAS 98 (4 Acid) Cert	
NCS DC86318 Meas	
NCS DC86318 Cert	
USZ 25-2006 Meas	
USZ 25-2006 Cert	
DNC-1a Meas	
DNC-1a Cert	
BCR-2 Meas	
BCR-2 Cert	
USZ 42-2006 Meas	
USZ 42-2006 Cert	
GS311-4 Meas	
GS311-4 Cert	
GS311-4 Meas	
GS311-4 Cert	
GS311-4 Meas	
GS311-4 Cert	
OREAS 903 (4 Acid) Meas	
OREAS 903 (4	

Analyte Symbol	U
Unit Symbol	ppm
Lower Limit	0.01
Method Code	FUS-MS
Acid) Cert	
SiO2 Meas	
SiO2 Cert	
SiO2 Meas	
SiO2 Cert	
SiO2 Meas	
SiO2 Cert	
OREAS 45d (4-Acid) Meas	
OREAS 45d (4-Acid) Cert	
REE-1 Meas	139
REE-1 Cert	137
OREAS 96 (4 Acid) Meas	
OREAS 96 (4 Acid) Cert	
Oreas 72b (4 Acid) Meas	
Oreas 72b (4 Acid) Cert	
GS316-3 Meas	
GS316-3 Cert	
W-2b Meas	0.55
W-2b Cert	0.530
OREAS 681 (4 Acid) Meas	
OREAS 681 (4 Acid) Cert	
OREAS 147 (4 Acid) Meas	
OREAS 147 (4 Acid) Cert	
Oreas 521 (4 Acid) Meas	
Oreas 521 (4 Acid) Cert	
GS317-5 Meas	
GS317-5 Cert	
GS317-5 Meas	
GS317-5 Cert	
GS317-5 Meas	
GS317-5 Cert	
OREAS 70b (4 Acid) Meas	
OREAS 70b (4 Acid) Cert	
OREAS 620 (4 Acid) Meas	
OREAS 620 (4 Acid) Cert	
DMMAS 125 Meas	
DMMAS 125 Cert	
IG_BH04_MG060	

Analyte Symbol	U
Unit Symbol	ppm
Lower Limit	0.01
Method Code	FUS-MS
Orig	
IG_BH04_MG060 Dup	
IG_BH04_MG064 Orig	
IG_BH04_MG064 Dup	
IG_BH04_MG065 Orig	0.91
IG_BH04_MG065 Dup	0.90
IG_BH04_MG071 Orig	
IG_BH04_MG071 Dup	
IG_BH04_MG074 Orig	
IG_BH04_MG074 Dup	
IG_BH04_MG081 Orig	
IG_BH04_MG081 Dup	
IG_BH04_MG082 Orig	1.01
IG_BH04_MG082 Dup	0.91
IG_BH04_MG085 Orig	
IG_BH04_MG085 Dup	
IG_BH04_MG086 Orig	
IG_BH04_MG086 Dup	
IG_BH02_LG033 Orig	
IG_BH02_LG033 Dup	
IG_BH01_LG047 Orig	
IG_BH01_LG047 Dup	
IG_BH01_LG048 Orig	0.90
IG_BH01_LG048 Split PREP DUP	0.86
Method Blank	

Analyte Symbol	U
Unit Symbol	ppm
Lower Limit	0.01
Method Code	FUS-MS
Method Blank	< 0.01
Method Blank	
Method Blank	